

## Durham E-Theses

---

### *The electrical breakdown of gases at microwave frequencies*

Lane, P. E.

#### How to cite:

---

Lane, P. E. (1953) *The electrical breakdown of gases at microwave frequencies*, Durham theses, Durham University. Available at Durham E-Theses Online: <http://etheses.dur.ac.uk/9291/>

#### Use policy

---

The full-text may be used and/or reproduced, and given to third parties in any format or medium, without prior permission or charge, for personal research or study, educational, or not-for-profit purposes provided that:

- a full bibliographic reference is made to the original source
- a [link](#) is made to the metadata record in Durham E-Theses
- the full-text is not changed in any way

The full-text must not be sold in any format or medium without the formal permission of the copyright holders.

Please consult the [full Durham E-Theses policy](#) for further details.

THE ELECTRICAL BREAKDOWN OF GASES AT MICROWAVE FREQUENCIES,

by

P.E. LANE, B.Sc., A.Inst.P., Grad.I.E.E.

Being an account of work carried out at the  
University of Durham during the three  
years ending in September 1953.

-----

Thesis submitted to the University of Durham for  
Ph.D. degree examination.

-----

## ACKNOWLEDGEMENTS.

The author wishes to thank Professor J.E.P.Wagstaff and the staff of the Physics Department, South Road, Durham, for the facilities and advice made available during the period of the investigation.

He is deeply indebted to Dr.W.A.Prowse for his patient guidance and valuable criticism while acting as Research Supervisor.

Grateful acknowledgements are also made to the Department of Scientific and Industrial Research for a maintenance grant for the three years, and to the British Electrical and Allied Industries Research Association for a grant towards the apparatus.

-----

C O N T E N T S.

	Page
Historical Outline of High Frequency Discharge in Gases.	1.
General Introduction.	26.
Introduction to Part I.	26.

PART I.CHAPTER I.Variation of breakdown stress with irradiator position at 10,000 Mc/s.

1. Apparatus as taken over from Laverick and Jasinski	27.
1.1. Requirements of apparatus	27.
1.2. The microwave apparatus	28.
1.3. Field measurement in the resonator	31.
1.4. Determination of mode of resonance of the resonator	32.
1.4.1. Rotation of pick-up loop	32.
1.4.2. Positions of resonance	32.
1.5. Initiation of breakdown	33.
1.6. Apparatus as a whole	35.
1.7. Vacuum apparatus	37.
1.7.1. General	37.
1.7.2. Pressure measurements	37.
2. Preliminary results using apparatus as taken over from Laverick and Jasinski	38.
3. Development of apparatus and technique	41.
3.1. First improvement	41.
3.1.1. Apparatus	41.
3.1.2. Results	42.
3.2. Second improvement	43.
3.2.1. Apparatus	43.
3.2.2. Results	44.
3.3. Final development of the apparatus	45.
3.3.1. Apparatus	45.
4. Results with the apparatus as developed	47.
4.1. Air	47.
4.1.1. Variation of breakdown stress with irradiator position	47.
4.1.2. Variation of breakdown stress with pressure for a fixed irradiator position	49.
4.1.3. Variation of breakdown stress with pressure using a mesothorium source of radiation	49.



4.1.4. Effect of variation in the angle of incidence of the ionising beam	52.
4.1.5. Recovery of air after breakdown	54.
4.1.6. Effect of pulse repetition rate on breakdown stress	56.
4.2. Oxygen	56.
4.2.1. Recovery of oxygen after breakdown	57.
4.2.2. Variation of breakdown stress with irradiator position	59.
4.2.3. Variation of breakdown stress with pressure for a fixed irradiator position	60.
4.2.4. Variation of breakdown stress with pressure using a mesothorium source of irradiation	61.
4.2.5. Variation in the position of the mesothorium source	61.
4.2.6. Effect of variation in the angle of incidence of the ionising beam	62.
4.3. Nitrogen	62.
4.3.1. Recovery of nitrogen after breakdown	62.
4.3.2. Variation of breakdown stress with irradiator position	68.
4.3.3. Variation of breakdown stress with pressure for a fixed irradiator position	69.
4.3.4. Variation of breakdown stress with pressure using a mesothorium source of irradiation	70.
4.3.5. Effect of variation in the angle of incidence of the ionising beam	70.
4.4. Hydrogen	70.
4.4.1. Recovery of hydrogen after breakdown	70.
4.4.2. Variation of breakdown stress with irradiator position	73.
4.4.3. Variation of breakdown stress with pressure for a fixed irradiator position	75.
4.4.4. Variation of breakdown stress with pressure using a mesothorium source of irradiation	76.
4.4.5. Effect of variation in the angle of incidence of the ionising beam	76.
4.5. Neon.	76.
4.5.1. Variation of breakdown stress with pressure	77.
4.5.2. Spontaneous breakdown of neon	79.
5. Brief résumé of the microwave results	81.
6. Further development	83.

## CHAPTER II.

### Variation of breakdown stress with irradiator position at 11 Mc/s.

1. Apparatus	83a.
2. Experimental results	84.

	Page.
2.1. Distance effect	84.
2.1.1. Conditions of measurement	84.
2.1.2. Air (Dry)	86.
2.1.3. Oxygen (Cylinder)	89.
2.1.4. Hydrogen (Pure)	91.
2.1.5. Brief résumé of the three sets of results	92.
2.2. Variation of intensity of irradiating spark	93.
2.2.1. Apparatus	93.
2.2.2. Results: Air only	94.
2.2.3. The effect of an external metal sleeve: Air	95.
2.3. Metal sleeve inside the irradiator tube	98.
2.3.1. Air. Metal sleeve fixed; irradiator position varied	98.
2.3.2. Air. Irradiator fixed; metal sleeve position varied.	99.
2.3.3. Hydrogen. Metal sleeve fixed; irradiator position varied	100.
2.3.4. Hydrogen. Irradiator fixed; metal sleeve position varied	101.
2.4. A brief discussion on these results as a guide to the next experiments	102.
2.5. Breakdown stress measurements: irradiator in side tube	104.
2.5.1. Air (Dry)	105.
2.5.2. Hydrogen (Pure)	108.

### CHAPTER III.

#### Discussion of the experimental results.

1. Introduction	111.
1.1. Aspects of triggering processes	111.
1.2. Products from the irradiating spark	113.
1.2.1. Ultra-violet light	113.
1.3. Products not originating at the irradiating spark gap	114.
2. Experimental discrimination	115.
3. Conclusion	120.
4. Lowering of breakdown stress	120.
4.1. General résumé and comparison between microwave and h-f results	120.
5. Possible causes of the lowering of the breakdown stress	123.
6. Frequency effect	125.

PART II.

	Page.
Introduction to Part II	127.
Previous work undertaken with combined fields	129.
<u>CHAPTER I.</u>	
<u>The apparatus.</u>	
1. The Problem	131.
2. Apparatus	132.
2.1. Requirements to be satisfied by resonator	132.
2.2. Theory and design of the $H_{011}$ resonator	133.
2.2.1. General Theory	133.
2.2.2. Application of theory to given waveguide	136.
2.2.3. The Limiting Case	137.
2.2.4. Variation of $H_{011}$ in waveguide with $y$	137.
2.2.5. Variation of the Poynting Flux down the waveguide due to a change in A.	139.
2.2.6. Final choice of dimensions	139.
2.3. Steady field distribution within resonator	140.
2.4. Constructional details of resonator	142.
2.5. The other microwave components	143.
2.5.1. The tapering wave guide section	143.
2.5.2. The tuning stub sections	143.
2.5.3. The choke couplings	143.
2.5.4. The magnetron load and feed sections	144.
2.6. Coupling adjustments and initial use of apparatus	145.
2.7. The unidirectional field	146.
2.7.1. General	146.
2.7.2. Measurement of the steady pulse magnitude	147.
<u>CHAPTER 2.</u>	
<u>Crossed fields, microwave and unidirectional fields.</u>	
1. Initial results in air and hydrogen	148.
2. Air (dry)	149.
3. Hydrogen	151.
4. Oxygen (cylinder)	155.
5. Neon (pure)	156.
6. Discussion	156.
<u>CHAPTER 3.</u>	
<u>Crossed fields, microwave and 0.86 Mc/s fields.</u>	
1. Introduction	160.
2. Apparatus	160.

	Page.
2.1. The Oscillator	160.
2.2. Voltage measurement	161.
3. Results	162.
3.1. Pure electrolytic hydrogen	162.
3.1.1. Variation of the microwave stress with alternating field	162.
3.1.2. Auxiliary field cut off voltages	163.
3.1.3. General comments, hydrogen	165.
3.2. Spectroscopically pure neon	166.
3.2.1. Variation of the microwave stress with alternating field	166.
3.2.2. Auxiliary field cut off voltages	167.
3.2.3. Electron ambits under crossed fields, neon	168.

#### CHAPTER 4.

##### Crossed fields, microwave and 2.66 Mc/s. fields.

1. Apparatus	171.
2. Results	171.
2.1. Pure electrolytic hydrogen	171.
2.1.1. Variation of the microwave breakdown stress with alternating field	171.
2.1.2. Alternating field cut off voltages	172.
2.1.3. Electron ambits under crossed fields, hydrogen	173.
2.1.4. Statistical lag variations with auxiliary field voltages	174.
2.2. Neon, spectroscopically pure	175.
2.2.1. Variation of microwave breakdown stress with alternating field	175.
2.2.2. Breakdown of neon under the alternating field (2.66 Mc/s) alone	178.
2.2.3. Electron ambits under crossed fields, neon	178.
2.3. Spectroscopically pure nitrogen	179.
2.3.1. Variation of the microwave breakdown stress with auxiliary field	179.
2.3.2. Alternating field cut off voltages	181.
2.4. Cylinder oxygen	181.
2.4.1. Variation of the microwave breakdown stress with auxiliary field	181.
2.5. Dry air	183.
2.5.1. Variation of the microwave breakdown stress with auxiliary field	183.
2.6. Résumé of the 2.66 Mc/s. work	184.

#### CHAPTER 5.

##### Crossed fields, microwave and 9.7 Mc/s. fields.

1. Apparatus	186
--------------	-----

	Page.
2. Results	186.
2.1. Pure electrolytic hydrogen	186.
2.1.1. Variation of the microwave breakdown stress with auxiliary field	186.
2.1.2. Electron ambits under crossed fields, hydrogen	187.
2.2. Spectroscopically pure neon	188.
2.2.1. Variation of the microwave breakdown stress with auxiliary field	188.
2.2.2. Electron ambits under crossed fields, neon	189.
2.3. Dry air	190.
2.3.1. Variation of the microwave breakdown stress with auxiliary field.	190.
2.3.2. Electron ambits under crossed fields, air	191.
3. Discussion	191.

#### CHAPTER 6.

##### Calculation of electron ambits.

1. Electron drift velocity correction under crossed fields	193.
2. Calculation of electron ambits using corrected drift velocities	194.
2.1. Most precise method	194.
2.2. Sinusoidal variation of $eWx$	196.
2.3. Using the R.M.S. value of the field	197.
3. Conclusions	198.

#### CHAPTER 7.

##### The parallel electrode work at 2.3 and 11.5 Mc/s.

1. Introduction	199.
2. Apparatus	199.
3. Results	200.
3.1. The 2.3 Mc/s. experiments	200.
3.1.1. Hydrogen pure electrolytic	200.
3.2. The 11.5 Mc/s experiments	203a.
3.2.1. Hydrogen	203a.
3.2.2. Nitrogen	204.
3.2.3. Dry air	205.
3.2.4. Cylinder oxygen	206.
4. Conclusions	206.

#### CHAPTER 8.

##### Microwave breakdown stresses.

1. Calibration of 10,000 Mc/s. E-p curves.	208.
--	------

2. Comparison with the 2,800 Mc/s results of Prowse and Jasinski	211.
3. Comparison with the American work	212.
4. The minimum pressure on the E-p curves	213.

## CHAPTER 9.

### Discussion.

1. Comparison of the 11 Mc/s. and 10,000 Mc/s. results with the American Diffusion Theory	215.
2. The work under crossed fields	222.
2.1. A possible expected result with orthogonally applied fields	222.
2.1.1. Case 1. Microwave and unidirectional fields	222.
2.1.2. Case 2. " " alternating fields	223.
2.2. Summarised results	223.
2.3. Discussion of the results obtained under the action of the combined fields	225.
2.4. Further considerations	229.
2.4.1. Formative time for discharge	229.
2.4.2. Diffusion at the ends of the trajectories	230.
2.4.3. Variation of statistical lag with applied auxiliary field	231.
3. The neon results	232.
3.1. General	232.
3.2. The neon results for the crossed field experiments	235.
3.3. Further considerations for neon	236.

## APPENDICES.

1. The pressure gauges	238.
2. Calibration of crystal diodes	239.
3. The circulating pump	240.
4. Hydrogen generating plant	241.
5. Irradiator pulse generator	242.

BIBLIOGRAPHY	243.
--------------	------

### Historical Outline of High Frequency Discharge in Gases.

The expression "Electric Discharge" for the conduction of electricity through a gas is derived from an experiment performed by Coulomb<sup>1\*</sup> in 1785. He showed that a charged electroscope became discharged by the action of the air and not by defective insulation. Michael Faraday<sup>2</sup> in 1835 investigated low pressure discharges, which he called "glow discharges"; similar work by Righi<sup>3</sup> in 1876 showed that the breakdown stress of air was independent of the material of the electrodes.

High frequency gas discharges can now be conveniently divided according to their mode of oscillation, (Mehta<sup>4</sup>, Morgan<sup>5</sup>) :-

(a) The Electromagnetic discharge ("H" type of discharge), or as J.J.Thomson<sup>6</sup> called it the "Ring Discharge", where the conduction current in the gas is a closed path in form of a ring.

(b) The Electrostatic discharge ("E" type of discharge), or glow discharge where the conduction current in the gas is continued via displacement currents.

Electrodes are present for this type of discharge and may

\* For this and subsequent references see the end of this work.

be inside or outside the discharge vessel.

The electromagnetic discharge was discovered by Hittorf<sup>7</sup> using a spiral of wire, round the tube containing the gas, and connected across a Leyden Jar to an induction coil. Thus a series of highly damped current pulses were sent through the coil causing a brilliant glow in the tube.

Lehrmann<sup>8</sup>, Tesla<sup>9</sup>, Lecher<sup>10</sup> and Steiner<sup>11</sup>, conducted similar experiments claiming that the discharge was due to the large alternating potential differences which existed between the ends of the coil encompassing the discharge tube, i.e. the discharge was electrostatic in origin.

The work of J.J. Thomson<sup>12</sup>, from 1891 onwards supported the original work of Hittorf that the discharge was electromagnetic in origin (i.e. the ring discharge); he showed that the type of discharge obtained between two electrodes connected to an alternating source of potential produced a discharge which has none of the peculiarities of the ring discharge. The first actually to conduct such an experiment appear to have been Widemann and Ebert<sup>13</sup>. It is interesting to note that Thomson<sup>14</sup> found that ordinary light when passed through a screen, not opaque to ultra violet, caused the ring discharge to pass more easily. The ultra violet light did not actually ionise the gas, but, as he states, put



the molecules in a state where they are more easily ionised. The gases used in these experiments were air, hydrogen, oxygen, nitrogen and the two monatomic gases helium and argon.

Thomson's<sup>15</sup> paper of 1927 was followed by a paper by Townsend and Donaldson<sup>16</sup> criticising the electromagnetic theory of gas breakdown. They claimed that the ring discharge observed for the two gases used, neon and nitrogen, was due to an electrical and not to a magnetic effect.

With these two conflicting schools of thought it was only natural to find several workers, MacKinnon<sup>17</sup>, Knipp<sup>18</sup>, Smith Lynch and Hilberry<sup>19</sup>, Yarnold<sup>20</sup>, and Brasfield<sup>21</sup>, undertaking experiments in an endeavour to clarify the position. MacKinnon showed that the mean free path of an electron was the predominating factor in determining breakdown. For short mean free paths the high electrostatic force between the electrodes causes intense ionisation, but the electromagnetic force present is too small to cause any ring discharge; under the action of the electromagnetic force the electrons are unable to acquire sufficient energy between collisions to cause intense ionisation. When the pressure is reduced the mean free path becomes of the

same order as the separation of the electrodes, and the discharge ceases. However in the ring discharge the electrons have paths sufficiently long to acquire enough velocity to cause ionisation. It is recalled that Thomson's work was always at low pressure; Townsend and Donaldson worked over a wider range of pressures. It appears that both types of discharge can occur in the electrodeless discharge, the occurrence of either being dependent on the pressure; for example in nitrogen for pressures from 1.16m.m. Hg. to 0.0062m.m. Hg. the E type of discharge is obtained, while below 0.0062m.m. Hg. the E type ceases and the H type, or ring discharge, commences.

Meanwhile workers were endeavouring to establish the breakdown stresses of gases, in particular air, under the action of high frequency fields up to a frequency of about 100 Mc/s. Clark and Ryan<sup>22</sup> in 1914 describe experiments for the establishment of the breakdown stress for air at atmospheric pressure between 7 inch copper spheres, for frequencies up to 600 Mc/s. The first comparison between true high frequency discharge voltages and unidirectional discharges is given in a paper by Gill and Donaldson<sup>23</sup> in 1926, where there was a small decrease in the breakdown stresses between steady conditions and the high

frequency discharge ( $2.10^5$  c/s.); and a striking decrease for a frequency of  $3.6.10^7$  c/s. These results should be treated with some reserve as the pressures were low, 1 to 3 m.m.Hg., and the gases could have been contaminated with mercury vapour from the McLeod Gauge. Taylor<sup>24</sup>, Hulbert<sup>25</sup>, Thomson<sup>26</sup>, Lassen<sup>27</sup>, Kirchner<sup>28</sup>, and Rohde<sup>29</sup>, together with many other workers showed that from 0 to  $10^6$  c/s. the breakdown stress diminished slightly but steadily with increase of frequency, and the curve breakdown stress against pressure showed a single minimum. This minimum can be explained in two ways depending on the frequency range used. (See Gill and Donaldson, or Margenau. This point is further considered on page 22).

Cambell<sup>30</sup> first realised the double nature of the time lags encountered between application of the voltage and the breakdown of the gas. He concluded that one lag was irregular and connected with the presence of the casual electron, and one a regular lag.

A very useful summary of most work before 1932 is contained in a review by Darrow<sup>31</sup>, and the later work up to 1950 by von Engel<sup>32</sup>.

In contrast to the previous work the results obtained by C. and H. Gutton and their collaborators<sup>33</sup> are of considerable interest. The  $(E - p)^*$  curves they obtained

\* E = breakdown stress of gas measured in volts.cm., and  
p = gas pressure in m.m.Hg.

for hydrogen using a 10 cm. discharge tube with external electrodes for the frequency range 50 Kc/s to 99 Mc/s were of a complex nature. In some cases there were no minima, and others showed maxima. They concluded that these peculiarities were due to a resonance phenomenon in the gas. Gill and Donaldson<sup>34</sup> however showed that the phenomenon could be explained in terms of the removal, or non removal, of the electrons from the gap. In the earlier work electrons were evidently removed to the electrodes in each half cycle of the field; at the lower frequencies the positive ions would also be removed. As electrons are enormously more mobile than positive ions, the latter are not considered as reaching the electrodes in a high frequency discharge.

The experiments of Gill and Donaldson were designed expressly to investigate the change of breakdown stress of a gas (air) between the conditions of non-removal and removal of the electrons in one half cycle of the applied field. A long cylindrical discharge tube was arranged to be in one of two positions, parallel to the electrodes (a), or at right angles to the electrodes (b).

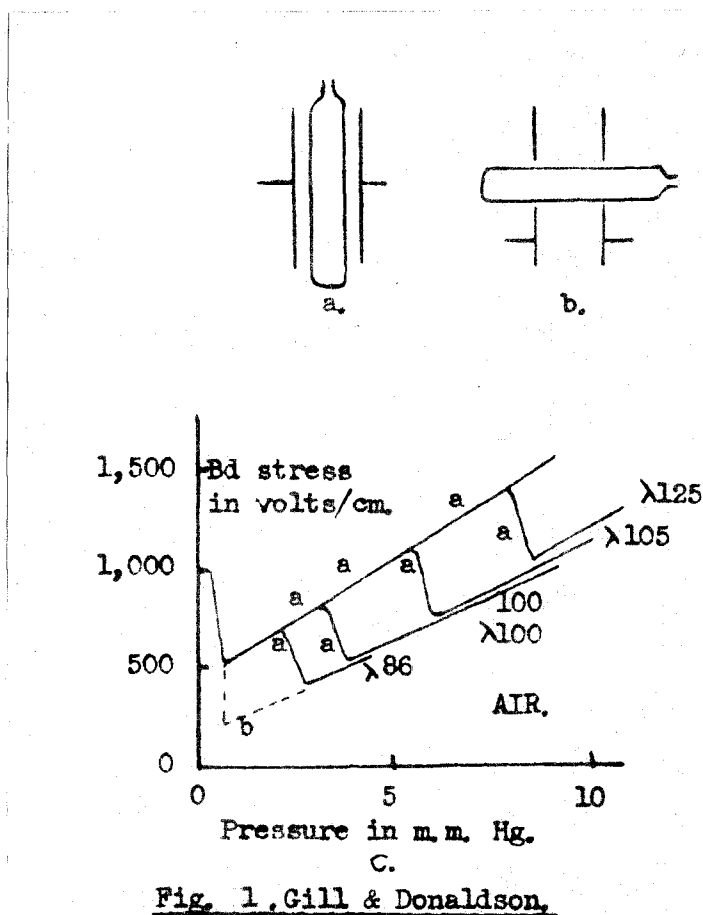


Fig. 1. Gill & Donaldson.

In the first arrangement when the excitation was by a field at right angles to the long axis of the discharge tube curves with two minima were obtained, curve "A" fig. 1c. In the second orientation the minimum independent of frequency was only observed, curve "b" fig. 1c.

They found the attributing of these facts to some form of resonance phenomenon in the gas difficult to support. Explaining the results, in the first experiment by the non-

removal of the electrons at the higher frequencies, that is when the electron orbit was less than the diameter of the tube. In the second case the minimum was the normal minimum observed in most high frequency (E - p) curves, where the collisional frequency of the electron is of the same order as the frequency of the applied field. They deduced from their results electron velocities which gave good agreement with previously obtained values.

This experiment by Gill and Donaldson can be assumed as the starting point for the modern work on h-f and u-h-f gas discharges. Similar work to the above has more recently been published by Mlle. Chenot<sup>35</sup>, and by Pim<sup>36</sup>. (See later pages for a discussion on Pim's work).

It would seem expedient to define in the broadest sense the types of gas discharge obtainable before proceeding with a discussion of more modern work

1. Low frequency discharge :- up to a few cycles per second, where neither the positive ions nor the electrons are removed from the gap during a half cycle; and the peak stress values differ but slightly from the unidirectional breakdown stress.

2. High frequency discharge, (h-f) :- a region where a gradual decrease in the breakdown stress is observed, a maximum of a few per cent below the steady field value.

This reduction is due to the non-removal of the slow moving positive ions during a half cycle. The space charge thus produced results in an increase in the ionisation and a lowering of the necessary stress to initiate breakdown.

### 3. Ultra-high frequency discharge (u-h-f):-

here the movement of the electron is so limited that there is no electron removal in one half cycle of the oscillation. Again a further lowering of the breakdown stress of 30% or more is observed compared with the steady field values. A fuller consideration of the types of discharge obtainable is given by Prowse<sup>37</sup>.

J. Thomson<sup>26</sup> in 1930 gave an approximate theory for electrodeless discharge in which he stated that a h-f discharge may be maintained by the ionisation produced by electronic collisions. The theory gave good agreement with experimental results for air and neon, and with the results obtained by Kirchner<sup>28</sup> for oxygen. Later work<sup>38</sup> in 1937 in hydrogen by J. Thomson using higher frequencies, 2 to 100 Mc/s, and parallel plate electrodes gave curves similar to those obtained by C. and H. Gutton<sup>39</sup>. (Double minima at lower frequencies and single minima at the higher frequencies). Prowse<sup>37</sup> states that the steps or minima at

the higher pressures correspond to the electrons just crossing the gap in one half cycle. This work is in agreement with that of Gill and Donaldson and other workers. Seward<sup>40</sup> working in air at frequencies between 200 to 1000 Kc/s. showed that there was a marked reduction in the breakdown stress as the frequency increased.

Following a chronological development, the work of Githens<sup>41</sup>, and of Pim<sup>36</sup>, is of interest. These data presented by Githens were the most accurate in this field to date; great care being used to eliminate mercury vapour (see Thomson<sup>42</sup>). (The action of the hydrocarbon vapour produced by the discharge of Apiezon products under the influence of a h-f discharge is apparently insufficient to influence the breakdown stress.) For frequencies 5 to 11 Mc/s. and pressures between 40 and 150 m.m.Hg. the h-f and steady field curves for (E - p) are linear.

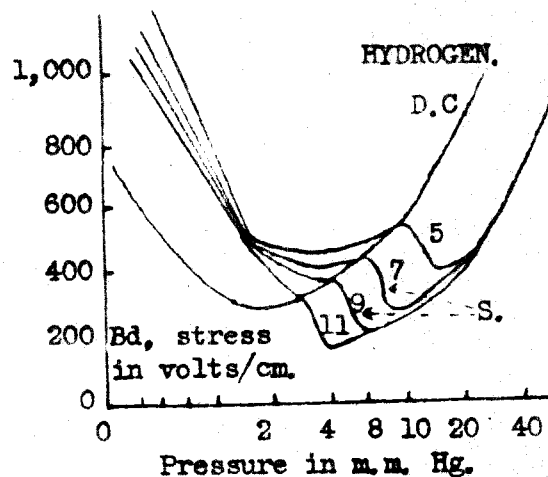


Fig. 2 . Githens



The curves obtained by Githens for pressures below 40 m.m.Hg. are shown in figure 2. The steps marked "s" again occur where the electrode separation becomes too short, and insufficient space charge is built up to give the mode of breakdown found at the higher pressures.

Pim determined the breakdown strength of air under the action of alternating electric fields, between 100 and 200 Mc/s., using parallel plane electrodes; for completeness the curves obtained for 1 m.m. gap are shown in figure 3.

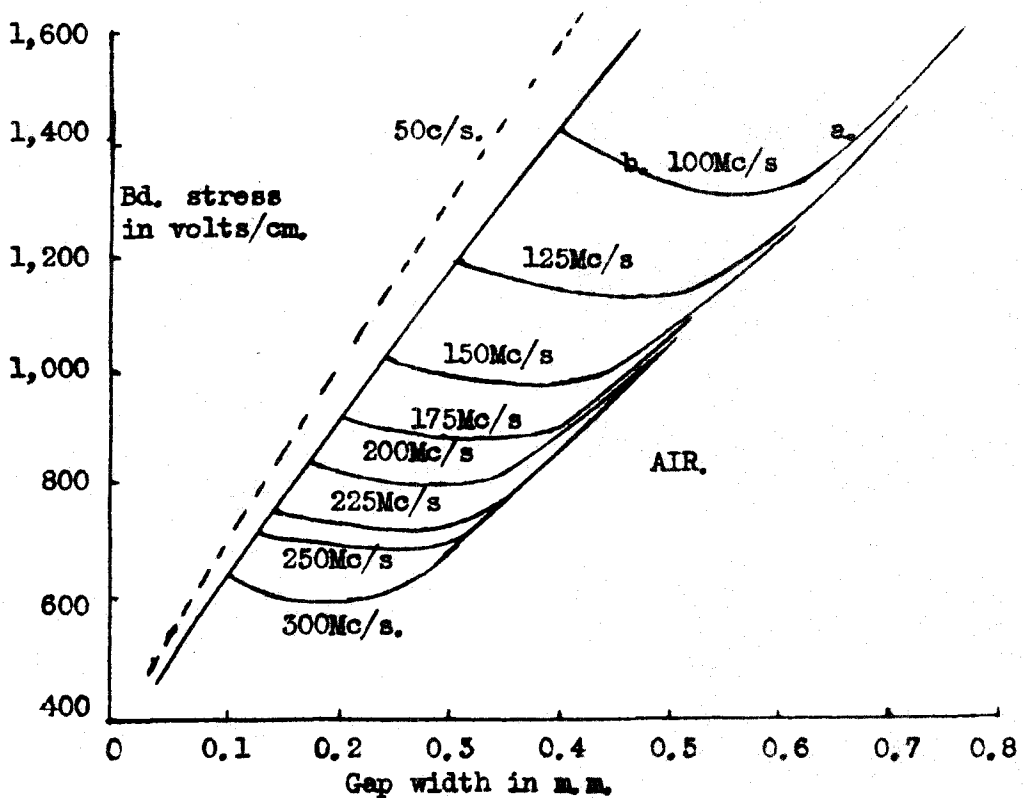


Fig. 3 . Pim.

The curves obtained by Githens for pressures below 40 m.m.Hg. are shown in figure 2. The steps marked "s" again occur where the electrode separation becomes too short, and insufficient space charge is built up to give the mode of breakdown found at the higher pressures.

Pim determined the breakdown strength of air under the action of alternating electric fields, between 100 and 200 Mc/s., using parallel plane electrodes; for completeness the curves obtained for 1 m.m. gap are shown in figure 3.

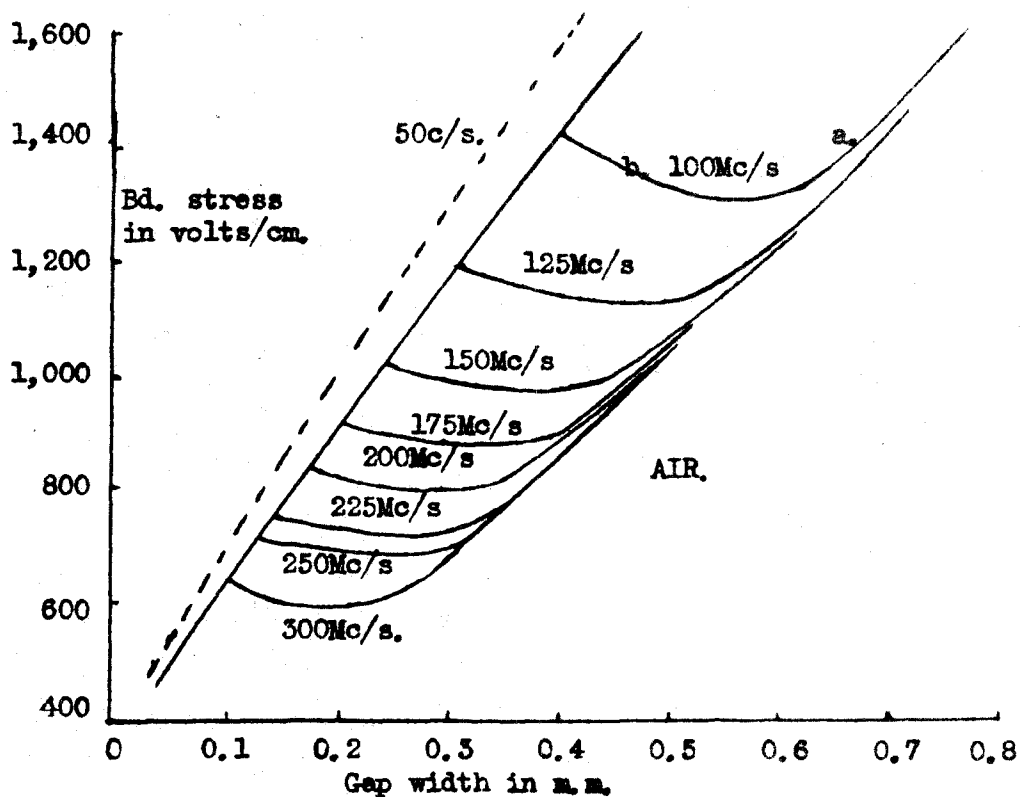


Fig. 3 . Pim.

It can be seen from figure 3 that as the gap width decreases the breakdown stress increases, i.e., between say "a" and "b" in the curve for 100 Mc/s. An explanation is offered by Prowse<sup>43</sup> as to why breakdown does not transfer to the longer gap found nearer the edge of the electrodes.

At very low pressures,  $10^{-3}$  m.m.Hg., Gill and von Engel<sup>44</sup> found for hydrogen, air, helium, and mercury vapour that the starting high frequency (3 to 6 Mc/s) field strength was independent of the gas. At these pressures a collision between an electron and a molecule is a rare occurrence and therefore the build up of ionisation by this means is impossible. A theory is developed where the secondary emission of electrons from the walls is the operative factor. For various lengths of the discharge tube a cut off frequency is observed, below which it is impossible to obtain breakdown.

In a second paper<sup>45</sup> the pressure range of their experiments was extended up to 350 m.m.Hg. for hydrogen. The results showed with the increase in pressure the nature of the gas became important. The starting stress of the high frequency field increased with increase in the wavelength of the applied field up to a region where a step occurred in the  $(E - \lambda)$  curve; this step was shown to occur

where the electron ambit was such that the electron could be lost to the end walls of the discharge vessel. (Figure 4).

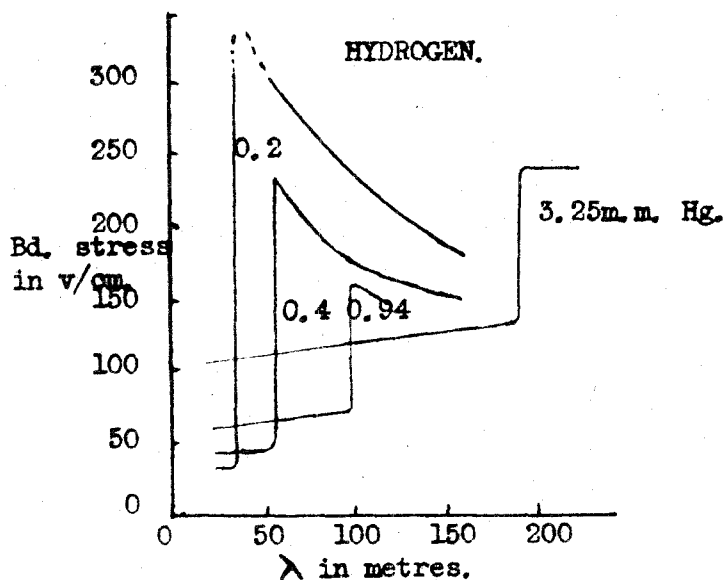


Fig. 4. Gill & von Engel.

Before leaving this section of the history the work of Lodge and Stewart<sup>46</sup> is of interest; where a qualitative theory of high frequency discharge is developed with special reference to the use of sleeve electrodes, on the assumption that the discharge is largely determined by its D.C. wall and space charges. The chief function of the high frequency field is to maintain the electron temperature, leading to the conclusion that under the electrodes there are high negative wall space charges and

the positive ions are driven by a high radial field to the walls of the vessel. Examination of the discharge tube walls helped to substantiate the theory.

Very few, if any, papers were published during the war years. However, because of the development of magnetrons and klystrons for use in radar work, much work has since been undertaken at centimetre wavelengths, (Microwaves). At these frequencies 3,000 to 10,000 Mc/s. the electron orbit during a half cycle is extremely limited; e.g. for hydrogen at breakdown stress at a pressure of 115 m.m.Hg., and a frequency of 10,000 Mc/s., the orbit becomes 0.0025 m.m.

Cooper<sup>47</sup> for wavelengths of 10 cm., and 3 cm. using 1  $\mu$ sec. pulses at a repetition rate of 40 p.p.s. has recorded the breakdown stress for air in both rectangular and co-axial wave guides. Comparison of the results with direct current breakdown stress shows a reduction to about 70% of the unidirectional breakdown stress, this reduction being independent of the gap width, or wavelength used. Cooper states a value for air of 28 Kv/cm. peak at atmospheric pressure.

Posin<sup>48</sup> claimed to have found that the breakdown stress of a gas was dependent on the duration of the microwave pulse, and upon the intensity of the irradiation illuminating

the gap between the electrodes. However, Cooper showed that only the sparking probability was dependent on the intensity of the irradiation, the onset value of the breakdown stress was fixed.

Working in Australia, Labrum<sup>49</sup> determined the breakdown stresses for air, neon and argon for wavelengths of 10 and 3.2 cms; unfortunately only for a limited pressure range 1 to 30 m.m.Hg. In air he found little or no dependence of the breakdown stress on repetition rate, or pulse duration; for neon an increase in either the pulse repetition rate or the pulse length resulted in a reduction in the microwave breakdown stress.

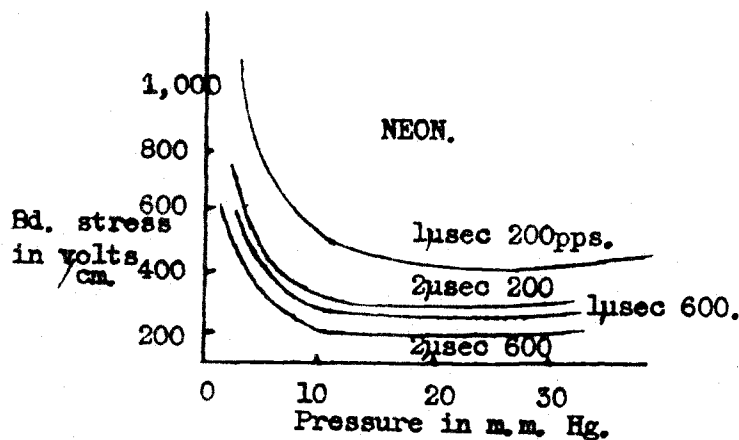


Fig. 5 . Labrum.

The explanation offered for the effect of pulse repetition rate for neon is the presence of residual ionisation

in the gap between pulses. The reduction due to an increase in pulse length is more complex; neon being a non-attaching gas, diffusion is assumed to be the only removal mechanism, but this is negligible in the times involved, (microseconds), also the electron ambipolarity is very limited at such frequencies. A necessary total ionisation is envisaged as the criterion for breakdown. As no losses of ionisation are assumed one can imagine that a large pulse, giving more time for build up of the necessary electron concentration, would require a lower stress to produce breakdown; such is the general argument advanced. (See chapter 9, Part II).

Hale<sup>50</sup> in 1942 proposed a theory for the monatomic gases xenon, and argon, where it is suggested that breakdown is determined by the electrons acquiring the necessary energy to produce ionisation at the end of one mean free path. Good agreement for argon was found at frequencies of 5 to 50 Mc/s., and with Thomson's<sup>38</sup> work for 100 Mc/s.

Turning now to the considerable amount of work by the American school in the microwave frequency region, Herlin and Brown<sup>51</sup> in 1948 developed the "diffusion theory" where electron loss is assumed to be only due to diffusion to the walls of the discharge vessel. If the volume rate of production of electrons per electron is " $\phi$ ", then the

criterion is that the rate of electron generation is just greater than the rate of loss by diffusion, expressed mathematically by :-

$$\nabla n^2 + (\phi/C)n = 0$$

Where  $n$  is the electron concentration, and  $C$  the coefficient of diffusion.

Attachment and recombination are considered negligible, the space charge at breakdown also being low enough to be neglected. (Hartman<sup>52</sup>). Particular solutions for a resonator in the  $TM_{010}$  mode have been given by Herlin and Brown<sup>51</sup> where the ratio  $r/L$  was small, and therefore can be considered a parallel plate system. ( $r$  - radius of resonator,  $L$  - length of resonator). The frequency used in these experiments was 3000 Mc/s. (sustained field). Preliminary results in air gave good agreement with theory. The work for air was extended<sup>53</sup> to an  $r/L$  ratio of 0.5, and to breakdown of gases under the action of non uniform fields between coaxial cylinders<sup>54</sup>.

The limitations of the diffusion theory are discussed by Brown and McDonald<sup>55</sup>; these are:-

(a) The dimensions of the gap must be small compared to the wavelengths used.

(b) The electron mean free path must be less than



the gap width.

(c) The electron orbit under the action of the microwave field must also be less than the gap length.

The diffusion theory has been extended to helium<sup>56</sup> and hydrogen<sup>57</sup>, and in both cases the ratio  $r/L$  was small, (i.e. approximately to a parallel plate system of electrodes). The results for hydrogen gave good agreement with the work of Githens<sup>41</sup> and Thomson<sup>38</sup>, both of whom worked at much lower frequencies.

MacDonald<sup>58</sup> in 1952 further extended the theory to deduce the variation of the microwave breakdown stress for neon with gas pressure. The collision cross sections have different functional forms to those found for helium and hydrogen, and lead to a more complex differential equation. Approximate solutions have been derived and show that there is reasonable agreement between theory and experiment for small gap widths,  $L = 0.317$  and  $0.634$  cms, (the value of  $r$  was  $4.1$  cms.)

In all the results the curves ( $E-p$ ) show a minimum; the breakdown stress decreases with the pressure as the energy gained between collisions increases and therefore more ionisation is available to compensate for the increased diffusion losses at the lower pressures. However where the transition from many oscillations per collision, to many

collisions per oscillation occurs the energy transfer is no longer at its maximum efficiency, therefore a higher field is required to compensate for the diffusion losses. The minimum is not a Paschen minimum.

Allis and Brown<sup>59</sup> in 1952 took the diffusion theory a stage further, presenting a simple solution which is applicable to any gas, and for a wide pressure range; the same limits as imposed by Brown and MacDonald<sup>55</sup> still applied. Their results show reasonable agreement between theory and experiment for the  $E/p$  range of 8 to 50 in hydrogen.

Using the non-attaching monatomic gas argon Krasik, Alpert and McCoubrey<sup>60</sup> found for uniform discharge at a frequency of 3000 Mc/s. good agreement with Holstein's<sup>61</sup> theory of ultra high frequency breakdown. Holstein showed that for a uniform field between parallel plane electrodes and for an applied frequency less than the frequency of elastic collisions of the electrons with the gas molecules, the electron distribution in energy for the microwave field is nearly the same as that for a steady field, of value equal to the r.m.s. value of the microwave field.

Returning now to workers in this country Prowse and Cooper<sup>37,62,63</sup> obtained photographs of discharges in a resonator working in the  $H_{010}$  mode at a frequency of 2,800 Mc/s.

The resonator was energised with 1  $\mu$ sec. pulses either individually or at a rate of 400 per second. The work showed that the true breakdown voltage is unaffected by irradiation, being in agreement with Cooper's<sup>47</sup> earlier work. The irradiation increased the probability of breakdown, especially when individual pulses were employed.

Using a nosed in cavity resonator energised with pulses from 0.25 to 2.5  $\mu$ secs. duration, Prowse and Jasinski<sup>64</sup> have investigated electrical discharge at 2,800 Mc/s. Mid gap irradiation produced the random electrons which initiated the discharge. Streamer photographs were taken of the discharges through a window in the wall of the resonator. The mid gap streamer photographs thus obtained were characteristic of the gases used; air, nitrogen, oxygen, argon and neon. The breakdown oscillograms of the envelope of the field in the resonator showed a very rapid collapse, in nitrogen for example 1/20th  $\mu$ sec. Hydrogen showed remarkable consistency in these breakdown times. No alteration in breakdown stress with pulse length was recorded in air, hydrogen, nitrogen and oxygen.

The processes leading to electron removal are discussed, recombination and attachment are not considered to be very effective methods. With regard to the American school, diffusion is not thought to have been the removal

mechanism; for nitrogen at atmospheric pressure the diffusion radius is 0.59 m.m. for the pulse duration used in these experiments. As the gap across the resonator was 1.4 cms. it therefore seems that diffusion of the electrons to the electrodes is not the removal mechanism in pulsed high frequency breakdown. These results support the view that the ultra high frequency breakdown stress of a gas is a true characteristic of the gas and is independent of the gap width.

In a subsequent paper<sup>65</sup> using similar experimental techniques, the formative and statistical time lags of the four gases, air, hydrogen, nitrogen and oxygen were determined. The statistical lags for air and nitrogen were very similar but far greater than the statistical lags found for hydrogen and oxygen. Relative breakdown stresses for pressures 100 m.m.Hg. to one atmosphere are given, these are based on a spot value of 28 K.V./cms. at atmospheric pressure as obtained by Cooper.

The monatomic gases exhibited a dependence of breakdown stress on time of application of the field, in support of Labrum's work, and also the work of Gill and von Engel. This result is in accordance with the suggestion that no appreciable electron removal occurs during the pulse. Thus the formative time is considered to be the time

required to build up the desired degree of ionisation for breakdown. The fact that no measurable formative time was recorded for the polyatomic gases suggests that the voltage stresses recorded were the minimum necessary to produce instability.

The minimum found in (E - p) graphs has been investigated by several workers. Gill and Townsend<sup>66</sup> presented a general theory of electrical breakdown in which they assumed that an electron's energy is increased by successive collisions until it possesses sufficient energy to ionise a gas molecule. It then loses all its energy in one ionising collision and the process is repeated. Based on this idea they developed an expression for the breakdown stress of a gas, the solution of which gave a minimum in the (E - p) curves.

A second type of minimum in the (E - p) curves is found when considering microwave discharge, this occurring when the frequency of the applied field ( $\nu$ ), is of the same order as the collision frequency of the electrons with the gas molecules. This has been treated mathematically by Margenau<sup>67</sup>. As the frequency of the applied field increases the electron will no longer move completely in phase with the field, and hence energy transfer becomes less efficient, i.e. ionisation efficiency decreases. By considering an

increase in the parameter  $\nu/p$ , Margenau shows that the  $E - p$  and the  $E - \nu$  curves should have a minimum where the applied frequency and the collision frequency are of the same order.

The original similarity theorem proposed by Townsend<sup>68</sup> was extended by Holm<sup>69</sup> and later by Llewellyn-Jones and Morgan. The latter two workers considered h-f breakdown between a wire and a coaxial cylinder, for a frequency range of 3.5 to 70 Mc/s., at pressures below 20 m.m.Hg. They found that geometrically similar systems broke down at the same stress ( $E_s$ ) provided the parameters  $a.p$  and  $\nu/p$  were invariant, where

$$E_s = f(a.p, \nu/p)$$

$a$  = a linear dimension.

$P$  = the pressure.

$\nu$  = the frequency of the applied field.

Their experiments gave general agreement for the two gases used air and hydrogen, provided the conditions imposed by Brown and McDonald were observed; the high frequency breakdown was determined by the primary ionisation in the gas and loss of electrons by diffusion to the boundaries of the vessel.

Further work<sup>71</sup> showed that the similarity theorem also applies to the maintenance of h-f currents, but the dependence of the minimum maintenance potential on the parameters  $a.p$  and  $\nu/p$  were not so well defined.

The validity of the similarity theorem for the frequency range 5 to 70 Mc/s. has also been established by the same workers<sup>72</sup> in helium. However the theorem was shown to be extremely sensitive to changes in the gas purity. Elaborate precautions were taken to ensure great purity of the helium. Results for (E - p) show a progressive increase of breakdown stress as the gas purity improved, reaching a limiting value. These final data were used in establishing the validity of the similarity theorem for helium. The complete failure of the theorem for impure helium is accounted for by the occurrence of collisions of the second kind between metastable atoms of the gas and molecules of the impurity.

Formative time measurements by Fisher and his collaborators<sup>73,74,75</sup> are of considerable importance. Working in air and nitrogen with parallel plate electrodes they found that the formative times were of the order of 100  $\mu$ secs. and longer, for gas pressures in excess of 200 m.m.Hg. (The gap widths were between 0.3 and 1.4 m.m.) However a rapid decrease in these times was established for slight over-voltages; for example 2% over-voltage produced a formative time of 1  $\mu$ sec. The time lags were independent of pressure for the same percentage over-voltage from 200 to 760 m.m.Hg. increasing however with separation of the electrodes. Using

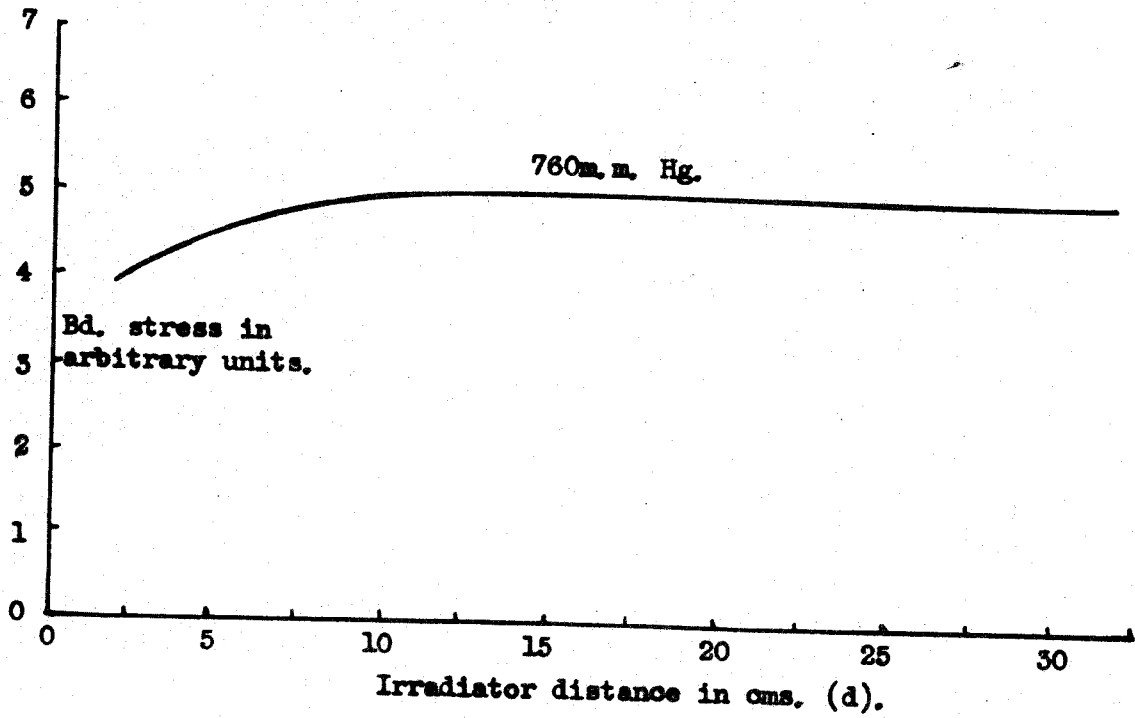
positive point corona in air<sup>75</sup> variation in the intensity of the irradiating ultra violet light produced no appreciable effect on the formative time lags.

Finally the development of the microwave technique has produced a method of studying the variation of electron concentration in after-glow, (Biondi and Brown<sup>76</sup>); this naturally lead to an extensive study of the recombination process. The method was based upon the change in the resonant frequency of a cavity, in the  $H_{010}$  mode for a frequency of 3,000 Mc/s., enclosing the gas at breakdown. The change in the frequency was measured by means of a probing signal of variable frequency. With the use of different probing signals the cavity frequency at a known time after cut off could be determined, and thus the electron concentration was calculated.

One unusual feature found by Biondi<sup>77</sup> was that the electron density in neon and argon actually increased for approximately one microsecond after removal of the ultra high frequency field. Calculations showed that this was due to ionisation resulting from collisions between pairs of metastable atoms as originally suggested by Holstein. A good survey of this recent work on recombination processes in gases is given by Massey<sup>78</sup> 1952.



Graph 1, AIR, Breakdown v. Irradiator Position, 2,800 Mc/s.  
(Prowse and Jasinski,)



GENERAL INTRODUCTION.

The research work undertaken can be broadly divided into two parts.

PART I. An investigation into the variation of the breakdown stress of a gas at both microwave, (10,000 Mc/s.), and high frequency, (11.5 Mc/s.), with the position of the triggering or irradiating spark.

PART II. An investigation into the variation of the microwave breakdown stress of a gas when a unidirectional or high frequency field is simultaneously applied orthogonally to the microwave field.

-----

PART I.Introduction to Part I.

Prowse and Jasinski<sup>65</sup> established that the microwave breakdown stress of air, at 760 m.m.Hg., was dependent on the position of the triggering or irradiating spark. Graph I shows how the microwave breakdown stress decreased as the position of the irradiating spark approached the resonator. (They used the E 110 mode of a nosed in cavity resonator and a frequency of 2,800 Mc/s.).

This phenomenon was further investigated at 10,000 Mc/s. by Prowse, Laverick and Jasinski<sup>79</sup>. They constructed the present apparatus in an exploratory form, and established that the distance between the irradiating spark and the resonator, (i.e., gas discharge vessel), influenced the microwave breakdown stress of air.

The work described in this thesis commenced from this point; a description of this initial apparatus as taken over from Laverick and Jasinski is now given.

## CHAPTER I.

### Variation of breakdown stress with irradiator position at 10,000 Mc/s.

#### 1. Apparatus as taken over from Laverick and Jasinski.

##### 1.1. Requirements of apparatus.

1. It was proposed to use gases other than air, so some form of discharge chamber that could be evacuated was necessary.

2. The microwave electrode system had to be of such a design that a unidirectional field could be applied at right angles to the microwave field.

3. To ensure that the gas breakdown was not influenced by the electrodes, it was considered necessary to use an electrodeless system.



### 1.2. The Microwave apparatus.

The most suitable way to realise these stipulations was by the employment of the ring electric field as present in a cavity resonator, oscillating in the H 011 mode. The field configuration for such a resonator mode is shown in figure 6: the electric field "E<sub>θ</sub>" is in the form of a closed loop.

A resonator oscillating in the H 011 mode can be easily tuned by the movement of one end plate. The resulting currents in the H 011 mode flow on the surface of the resonator, as indicated in figure 7; no current flow occurs across the junction between the curved wall of the resonator and the end plate. The distribution of the current for the H 011 mode is therefore not affected by a small gap between the movable plate and the sides of the resonator. This gap also helps to suppress unwanted modes, in particular the H<sub>l,mn</sub> modes ( $l \neq 0$ ); In the H<sub>l,mn</sub> modes current is required to flow from the curved resonator wall to the end plates.

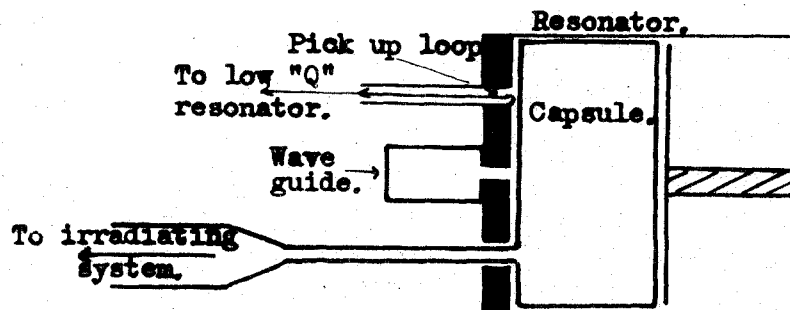


Fig. 9. Section of resonator.

This type of resonator construction allowed the easy insertion of a tight fitting glass capsule within the resonator; (figure 9); therefore the discharge chamber could be evacuated. The presence of the glass vessel did not alter the oscillation of the resonator, due to the fact that the electric field is zero at the walls of the resonator. The tuning position of the movable plate, for resonance, in the H 011 mode was moved slightly further out due to the presence of the glass capsule.

A resonator of such a design was used for these experiments, with an internal diameter "D" of 4.65 cms., and a length "L", when tuned for the H 011 mode, of 2.80 cms. at a frequency of 10,000 Mc/s., (Air dielectric). The resonator was energised by magnetic coupling to an H 01 wave, (generated by a magnetron), travelling down a rectangular wave guide; the general arrangement is shown in figure 8. The magnetic coupling was achieved by means of two holes  $\lambda_g/2$  apart. ( $\lambda_g$  being the wavelength of the H 01 wave in the rectangular guide). However, feed by means of two holes was found to be insufficient when the glass capsule was present within the resonator; the capsule damped the oscillation. The use of a resonant slot between the two holes increased the

electric field within the resonator; the coupling system finally used can be seen in figure 12. It was found possible to produce electrodeless gas discharge within the resonator for air up to a pressure of 130 m.m.Hg.

The rectangular waveguide was fed in turn by means of a choke coupling from a 3 cm. magnetron; originally a British CV108. (Actual frequency 9375 Mc/s., giving  $\lambda = 3.198$  cms.). The waveguide could be tuned by means of two resonant stubs placed on either side of the resonator, and an odd number of  $\lambda_g/4$ 's apart. (See figure 12). Manipulation of these stubs matched the waveguide to the magnetron, and also varied the standing wave system in the wave guide. In this way the feed of energy to the resonator could be easily and effectively controlled.

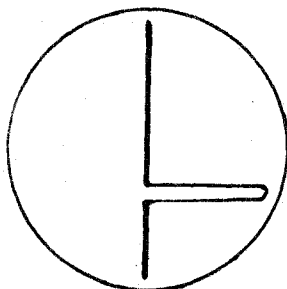
The magnetron was energised by one microsecond duration pulses derived from the discharge of a delay line in the modulator pulse unit. The repetition rate of these pulses could be varied from 400 to 1200 p.p.s. The magnetron output as fed by means of the tunable choke coupling to the wave guide was therefore one microsecond pulses of approximately 3 cms. wavelength radiation, at a repetition rate of 400 to 1200 p.p.s.

Provision was also made for the employment of non-repetitive pulses; however, due to the low probability

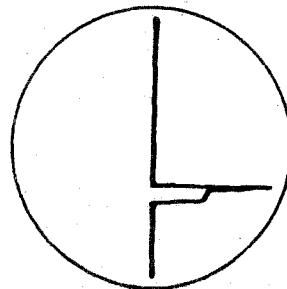
of breakdown within a microsecond at very small over-voltages single slot work was abandoned. All the results recorded were for a pulse repetition rate of 400/sec. unless otherwise stated.

### 1.3. Field measurement in the resonator.

In order to measure the energy fed into the resonator a small magnetic pick up loop was inserted into the end wall of the resonator, (as shown in figures 9 and 12); the output of this magnetic loop fed to a tunable low "Q" resonator and crystal detector system. The rectifier was a crystal diode, CV 111. The rectified output from this low "Q" resonator was fed to a wide band amplifier of variable gain, the output of which was displayed on a high speed cathode ray oscillograph. A characteristic trace can be seen in figure 10. Very careful screening of all leads was necessary in these circuits to avoid spurious pickup. Automatic synchronisation of the oscilloscope was achieved by means of an early warning pulse derived from the modulator unit.



Before  
breakdown.  
Fig. 10a.



After  
breakdown.  
Fig. 10b.



#### 1.4. Determination of mode of resonance of the resonator.

##### 1.4.1. Rotation of pick up loop.

When the field distribution inside the resonator is of the form shown in figure 6, (the H 011 mode), maximum pick up by the magnetic loop is indicated when the plane of the loop is perpendicular to, and threaded by, the magnetic field. With the plane of the loop in line, i.e., parallel to the magnetic field, the pick up is reduced to zero.

Upon rotating the pick up loop through  $180^\circ$  it was observed that the output, as indicated by the height of the pulse envelope displayed on the oscilloscope screen, passed through a maximum for one position of the loop, and was negligible upon a further  $90^\circ$  rotation of the loop. (An indicator on the input cable to the loop showed the plane of the loop). This sequence of amplitudes indicated that the mode present in the resonator was the required H 011 mode.

##### 1.4.2. Positions of resonance.

As the piston of the cavity resonator is withdrawn resonances occur for various positions of the piston. Knowing the wavelength of the radiation in free space ( $\lambda$ ), and the dimensions of the resonator, the wavelength of the radiation for the H 011 mode in the resonator

can be deduced ( $\lambda_{011}$ ). The initial setting of the piston for resonance is, therefore, known and the actual position is in this neighbourhood and can be checked by pick up loop rotation.

An absorbing disc was placed behind the piston to suppress any spurious oscillations in this region.

### 1.5 Initiation of breakdown.

It can be stated generally that two conditions are necessary before breakdown can occur in a gas:-

1. The field strength must be of sufficient magnitude to be capable of producing breakdown at the particular pressure chosen.
2. A triggering, or casual, electron must be in a suitable position to initiate the breakdown. The statistical component of the time lag preceding breakdown is usually associated with the wait for this casual electron.

The first condition can only be satisfied if enough energy is available within the resonator.

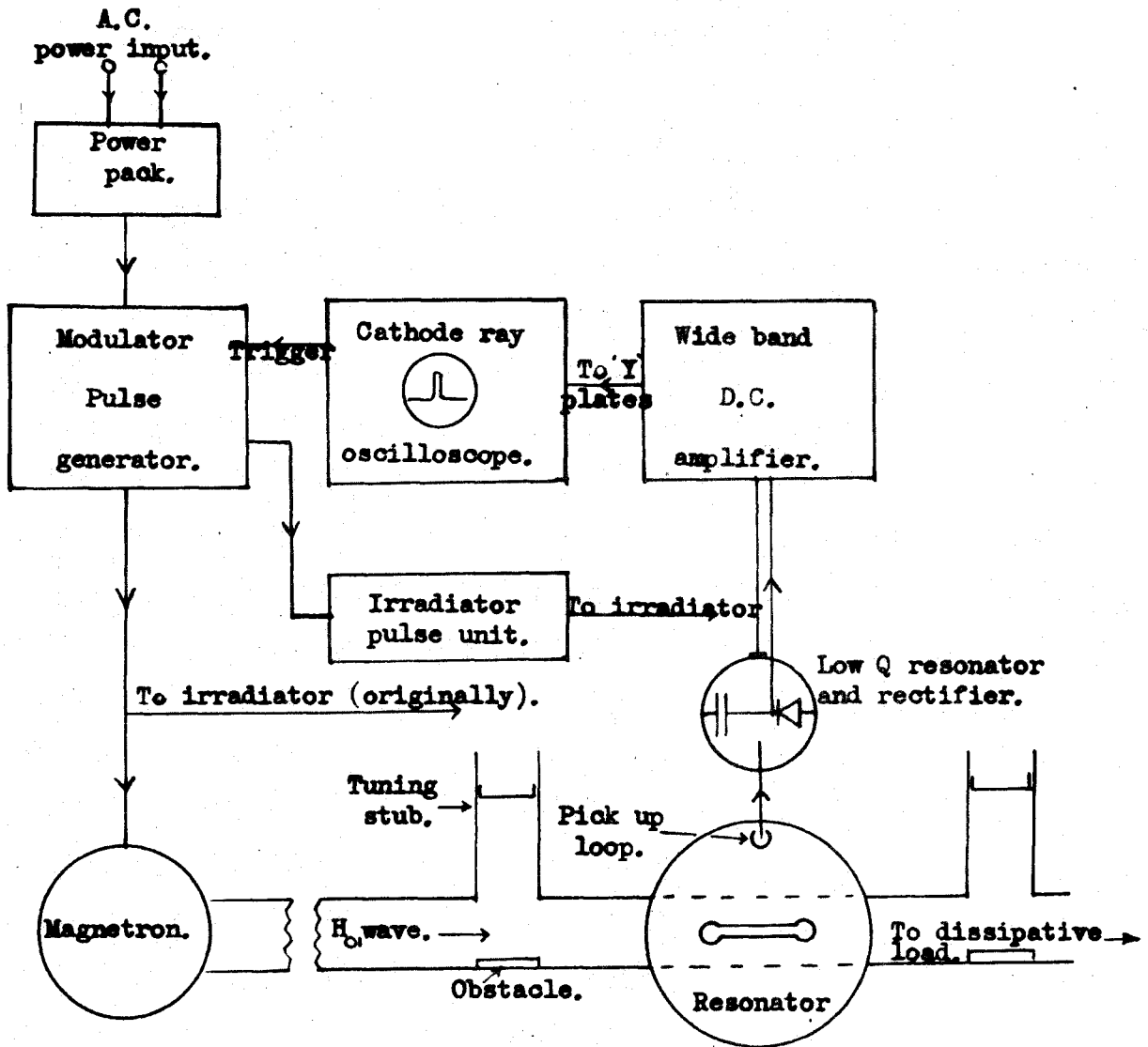
The second condition can be achieved by irradiating the gas within the resonator by means of a small irradiating spark. Earlier experiments by Prowse and Jasinski<sup>65</sup> showed that effective radiation is completely excluded by any film thick enough to withstand the gas

pressure, therefore the irradiating spark must be within the gas system.

The irradiating spark, (as it will now be called), necessary to trigger the discharge had therefore to satisfy the following conditions:-

1. Situated within the gas system.
2. Placed in such a position as to be visually in line with the gas within the resonator.
3. Capable of movement with respect to the resonator whilst still situated within the gas system.

The irradiating system used is shown in figure 11, and depends for its operation upon the capacitive coupling between the metal sleeves outside and inside the glass tube. The inner sleeves were made of iron, therefore the irradiator could be easily moved by a magnet. The term irradiator is used to describe the system.



Block diagram of apparatus, Fig 12.

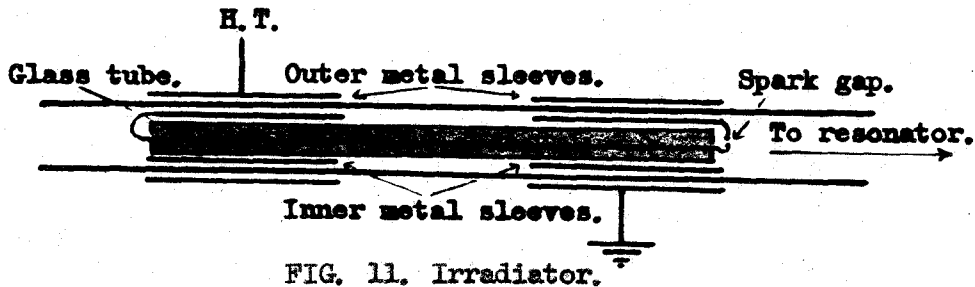
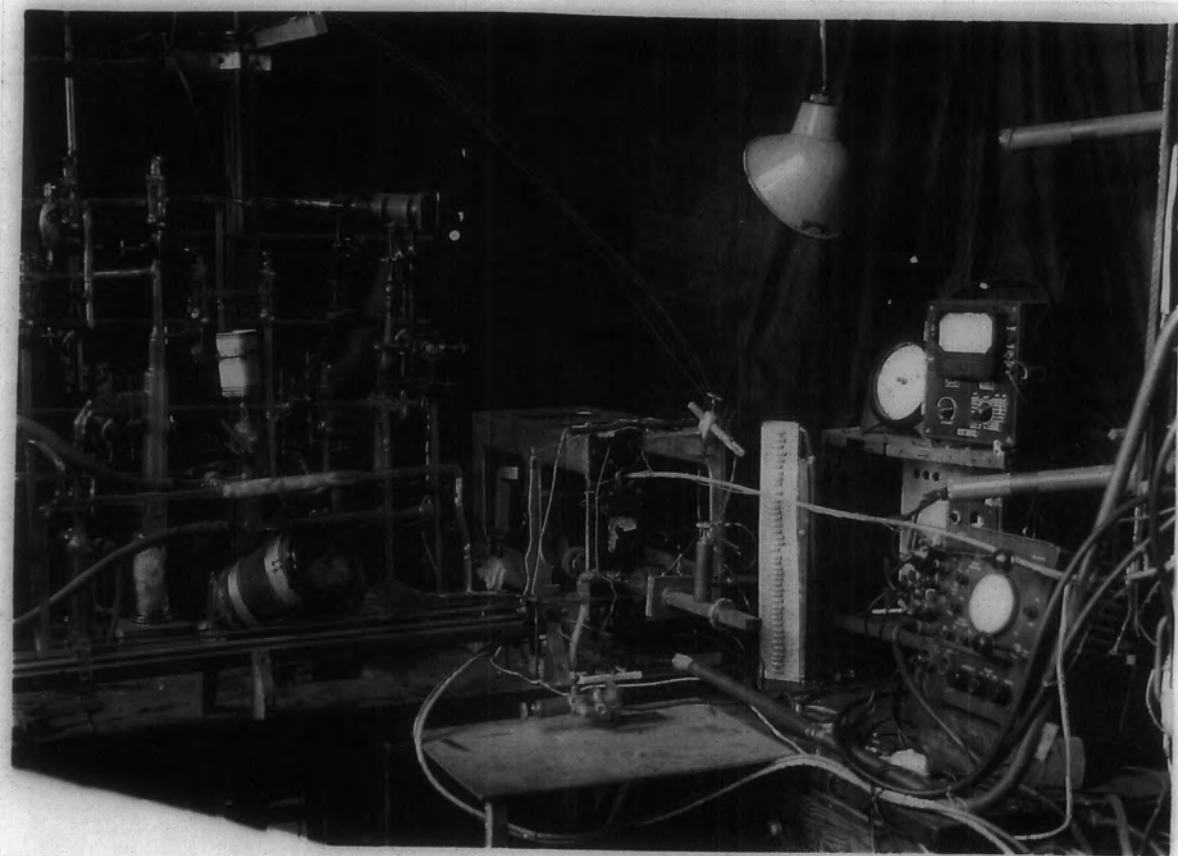


FIG. 11. Irradiator.

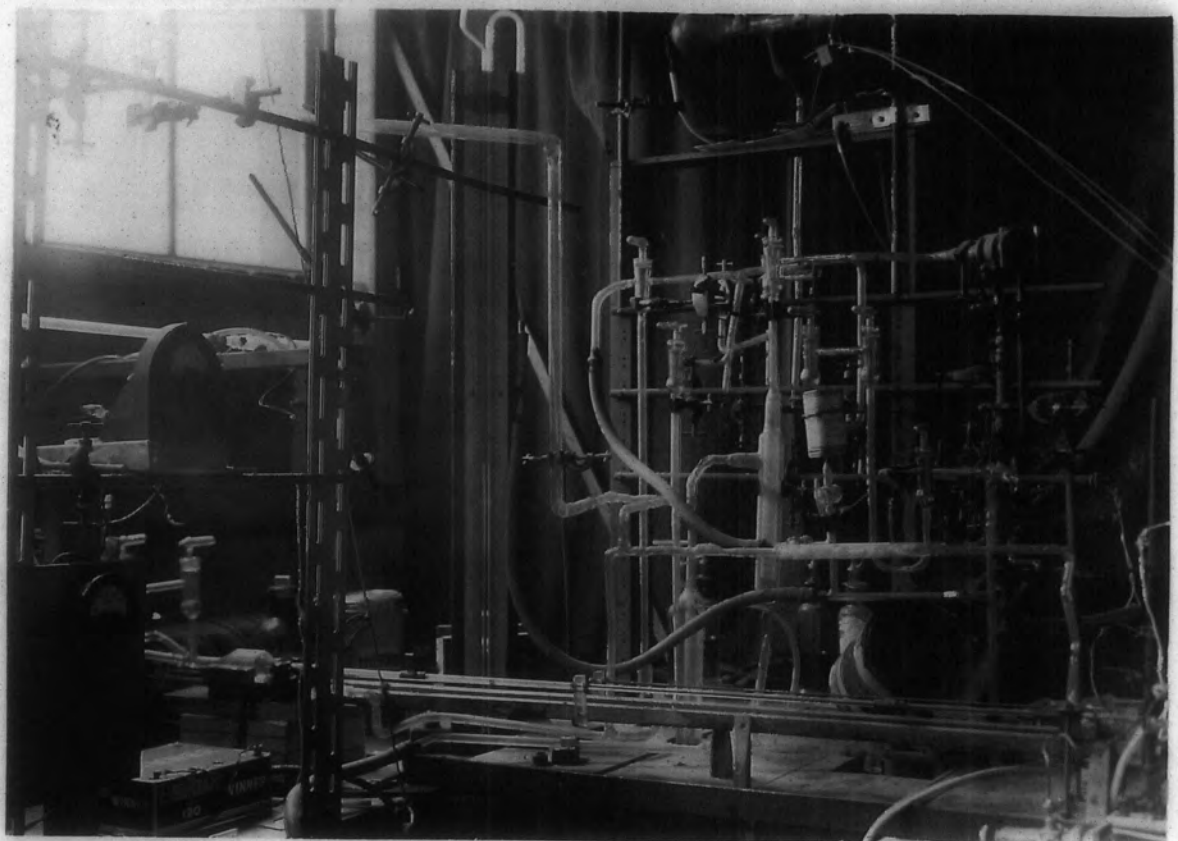
A high voltage pulse, about 4 K.V., was applied to one external sleeve, the second external sleeve being earthed; a spark resulted at the irradiator spark gap. This spark was therefore within the gas, and could irradiate the gas within the resonator. In these initial experiments the high voltage pulse was derived from the modulator unit by a feed run in parallel to the magnetron feed. This was altered in the latter experiments so as not to affect the input to the magnetron. See section 3.3.1.

#### 1.6. Apparatus as a whole.

A block diagram of the whole apparatus



Figs. 13 & 14. General view of apparatus.



is shown in figure 12: figures 13 and 14 show the general lay out of the system. The modulator unit had its own power packs; a 300 volt D.C. power pack, and an 80 volt, high cycle, power pack; (motor generator). The peak power output of the modulator unit was of the order of 160 K.watts at a repetition rate of 1200 p.p.s. feeding to an output impedance of 76 ohms.

The one-microsecond pulses from the modulator unit were transformed from 4 to 11.5 K.V. by a pulse transformer and applied to the magnetron; the latter being capable of a peak output of 7.5 watts, C.W.

Great care had to be exercised in earthing and screening leads to reduce interference between one circuit and another, particularly from the pulse generator to the amplifier and oscilloscope. The amplifier had to be double screened. Matching resistors were placed in the oscilloscope feed from the amplifier to suppress reflected waves: and all leads in the detector circuits were kept as short as possible.

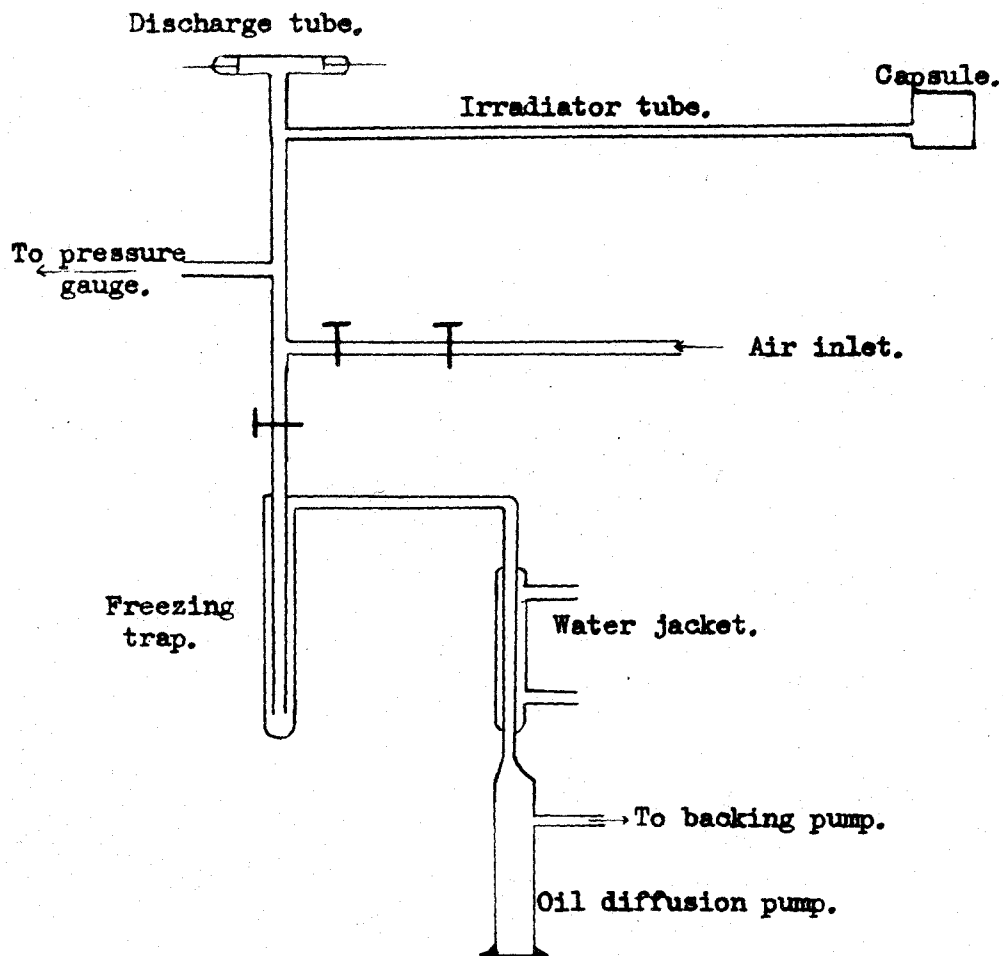


Fig 15 Original vacuum apparatus



## 1.7. Vacuum apparatus.

### 1.7.1. General.

The vacuum apparatus had to satisfy the following conditions:-

1. Suitable for various gases.
2. Provision for pipetting into the system small quantities of gas.
3. No mercury vapour to be present within the system; i.e. eliminating any Penning<sup>80</sup> effect.

The first condition was satisfied, as has been stated in section 1.2. by placing a glass capsule within the resonator, the capsule being constructed to be a snug fit to the walls of the resonator. The presence of the capsule within the resonator lowered the Q of the resonator, so the coupling between the resonator and the waveguide had to be increased if the maximum electric field was to be attained. The outlet of the glass capsule joined the irradiator tube; this coupling was originally a polythene sleeve.

The irradiator tube in turn was connected to the main vacuum plant, a diagram of which is given in figure 15

### 1.7.2. Pressure measurements.

Pressure measurements were initially

made by means of a bellows gauge of the differential type. The action of this gauge was somewhat limited and has since been modified. As a differential type of gauge no mercury vapour was introduced into the gas system during the calibration of the gauge against a mercury monometer. A second gauge, a modified Bourdon gauge, was also used but was found to be too insensitive: later modifications made it a reliable differential gauge. The modified Bourdon gauge was used almost exclusively in all the later experiments.

Further details of the modified pressure gauges and their calibration are given in Appendix 1.

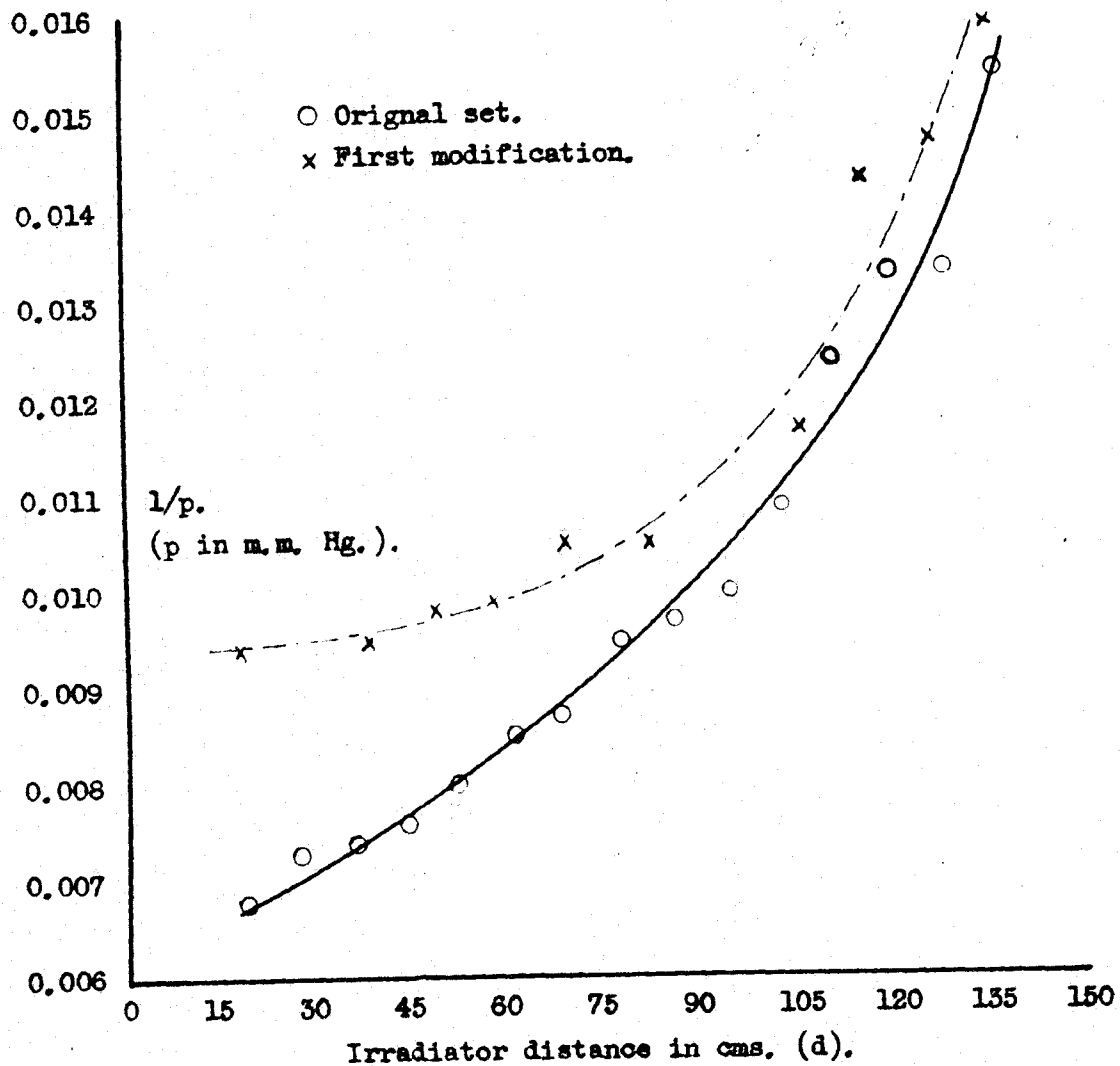
A small discharge tube was used to give a rough indication of the hardness of the vacuum. The tube was fed by either 7 or 15 K.V., D.C. with series resistors to limit the current.

2. Preliminary results using apparatus as taken over from Laverick and Jasinski.

Laverick and Jasinski<sup>79</sup> had made initial experiments on the variation of breakdown stress of gas with the distance between the irradiating spark and the resonator. It was thought advisable to repeat some of these measurements to gain experience and to find how the apparatus could be modified.

The general experimental procedure was as follows. The irradiator was set at one of its fixed positions with

Graph 2 , AIR,  $1/p$  v. Irradiator Position.



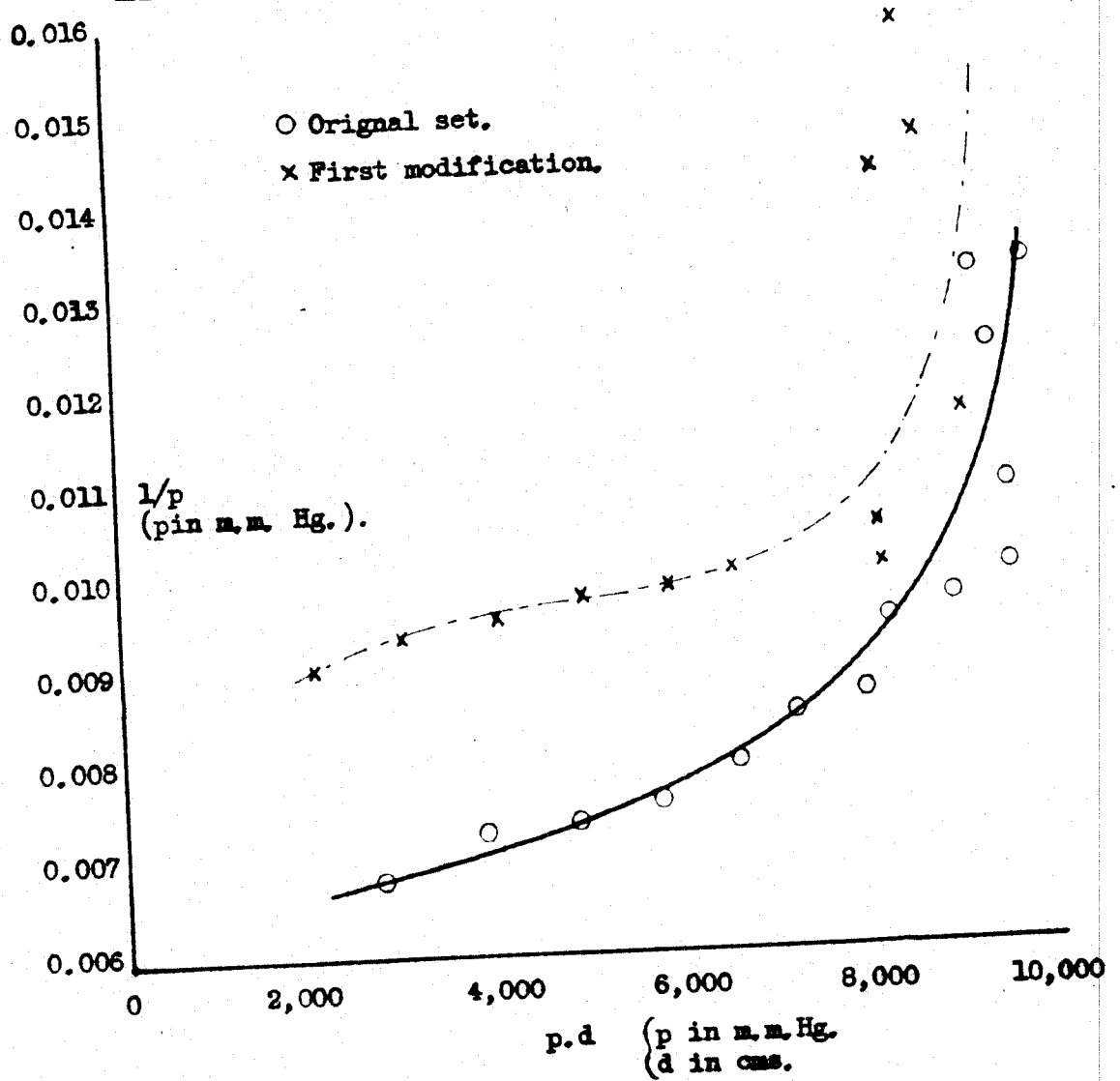
respect to the resonator, that is between 15 and 140 cms. from the resonator. The tuning stubs were then adjusted to give maximum input to the resonator; this was evident by the height of the pulse envelope displayed on the oscilloscope screen. (Figure 10 left hand). Naturally the mode of oscillation of the resonator was carefully checked ensuring the H 011 mode: details of this process have been given in section 1.4.

The pressure was then gradually and continuously reduced until breakdown occurred; this was evident by the collapse or partial collapse of the pulse envelope. (Figure 10 right hand). The pressures ( p ) at which breakdown occurred for various irradiator positions were determined. Typical graphs plotting  $\frac{1}{p}$  against the distance of the irradiator from the resonator (d), and against the product of the pressure in m.m.'s. and the distance in cms. (p.d.), are shown in graphs 2 and 3 respectively.

The value  $\frac{1}{p}$  was plotted because the breakdown stress is approximately proportional to the reciprocal of the pressure. Each point on the graphs represents a mean value of  $\frac{1}{p}$  for at least 10 readings.

The apparatus in its then present state was considered unsuitable for further detailed study of the variation of breakdown stress with irradiator position. The reasons for

Graph 3 , AIR,  $1/p$  v. p.d.



this were -

1. To study gases other than air an all glass vacuum apparatus was necessary, with provision for proper pumping out.

2. During these experiments it was noticed that especially when the distance between the irradiator and the resonator was great, a large statistical lag occurred. This might have given rise to pressure overshooting, i.e., had the pressure remained constant for a considerable time at a value higher than the one recorded for breakdown, the discharge might have occurred at this higher pressure. Further evidence for this possible overshoot was the greater scatter of the results for the greater distances. This is clearly shown in the graphs. It was also impossible to always ensure that the pressure was reduced at the same constant rate.

3. The pressure gauges were not of the required degree of sensitivity.

4. Another difficulty was that, as the pressure varied, so did the absorption of the irradiation from the irradiating spark; these results would be therefore extremely troublesome to unravel.

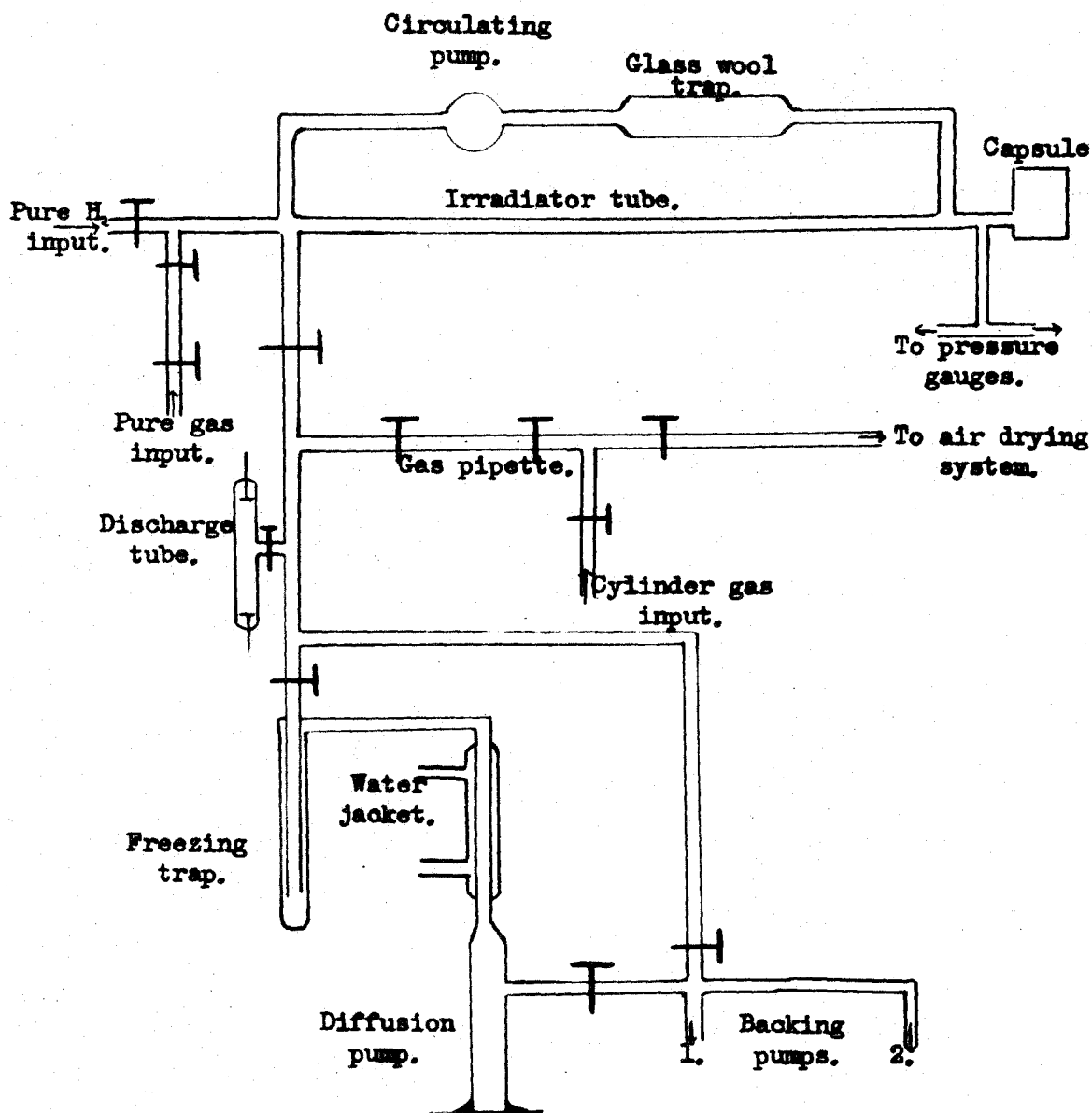


Fig 16. Improved vacuum apparatus. (Final design).

The development of the apparatus can be divided into three stages; each step will be discussed separately, together with the results obtained at that stage. The third, or final stage, includes the results for all the gases used, air, oxygen, hydrogen, nitrogen and neon.

### 3. Development of apparatus and technique.

#### 3.1. First Improvement.

##### 3.1.1. Apparatus.

The vacuum system was remade and extended, all rubber and polythene connections were removed. The resonator was now joined to the irradiator tube by means of a small glass cone joint. A second rotary pump and a high vacuum pump bypass, pure gas inlet with pipette, together with a drying system for air were added. The now modified vacuum system is shown in figure 16.

Both pressure gauges were remade; the bellows gauge now worked reliably over a limited range. The Bourdon gauge was itself encased in a vacuum tight cylinder with a glass end window; it was now possible to calibrate this directly against a mercury manometer without the indirect method employing the bellows gauge. This modified Bourdon gauge functioned very satisfactorily throughout these experiments and has been used continuously for almost all later pressure readings. An optical lever system



was used as a pointer. A more detailed description and the method of calibration of these gauges is given in Appendix 1.

It will be seen that the lead to the pressure gauges is now placed as close to the resonator as possible to avoid any build up of a pressure head in the irradiator tube.

In this state the apparatus could be pumped black even for a Tesla coil discharge and would maintain this condition for several hours; the length of an experimental run.

### 3.1.2. Results.

Further results were obtained with the modified apparatus following a similar experimental technique to that described in the previous section. (Section 2.) Typical results are given for dry air on graphs 2 and 3, the dotted lines. The air was dried by passing it through four wash bottles of  $H_2SO_4$  and then a spray trap. The results show the same general variation of the pressure for breakdown with respect to the distance of the irradiator from the resonator, for a fixed resonator input energy.

Due to the reasons given in paragraph 2 of the previous section, (Section 2), it was felt that the

apparatus should be modified so that the pressure could remain constant, and the input to the resonator from the waveguide varied.

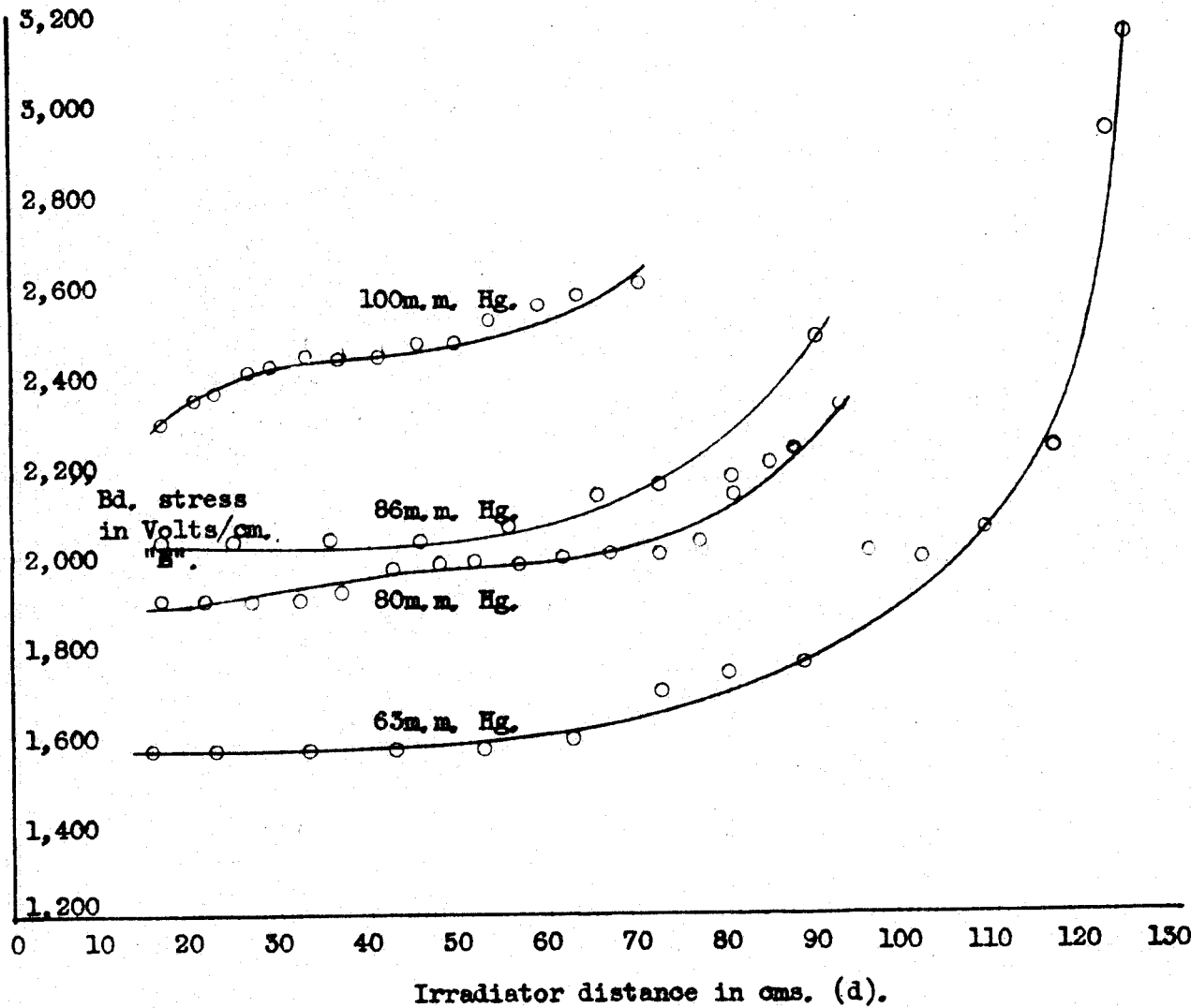
### 3.2. Second Improvement.

#### 3.2.1. Apparatus.

Over a considerable range the height of the pulse envelope as viewed on the oscilloscope is directly proportional to the microwave stress in the resonator. The crystal diode rectifier and amplifier were found to have linear response curves; Appendix 2. By means of a variable backing off voltage applied to the X plates of the oscilloscope, the pulse envelope could be displaced and the voltage necessary to displace it a distance equal to its own height recorded. This voltage was therefore directly proportional to the microwave stress in the resonator.

The experimental procedure now followed was to increase, by small steps, the energy fed to the resonator, allowing some two minutes between adjustments to account for any statistical lag. The height of the pulse envelope at breakdown was recorded in this manner, for a particular irradiator position, for a known fixed pressure. A typical pulse envelope as viewed on the oscilloscope has been shown in figure 10.

Graph 4 . AIR. Breakdown Stress v. Irradiator Position.



### 3.2.2. Results.

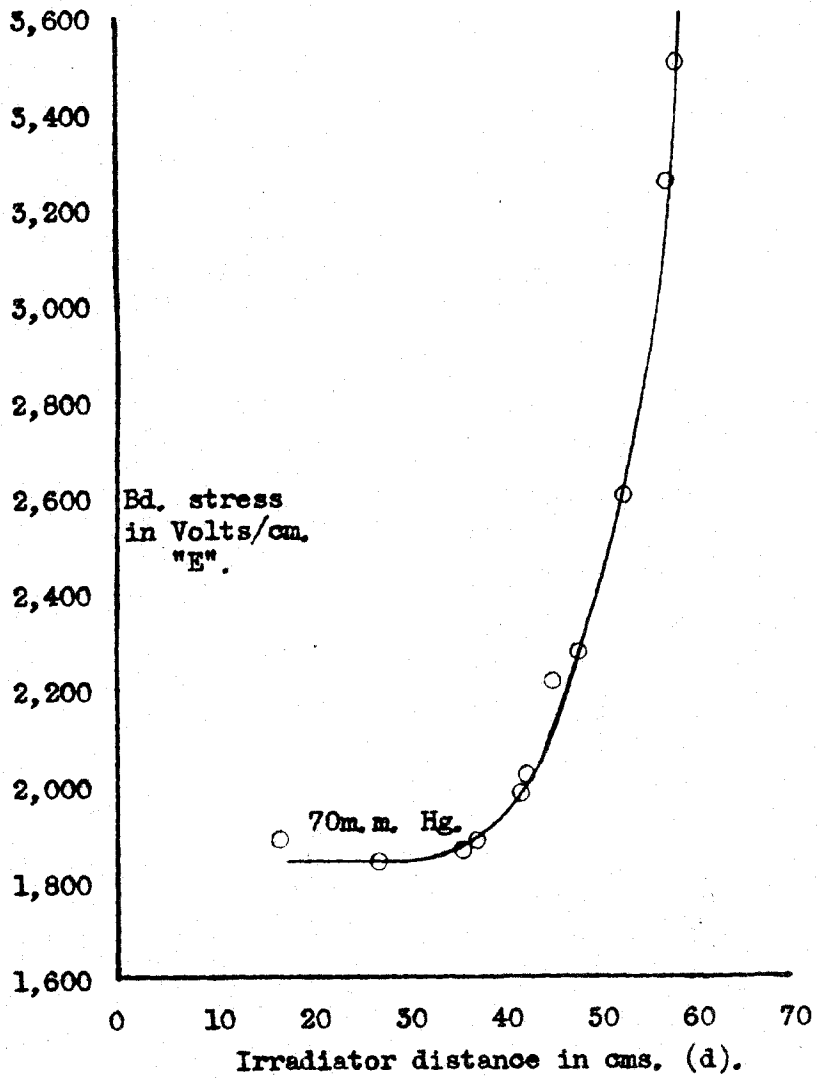
Using this new technique preliminary results for air and oxygen were obtained: graphs 4 and 5 show the relation between breakdown stress, and the distance between the irradiating spark and the resonator. Dried atmospheric air and commercial oxygen were used.

In the graphs the breakdown stress plotted is shown in volts per cm.: a description of the method used in establishing these absolute values is given below. (See Part II, Chapter 8.)

It can be seen that the new results indicate a smaller increase in the breakdown stress for air than the previous results, the upswing of these graphs now occurring at distances greater than 60 to 100 cms., depending on the pressure. This again agrees with the suggestion that in the earlier experiments insufficient time allowance was made, so that the statistical lags were misinterpreted as an increase in breakdown stress.

The interim results of graphs 4 and 5 serve only as a record of the effect of the changes made, and as a guide to further development. A more complete set of results is presented in sections 3.3. and 4 below for the following gases; air, oxygen, nitrogen, hydrogen and neon.

Graph 5 . OXYGEN. Breakdown Stress v. Irradiator Position.



### 3.3. Final development of the apparatus.

#### 3.3.1. Apparatus.

To obtain greater power an American magnetron, (Raytheon 725A or CV 722) of the same frequency 9,375 Mc/s. was substituted, and to reduce the statistical lags the aperture into the glass capsule was increased from an internal diameter of 1.5 m.m. to 3.5 m.m. The filament of gas thus irradiated was increased, i.e., the total flux but not the flux density was increased. Jasinski<sup>65</sup> had shown that in his experiments the size of the aperture did not alter the breakdown stress.

To ensure a steady input voltage to the magnetron the irradiating spark pulse was now derived from an auxiliary trigatron, not from the trigatron feeding the pulse forming circuits. The circuit diagram of this auxiliary circuit is given in figure 17. One further advantage of the double trigatron arrangement is that the auxiliary spark just precedes the magnetron output pulse.

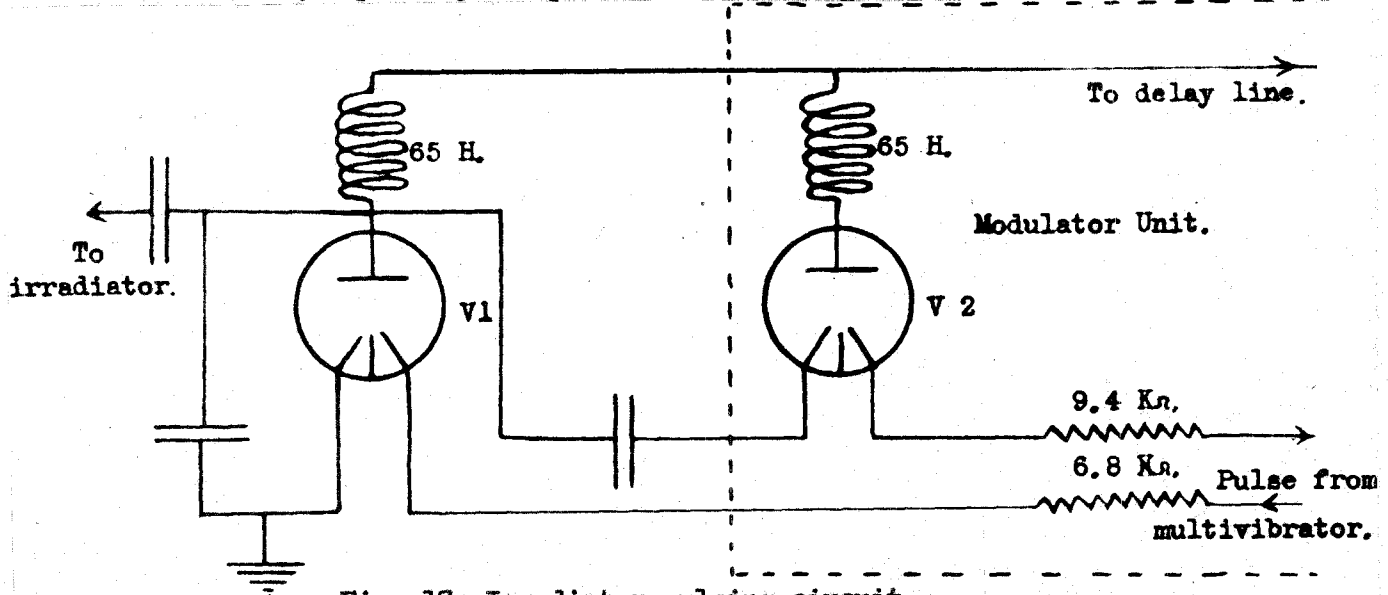


Fig. 17. Irradiator pulsing circuit.

The pulse envelope viewed on the oscilloscope screen had shown a tendency to fluctuate in amplitude; by the use of an entirely separate high cycle generator for the oscilloscope alone, these fluctuations were completely eradicated. A voltage regulator control was also fitted on both inputs, i.e., to the modulator unit and the oscilloscope; thus the applied voltage to either of these units could be maintained constant for a complete run. With these modifications to the modulator and recording circuits, the amplitude of the pulse envelope for one particular resonator input feed would remain constant within the oscilloscope discrimination for many hours, i.e., the length of a run, say up to seven hours.

Finally the input to the low  $Q$  resonator from the pick up loop in the main resonator was changed from an electrostatic input feed to a magnetic input feed, this eliminated all the slight spurious pick up previously noticed on the oscilloscope trace. The degree of projection of the magnetic pick up loop into the main resonator was reduced, thus increasing the  $Q$  of the resonator. This was found to be possible by a redesign of the magnetic loop; if the projection is too great the resonator  $Q$  is quite appreciably reduced.

With these improvements to the electronic side of the apparatus and the previous clean up of the vacuum plant, the apparatus was now considered suitable for making more extensive observations; these are recorded separately for each gas studied.

#### 4. Results with the apparatus as developed.

##### 4.1. Air.

##### 4.1.1. Variation of breakdown stress with irradiator position.

By a careful and prolonged series of experiments where the breakdown stress was measured in the manner described for various positions of the irradiating spark, it soon became evident that the increase in the breakdown stress for air for an irradiator movement of some 110 cms. was only of the order of a few per cent. It was therefore decided to measure the breakdown stress for the two extreme irradiator positions only, i.e., d minimum, and d maximum. Some nine complete sets were taken in all: a typical complete set is given in table 1.

The general procedure was to increase in small stages ( $\approx 1\%$ ) the input feed to the resonator allowing in some cases 10 minutes for statistical lag: it will therefore be appreciated that a set for complete pressure range took many hours, and in many cases could not



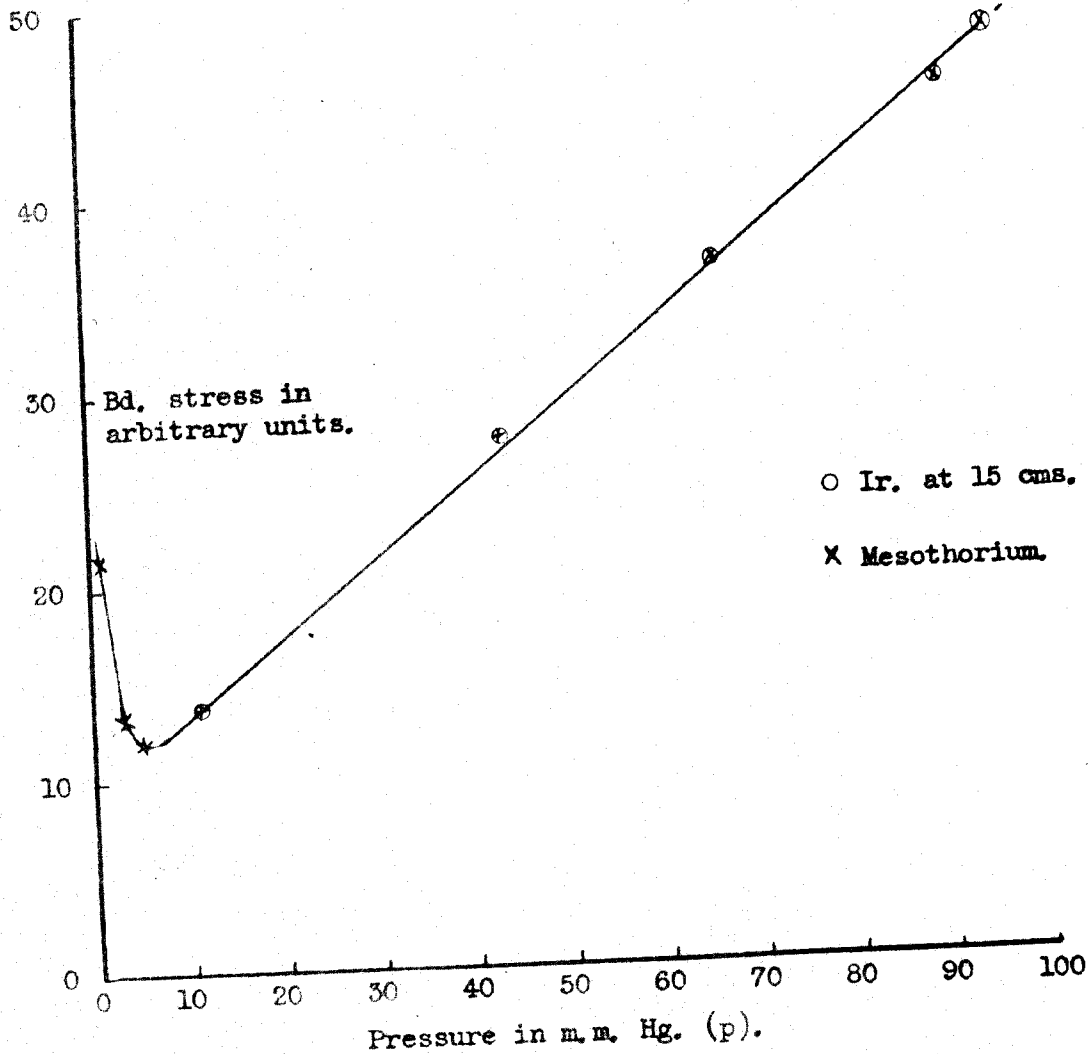
be completed in one day. The percentage increases shown were found to vary slightly for one particular pressure but the maximum percentage increase recorded was never more than 16% and usually of the order of 5 to 7% as shown.

It can thus be said there is an increase in the breakdown stress as the irradiator moves away from the resonator, but this increase is far smaller than determined previously. In the earlier experiments the pressure change took place at a slow but not infinitesimal rate which would give a greater overshoot the greater the statistical lag and therefore changes in statistical lag were misinterpreted as changes in pressure for breakdown.

TABLE 1. Percentage increase of breakdown stress for the two extreme irradiator positions in air.

Pressure in m.m.Hg.(p).	Irradiator position.		% increase in breakdown stress.
	d min. in cms.	d max. in cms.	
5	16	130	0
15	"	"	4.3
25	"	"	7.6
30	"	"	7.9
35	"	"	8.3
41	"	"	16.0
45	"	"	8.2
50	"	"	7.8
55	"	"	7.6
65	"	"	8.2
75	"	"	6.6
84	"	"	3.0
94	"	"	1.0
112	"	"	3.9
142	"	"	3.5

Graph 6 . AIR. Breakdown Stress v. Pressure.



#### 4.1.2. Variation of breakdown stress with pressure for a fixed irradiator position.

The relationship between the breakdown stress and the pressure for a constant position of the irradiating spark, i.e. 15 cms., is shown in graph 6. The breakdown stress is plotted in arbitrary units, the values actually plotted are the voltages applied to the X plates of the oscilloscope to deflect the pulse envelope its own height. These graphs are only intended to show the general shape of the curves, and a separate chapter, (8), in Part II is devoted to the absolute calibration of the curves relating breakdown stress and pressure. The curvature at the high pressures was later shown to be caused by saturation of the amplifier.

These results are really auxiliary to the main experiment, but are given for completeness. Attention is drawn to the upsweep of these p - E graphs for low pressures, (E = breakdown stress in volts/cm.)

#### 4.1.3. Variation of breakdown stress with pressure using a mesothorium source of radiation.

The effect of a second ionising agent was investigated. A relatively weak  $\gamma$  ray source was first tried, but this did not reduce the statistical lag to a reasonable value; then a  $\beta$  ray source  $\text{CO}^{60}$ , which did not

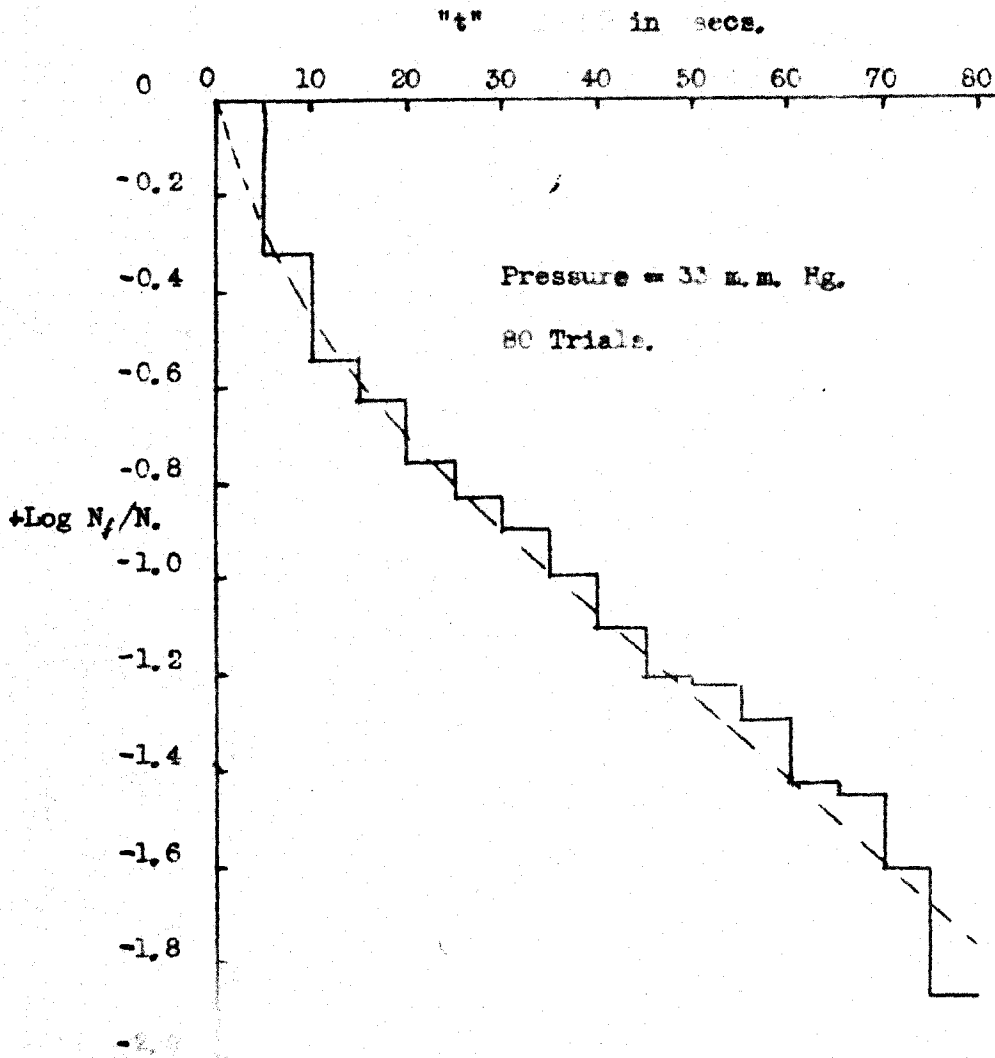
produce breakdown. Finally 0.93 millegammes of mesothorium was used: this initiated breakdown. On graph 6 is also shown the breakdown stress recorded for various pressures using this source of ionisation.

As will be seen, for air the curves coincide, there being no difference between the breakdown stress at a particular pressure, whether the ionising radiation was obtained from the irradiating spark at 15 cms. or from the mesothorium source placed on the outside of the capsule. This held for all pressures, even for the low pressures, i.e. below 10 m.m.Hg., where the curve sweeps upwards. It was found easier to use the radio active source for these low pressures as the irradiator tended to produce a visible discharge between the irradiating spark gap and the resonator. This point was always watched, and the coupling between the inner and outer metal sleeves of the irradiator reduced accordingly to eliminate such a discharge

When using the mesothorium source quite long statistical lags were still encountered: a plot showing the distribution of these statistical lags for eighty successive breakdowns, for a constant pressure and applied voltage, is shown in graph 7.

The statistical lags for the eighty

Graph 7 . AIR. Statistical Lag Variation



successive breakdowns were recorded; these lags varied between 0 to 80 seconds, i.e. 0 to 3,200 trials, (p.r.f. = 400).

Let the total number of trials be "N", and let the number of trials when breakdown occurred within a time "t" be  $n_t$ , then the number of trials when breakdown did not occur within the time t was  $N - n_t = n_f$ . Therefore the probability of breakdown not occurring within the time t was  $\frac{n_f}{N}$ , the logarithm of  $\frac{n_f}{N}$  is plotted against the time interval "t" in graph 7. The values of "t" shown are the values of the observed lags for breakdown, the actual time during which the microwave field was operative was, of course,  $t \cdot 400 \cdot 10^{-6}$  seconds, (p.r.f. = 400, and pulse duration 1 microsecond).

It is interesting to note that in air the breakdown stress recorded using either the mesothorium or the irradiating spark as the source of the ionising radiation was the same, provided the irradiating spark was situated at the minimum distance from the resonator, (15 cms.) The range of wave lengths of the radiation from the irradiating spark is very great, and there are probably quanta present with insufficient energy to directly ionise the gas molecules but with enough energy to raise the molecules to a series of excited states. It would seem probable that the lower

energy quanta would be more easily absorbed by the gas molecules between the irradiator and the resonator, and at large distances could possibly be completely absorbed in the intervening cylinder of gas between resonator and irradiator. This may be a part explanation of the lowering of the breakdown stress which occurs as the irradiator approaches the resonator. The problem is more fully explored in the discussion section, (i.e., chapter 3, Part I.).

On the other hand, it would seem that mesothorium, being a  $\gamma$  ray source would produce by ejection of electrons from the walls of the capsule, and possibly some by direct ionisation, a limited number of free electrons in the gas: it would therefore be expected that the stress necessary for breakdown with this form of irradiation would be greater than that for breakdown using the irradiator at the minimum distance. This is in direct contradiction with the observations. It is possible that the spatial distribution of the electrons is a factor of some importance.

#### 4.1.4. Effect of variation in the angle of incidence of the ionising beam.

It can be assumed that the lowest breakdown stress will occur when the ionisation of the gas

occurs in a filament enclosing the region of maximum circuital electric stress, ( $E_e$ ). To ensure that in these experiments the lowest values of the breakdown stress were recorded for a given pressure, the piece of apparatus shown in figure 18 was devised. This enabled the beam of ionising ultra-violet light to be moved about, within a limited solid angle, thus ensuring that in one position the filament of maximum circuital field was irradiated.

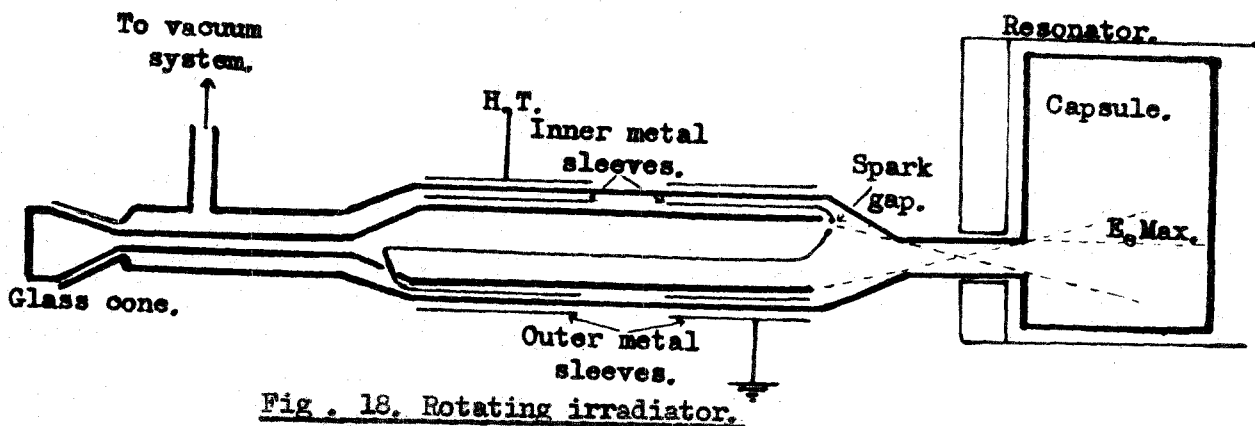


Fig. 18. Rotating irradiator.

Results from this showed that for the pressure range used in these experiments no change in the breakdown stress could be detected with variation in the angle of the irradiation. It is therefore to be concluded that the strong filament of the electric stress



had been irradiated in all the previous experiments.

#### 4.1.5. Recovery of air after breakdown.

During the period of these experiments in air a trial set was undertaken in oxygen, from which it appeared that there was some form of residual ionisation remaining in the gas after breakdown: this then lowered the breakdown stress for subsequent breakdowns at the same pressure.

A gas sample is said to have "recovered" if, after the discharge has been established in the gas, the microwave field is switched off, (the discharge obviously ceases), reapplication of the microwave field does not result in spontaneous breakdown, the discharge not reappearing until the gas is irradiated by either the irradiator or the mesothorium source .

To ensure that no such mechanism was operative in air the following experiments were undertaken.

The capsule was recharged with fresh air and the energy input was increased in stages, allowing several minutes between adjustments until the breakdown stress was established. The gas was then allowed to recover and was heavily overvolted, (i.e., the input to the resonator increased above that necessary for irradiated breakdown), therefore as soon as the irradiating spark was connected, the

gas broke down. Switching off the irradiator and magnetron the air recovered: the voltage was then gradually reduced in stages from this overvolted state, switching on the irradiator each time to see if breakdown would occur; by this means a minimum breakdown stress was established. This value was identical with the value determined by gradually increasing the input to the resonator. The experiment when the input was decreased was undertaken at speed, thus ensuring that, if the previous and immediate history of the gas affected the future breakdown stress, it would surely have been evident. This type of experiment was performed many times for different pressures and irradiator distances, and in no single instance did the previous history of the gas affect subsequent breakdown stress values.

The only real recovery trouble encountered for air was for low pressures up to 10 m.m.Hg. when using the mesothorium as an irradiating source. After breakdown for these low pressures the air would appear to recover: however, leaving the same sample of gas in the capsule with the microwave field on and no irradiation operative, the gas would breakdown after a statistical lag of some 100 seconds. To obtain complete recovery for these pressures, it was found necessary to reduce the microwave

stress below the breakdown stress, and allow the gas to remain under the influence of the reduced field for some time. Then on increasing the electric stress, even above the breakdown stress, no discharge occurred; of course provided the irradiator was not operative. (Naturally by switching off completely for say two minutes or more the gas also recovered).

#### 4.1.6. Effect of pulse repetition rate on breakdown stress.

Alteration of the pulse repetition rate from 400 to 600, 800 and 1000 pulses per second did not alter the breakdown stress for a given pressure. Unfortunately the modulator unit became unstable if the pulse repetition rate was altered too frequently, therefore only two sets for two pressures were obtained, but these showed no variation within experimental error in the breakdown stress for air with pulse repetition rate.

One final note for air: several types of irradiators were used, being constructed of different metals, and no change in the breakdown stress, for a particular pressure, with any type of irradiator was recorded.

#### 4.2. Oxygen.

The first gas tried other than air was Oxygen, and from the early experiments with oxygen it became

evident that the previous and immediate history of the gas affected subsequent breakdown stresses. On switching on the microwave field spontaneous breakdown of the gas occurred, independent of the irradiating spark, if the gas had previously broken down and presumably recovered. Thus there appeared to be some residual effect in the gas that caused this spontaneous breakdown even after a minute (or more), if the gas were now subjected to the microwave field with no irradiating spark operative.

The term spontaneous breakdown is used to describe breakdown not initiated by the radiation from the irradiating spark, or by the  $\gamma$  rays from the radio active source. Naturally it was necessary to investigate fully this troublesome effect before proceeding with the main experiments.

#### 4.2.1. Recovery of Oxygen after breakdown.

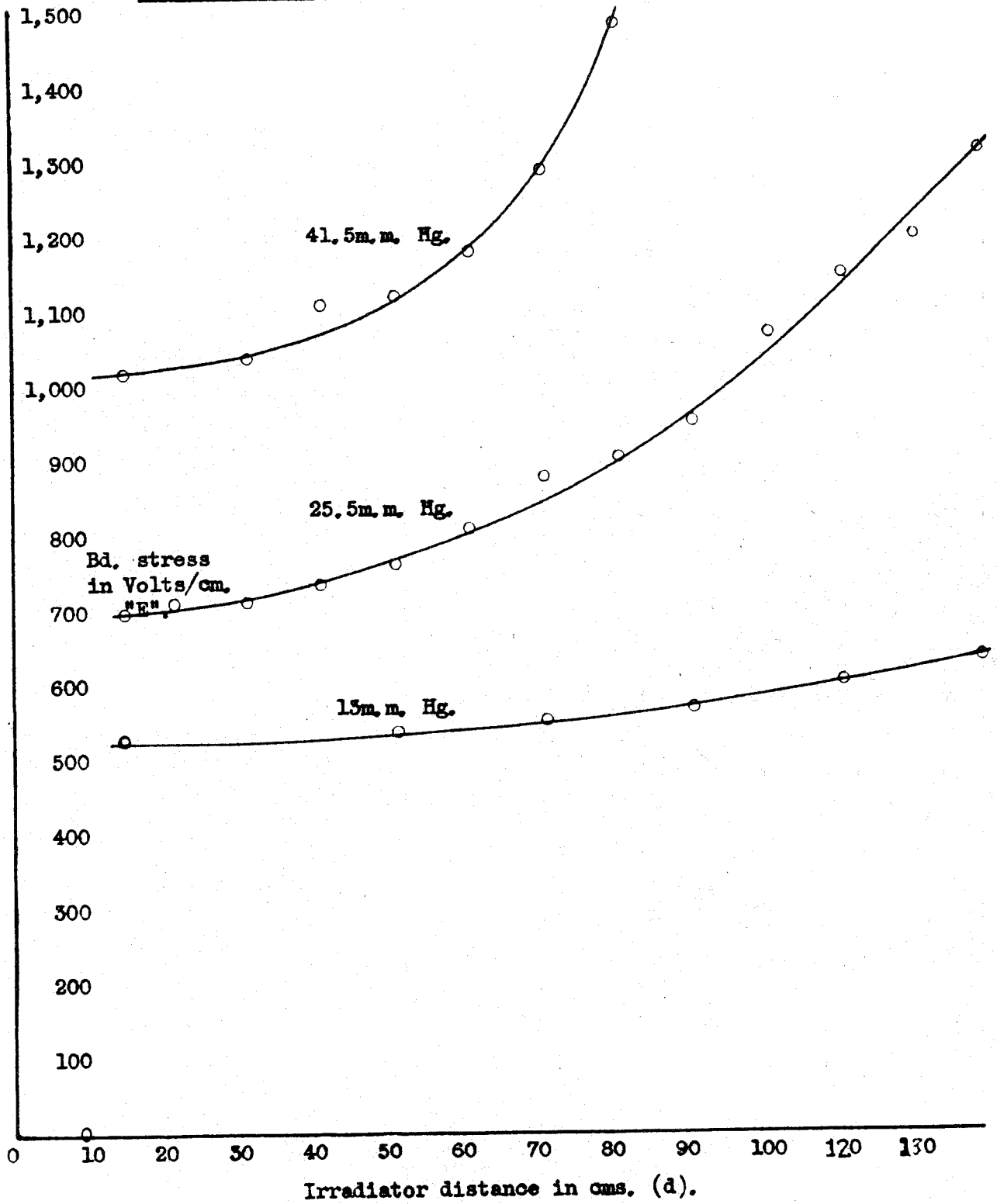
The application of a unidirectional clearing voltage along the axis of the capsule, when the microwave field was off, did not remove the cause, even for a 60 seconds application of the steady field.

It seemed probable that atomic oxygen and ozone formed during the discharge might still be present in the gas within the capsule, and thus produce this spontaneous breakdown. In order to test the

possibility that chemical products of the discharge (e.g. O, O<sub>3</sub>) might still be of importance, the capsule was pumped out and refilled, passing the incoming gas through a Tesla discharge maintained in the filling tube. However, with no irradiation no spontaneous breakdown could be recorded however long the microwave stress was applied to this sample of gas. This was true for the complete pressure range. The gas could be heavily overvolted and no spontaneous breakdown occurred; naturally the irradiator was switched off for these tests. Once any particular sample of gas had broken down, being triggered by the irradiator, the same spontaneous breakdown effects reappeared. It therefore seemed that the effect was not caused by the presence in the gas of atomic oxygen or ozone.

It was thought that circulation of the gas through a glass wool trap would filter the gas and possibly aid the recombination processes: the circulating system is shown in figure 16. A small circulating pump drove the gas round this closed system and it was hoped that the gas would be dragged from the capsule by the gas movement across the capsule inlet. The gas in this circular path was caused to flow through a glass wool trap.

Graph 8 . OXYGEN. Breakdown Stress v. Irradiator Position.



The switching on of the pump after a discharge did help recovery but it was not as successful as had been hoped. Details of the circulating pump are given in Appendix 3.

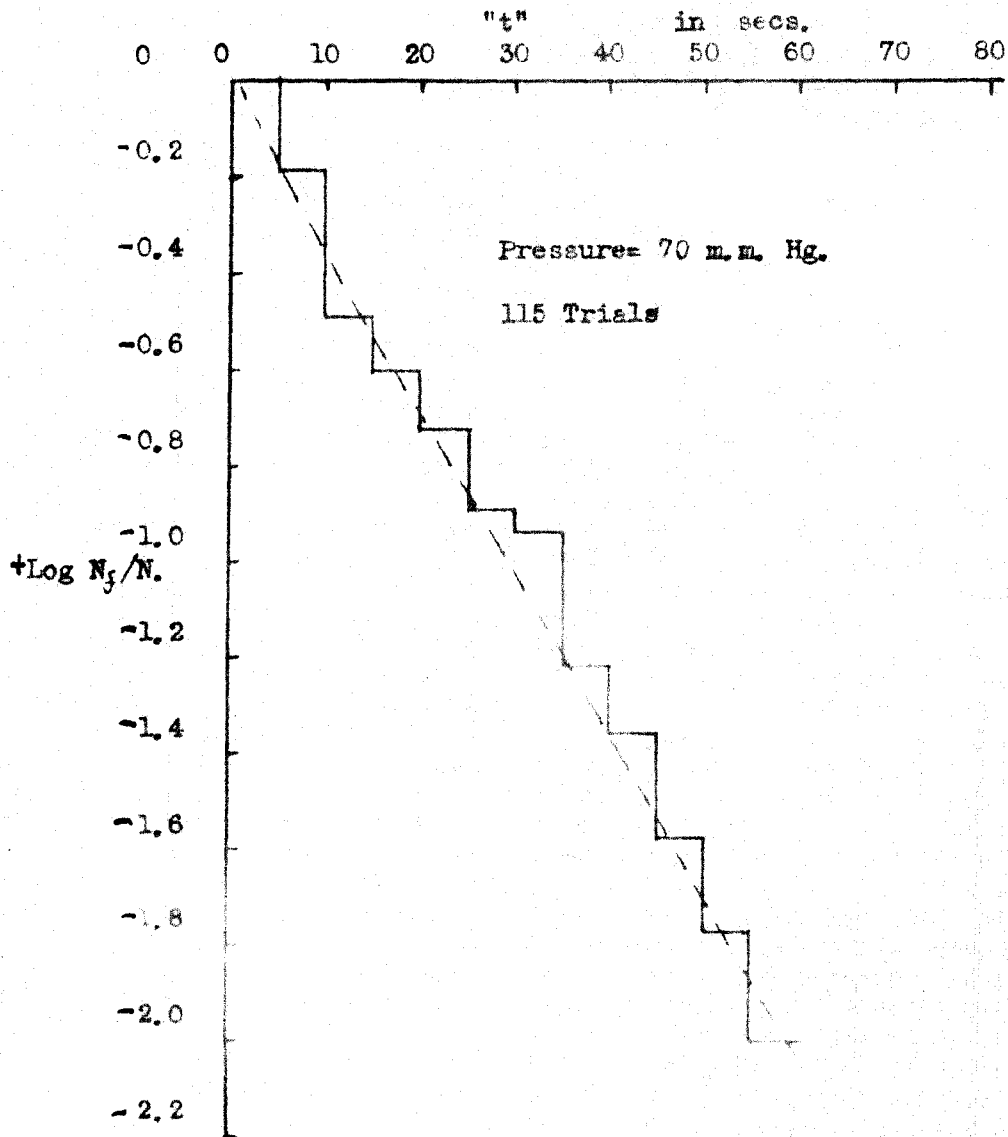
Eventually it was therefore decided to pump out the gas and refill with fresh oxygen for each measurement. Even so, large overvoltages (that is, large overvoltages as compared to the breakdown stress required when the irradiator was at  $d$  minimum), did occasionally give spontaneous breakdown of the gas. This can probably be attributed to natural ionisation, e.g. cosmic rays.

To ensure that the pressure on refilling was identical to the pressure before exhaustion the sensitivity of the pressure gauge was increased by tripling the optical lever, hence tripling the sensitivity. It was then estimated that the pressure could be reset to well within  $\pm 0.5$  m.m.Hg.

#### 4.2.2. Variation of breakdown stress with irradiator position.

The variation of the breakdown stress with the distance of the irradiating spark from the resonator can be seen in graph 8, for pressures between 13 and 41.5 m.m.Hg. In all cases the gas was changed between readings, so that the previous history of the gas

Graph 9, OXYGEN, Statistical Lag Variation,





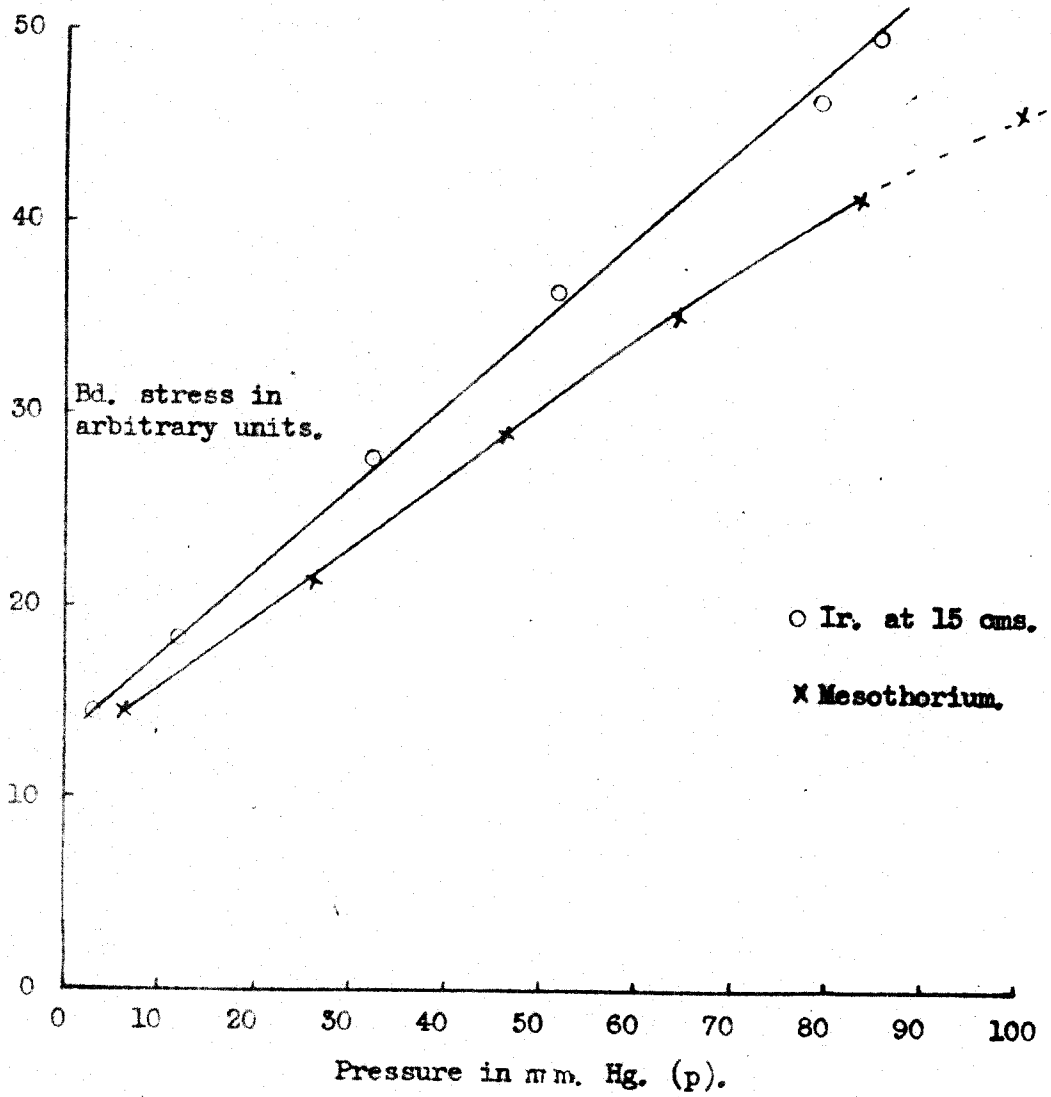
did not affect the breakdown stress. The statistical lags for oxygen were large especially for the greater values of "d", up to 120 seconds. The same experimental technique was used as for air; that is, gradually increasing the resonator input, (approximately 1% steps), allowing 3 to 5 minutes between adjustments. A plot of the statistical lag variation for oxygen is shown in graph 9, for some 115 readings for a fixed pressure and applied voltage. The nomenclature is identical to that used in the statistical lag curve for air. (Section 4.1.3).

These results were consistent and reproducible, and they show substantially the same increase as the earlier results in the breakdown stress with position of the irradiating spark. Thus, unlike air, the refined apparatus made no major difference to the results.

#### 4.2.3. Variation of breakdown stress with pressure for a fixed irradiator position.

Graph 10 shows the variation of breakdown stress with pressure for a fixed irradiator position of 15 cms. As before, the breakdown stress is plotted in arbitrary units, and the graph is just intended to indicate the general variation of stress with pressure. The complete voltage-pressure variation for all gases is more fully covered in the chapter on the absolute calibration

Graph 10, OXYGEN, Breakdown Stress v. Pressure.



of the microwave breakdown stress. (Chapter 8, Part II).

Again the gas was changed for each reading, and due allowance was made for statistical lag which is at its minimum for the near position of the irradiator. The curve over at the top of the graphs was later shown to be caused by amplifier saturation.

#### 4.2.4. Variation of breakdown stress with pressure using a mesothorium source of irradiation.

This relationship between breakdown stress and pressure for oxygen is also given in graph 10. The same surprising result emerges, that the mesothorium source of irradiation produces breakdown at a stress not equal to that found for the irradiator at  $d$  minimum but at an even lower stress.

The two sets were obtained concurrently and the gas was changed for each individual reading for each method of irradiation. Using the mesothorium source breakdown could be obtained at higher pressures than those obtainable using the irradiating spark at  $d$  minimum.

#### 4.2.5. Variation in the position of the mesothorium source.

There seemed to be a possibility that the direction of the  $\gamma$  ray irradiation might affect the breakdown stress. The breakdown stresses for a series of positions of the mesothorium capsule were determined, and

the same value of the stress was found whether the mesothorium was placed above or at the ends of the resonator. Therefore the idea that the mesothorium produced electron trails radiating from the source is considered spurious, and it is assumed that the trails would chiefly be produced by secondaries.

#### 4.2.6. Effect of variation in the angle of incidence of the ionising beam.

No variation in the breakdown stress could be detected when the angle of incidence of the ionising beam was varied; the apparatus was so designed that in one position the filament of maximum circuital stress was irradiated. It was therefore concluded that in all experiments in oxygen the filament of maximum circuital stress had been irradiated; this conclusion was also reached for the air experiments.

#### 4.3. Nitrogen.

Nitrogen was not used in these experiments until the apparatus had reached stage 3, or the last stage in its development. The results for this gas can be conveniently divided into five sections.

##### 4.3.1. Recovery of Nitrogen after breakdown.

As with oxygen it became immediately obvious from initial experiments that previous breakdown of

a particular sample of gas in the capsule did affect the future breakdown stress of the gas. The first problem therefore was to find when it could be assumed that the immediate history of the gas was not influencing the breakdown stress. The following results give a brief summary of these experiments.

Preliminary experiments seemed to indicate that for complete recovery the magnetron had to be switched off for a considerable time after each breakdown; of the order of a minute. Also provided the duration of the discharge was short, 1 to 2 seconds, recovery was more easily effected than for a discharge lasting, say 10 to 20 seconds. These results led to the more conclusive set of experiments explained below.

1. The apparatus was filled with nitrogen and the gas heavily overvolted, for the pressure used, the tuning stubs were then locked and the pressure carefully recorded. The capsule was then evacuated and refilled with fresh nitrogen. By applying the microwave field and the irradiator, breakdown immediately occurred; this was allowed to continue for 4 to 5 seconds. All was switched off, and after 5 seconds the microwave field reapplied (no irradiator operative however), the gas broke down spontaneously. Once again the capsule was evacuated and refilled with fresh gas, and the whole procedure repeated, switching off for 10 seconds

this time, and so on. The table below summarises the results: it would appear that provided the initial breakdown only has a duration of a few seconds (up to 5), and some 55 to 60 seconds are allowed for gas recovery, any subsequent breakdown will only occur when the gas is irradiated.

TABLE 2. Recovery times for nitrogen after a discharge of duration 4 to 5 seconds.

Time apparatus is switched off in secs.	Comments.
5	No recovery.
10	"
15	"
20	"
25	"
30	"
35	"
40	"
45	"
50	Almost recovery.
55	Complete "
60	" "
65	" "
70	" "

2. It was now decided to evacuate and refill the capsule with fresh nitrogen during the switch off times recorded in the last experiment. If the residual effect could be removed by this process the cause of the spontaneous breakdown could not be attributed to the presence of the

walls of the capsule. The actual duration of a discharge was increased to 10 seconds to assimilate the worst possible conditions. The table below shows the results: it was impossible to evacuate and refill the capsule in a shorter time than 10 seconds.

TABLE 3. Recovery times for Nitrogen, refilling between trials.

Time of switch off of microwave field; apparatus refilled with fresh N <sub>2</sub> in this period. In seconds.	Comments.
30 20 15 13 12 10	Complete recovery on refilling, though no recovery before refilled for the same times of switch off.

The residual effect was completely removed by pumping out the affected gas and refilling; it would therefore seem that the spontaneous breakdown effect could not be attributed to the presence of the walls of the capsule. It should be mentioned that this conclusion is not completely certain as any contamination of the walls might itself disappear at low gas pressures.

3. Finally, the duration of the initial breakdown was varied, together with the times of switch off. In this

set of observations the gas was changed for each test and the applied microwave stress was the minimum stress necessary to give breakdown, with the irradiator at d minimum. In paragraph 1 the microwave stress applied was far higher than the minimum breakdown stress for the given pressure; the switch off times for recovery in the latter case are seen to be greater.

TABLE 4. Recovery times for Nitrogen varying the duration of the initial breakdown.

Duration of initial breakdown in seconds.	Duration of switch off of microwave field in seconds. Comments.
1 to 2.	$\left\{ \begin{array}{l} 1 \text{ to } 2 \text{ No recovery.} \\ 3 \text{ Recovery.} \\ 5 \text{ "} \\ 10 \text{ "} \end{array} \right.$
3.	$\left\{ \begin{array}{l} 2 \text{ No recovery.} \\ 3 \text{ Recovery.} \\ 5 \text{ "} \end{array} \right.$
4.	$\left\{ \begin{array}{l} 2 \text{ No recovery.} \\ 3 \text{ Recovery.} \\ 5 \text{ "} \end{array} \right.$
5.	$\left\{ \begin{array}{l} 3 \text{ No recovery.} \\ 5 \text{ Recovery.} \end{array} \right.$
10.	$\left\{ \begin{array}{l} 5 \text{ No recovery.} \\ 7 \text{ No recovery.} \\ 10 \text{ Recovery.} \end{array} \right.$
15.	$\left\{ \begin{array}{l} 20 \text{ No recovery.} \\ 25 \text{ Recovery.} \end{array} \right.$



20 .	{15 {20 {25 {30	No recovery. No recovery. Almost " Recovery.
25.	{20 {25 {30	No recovery. No recovery. Recovery.
30.	{20 {25 {30	No recovery. No recovery. Recovery.
40.	{30 {35 {40 {60	No recovery. No recovery. Recovery. Recovery.

As a final test the apparatus was again filled with fresh nitrogen and allowed to stand, with no irradiating spark operative, for 5 minutes or more, and the microwave field failed to produce breakdown.

It can be seen from these observations that provided the initial breakdown has a duration of the order of 1 to 2 seconds only the switch off time of the microwave field for complete and absolute recovery of the gas is very short, (i.e. switch off time of the order of 5 seconds).

It so happened that further investigations revealed that the variation of the breakdown stress of nitrogen with irradiator position was slight, (similar to the results for air); therefore only two positions of the irradiator were used, d minimum and d maximum. The same gas specimen was therefore used for the two positions, provided the

precautions outlined above were taken. As an added precaution the gas was changed for each pressure used, though this would seem unnecessary.

#### 4.3.2. Variation of breakdown stress with irradiator position.

These results are very similar to those in air: only a small percentage increase in the breakdown stress for the two extreme positions of the irradiating spark. The two positions of the irradiator used were 15 and 130 cms. from the resonator, and a pressure range from 15 to 170 m.m.Hg.

The usual procedure was adopted; that is, gradually increasing the microwave stress in small steps, (i.e. order of 1%), whilst allowing several minutes at each adjustment for any statistical lag in the breakdown. In all experiments of this type some limit must be imposed on the time allowed at each adjustment as a complete run even with such a limit takes some 9 hours or more. The gas was changed as discussed in the previous section.

A sample set of the results is given in Table 5 below, each reading being the mean of three trials at that particular pressure.

Graph 11, NITROGEN, Breakdown Stress v. Pressure.

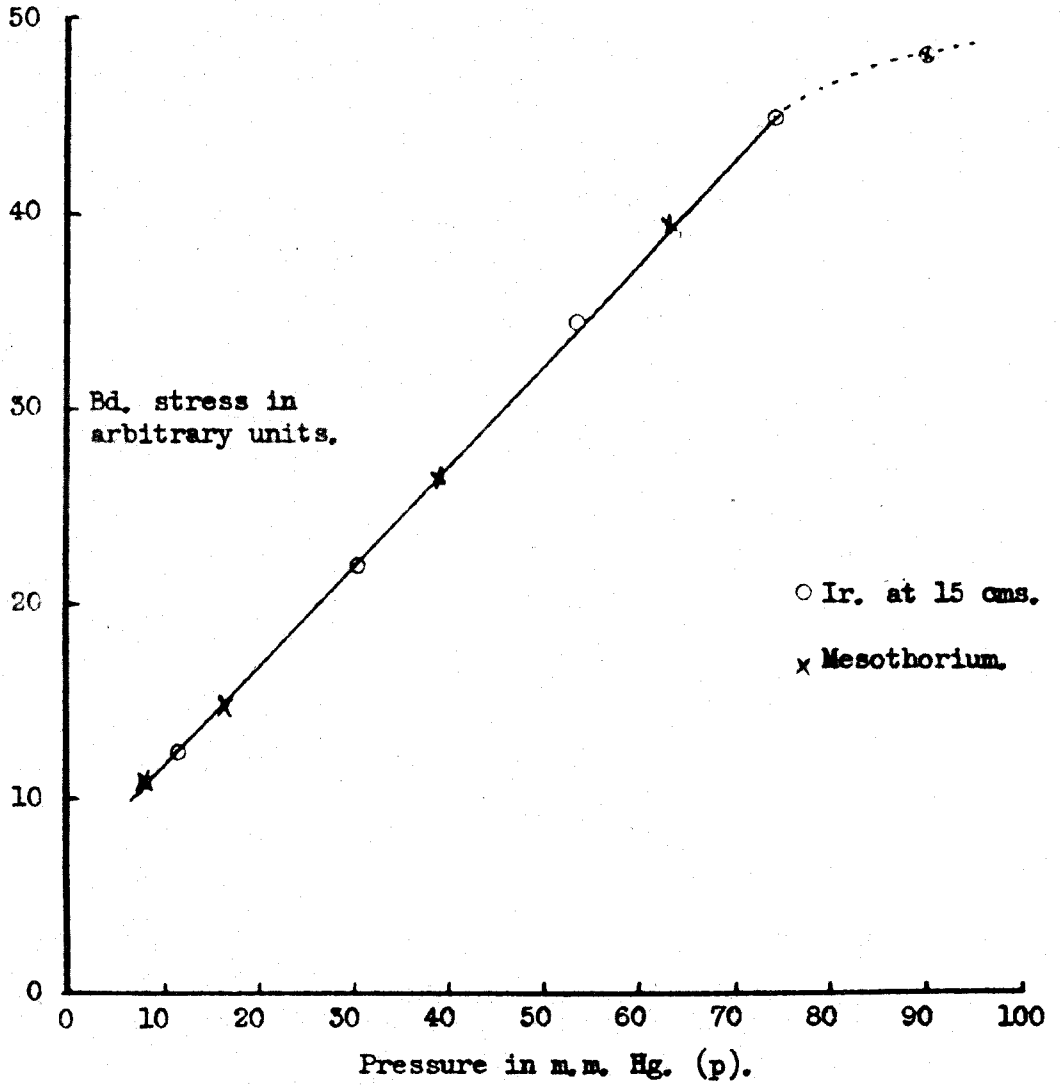


TABLE 5. Percentage increase of breakdown stress for the two extreme irradiator positions in Nitrogen.

Pressure in m.m.Hg. (p)	Irradiator position.		% Increase in breakdown stress.
	d min. in cms.	d max. in cms.	
15	15	130	6
35	"	"	2.2
56	"	"	2.4
79	"	"	0.7
96	"	"	4.0
116	"	"	1.9
140	"	"	4.5
154	"	"	5.5
174	"	"	4.0

The greatest increase observed was of the order 7%. The apparent casual variation of the percentage increase was found to be not repeatable; it can be definitely stated, however, that there always was a slight increase up to 7% maximum between the two irradiator positions. The experimental error was estimated at 1%. Little significance can therefore be attached to the absolute value of the percentage increases quoted. This remark, however, is not true for air where the results showed far more consistency.

4.3.3. Variation of breakdown stress with pressure for a fixed irradiator position.

Graph II gives the general shape of the breakdown stress variation (plotted in arbitrary units)

with pressure for a fixed position of the irradiating spark, the near position, 15 cms: the same remarks as those for air and oxygen apply to these results.

4.3.4. Variation of breakdown stress with pressure using a mesothorium source of irradiation.

As for air, the employment of mesothorium as an ionising source gave substantially the same results as those for the irradiating spark at a distance of 15 cms. from the resonator. The breakdown stresses recorded under the influence of the  $\gamma$  ray source are also plotted on graph II.

4.3.5. Effect of variation in the angle of the ionising beam.

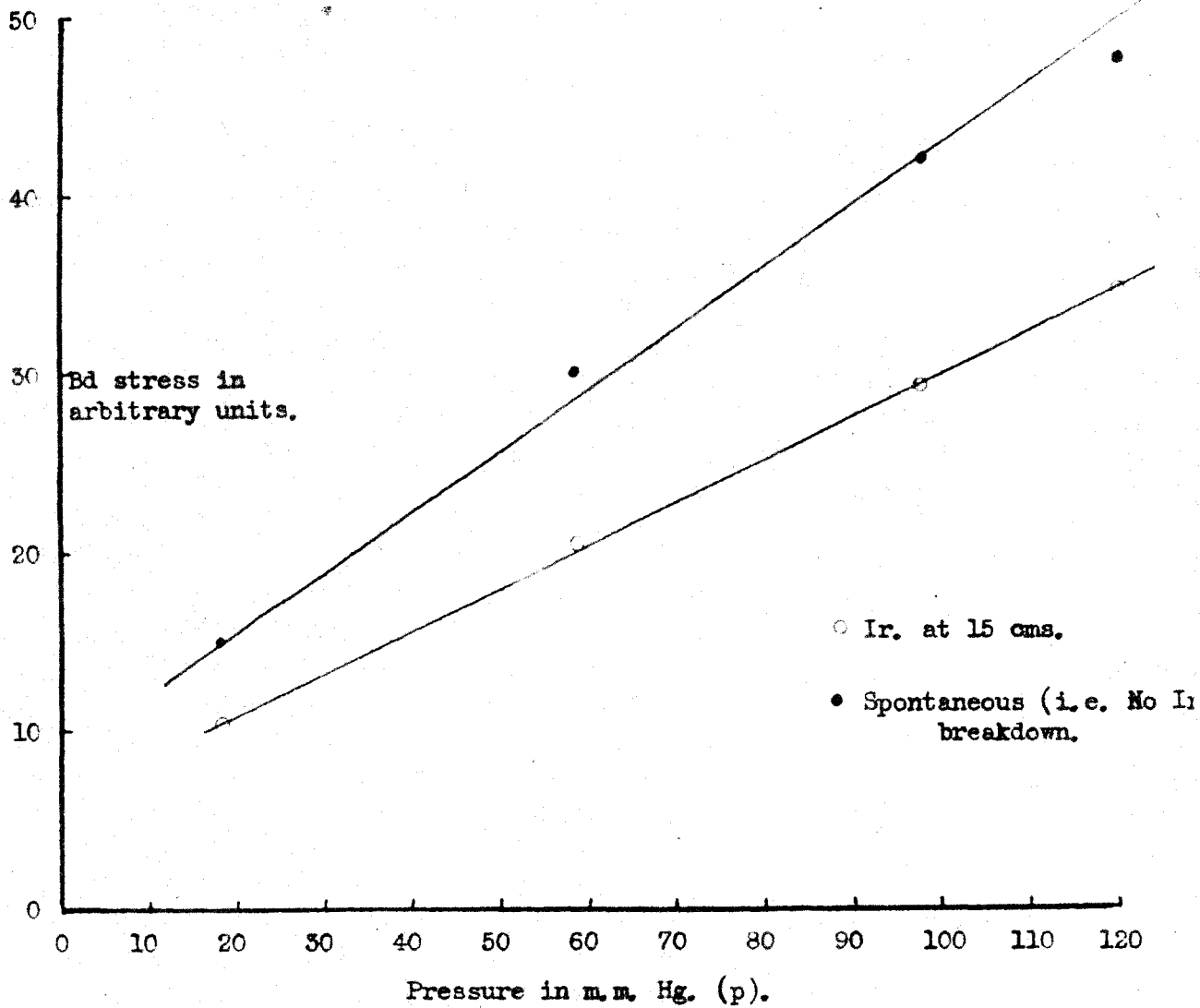
Once again no variation of breakdown stress with the direction of the ultra-violet beam was discernible, agreeing with the findings for air and oxygen.

4.4. Hydrogen.

Experiments in hydrogen were not undertaken until the development of the apparatus had reached its last stage. For the initial experiments commercial hydrogen was used, and later pure hydrogen. No difference in any of the results could be observed with the pure hydrogen. The pure hydrogen was produced by the electrolysis of barium hydroxide<sup>38</sup>. See appendix 4.

4.4.1. Recovery of hydrogen after breakdown.

Graph 12. HYDROGEN, Breakdown Stress v. Pressure.



This problem took a slightly different form in the case of hydrogen, and the spontaneous breakdown of the gas when overvolted seemed the principal difficulty. The phrase spontaneous breakdown is used to mean the breakdown of the gas without any applied irradiation, (i.e. no mesothorium irradiation or the irradiator switch off). This spontaneous breakdown of the gas usually occurred when the microwave field was re-applied to a specimen of the gas that had presumably recovered from a previous discharge.

That is, if the breakdown stress was set for the irradiator at 15 cms., say, and it was then desired to measure the stress for  $d = 130$  cms., the applied microwave stress had to be increased but this increase might cause breakdown with no irradiation depending on the immediate history of the gas. The possible increase in the breakdown stress with distance was masked by this spontaneous breakdown. Changing the gas for each individual reading completely overcame this difficulty, and incidentally showed that the increase in the breakdown stress with distance was small, a few per cent.

Determination of the variation of the breakdown stress with pressure with the irradiator at 15 cms. gave the graph shown (graph 12): the gas was

changed for each reading. Spontaneous breakdown of hydrogen could also be obtained for the lower pressures; with a fresh filling of gas, the stresses observed for such discharges are also shown on graph 12; the gas was again changed for each individual observation. The increase in the stress between irradiated and non-irradiated breakdown could not be attributed to insufficient time allowance for statistical lags. These lags were subsequently shown to be small for hydrogen, and several minutes, (up to 10 minutes) was allowed between adjustments in these experiments.

From these results it was felt that provided the breakdown stress for a particular pressure was approached carefully by gradually increasing the energy input to the resonator, and allowing for any statistical lag, the microwave breakdown stress recorded was for breakdown initiated by the irradiator, and not by any spurious effects. As has been subsequently shown this is justifiable for both irradiator positions as the percentage change between the two curves in graph 12 is far greater, (factor of 2), than the percentage change in the breakdown stress between the two extreme irradiator positions. However, to further validity of the results it



was decided to refill with fresh gas for each observation. Use of the circulating system for the gas helped recovery, but it was probably more expeditious to refill each time with fresh hydrogen.

Variation of  
4.4.2. Breakdown stress with irradiator position.

The resonator input for each trial was increased in small stages, (e.g. 1%), allowing the usual time for statistical lag at each stage. The lags observed were small for the minimum distances, and somewhat longer for the position of the irradiator far removed from the resonator.

The percentage increase of the breakdown stress between the two positions,  $d$  minimum and  $d$  maximum was again small, a maximum of 8%: a table of specimen results is given. The gas was changed for each reading and comparative breakdown stresses for three cases are noted:

1. Irradiator at 15 cms. ( $d$  min).
2. Irradiator at 130 cms. ( $d$  max).
3. Spontaneous breakdown.

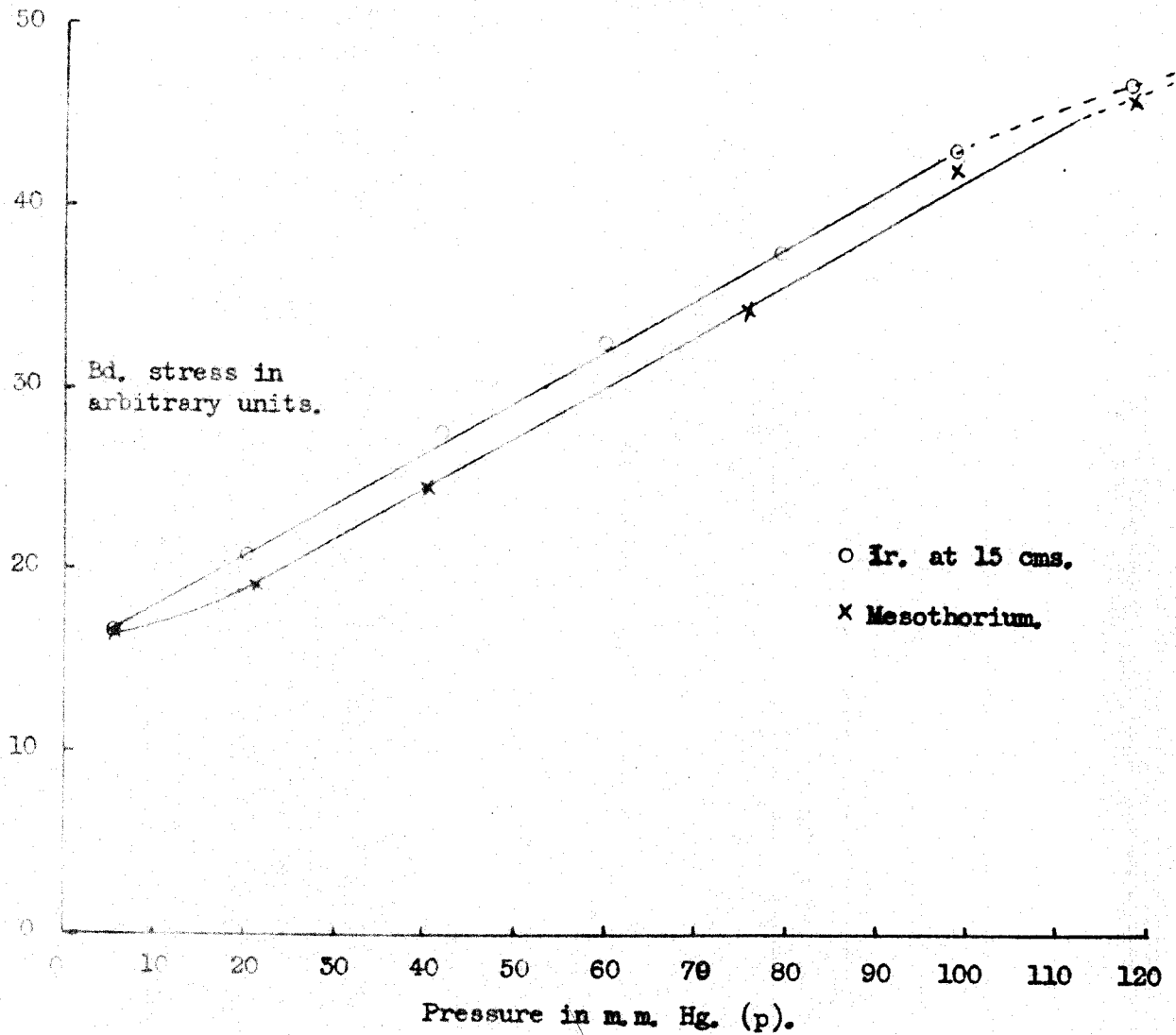
As is seen the stress recorded for spontaneous breakdown was in all cases considerably higher than that determined for the far irradiator position. Therefore it can be assumed that the breakdown for this

position was initiated by the irradiating spark. Four complete sets of results were obtained. The percentage variations were substantially the same in all sets: each set took at least one day to complete. It was estimated that the pressure could be reset to  $\pm 0.5$  m.m.Hg.

TABLE 6. Percentage increase of breakdown stress for the two extreme irradiator positions in hydrogen.

Pressure in m.m.Hg. (p).	Irradiator position.	Breakdown stress. Arbitrary units.	%Increase of breakdown stress. $d_{\min} - d_{\max}$
200.	Min. Max. No Ir.	54 No breakdown 54 " " 54	-
180.	Min. Max. No Ir.	52.0 53.3 No breakdown 54	2
158.	Min. Max. No Ir.	48 52 54.5	8
139.	Min. Max. No Ir.	47 50 52	6.5
122.	Min. Max. No Ir.	45 46.4 52	3
101.	Min. Max. No Ir.	40.8 43.2 51	8
81.	Min. Max. No Ir.	34.9 37.4 47.0	7.5

Graph 13 . HYDROGEN, Breakdown Stress v. Pressure.



63.	Min. Max. No Ir.	31 32 47	3
43.	Min. Max. No Ir.	24.8 26.1 37.2	4.5
35.	Min. Max. No Ir.	21 22 35?	4

The use of lower pressures was found impossible as a general glow discharge between the irradiating spark and the resonator developed for d minimum. This could be stopped by decreasing the irradiator coupling feed but not then a true comparison of the two positions.

4.4.3. Variation of breakdown stress with pressure for fixed irradiator.

Graph 13 shows the variation of the breakdown stress with pressure for a fixed position of the irradiator, i.e. 15 cms: the gas was changed for each reading, little or no statistical lag was observed for this irradiator position. To obtain the breakdown stress values for pressures below 33 m.m.Hg. the coupling to the irradiator had to be reduced to obviate the glow discharge that was otherwise established in the irradiator tube.

#### 4.4.4. Variation of breakdown stress with pressure using a mesothorium source of radiation.

The  $\gamma$  ray source produced breakdown stresses that were slightly lower than those determined for similar pressures with the irradiator at d minimum. The comparison can be seen in graph 13. The gas recovery after breakdown initiated by the radio active source was, if anything, more difficult than for breakdown initiated by the irradiating spark. For this reason the gas was again changed for all readings, and the results taken concurrently with those for the irradiator at d minimum. A direct comparison was possible. The significance of these results is discussed in Chapter III.

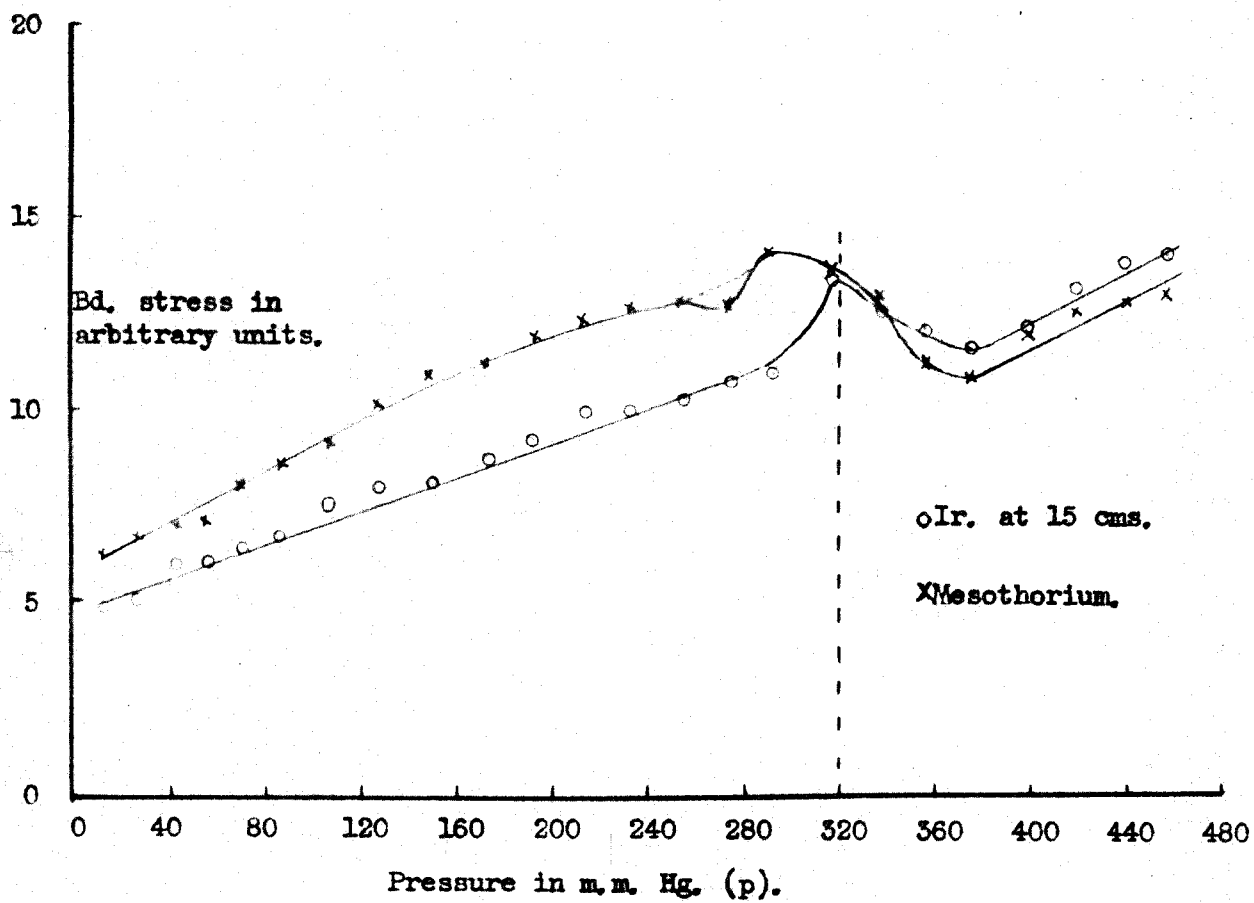
#### 4.4.5. Effect of variation in the angle of incidence of the ionising beam.

No change was observed in the breakdown stress with the direction of the ultra-violet beam, and it was therefore again concluded that the filament of maximum circuital electric stress had been irradiated in all experiments using hydrogen.

#### 4.5. Neon.

Spectroscopically pure neon was used for a final series of results, the vacuum apparatus was thoroughly pumped black before filling with neon. A further sequence/

Graph 14, NEON, Breakdown Stress v. Pressure.



of pump refill, repump refill was carried out: this procedure of course was adopted for all gases, together with leakage tests, where the apparatus was left for at least two days and the vacuum again tested. It was then assumed that if the apparatus had remained hard for such a length of time it would certainly remain so for the time required to make a complete set of readings.

The range of experiments with neon was strictly curtailed due to the occurrence for pressures below 320 m.m.Hg. of a general glow in the irradiator tube as well as the normal irradiating spark. There was, therefore, considerable uncertainty whether the microwave discharge within the resonator was being initiated by the irradiator spark or by the general glow due to the irradiator.

#### 4.5.1. Variation of breakdown stress with pressure.

With neon far higher pressures could be employed (up to 460 m.m.Hg.) due to its low striking voltage. Two curves are shown in graph 14, one displaying the breakdown stress variation with pressure when the gas was irradiated by the irradiating spark, the other when the  $\gamma$  ray source was employed.

The results are of considerable interest as below a pressure of 320 m.m.Hg. the breakdown stress recorded using the  $\gamma$  ray source is higher than that

recorded under the radiation from the spark gap. While above this pressure the positions reverse.

As mentioned, a general glow discharge in the irradiator tube also accompanied the irradiator spark when the H.T. was applied to the metal sleeves of the irradiator, this was true for pressures up to 320 m.m.Hg. Above this pressure conditions seemed normal, i.e. just a spark in the gap of the irradiator being visible. Again, whereas no statistical lag was observed for irradiated breakdown below 320 m.m.Hg. a lag began to appear above this pressure. It will also be noticed that the striking voltages are lower above 320 m.m.Hg. than those indicated by a continuation of the curves for lower pressures. No explanation can really be advanced for this unusual lowering of the stress. The graphs were reproducible together with the irregularity in the curves around 300 m.m.Hg.

It would seem that above 320 m.m.Hg. conditions comparable with the other gases existed. A very definite resonator input was required to produce breakdown for both sources of irradiation for all pressures: the breakdown stress was far easier to establish than for the other gases, mainly due to the lack of any high statistical lag.



As in hydrogen, it was noticed that the gas recovery from breakdown initiated by the irradiating spark was good, but the recovery was not so rapid for breakdown initiated by the  $\gamma$  ray source.

#### 4.5.2. Spontaneous breakdown of neon.

The microwave stress necessary to produce spontaneous breakdown in neon gradually decreased for each successive trial: the decrease in stress tended to a minimum value.

A typical set for a pressure of 463 m.m.Hg. is tabulated below, the first value being the microwave stress, (in arbitrary units), determined for the spontaneous breakdown of a fresh sample of gas. The 2nd, 3rd, 4th and 5th were taken as rapidly after each other as possible; the gas was then allowed to stand unstressed for two minutes, a partial recovery occurred (No.6). Breakdown stresses immediately following the partial recovery again showed the lower values, (Nos. 7 and 8).

Circulation of the gas by the pump appeared further to restore the gas towards its initial state, (No. 9); however, the stress was again found to be low on a determination immediately following No. 9. The gas recovery therefore seemed to be helped by its circulation through the glass wool trap.

Two more such sets for the same pressure confirmed that the breakdown stress for neon for spontaneous breakdown tended towards a minimum for successive breakdowns. It should be stated that in the experiments on the variation of breakdown stress with pressure (4.5.1.) the spontaneous breakdown stresses were also recorded following each triggered discharge. These stresses for spontaneous breakdown were, in all cases, far greater than the voltage recorded for irradiated discharge, whether  $\gamma$  ray or spark irradiation. Therefore the results shown in the previous section can be attributed to the action of the  $\gamma$  ray source or the irradiator. The immediate history of the gas affects the spontaneous breakdown stress, but does not affect the irradiated breakdown stress.

TABLE 7.    Breakdown stress values for neon.

No. of Discharge.	Breakdown stress in arbitrary units.
Initial breakdown 1.	37.5
Following rapidly (2.	33.5
(3.	29.5
after each other (4.	29.5
(5.	30.0
2 Minute wait. 6.	36.0
7.	30.0
8.	30.0
Circulation by pump. 9.	33.5
10.	31.0

Unfortunately a gas leak interrupted this work on neon, and in the absence of a spare bottle of neon work was continued on to other experiments.

5. Brief résumé of the microwave results.

1. Examination of the results suggested that further experiments of this type were not likely to lead to an explanation of the mechanism.

2. The lowering of the breakdown stress with the closer proximity of the irradiator to the resonator is established. Greater in oxygen than in hydrogen; the small value in hydrogen suggests this is a useful gas as a reference standard.

3. The agreement between the  $\gamma$  ray source of irradiation and the  $d$  minimum position of the irradiator suggests the use of the near position of the irradiator in future experiments. This has the incidental advantage of short statistical lags.

4. The main object of the work was to undertake experiments in crossed fields.

5. It was hoped that further work on the main problem might suggest lines on which an explanation is to be sought.

6. The following limited conclusion relating to the

mechanism can be stated, i.e., the inadequacy of the simple explanation; viz., that interpretation of the action of external ionising agent is :- (a) producing merely a casual electron when a weak source of ionisation, (b) to produce a greater number of independently acting casual electrons when the ionising source is stronger.

The following possibilities ought to be borne in mind:-

1. Interaction of electrons close to one another, i.e., two beaten zones may overlap.
2. Possible chemical effects; the dissociation into the atomic forms, formation of temporary molecules such as  $O_3$ ,  $NO_2$ ,  $H_3$ .
3. Concentration and space change effects due to the ionising beam; developing a cone of positive ions.
4. Differences as between penetrating and non-penetrating radiation in producing clumps of electrons.
5. Introduction of components other than direct radiation. (See Chapter II).

Not knowing of any certain means of producing the ideal condition of merely introducing a succession of non-interacting casual electrons into the gas, it seems best to use conditions in which two different agents produce the same results, i.e. d minimum position of the irradiator, and the  $\gamma$  ray source, especially as the  $\gamma$  ray source is suitable

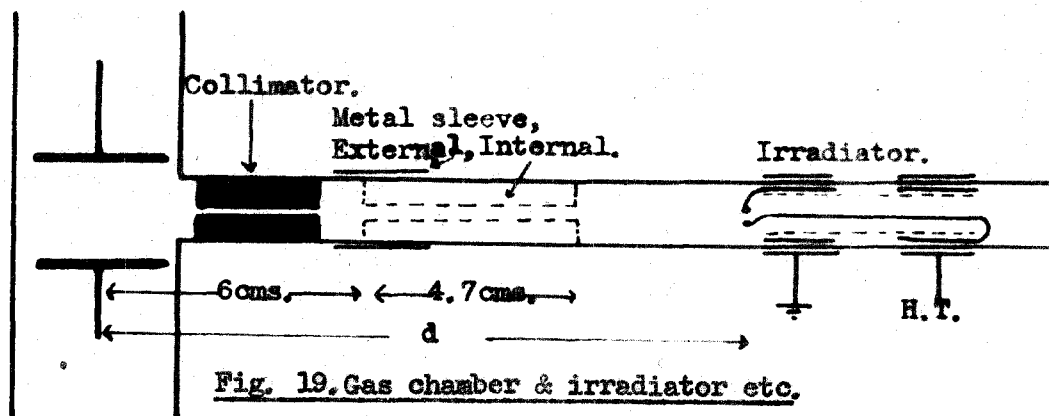
for the low pressure work.

#### 6. Further Development.

The main problem, the measurement of the microwave breakdown stress of a gas when an orthogonally placed second field is also present, was then begun. This work necessitated the construction of a high frequency oscillator; using this oscillator and a conventional parallel electrode system, the variation of breakdown stress with irradiator position was further explored, this time at the lower frequency of 11.5 Mc/s. For convenience these results in the lower frequency field are presented next, although this represents a departure from the chronological sequence of the experiments.

CHAPTER II.Variation of breakdown stress with irradiator position  
at 11 Mc/s.1. Apparatus.

The apparatus consisted of a parallel electrode system enclosed in a vacuum chamber. The separation of the electrodes could be varied without breaking the vacuum. The complete apparatus is shown in figure 38, Chapter 7, Part II. A long glass side tube (40 cms. x 9 m.ms) was attached to the main vacuum chamber in an approximately central position between the electrodes, see figure 19.



The irradiating spark gap system was of similar construction to that used in the microwave experiments. The irradiator pulse was obtained by cutting off an inductively loaded

pentode; i.e., a negative pulse was applied to the grid of the pentode when the H.T. pulse was required. The repetition rate of the irradiator pulses was controlled by a multivibrator at a frequency of approximately 400 pulses per second, therefore similar to the microwave repetition rate. The complete circuit diagram is given in appendix 5. The internal sleeves of the irradiator were again constructed of iron: by use of an external magnet the irradiator position could, therefore, be varied with respect to the electrode system. The high frequency oscillator had a frequency of 11.5 Mc/s, and a peak output of some 3,000 volts; the oscillator, together with the diode voltmeter, are fully described in a later chapter. (Chapter 3, Part II).

## 2. Experimental Results.

The experiments undertaken can be conveniently divided into four sections; each section will be described separately.

### 2.1. Distance effect.

#### 2.1.1. Conditions of measurement.

When the drift oscillation of an electron under the influence of the applied field in the test gap is less than the gap width the onset of discharge can properly be referred to as u-h-f breakdown. This

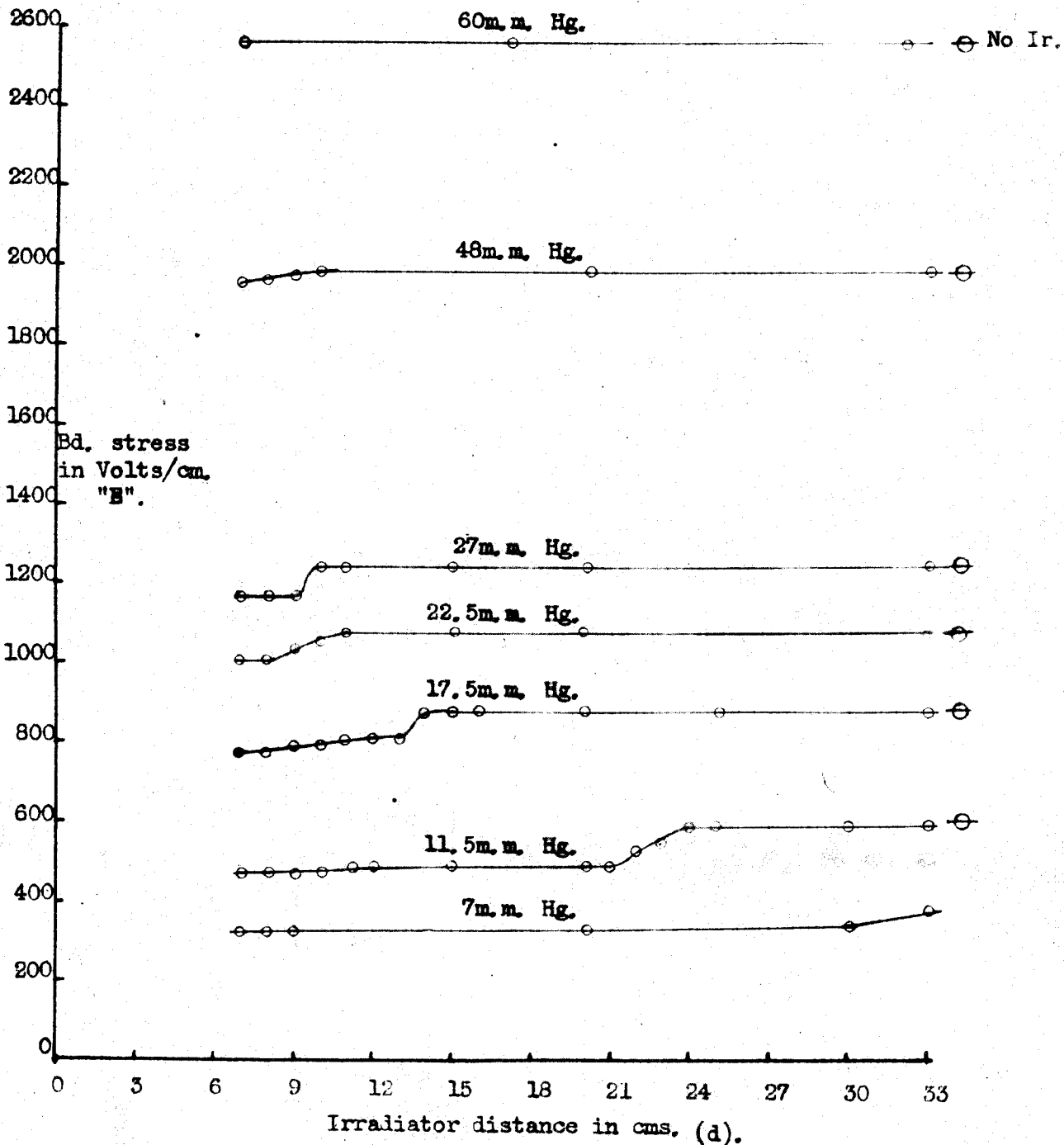
This condition is satisfied in the experiments to be described: it is readily established by measuring the breakdown voltage as a function of gap width and observing the step in the resulting graphs. (e.g. see graphs 48, 50, 52, 54, Chapter 7, Part II). Despite the presence of the electrodes in the gas vessel this breakdown is electrodeless in character provided the discharge starts in the middle of the test gap. This condition was observed in these experiments, where the pre-ionisation of the gap was provided by the radiation from an auxiliary spark. It should be noted that there is no evidence to show that the point from which the discharge starts affects the breakdown voltage in any way.

No ionisation is present in the gas chamber (except casual ionisation by cosmic rays, etc.) until irradiation, the amount is then only small; however at breakdown the density of ionisation is high and after this occurrence clearing time is needed. It was therefore found necessary, to ensure reproducible results, to switch off the h-f field for several minutes between breakdowns. A unidirectional sweeping field was found to reduce the ionisation clearance time.

To ensure only mid gap irradiation of the gas the radiation from the spark gap was collimated by means



Graph 15. AIR, Breakdown Stress v. Irradiator Position.



of an ebonite plug 2.5 cms. long, with a central hole of 1.5 m.m. diameter: it was later found possible to increase the diameter to 2.0 m.m. and then 2.5 m.m. without allowing irradiation from the irradiator spark gap to impinge on either electrode.

The statistical lags were sometimes long, especially when establishing the breakdown stress with no irradiation from the spark gap. (No. In). This is the real reason for the use of 400 p.p.s. of irradiation, i.e. rapid rate of trials before breakdown; the use of individual pulses was not practicable.

#### 2.1.2. Air; (Dry).

The variation of the breakdown voltage as a function of distance 'd' between the irradiator and the axis of the test gap is shown in graph 15 for the pressure range 7 to 60 m.m.Hg; above these pressures no alteration in the stress could be detected. It was impossible in the early experiments due to the position of the collimator to use irradiator distances less than 7 cms.

The results were obtained with great care especially, as commented, in ensuring clearance of the residual ionisation from the inter-electrode space between breakdowns. The voltage applied to the electrodes was increased in small stages and many minutes allowed for

one setting before no breakdown was recorded. It can be stated, as a general rule, that the statistical lags decreased as the irradiator distance from the electrode system decreased. Usually when the irradiator did not produce any reduction in the breakdown stress it did produce a reduction in the lag as compared to the non-irradiated breakdown at the same pressure. It can therefore be seen, as each individual reading required about four voltage settings, a complete run, (i.e. all distances) occupied several hours. The stresses recorded for non-irradiated breakdown are also shown on graph 15 and marked thus  $\ominus$  : the statistical lags were greatest in these trials. It was particularly important that the applied field was sustained over a long period compared with the statistical time to avoid serious overvolting when working without artificial irradiation. The error in measurement of the breakdown voltage was estimated as 1 to 1.5% and the pressures recorded to  $\pm 0.5$  m.m.Hg., and the irradiator distances to 1 m.m.

The steps shown in the curves in graph 15 were reproducible provided care was taken to clear residual ionisation, and due allowance made for statistical lag.

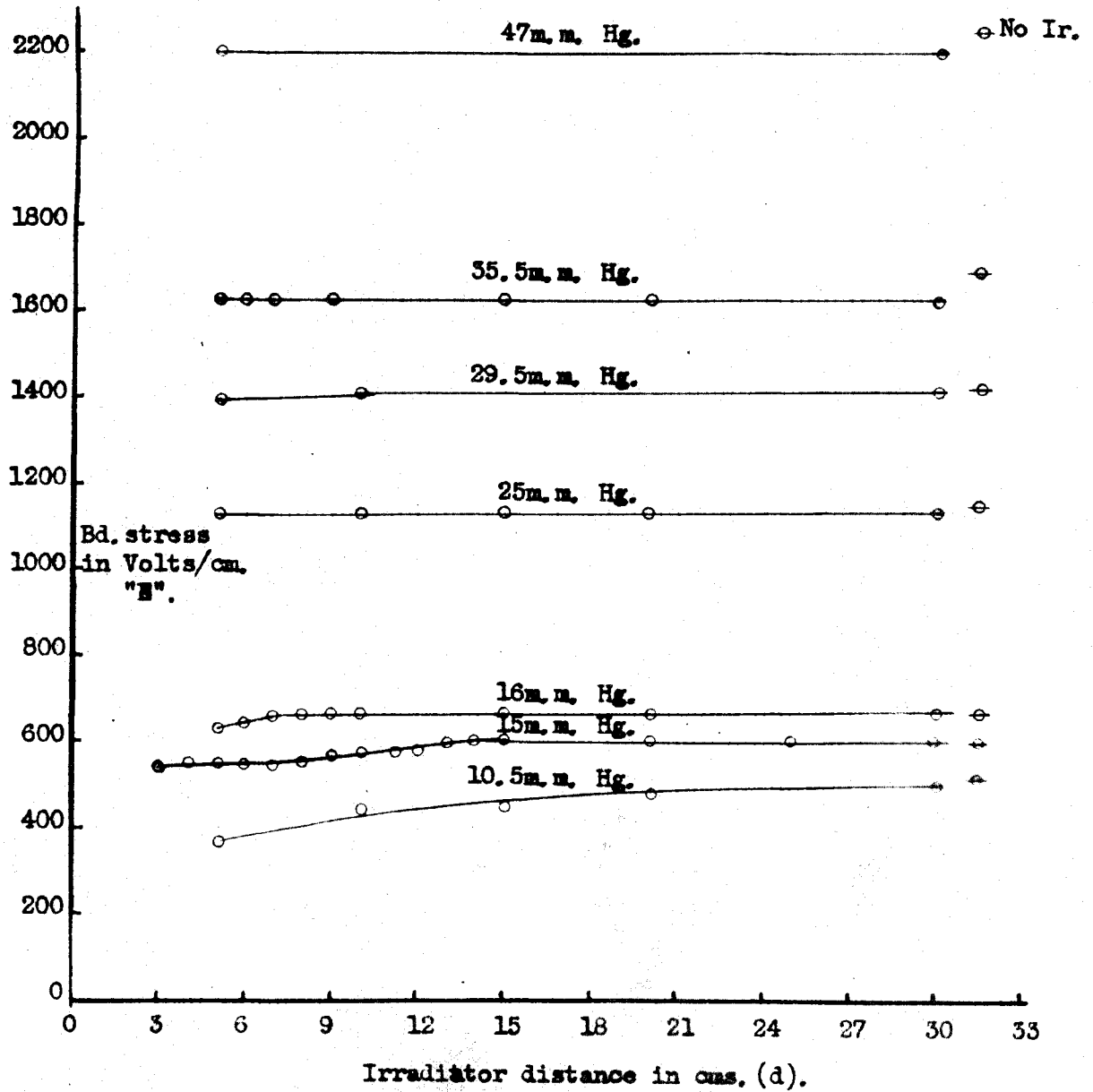
A point of considerable interest is the breakdown stress of air under the action of a mesothorium source of ionisation, (0.93 mg), placed just outside the electrode chamber. The stress recorded in all cases agreed with the upper part of the step, i.e. the non irradiated breakdown stress, or the stress recorded when the irradiator was far removed from the test gap.

The breakdown stress obtained in these experiments is again a function of the irradiator distance, the curves showing this relationship are of a different form from those obtained in the microwave work. The following table shows the p.d. value ('p' in m.m.Hg., 'd' in cms.) at which the steps in graph 15 occur, the values show reasonable constancy. Discussion of these and the following results for other gases has been reserved until Chapter 3.

TABLE 8. values of p.d at the steps in the curves of graph 15.

Pressure in m.m.Hg.	p d. p in m.m.Hg. d in cms.
48	(Less than) 275
27	240
22.5	205
17.5	235
11.5	240
7	220

Graph 16. OXYGEN, Breakdown Stress v. Irradiator Position.



### 2.1.3. Oxygen, (Cylinder).

The same general procedure as used for air was followed covering the pressure range 10.5 to 47 m.m.Hg. The results are shown in graph 16: a decrease in the breakdown stress only being apparent for the lower pressures, ( $< 25$  m.m.Hg.) The apparatus had been slightly modified to allow a nearer approach of the irradiator to the electrodes.

The breakdown voltage recorded using the  $\gamma$  ray source was identical to the non irradiated voltage or with the irradiator at its extreme range at the same pressure. (Similar to the results for air). The stresses recorded using the  $\gamma$  ray source are shown on graph 16 by the symbol  $\ominus$ .

Several minutes were allowed between trials to ensure the complete disappearance of residual ionisation in the electrode chamber. The statistical lags encountered were large, (from 1 to approximately 120 seconds), and the lags increased as the irradiator distance increased; e.g. for a pressure of 29.5 m.m.Hg. the position of the irradiator did not affect the breakdown stress of the gas but the lags decreased as shown in the following table. The results were obtained in the following manner.

1. A known stress was applied to the electrodes and the irradiator switched on; this stress was sustained for several minutes.

2. If no breakdown occurred the stress was increased by a known amount, (usually of the order 1 per cent, say 5 volts in 500 volts.); the stress was again sustained for the same duration as before.

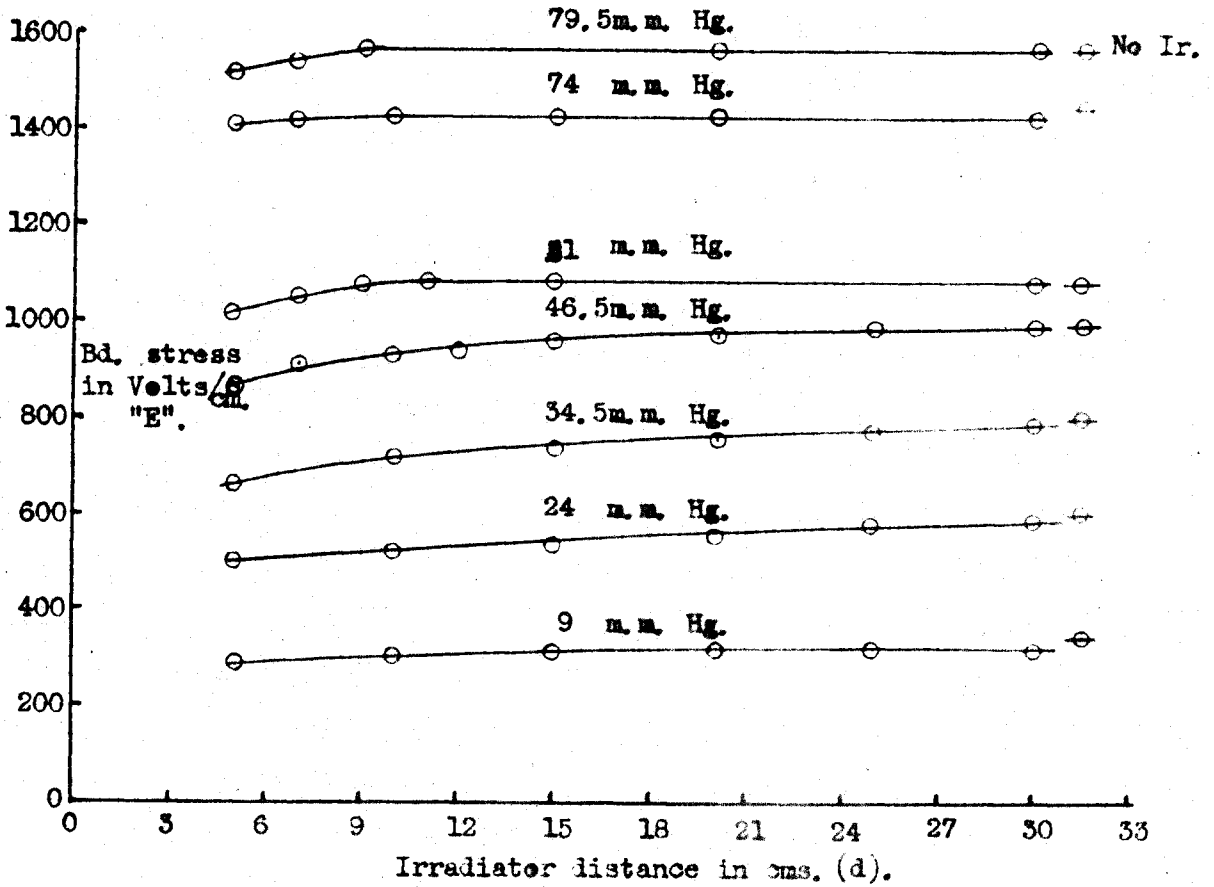
3. This procedure was followed until breakdown occurred. Some limit had to be imposed on the time of duration of each test in order that one complete run could be accomplished within a reasonable time, (i.e. 3 hours or more).

4. The statistical lags shown in the table are a mean of many results and all were taken following the same outlined procedure.

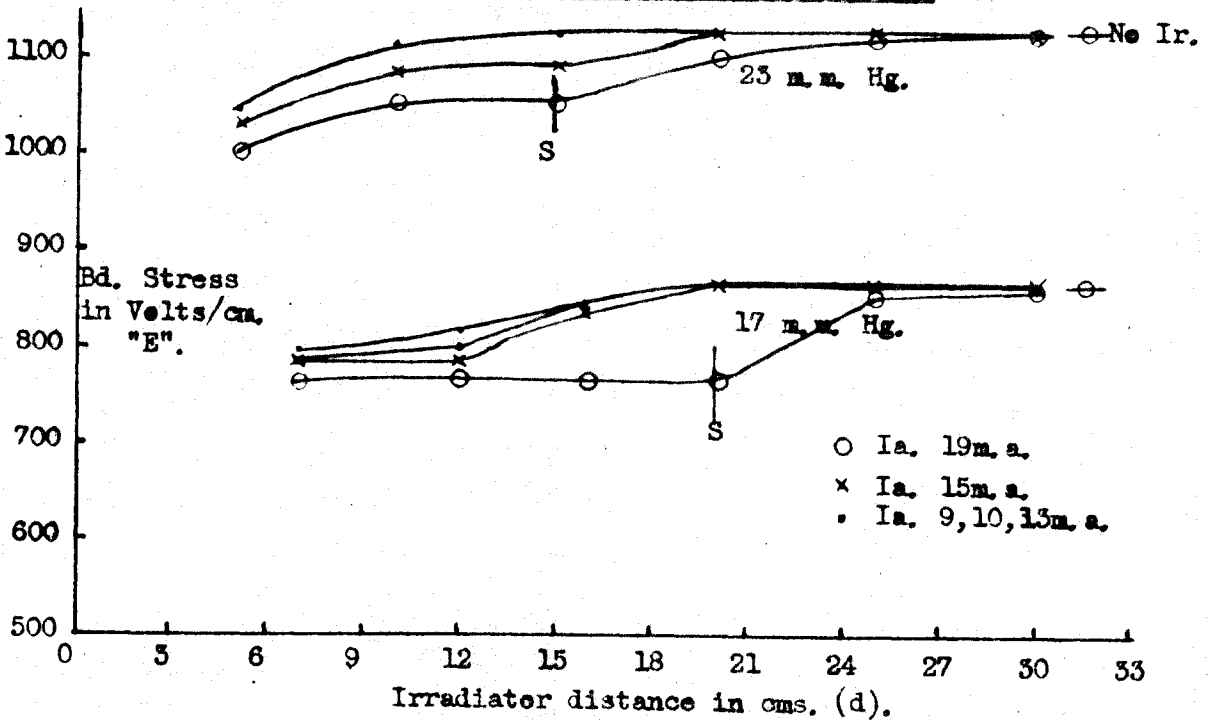
TABLE 9. Statistical lag variation with irradiator position for oxygen.

Distance d. in cms.	Stat.Lag in seconds.
6	Small lags < 5
15	5 to 10
20	20 to 30
25	≐ 40
30	≐ 90
No Ir.	≐ 120
⊗ Ray Source	≐ 120

Graph 17, HYDROGEN, Breakdown Stress v. Irradiator Position.



Graph 18, AIR, Intensity Variation of Irradiator.





A slight overvoltage, (i.e. greater than the errors of measurement), caused a large reduction in the statistical lags, so naturally the lags were difficult to assess.

#### 2.1.4. Hydrogen, (Pure).

The electrode separation was again chosen so that the electron ambit under the applied field at breakdown stress was less than the separation: the discharge could again be described as electrodeless. The experimental technique for hydrogen was as for the other two gases: time allowed for clearance of residual ionisation between breakdowns and for a reasonable statistical lag (i.e. up to 5 minutes)

The results thus obtained are shown in graph 17. The voltage recorded for breakdown when the gas was exposed to the irradiation from the mesothorium agreed once more with the non-irradiated values. It can also be generally stated that the statistical lag increased with increasing irradiator distance. There was also an indication that the irradiator at large distances caused a slight reduction in the statistical lag as compared to the lag encountered for a non-irradiated discharge, at the same pressure. The irradiator at these large distances did not

however produce any lowering of the breakdown stress from that found for the non-irradiated case. The lags involved were of the order one to three minutes so any marked variation was difficult to establish.

TABLE 10. Statistical lag variations with pressure for hydrogen.

Pressure in m.m.Hg.	Statistical lags in seconds.	
	No Ir.	Ir. at 30 cms.
9	120	90
20.5	120 - 180	70
46.5	120 - 180	60 - 90
74	120 - 180	80

2.1.5. Brief résumé of the three sets of results.

The results for air exhibit a quite different character from those for oxygen and hydrogen. No steps in the curves for oxygen or hydrogen are evident, these curves show a gradual reduction of the stress as the irradiator approaches the electrodes.

The sharpness of the steps in the air curves is not of the form associated with multiple absorption: the sum of several exponential curves will still give a monotonic curve. These steps occur at roughly constant p.d values and could indicate particle absorption; the particles having a defined range dependent on the pressure.

The probability of a particle originating from the irradiator spark and traversing some 20 cms. (including a collimator 2.5 cms. long and orifice 1.6 m.m.) would seem very small.

An alternative explanation could be the formation of a discharge (not visible) from the irradiator to the electrodes, having a maximum path which it could traverse: the length of this path indicated by the step positions.

In an endeavour to explore the problem, the intensity as well as the position of the irradiating spark was controlled, as described below.

## 2.2. Variation of intensity of irradiating spark.

### 2.2.1. Apparatus.

Variation of the irradiating spark intensity was accomplished by alteration of the anode current through the inductively loaded pentode. (See appendix 5). Anode currents between 9 and 19 m.a. were used, the greater the current the greater the apparent, (or visual) intensity of resulting spark. Naturally no absolute value of the spark intensity could be measured: the spark intensities have therefore been referred to by the value of the appropriate anode current. (9, 10, 12, 13, 15 or 19 m.a.)

### 2.2.2. Results: Air only.

Two pressures only were used and the results are shown on graph 18. The breakdown stress decreased with increasing spark intensity for all but the longest distances. The three lines then unite as is clearly seen for a pressure of 23 m.m.Hg. The results for spark intensities corresponding to 10 and 13 m.a. are identical for this pressure and join the 15 m.a. curve when the irradiator distance exceeds 20 cms. This overlap of the curves could indicate that the upper limit of the curves had been reached. It should be noted that at this pressure a current of at least 10 m.a. was required to produce a spark at the irradiator points.

No glow could be seen between the irradiator and the electrodes at any pressure for any spark intensity. The usual time intervals had to be allowed for residual ionisation clearance, and for statistical lags.

At both pressures only the higher spark intensities produced steps in the curves, possibly indicating some form of discharge between the irradiator and the electrodes which ceases at a certain p d value.

(i.e. at these two pressures for  $I_a = 19$  m.a. the steps occurred at -

p.d = 340	for 17 m.m.Hg.)
p.d = 340	for 23 m.m.Hg.)

This discharge could be possibly of two forms:-

1. A continuous discharge from the irradiator to the electrodes
- or
2. A travelling discharge reaction from the irradiator to the electrodes. (Shown to be the preferred explanation). The presence of the collimator must not be overlooked which because of its small orifice could possibly cool any such discharge.

2.2.3. The effect of an external metal sleeve:  
Air.

An external metal sleeve (1 c.m. long) was placed as shown in figure 19, and the irradiator set at distances corresponding to the bases of the steps in graph 18: i.e. at distances 15 and 20 cms. for the pressures 17 and 23 m.m.Hg. respectively. The positions of the irradiator for these trials are marked with an 'S' on graph 18.

With the external metal sleeve in position, and the irradiator placed as stated, the voltages necessary for breakdown were measured when known voltages were applied to the external metal sleeve. A summary of these results is given in table 11 below. The voltages applied to this external sleeve were derived from a potential divider network fed from the irradiator pulse.

TABLE 11. Summary of external metal sleeve results for air.

Pressure in m.m.Hg	17	23	
Irradiator distance	20 cms.	15 cms.	
Anode current through Pentode	19 m.a.	19 m.a.	
Breakdown stress in Volts/cm.			
<u>Applied voltage to External Metal Sleeve.</u>			
Irradi- ator on for all read- ings.	(No sleeve present	765	1050
	{ Sleeve floating	775 <sup>+</sup>	1070
	{ Earthed	770 <sup>+</sup>	1070
	{ Connected to Irradiator		
	earth	770 <sup>+</sup>	1070
	{ 1/4 of H.T.pulse applied		
	to Ir.	775	1070
	{ 1/2 do. do.	770 <sup>+</sup>	1030
{ 3/4 do. do.	705	1005	
{ Full H.T. do.	Visible dis- charge to electrodes from sleeve.	995 Tend- ing to pro- duce a visible discharge from electrodes to sleeve.	
No Irradiator, i.e. top of step (graph 18)	865	1120	

The higher pressure, and to a smaller extent the lower pressure, gave a definite increase in the stress necessary for breakdown when the earthed external sleeve was present. Both pressures showed (1) reduction in the stress when the applied voltage to the sleeve exceeds half the irradiator voltage; and (2) a visible discharge either from the irradiator to the sleeve, or from the sleeve to the electrode when the full potential was applied

to the sleeve. The visible glow from the sleeve is the glow seen in the gas, not any external sparking along the surface of the glass.

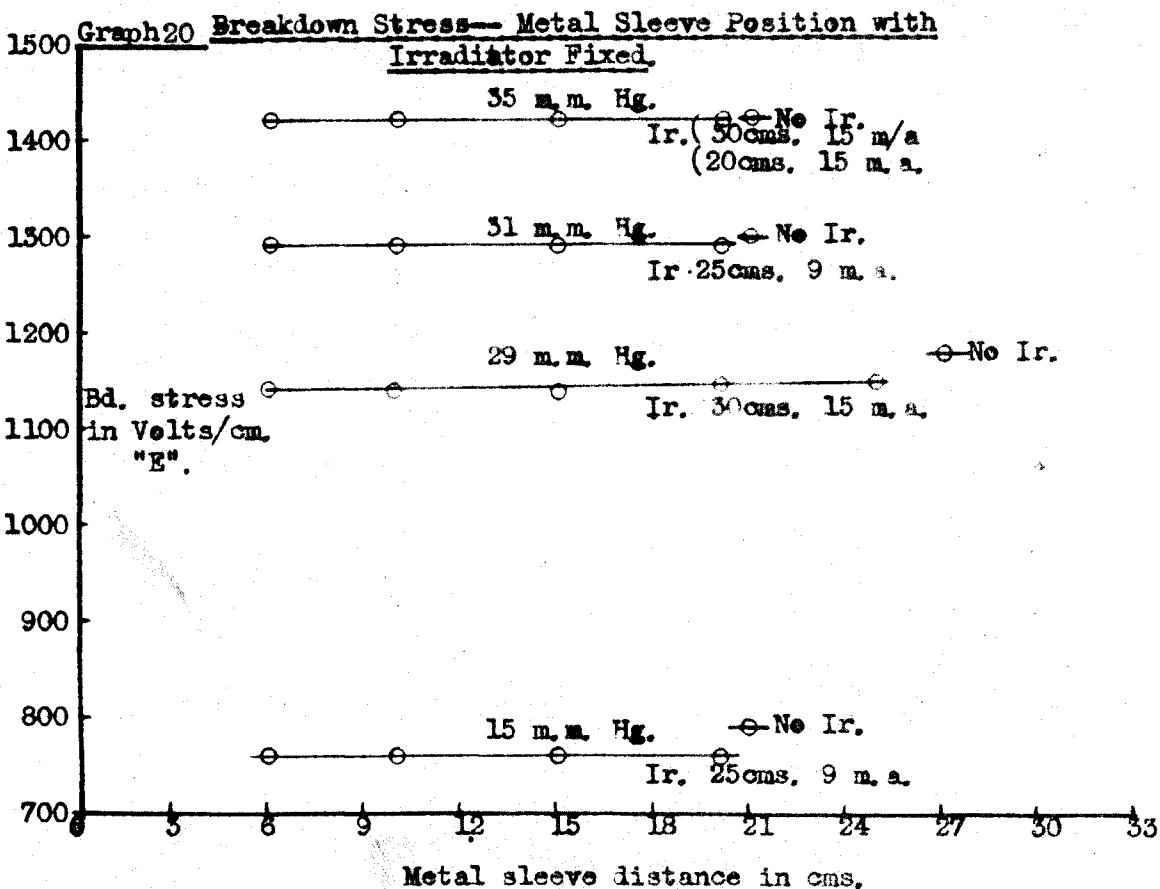
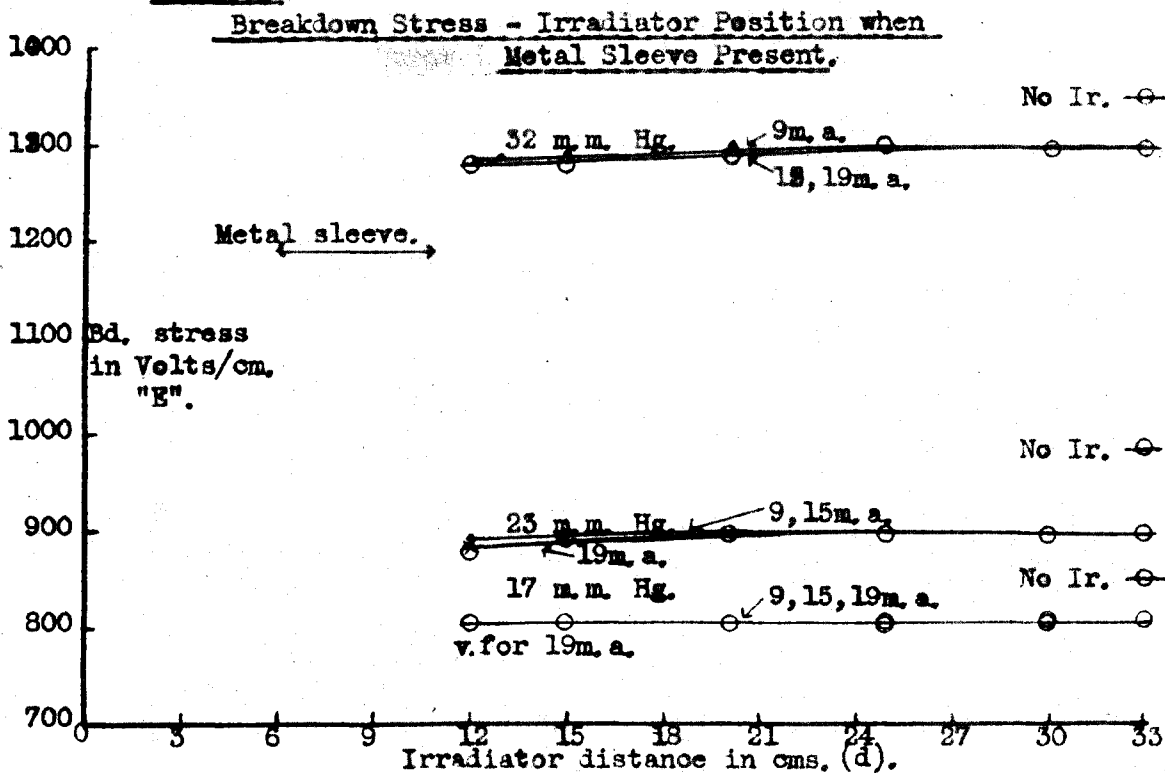
These results would again tend to support the hypothesis that the reduction in the stress necessary for breakdown could be partly explained by the action of some form of discharge originating from the irradiating spark and progressing down the tube towards the electrodes. The external earthed sleeve helped to quench such a discharge.

The experiments of Prowse and Jasinski<sup>65</sup> give a strong presumption that ultra-violet light from a spark gap will initiate the discharge, the insertion of thin films of different absorption coefficients affected the probability of breakdown. There is no reason to discount the action of the ultra-violet light, but definite indications of a second factor as well.

It was hoped to produce further evidence of these effects by placing within the irradiator tube a sliding metal sleeve (see figure 19), so constructed that it could be moved between the collimator and the irradiator. The sleeve could be expected to chill any discharge without obstructing the ultra-violet light, by

AIR ( DRY ).

Graph 19.





choosing a central hole of the right size. The following two experiments were proposed:-

1. Keep the metal sleeve fixed near the collimator and determine the breakdown stress for known positions of the irradiator.

2. Place the irradiator at a known position and then determine the breakdown stress for various positions of the metal sleeve as it is moved towards the collimator.

2.3. Metal sleeve inside the irradiator tube.

2.3.1. Air: Metal sleeve fixed; irradiator position varied.

The metal sleeve was placed between the collimator and the irradiator; the central hole through the sleeve was such that it did not affect the incidence of the ultra-violet on the gas between the electrodes. (Figure 19). The metal tube was 4.7 cms. long with a central hole of 2.5 m.m. diameter.

Three sets of results are given in graph 19, each set being for three irradiating spark intensities (9, 15 and 19 m.a.) The metal sleeve was placed between 6 and 10.7 cms. from the axis of the electrodes. A slight fall of breakdown stress with decreasing irradiator distance was observed for distances less than about 15 to 18 cms; all three curves for one pressure coincided for

greater irradiator distances. No steps in the curves were found. The constancy of the breakdown stress as the irradiator moved away from the metal sleeve helps to substantiate the hypothesis that the effective point of irradiation was now the metal sleeve, provided the plasma from the irradiating spark could traverse the distance between the sleeve and the irradiator. Due to the fact that the breakdown stresses for all the irradiated discharges were considerably lower than for the non-irradiated breakdowns, it would seem that the plasma was able to spread to the sleeve from the irradiator at all pressures and for all irradiator positions. (i.e. corresponding to the lower portion of the steps in graph 15).

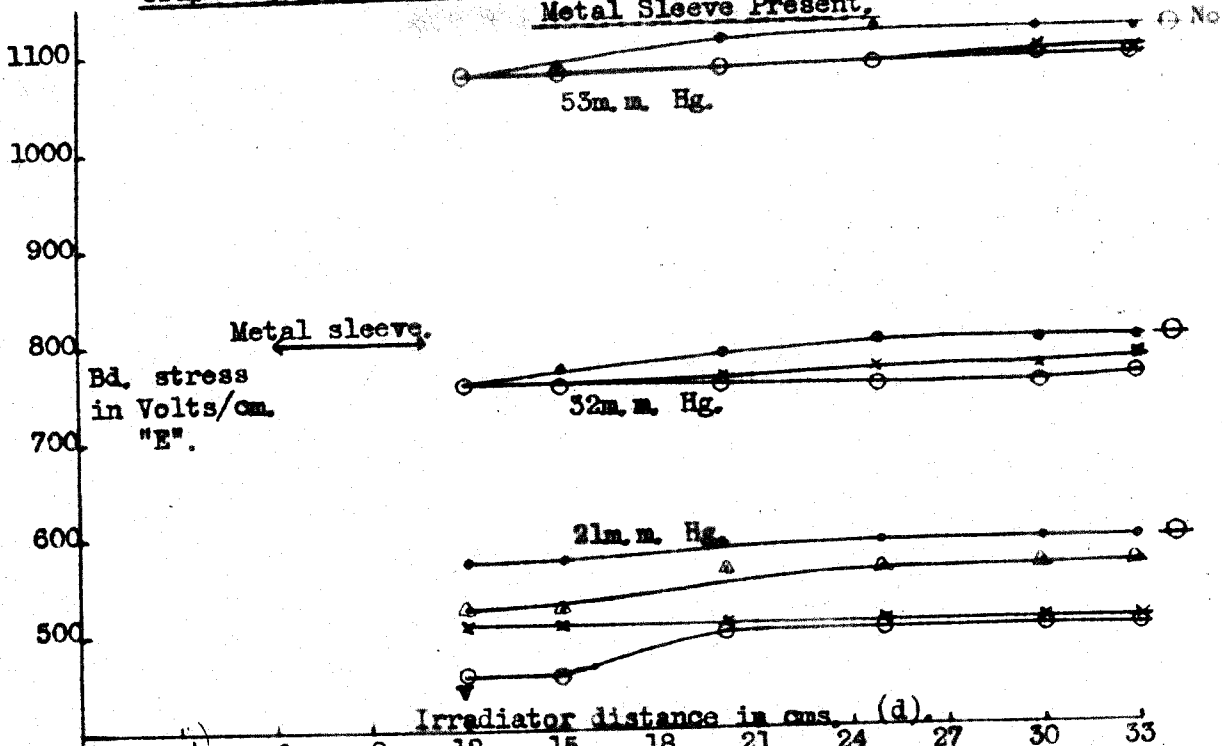
At the near positions for the pressure of 17 m.m.Hg. there tended to be a slight diffuse visual discharge from the irradiator to the sleeve, but only for the 19 m.a. intensity spark. No discharge was visible once 'd' exceeded 15 cms.

2.3.2. Air: Irradiator fixed; metal sleeve position varied.

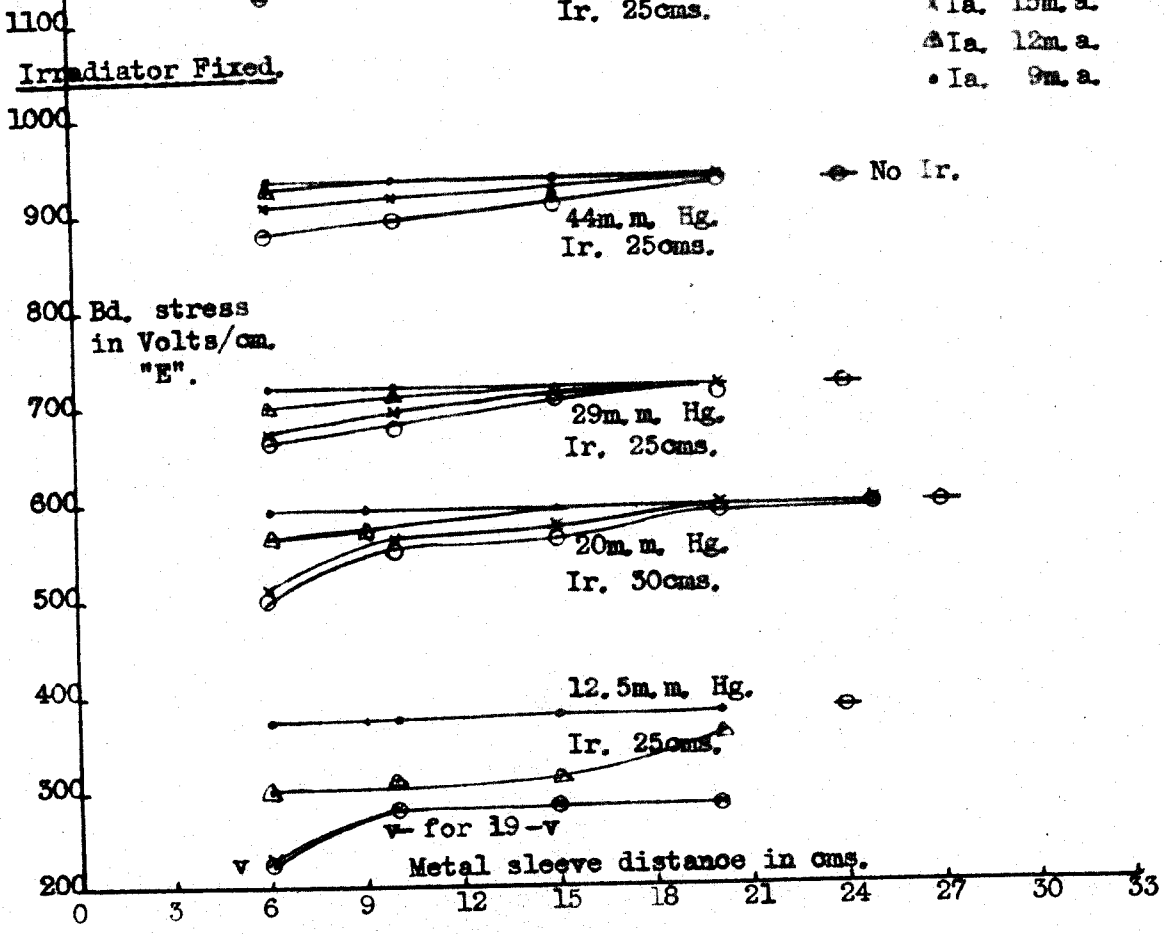
The iron sleeve could easily be moved by means of a magnet. Various irradiator positions and intensities were used, these are marked beside the appropriate curve on graph 20. The metal sleeve distances

HYDROGEN.

Graph 21. Breakdown Stress v. Irradiator Position when Metal Sleeve Present,



Graph 22. Irradiator Fixed.



were measured from the axis of the electrode system to the near edge of the sleeve.

Little or no stress variation could be determined except possibly a very slight decrease for the lower pressures when the metal sleeve was close to the collimator. The graphs again show no steps in the breakdown stress as the sleeve distance increases. The values observed seemed somewhat lower than the non-irradiated values for the lower pressure range. Discussion of these results is reserved until Chapter 3.

### 2.3.3. Hydrogen. Metal sleeve fixed: irradiator position varied.

This time four spark intensities were used 9, 12, 15 and 19 m.a., the results are given in graph 21.

For any given distance the breakdown stress appeared to depend on the irradiating spark intensity, the separation of the lines for each intensity of irradiating spark increasing with a reduction in the pressure. As the irradiator approached the metal sleeve the breakdown stress decreased for discharges initiated by the less intense sparks: the 19 m.a. results showed little variation with distance except for the lowest pressure when discharge was seen (for distances less than 12 cms) between the irradiator, metal sleeve and the electrodes. Whenever a discharge was seen

to actually go to the electrodes an unsteadiness in the voltmeter occurred. (A good check on this point).

There was quite definitely evidence that for one particular irradiator position the statistical lag increased as the irradiating spark intensity decreased.

2.3.4. Hydrogen. Irradiator fixed; metal sleeve position varied.

Again the same four intensities of irradiating spark were used; the position at which the irradiator was fixed is indicated on the appropriate curves, graph 22.

The rate of decrease of the breakdown stress depended on the intensity of the irradiating spark; the rate of decrease was greatest for the highest intensity spark. All the curves converged as the metal sleeve approached the irradiator, the breakdown stress values recorded in these positions were identical to the non-irradiated voltages necessary to produce breakdown at the same pressure.

The lowest pressure 12.5 m.m.Hg. was the only case where a visible discharge could be seen in the irradiator tube, or unsteadiness recorded in the voltmeter, and this only occurred for distances less than

15 cms. and for an irradiator spark intensity of 19 m.a. The graph is marked with a letter V at these points.

The breakdown between the parallel plate electrodes under this type of irradiation, (i.e. V positions) took the form of bursts of pulses for the near positions, and a very diffuse glow for the 10 and 15 cms. positions of the metal sleeve. ( $I_a = 19$  m.a.) Breakdown ceased when the irradiator was switched off.

2.4. A brief discussion on these results as a guide to the next experiments.

The relatively flat curves obtained for air and hydrogen ( $I_a > 15$  and 19 m.a. for hydrogen), when the metal sleeve was fixed and the irradiator moved all help to indicate that the effective point of irradiation is now the position of the metal sleeve and not the position of the irradiator. Any discharge arising from the irradiator was now quenched, or cooled, by the high radial diffusion rate within the metal sleeve aperture. It would therefore be expected that provided the intensity of the irradiating spark was high enough the stress necessary for breakdown would be the same for the whole range of irradiator positions; this is shown in air and to a lesser degree in hydrogen.

The departure of the  $I_a = 9$  m.a. curve from the family of curves in hydrogen could be explained by the intensity of the irradiating spark, even at the nearest

distances, being less than that necessary to establish the proposed discharge between the metal sleeve and the irradiator.

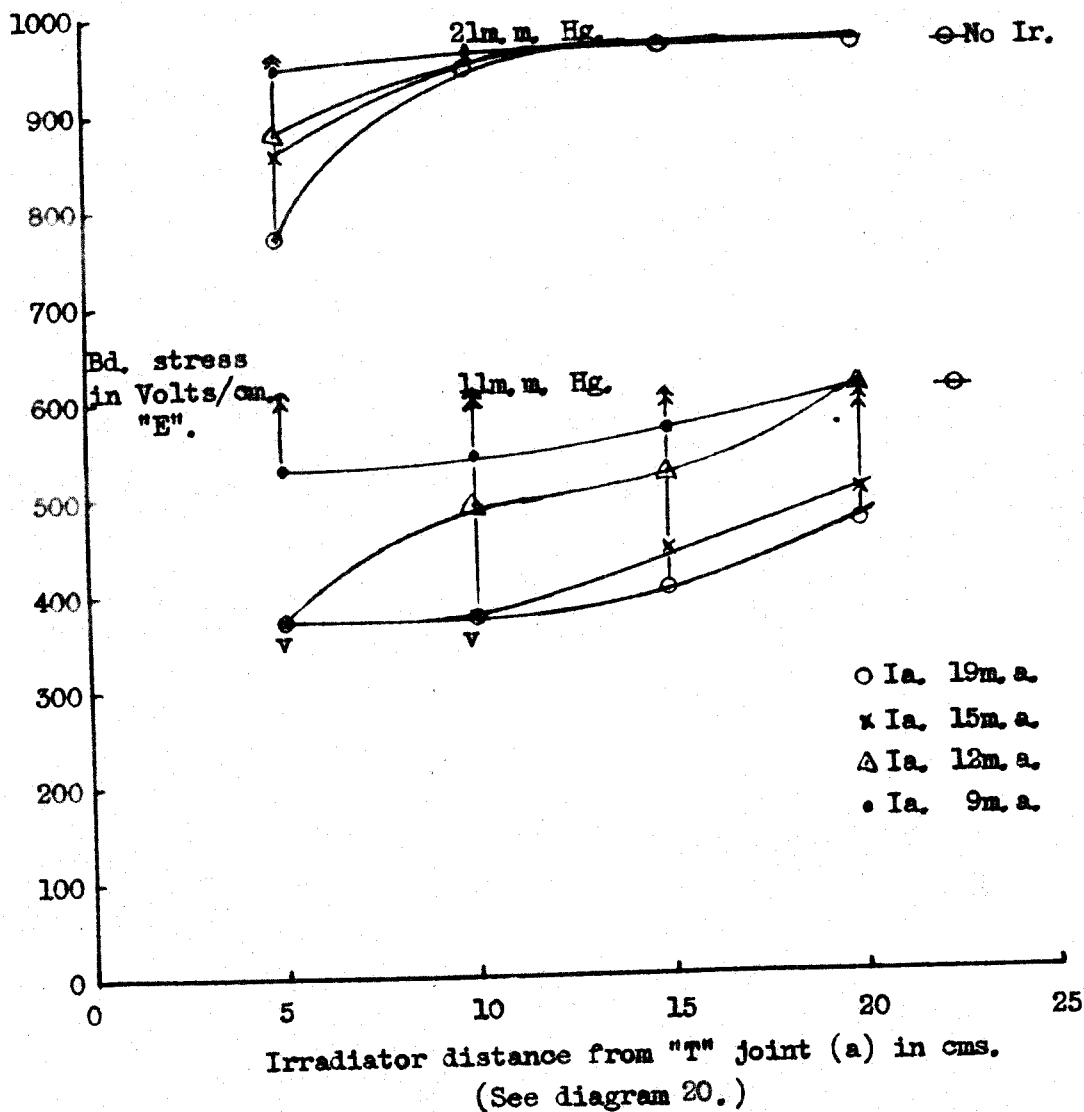
Again, the departure in the opposite direction of the high intensity spark line (Ia 19 m.a.) at the lowest pressure and smallest distances could be due to the discharge from the irradiator now being of such an intensity that it could traverse the metal sleeve. This is clearly the case when the discharge becomes visible in the irradiator tube.

If, as has been suggested, the effective point of irradiation becomes the metal sleeve's position movement of the metal sleeve towards the irradiator should produce the usual graphs as first discovered, graphs 15, 16 and 17. This is evident in hydrogen (graph 22) but is not very conclusive in air, where the variation is small. (graph 20).

From all the results so far there seems to be some evidence of a discharge down the irradiator tube, and it was felt necessary to definitely prove, or disprove, this point. The apparatus was therefore again modified; a tube being attached at right angles to the main irradiator tube in a horizontal plane. Figure 20 shows this; but for

AIR

Graph 23. Breakdown Stress v. Irradiator Position (Right angle expt.).





ease of presentation the added side tube is shown rotated through a right angle. The T joint was constructed as neatly as possible to avoid any optical reflexions of radiation from the irradiating spark to the electrodes.

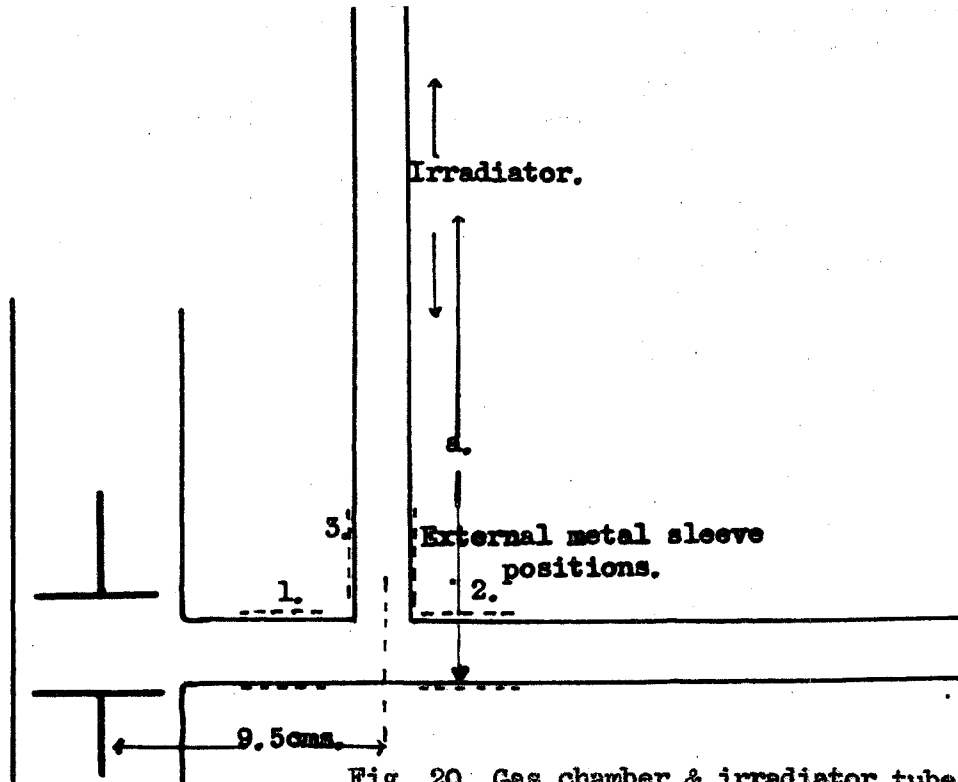


Fig. 20. Gas chamber & irradiator tube.

Breakdown stress measurements were taken for various positions of the irradiator in this side tube; no collimator or metal sleeve of any sort was present in the main tube thus avoiding influencing any discharge that might originate from the irradiating spark.

2.5. Breakdown stress measurements: irradiator in side tube.

### 2.5.1. Air (Dry).

Before discussing these results in any detail the most important outcome of these experiments should be stated: namely, that the irradiation can trigger the discharge from round the bend, also the irradiation can still cause a lowering of the stress necessary for breakdown even when the irradiator is situated some 20 cms. along the side limb. (Pressure 11 m.m.Hg. graph 23).

The graph shows two sets of results for pressures 11 and 21 m.m.Hg. four intensities of irradiation were used.

In the higher pressure set no visible discharge or unsteadiness in the voltmeter could be detected, not even when the irradiator was only 5 cms. along the side limb, and  $I_a = 19$  m.a. The distances (a) shown on the graph are measured from the irradiator to the further wall of the main irradiator tube. (Figure 20).

The 11 m.m.Hg. curves need further comment, for  $I_a = 19, 15$  m.a. and distances less than 10 cms.; and  $I_a = 12$  m.a. for 5 cms., the meter became unstable and a visible discharge from the irradiator to the electrodes could be seen, these voltages are therefore not true breakdown voltages in that the gas does not breakdown exclusively

in the direction of the applied high frequency stress.

When the irradiator had no influence on the breakdown stress, there was still slight evidence of a reduction in the statistical lag, compared to the non-irradiated breakdown cases. These lags were all high, of the order three minutes, and it was thus difficult to establish this point with absolute certainty. Hydrogen, as will be seen in the next section, gave more definite evidence on this point.

The effect of an external metal sleeve was next tried, this being placed around the irradiator tubes in the three positions indicated in figure 20. Positions 1 and 2 produced no change in the results, however, position 3 was far more effective. The breakdown stress was now raised to the non-irradiated level. The arrows on graph 23 clearly show the levels to which the stresses for breakdown for the particular irradiator positions were raised. The metal sleeve, (2.5 cms. long) was placed 2 cms. along the side tube, (a = 2 cms. for sleeve's near edge.)

In the particular case:- irradiator at 20 cm. pressure 11 m.m.Hg. and Ia = 19 m.a., the sleeve was placed at successive positions all giving the same value for breakdown.

TABLE 12. Effect of external metal sleeve for air.

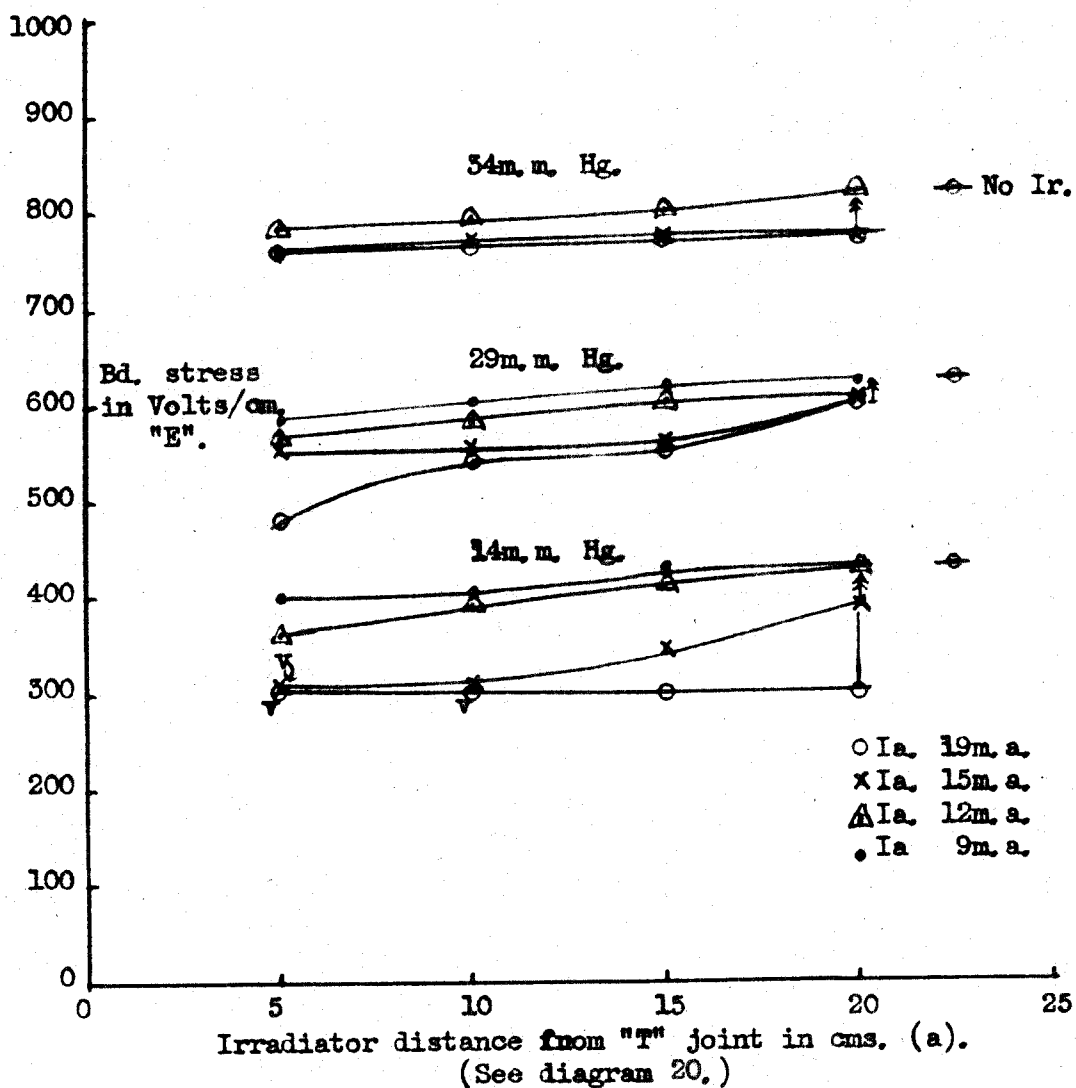
p = 11 m.m.Hg Ir. at 20 cms.(a) Ia = 19 m.a.	Sleeve position (a) in cms.	Breakdown stress Volts.cm.
Metal sleeve in position 3	2	610
	5	610
	10	610
	15	610
	No sleeve	470
	No irradiation	610

If, while the metal sleeve was in position 3, the stress was raised above the breakdown stress necessary for no sleeve present, removal of the sleeve resulted in immediate breakdown, a conclusive experiment. The sleeve was removable being constructed in two halves which hinged apart.

Finally to investigate if there was any influence on the statistical lag when the sleeve was present. The lags were measured for breakdown with and without irradiation, the sleeve being in position 3: the results (Table 13 below) show that when the irradiator was switched on the lags were reduced, there was as shown no change in the breakdown stress. The lags shown are the mean of only three sets of readings so cannot be called statistical lags. It was however generally noted that the irradiator with, or without, the metal sleeve present reduced

# HYDROGEN

Graph 24. Breakdown Stress v. Irradiator Position (Right angle expt.)



the lags compared to the non-irradiated measurement.

TABLE 13. Variation in lags with and without metal sleeve for air.

	Lags in seconds.	
	No Irradiator.	Irradiator + Metal Sleeve in position 3.
P = 21 m.m.Hg.	20	15
Ir. at 10 cms.(a)	47	12
Ia = 19 m.a.	25	8
Metal sleeve in position 3.	30	25
	40	30

### 2.5.2 Hydrogen (Pure).

Similar experiments to those made in air were tried giving much the same results; in that the irradiator in the side tube did (1) trigger the discharge, and (2) in some cases produce a lowering of the breakdown stress. The results are plotted on graph 24, and as before at the near positions and low pressures there was a visible discharge from the irradiator to the electrodes: these positions are labelled with a V.

When the irradiator produced no reduction in the breakdown stress, it did produce a very marked reduction in the statistical lag: in some cases the lag was reduced to apparently zero.

As before the first two positions of an earthed external metal sleeve caused no change in the stress

values. The third position (i.e. along the side tube) caused an increase in the stress required to give breakdown, the increase usually bringing the stress up to the non-irradiated value. These variations are once again shown by vertical arrows on graph 24.

TABLE 14. Variation of breakdown stress with and without metal sleeve in hydrogen.

Pressure m.m.Hg.	Ir Position 'a' cms.	Irradiator spark in- tensity m.a.	Breakdown Stress Volts/cm.		
			No Ir.	Ir. no sleeve.	Ir+sleeve earthed.
34	20	19	820	770	800 <sup>+</sup>
29	20	19	625	600	625
14	20	19	430	300	430

If with the metal sleeve in position a voltage was applied to the electrodes greater than that necessary to produce breakdown with no sleeve present, removal of the sleeve resulted in almost instantaneous discharge.

Finally when the presence of the metal sleeve raised the necessary stress for breakdown to be identical with the non-irradiated case, the irradiator still influenced the discharge by reducing the statistical lag. To test this and to ensure true results the following experimental procedure was used for both hydrogen and air.

1. The high frequency field and the irradiator were switched off for three minutes to allow time for complete residual ionisation clearance. The h - f field was then applied at breakdown stress level for non-irradiated breakdown, the lag for discharge was measured.

2. After the discharge the h - f field was again switched off for three minutes; before reapplying the h - f field the irradiator was switched on following immediately with the h- f field. (The value of the applied stress was as before); again the lag was measured.

3. The above procedure was repeated in order, the lag being measured each time. The earthed metal sleeve was left in position 3 the whole time.

TABLE 15. Variation in lags with and without metal sleeve for hydrogen.

		Lag measured in seconds.	
		No irradiation	Irradiation+metal earthed sleeve.
p = 14 m.m.Hg.		70	25
Ir at 20 cms. (a)		50	10
Ia = 19 m.a.		60	5
Metal sleeve in position 3		90	10
Stress breakdown value for H <sub>2</sub> at 14 m.m.Hg. with no irradiation.			



CHAPTER III.Discussion of the experimental results.1. Introduction.1.1. Aspects of triggering processes.

The possible mechanisms by which a discharge may be triggered are considered below.

1.1.1. The simplest form of triggering mechanism for a discharge is the production in the gas of one casual electron. This electron is then accelerated by the applied field producing ionisation, and so by a cumulative process this may lead to instability.

1.1.2. The next simplest mechanism is the simultaneous production of randomly distributed electrons within the gas. These electrons are so distributed that mutual interaction is impossible.

1.1.3. The production of a group of electrons in close proximity to each other : as such electrons drift under the action of the applied field they could traverse each other's ionised zones. A mutual reinforcement of the ionisation could therefore occur; this mechanism assumes that the breakdown stress is a function of the actual initial concentration of the electrons.

1.1.4. The production of quasi-chemical

effects: for example :-

- a. the dissociation of molecular gases into the atomic form.
- b. the production of ozone in oxygen, or nitrous oxide in air, etc.
- c. the formation of temporary molecules such as  $H_3$  and  $He_2$ .

The presence of such molecules may possibly help to produce instability in a gas.

1.1.5. The excitation of the gas molecules, i.e. change of species which could by successive collisions lead to step wise ionisation of gas molecules.

1.1.6. The introduction of an actual plasma into the test gap, e.g., from another discharge, (as has been discussed in the previous chapter).

The preferred mechanism that offers the more conclusive explanation of the observed phenomena is now indicated. The observed phenomena were seen to be, 1, the reduction of the breakdown stress (microwave, and h-f) with the closer proximity of the irradiator to the resonator, or electrode system, and 2, the triggering of the discharge by the irradiating spark, even when there was no visual path between the irradiator and the gas chamber.

As has already been suggested the preferred mechanism could possibly be a dual process:-

1. Some form of discharge originating at the irradiating spark and progressing down the irradiator tube towards the gas chamber, or into the electrode space.

2. There is still reason to think that the ultra violet light from the irradiating spark liberates electrons, and/or, produces excited states in the gas molecules.

### 1.2. Products from the irradiating spark.

1.2.1. Ultra-Violet Light. (a) Even if the effect of the ultra violet light may be overshadowed by other processes there is no reason to doubt its effectiveness in triggering discharges at all ranges. The experiments of Prowse and Jasinski<sup>64</sup> using various interposed films between the irradiator and the test gap show clearly that the emission of radiation from the irradiating spark is the cause of the initial ionisation in the test gap.

(b) If the absorption coefficient is thought to be complex (i.e. consisting of several absorption coefficients) the variation of the intensity of the radiation with distance will still be a continuous decrease, with no discontinuities. The sum of several exponential curves is a monotonic curve.

(c) At the near positions of the irradiating spark the range of wavelengths of the radiation reaching the test gap will be large, (the

absorbing cylinder of gas between the resonator and the irradiator being small for d minimum). This mixture of wavelengths of radiation may give rise to the production of

- i many randomly distributed electrons,
- ii quasi-chemical changes in the gas. and
- iii changes in the gas species (i.e. excitation of the molecules).

All of these processes could occur simultaneously.

(d) All these radiations in the simplest case originate at the irradiating spark gap itself.

### 1.3. Products not originating at the irradiating spark gap.

1.3.1. Plasma Spread. - The spread of an actual discharge from the spark gap down the irradiator tube: an electric field too weak to initiate such a discharge may extend the boundaries of the discharge once the discharge has started. The spread of the positive column down a side tube, to a pump head for example, occurs in a very weak field; or impulsive discharge can send flashes down side tubes without electrodes. All these types of discharge can be called plasma spread.

1.3.2. The low energy radiation from the irradiating spark though unable to ionise the gas molecules could raise the molecules (as stated above), to a series of excited states, and may so contribute to the outward spread

of the plasma.

1.3.3. If, however, quanta with sufficient energy to ionise the gas molecules are present then by initial, or preferential, recombination reradiation could occur from the intervening gas, ( i.e., the gas between the irradiator and the test gap), at the same frequency. A process of progressive radiation, at the same frequency, down the irradiator tube is therefore possible. Initial recombination occurs when negative ions are readily formed in the gas, (e.g. oxygen) and it is more frequent at higher pressures, (i.e.  $> 10$  m m Hg)<sup>81</sup> Preferential recombination is where the electron returns to its parent positive ion, and is usually associated with the absence of external fields and with low pressures.

## 2. Experimental discrimination.

2.1. The steps in the air curves, (Graph 15), do not appear to admit of explanation by the action of ultra-violet radiation originating at the irradiator. They might be explained by re-radiation (initial or preferred recombination processes), or by plasma spread: but there is no reason to expect a discontinuity in the re-radiation processes. Assuming the effect of breakdown stress reduction is due to some progressive form of activity, the air curves

show a fairly definite range for this spread. (Table 8. —p.d varied between 220 and 275 for the step positions).

In these early experiments the irradiating spark was made as intense as possible, so that any effect would, it was hoped, be made more obvious; these curves therefore correspond to the Ia 19 m.a. curves. (Later work confirmed this - graph 18). In the subsequent work in oxygen and hydrogen the apparatus was slightly modified to enable the minimum irradiator distance to be reduced, (from 7 to 4 cms). When working at these close positions, and the lowest pressures, it was found necessary to reduce the irradiating spark to obviate spark over, or the establishment of a visual glow between the irradiator and the electrodes. The oxygen and hydrogen curves (graphs 16 and 17) therefore correspond to the minimum intensity curves, i.e Ia 9 or 10 m.a.)

Subsequent work, as it happened, (Sections 2.3.2. and 2.3.3.) also included the effect of variation of the intensity of the irradiating spark for hydrogen: or as can be seen the results are in general agreement with the air results, a step is evident for the lower pressure range and higher spark intensities, (graphs 21 and 22).

2.2. The internal metal sleeve experiments: in hydrogen, and to a lower extent in air, the position of the

sleeve did affect the breakdown stress, graphs 21, 22 and 19, 20 respectively. The high radial diffusion rate of a plasma within the metal sleeve might cool or damp the discharge; the plasma spread from the irradiator would therefore be terminated at the sleeve. The effective point of irradiation might thus be moved from the irradiator position to the metal sleeve's position, i.e., nearer the electrode system. Movement of the irradiator away from the sleeve would not alter these conditions until the plasma was unable to spread as far as the metal sleeve. It would therefore be expected that the breakdown stress of the gas under the h-f field applied across the electrodes would be constant as the irradiator moved away from the fixed metal sleeve, the breakdown stress rising when the plasma failed to reach the sleeve. This was seen to be true for air and hydrogen: a constant h-f breakdown stress for all positions of the irradiator for all intensities of irradiating spark was recorded for air. It would appear for air that plasma spread to the metal sleeve from the irradiator occurred for all pressures, and distances between the sleeve and the irradiator. In hydrogen for the lower intensity irradiating spark the breakdown stress soon reached the valve for non-irradiated discharge as the irradiator receded from the metal sleeve. Plasma spread in hydrogen for the lower intensity irradiating

spark would therefore seem very limited.

However, control of a plasma by an internal sleeve, or electrode, is an uncertain process, e.g. in a thyratron variation of the grid potential will switch on the tube but will not easily switch off the gas relay. It is therefore to be expected for the near position of the irradiator that the plasma will penetrate the metal sleeve.

Following a similar line of thought, movement of the metal sleeve towards the irradiator, (the irradiator fixed at some large value of 'd'), should produce similar curves to the original graph showing the variation of the breakdown stress with irradiator position. This was found to be true for hydrogen, (graphs 17 and 22): the air curves show little variation of the stress with sleeve position, (graph 20).

2.3. The energy, i.e. intensity of the irradiating spark, could affect both the production of ultra-violet radiation, and the spread of plasma: the anode current ( $I_a$ ) in the pentode controls the rate of voltage rise at the irradiator spark gap, and thereby voltage overshooting. The variation in the breakdown stress with irradiating spark intensity may be explained by plasma spread, or the production of grouped electrons giving mutual reinforcement.



The ultra violet radiation may also produce quasi-chemical effects, or stepwise ionisation within the gas.

2.4. The action of an external metal sleeve could affect the plasma spread by controlling the pre-breakdown field distribution, but the results for air in section 2.2.3. Chapter II are not by themselves very certain. (See discussion at the end of section 2.2.3. Chapter II). The results found for the action of an external metal sleeve in the side arm experiments do favour the plasma spread hypothesis.

2.5. The irradiator in the side arm experiments might have triggered the discharge by re-radiation effects, i.e. initial or preferential recombination, but the discriminatory effect of an external metal sleeve on the side arm. (i.e. Position 3, Figure 20), is against this.

2.6. With the irradiator at its maximum distance from the electrode system, no breakdown stress reduction from the non-irradiated case was observed. However, a decrease in the statistical lag compared to the non-irradiated discharge was always observed, this was true whether the irradiator was situated in the main or in the side arm. This decrease in the lag was found to occur whether an earthed external metal sleeve was present or not. The triggering might be explained by the action of the ultra-violet radiation rather than plasma spread from the irradiating spark.

### 3. Conclusion.

The only process of those mentioned that satisfies all the conditions is plasma spread, i.e. the production of a progressive zone of activity from the irradiating spark down the irradiator tube, seen to have a fairly definite range in air. (Graph 15).

### 4. Lowering of breakdown stress.

This is not explained in the foregoing: only shown that whatever factor produces the lowering of the breakdown stress can be associated with the spread of a discharge away from the irradiator.

#### 4.1. General résumé and comparison between microwave and h-f results.

4.1.1. The results obtained by Prowse and Jasinski showed that there was a reduction in the breakdown stress for air as the irradiator approached the test gap. (Graph 1). This reduction was of the order 10% for an irradiator movement of 8 cms, (d from 10 to 2 cms), and a pressure of 760 m.m.Hg. The frequency was 2.800 Mc/S.

The present 10,000 Mc/S work gave a similar reduction, i.e. of the order 8%, but the irradiator distance change was some 115 cms, (d from 130 to 15 cms), and the pressure range only extended up to 75 m.m.Hg. This pressure range could not be extended due to power limitations.

Similar variations in the breakdown stress were found for hydrogen and nitrogen: the results for all three gases were not very reproducible.

Oxygen, however, at 10,000 Mc/S, did give reproducible results, (Graph 8), showing a large increase in the stress as the irradiator moved from 15 to 130 cms. The curves however exhibit an opposite curvature to the 11 and 2,800 Mc/S curves. A further difference was noted in that for 11 Mc/s no increase could be detected for pressures above 25 m.m.Hg and  $d > 5$  cms (Graph 16) as opposed to pressures up to 42 m.m.Hg and  $d$  up to 75 cms. for 10,000 Mc/s. One possible explanation may be that the 10,000 Mc/s. results correspond to one section of the curve relating breakdown stress with p.d, while the 2,800 Mc/s work corresponds to a second portion of the curve exhibiting an opposite curvature.

4.1.2. Flux density variation. Prowse and Jasinski also established that alterations in the aperture admitting the ultra-violet radiation altered the probability (i e. statistical lag) of breakdown only, and not the breakdown stress at a given pressure: these findings were confirmed at 11 and 10,000 Mc/s. (Section 2.1.1. Chapter 11, and Section 3.3.1. Chapter 1 respectively). A general decrease in the statistical lag was noted as the aperture

size increased.

No absolute values of the statistical lags for 11 or 10,000, Mc/s for a particular aperture size were determined: all that can be stated is that there was a reduction in the lag as the aperture size was increased but no change in the breakdown stress for a given irradiator position and pressure. This latter point is corroborated by the reproducibility of the  $p - E$  curves over a period of many months.

#### 4.2.2. Effect of radio active source.

A contrast between the microwave and h - f results is found: for microwave the breakdown stress values recorded using a  $\gamma$  ray source for the irradiating system were substantially the same as the stresses determined with irradiator at  $d$  minimum. The opposite is true for the 11 Mc/s work, where the breakdown stress using the mesothorium radiation was identical to the stress for non-irradiated discharge, or for the irradiator at  $d$  maximum. This is clearly seen in air, the step graphs (Graph 15). The pressure ranges for the microwave and h - f work were substantially the same, (5 to 100 m.m.Hg).

The agreement in the stress for breakdown initiated by the  $\gamma$  ray source or the irradiator in its near position, (i.e. at 10,000 Mc/s), suggests

the formation of grouped electrons: mutual reinforcement could therefore be operative, i.e. this assumes that breakdown is a function of the actual concentration of electrons. (Section 1.1.3.) There is no reason to think that the  $\gamma$  ray source could make any measurable contribution to the quasi-chemical effects. (Section 1.1.4.)

Where the breakdown stress recorded with the irradiator at the near position falls below the stress for a discharge initiated by the  $\gamma$  ray source, there is a presumption that quasi-chemical effects, excitation of the gas molecules, and plasma spread in the test gap, are contributing.

#### 5. Possible causes of the lowering of the breakdown stress.

The possible causes of the reduction in the breakdown stress of a gas as the irradiating spark approaches the resonator, or electrode system, are fourfold.

5.1. The formation of grouped electrons which will give mutual reinforcement: breakdown is a function of the actual concentration of electrons.

5.2. The dissociation of molecular gases into atomic form: quasi-chemical effects or the formation of temporary molecules, e.g.  $H_3$  ). Passing oxygen through a Tesla discharge before it entered the gas chamber did not however produce any lowering in the breakdown stress. The

time of decay of the created molecules ( $O_2$ , etc.) may be important here.

5.3. The production of excited states within the gas: these excited states might be produced by quanta from the irradiating spark, or by electrons.

It has been suggested<sup>65</sup> that the production of instability in a gas at microwave frequencies is partly due to the electron moving in an activated atmosphere. (Where activated atmosphere refers to a region in which some of the gas molecules have been raised by inelastic collisions with electrons to a series of excited states). In a microwave field an electron drifts back and forth along some defined track, being only dispersed by diffusion, and could thus return into its own activated zone. An electron of lower energy than the ionisation level could therefore produce a further electron by a collision with an excited molecule. Thus the random velocity to produce ionisation would not have to be that necessary for direct ionisation, but some lower velocity. As the random velocity is dependent on the applied stress, the stress necessary to produce ionisation of an excited molecule will be lower than that necessary for direct ionisation of a molecule. The life of a molecule in the excited state is short<sup>64</sup>,  $10^{-8}$  to  $10^{-7}$  secs., i.e. it rapidly returns to its ground state.

These excited states in the molecules might also be produced by quanta from the irradiating spark, (these quanta having insufficient energy for direct ionisation).

Considering the variation of breakdown stress with the position of the irradiator: the production of these excited states by the quanta from the irradiating spark will be greater for near positions of the irradiator as compared to the far positions. In the distant irradiator positions a proportion of the quanta capable of producing excited levels in the gas molecules will be absorbed in the gas column situated between the irradiator and the resonator. Therefore to produce the necessary electron concentration for instability the random velocity of the oscillating electrons must be increased: i.e. increase in the applied stress.

5.4. Finally the reduction in the breakdown stress of a gas as the irradiator approaches the resonator could be caused by plasma spread from the irradiator down the irradiator tube, as already enunciated.

#### 6. Frequency effect.

It has been suggested that the irradiator may be the source of two types of stimuli -

- 1 Ultra-violet radiation
- 2 A spreading discharge reaction (i.e. the

penetration of the test gap by a plasma).

At different frequencies the relative importance of these two stimuli is likely to be different, but in the most striking case, (10 Mc/s to 10,000 Mc/s), frequency is not the only factor changed. Notably at 10,000 Mc/s. the communication tube from the irradiator passes through an earthed metal sleeve (i.e. resonator end plate, figure 9). It seems that this will limit plasma spread, but not necessarily kill it. At lower frequencies the electron ambit is proportionally greater so that :

(a) the decay of excited states in the gas molecules and (b) the reduced probability of an electron re-striking a given molecule may reduce the importance of the excited atmosphere, i.e. the storage of energy in excited molecule states may only be important at a high level of activation, in which case the relatively small contribution of the ultra-violet may be unimportant.

It can be stated that for the special conditions of these experiments (only) plasma spread as compared with ionisation by quanta is likely to be more important in the lower frequency region, (1 to 11 Mc/s.)



PART II.Introduction to Part II.

An electron moving under the influence of a microwave field will follow an oscillatory path; the amplitude of oscillation will be dependent on the frequency and magnitude of the applied field; the electron displacement is also dependent on the gas pressure. At the frequency used in these experiments, 10,000 Mc/s., and within the pressure range 5 to 160 m.m.Hg., these electron displacements are small compared with the resonator dimensions.. An electron moving under such conditions will produce excited molecules in the gas by non-ionising collisions along its path: it can therefore be envisaged that the electron moves back and forth through its own excited atmosphere. Therefore by successive collisions the production of a further electron can occur, even though

the original electron did not possess sufficient energy to ionise by a single collision with a gas molecule. This second electron moves into an excited atmosphere and in turn raises the level of the stored energy. It has been suggested<sup>65</sup> that such a cumulative process can lead to breakdown of the gas, the electric stress necessary for this microwave discharge being somewhat lower than that required for a low frequency, or steady field, discharge at the same gas pressure.

Diffusion to the walls of the discharge chamber appears to be the chief electron removal mechanism in a non-attaching gas; volume recombination is dependent on the square of the ionic concentration and will not therefore be effective. Removal of electrons by attachment to gas molecules only applies to air and oxygen, for the other gases used in these experiments, hydrogen, nitrogen and neon, this removal mechanism cannot be assumed to be generally operative; a more widely applicable mechanism is required.

The American diffusion theory has already been outlined in the historical introduction (page 16), the time necessary to establish such an equilibrium process is far too long to be applicable to one microsecond pulsed breakdown. The diffusion theory also requires the breakdown stress of a

gas to be a function of the electrode separation. Pim's<sup>36</sup> results in air for frequencies 100 to 300 Mc/s. and gap widths 0.3 to 0.85 m.m. showed a constant breakdown stress for a given gas pressure; these results agree with Cooper's<sup>47</sup> values for pulsed breakdown at 2,800 and 10,000 Mc/s. This would suggest that air has a unique value of breakdown stress dependent only on the gas pressure. Unfortunately no comparative results are available for other gases.

The following experiments were therefore undertaken to explore the mechanism operative in the establishment of a microwave discharge in a gas.

By the application of a unidirectional field at right angles to the microwave field it was envisaged that the electron concentration in the gas would be reduced. The electron path will now become extended to form a zig-zag, thereby removing the electron from its own excited atmosphere. It would thus seem that with the simultaneous application of a steady field at right angles to the microwave field, the breakdown stress of the gas under the microwave field would be changed. Experiments of this nature are described in Part II of this thesis.

Previous work undertaken with combined fields.

Kirchner<sup>28</sup> and Varela<sup>82</sup> both established that a

unidirectional field applied parallel to the high frequency field either caused the high frequency discharge to vanish, or impeded its formation; a greater high frequency field was necessary to initiate the discharge. Varela employed 5 microsecond pulses of 120 Mc/s. oscillation at a pulse repetition rate of 400 pulses per second; the increase in the high frequency field necessary to produce breakdown was attributed to an increase in the deionisation of the gas. (Hydrogen at 50 m.m.Hg.) As the unidirectional field was operative continuously the deionisation of the gas was a continuous process as opposed to the increase in ionisation due to the steady field during the 5 microsecond high frequency pulses.

Similar results in air at 150 Mc/s. continuous wave, at 760 m.m.Hg. are recorded by Pim<sup>36</sup>; once again the unidirectional field was applied parallel to the high frequency field. The evidence of Pim's experiments supports the idea that breakdown is the result of the formation of a critical concentration of positive ions within the gap.

In all these experiments the two fields were applied in the same direction: it would appear that no work has been recorded for orthogonal electric fields.

CHAPTER I.The Apparatus.1. The Problem.

It was again considered expedient to use a resonator in the  $H_{011}$  mode as the most suitable means of investigating the electrodeless discharge of a gas, when under the combined influence of a microwave and a unidirectional field. The problem amounted to applying at right angles to the electric ring, ( $E_e$ ), a unidirectional field, the latter to be directed along the  $Z$  axis of the resonator, (i.e. along the axis of the cylinder).

The effect of a unidirectional field was first explored with the resonator described in Part I; the steady voltage was applied to the movable piston of the resonator. The construction of the resonator was such that the movable piston was carried on an insulated rod, and had no electrical contact with the curved walls of the resonator. Neither the application of a steady voltage of 7 K. volts to the movable piston nor the application of a potential of approximately 4 K volts (derived from the magnetron H.T. pulse) caused any observable reduction in the microwave stress necessary for breakdown.

However the field distribution for the applied voltage was not of the required magnitude or direction with respect to the microwave field. Later work using an electrolytic tank to plot the equipotential lines for the steady field confirmed this; a typical plot is shown in figure 27.

The conditions of the proposed investigation were not satisfied: a new resonator was therefore designed to give the necessary field distribution at the filament where the circuital microwave stress was a maximum.

## 2. Apparatus.

### 2.1. Requirements to be satisfied by resonator.

2.1.1. The resonator must be so constructed that a unidirectional field could be applied in such a manner as to be at right angles to the ring of maximum electric microwave stress, and parallel to the longitudinal axis of the resonator, (the Z axis.).

2.1.2. Magnetic coupling between the resonator and the wave guide was again envisaged. This was accomplished by means of two holes, as shown in figure 29. This type of coupling requires the holes to be separated by a distance equal to  $\lambda_g/2$ , ( $\lambda_g$ , wavelength of the  $H_{01}$  wave in the wave guide), the two coupling apertures then appear opposite the positions of maximum longitudinal magnetic field in the wave guide.

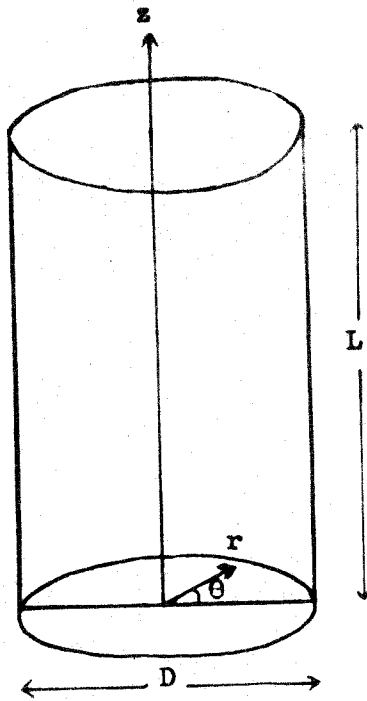


Fig. 21 . Resonator co-ordinates,  $r$ ,  $\theta$ , &  $z$ .

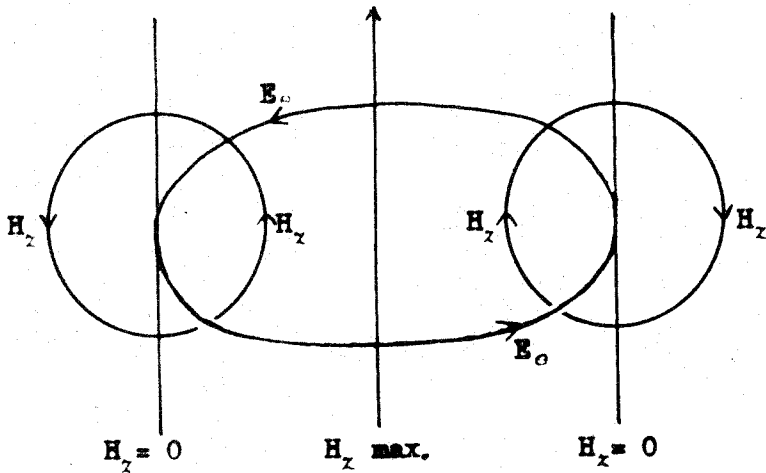


Fig. 22 . Field distribution in  $H_{01}$  mode.

2.1.3. It was further argued that if the two coupling holes were opposite the position of maximum circuital stress in the resonator, the maximum possible coupling efficiency would be achieved. Therefore the diameter of the ring of maximum electric stress,  $R$ , must be equal to half the distance between the coupling holes.

$$\text{i.e. } R = \lambda_g/4$$

2.1.4. The resonator had therefore to conform to the following conditions :-

(a) Must be designed so that a steady field could be applied at right angles to  $E_\theta$  and parallel to the  $Z$  axis.

(b) Separation of the coupling holes must equal  $\lambda_g/2$

(c) Radius to maximum circuital stress,  $R$  must be  $\lambda_g/4$

## 2.2. Theory and design of the $H_{011}$ resonator.

2.2.1. General Theory. Using the polar co-ordinates  $Z$ ,  $r$  and  $\theta$ , the field equations for a cylindrical resonator working in the  $H_{011}$  mode are<sup>83</sup> :-

$$\text{Electric Components } \left\{ \begin{array}{l} E_r = 0 \\ E_\theta = -J_0' \left( \frac{2 \chi_{011} r}{D} \right) \frac{\sin \pi Z}{L} \\ E_z = 0 \end{array} \right.$$



Magnetic Components.

$$\left\{ \begin{aligned} H_r &= \frac{\pi}{L} \frac{1}{\sqrt{\left(\frac{2x_{01}}{D}\right)^2 + \left(\frac{\pi}{L}\right)^2}} J_0' \left( \frac{2x_{01}r}{D} \right) \cos \frac{\pi z}{L} \\ H_\theta &= 0 \\ H_z &= 2 \frac{x_{01}}{D} \frac{1}{\sqrt{\left(\frac{2x_{01}}{D}\right)^2 + \left(\frac{\pi}{L}\right)^2}} J_0 \left( \frac{2x_{01}r}{D} \right) \sin \frac{\pi z}{L} \end{aligned} \right.$$

Where L = length of the resonator.  
 D = diameter -do-  
 $x_{01}$  = First root of  $J_0'(x) = 0$ .

In such a resonator the resultant electric, and magnetic, field patterns oscillate in quadrature; also at the position of maximum circuital electric stress, ( $E_\theta$  maximum), the longitudinal magnetic field  $H_z$ , will be a minimum; i.e.  $H_z = 0$ .

Therefore by equating  $H_z$  to zero the position of  $E_\theta$  maximum can be obtained:-

$$\therefore 2 \frac{x_{01}}{D} \frac{1}{\sqrt{\left(\frac{2x_{01}}{D}\right)^2 + \left(\frac{\pi}{L}\right)^2}} J_0 \left( \frac{2x_{01}r}{D} \right) \sin \frac{\pi z}{L} = 0$$

For this condition either 1.  $\sin \frac{\pi z}{L} = 0$

or 2.  $J_0 \left( \frac{2x_{01}r}{D} \right) = 0$

Now:- (1) Gives  $z=0, L$ ; not the condition required.

(2) This can be evaluated easily; knowing D

there is a series of values for  $r$ , where  $E_0$  is a maximum, (i.e. a series of values of  $R$ ), of these values only one is admissible.

Assuming a wave guide of Standard British Xband cross section, i.e. 2.54 cms. X 1.27 cms., the value of  $\lambda_g$  can be obtained from:-

$$\frac{1}{\lambda_g^2} = \frac{1}{\lambda^2} - \frac{1}{\lambda_c^2}$$

where  $\lambda_g$  = wavelength of  $H_{01}$  wave in wave guide.

$\lambda$  = " " T.E.M. wave in free space.

$\lambda_c$  = cut off wavelength, i.e. 2. x 2.54 cms.

For the frequency used, namely 9375 Mc/s,  $\lambda = 3.198$  cms., and the value of  $\lambda_g$  becomes 4.275 cms. for the given waveguide.

$\lambda$  is determined by the magnetron frequency, so that  $\lambda_g$  is also fixed.

As stated in section 2.1. the conditions to satisfy are:-

$$\frac{\lambda_g}{2} = 2R = \text{separation of coupling holes.}$$

Therefore  $R$  is fixed and is equal to 1.069 cms. Using this value in  $J_0\left(\frac{2\alpha_{01}R}{D}\right) = 0$ , a series of possible values for  $D$  can be obtained, the diameter of the resonator<sup>84</sup>.

For a given value of  $\mathcal{D}$ , by means of the relationship

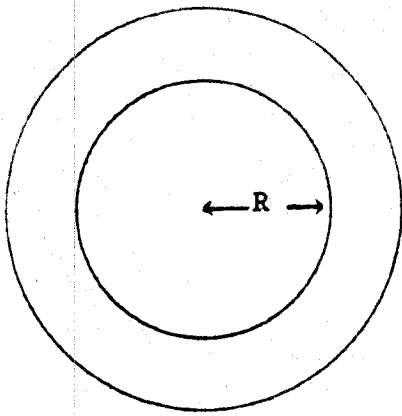
$$\lambda = \frac{2}{\sqrt{\left(\frac{2\pi c_0 l}{\mathcal{D}}\right)^2 + \left(\frac{1}{L}\right)^2}}$$

the corresponding value of  $L$ , the length of the resonator can also be determined. Thus knowing  $\mathcal{D}$  and  $L$ , the necessary dimensions, the resonator can be constructed to satisfy two of the three given conditions. The third requirement, i.e. to be constructed to allow the application of a longitudinal field is discussed in a later section, (Section 2.3.)

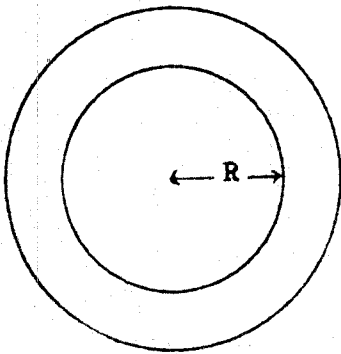
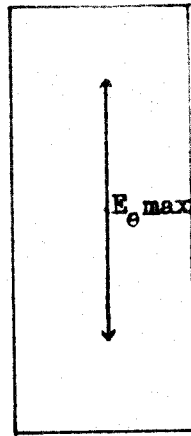
2.2.2. Application of theory to given waveguide. A series of values for  $\mathcal{D}$  can be determined for the given dimensions of the Standard British X band waveguide; however using these values of  $\mathcal{D}$  the value of  $L$  becomes an imaginary quantity. Therefore it is impossible to satisfy the given conditions using a waveguide of these dimensions. The values of  $\mathcal{D}$  so calculated are :- 3.406 cms., 1.484 cms., 0.947 cms., etc.

It can easily be shown that for real values of  $L$ , the value of  $\mathcal{D}$  must be greater than 3.902 cms., which in turn means that  $\lambda_g$  must exceed 4.898 cms.

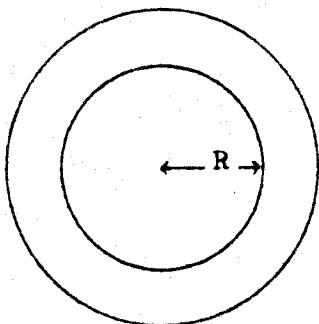
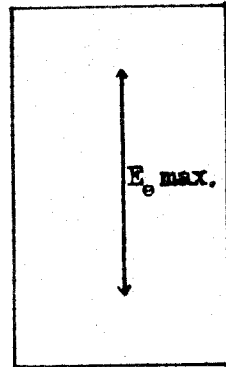
To increase  $\mathcal{D}$ ,  $\lambda_g$  must be increased



$B = 1.8\text{cms}$



$B = 1.9\text{cms.}$



$B = 2.0\text{cms.}$

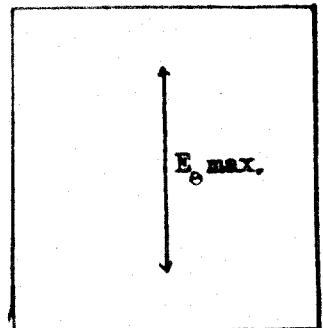


Fig. 23 , Plan & elevation views of resonators  
for  $B = 1.8, 1.9, \& 2.0\text{cms.}$

which is readily accomplished by a suitable adjustment, (a reduction), to the larger dimension, A, of the waveguide.

2.2.3. The Limiting Case. As shown, to satisfy the given conditions, we must have:-

$$\begin{aligned} \text{which gives:- } & D \geq 3.902 \text{ cms. (For real values of L)} \\ & R \geq 1.225 \text{ cms.} \\ & \lambda_g \geq 4.898 \text{ cms.} \\ \text{and} & \lambda_c \leq 4.224 \text{ cms.} \\ \text{or} & A \leq 2.112 \text{ cms.} \end{aligned}$$

The table below summarises the results obtained using values of A of 1.8, 1.9 and 2 cms; a series of sketches of corresponding resonator dimensions is given in figure 23.

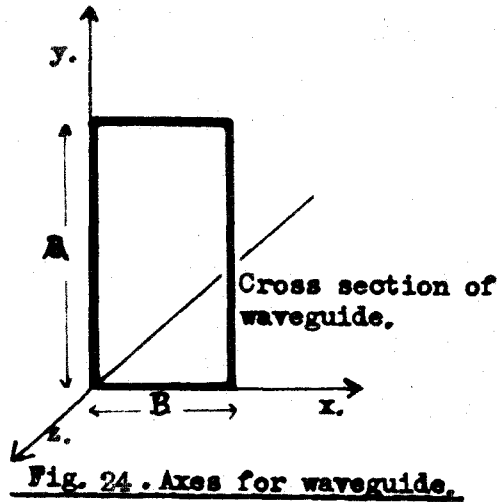
TABLE 16. Summary of possible resonator dimensions, etc.

A.	$\lambda_c$	$\lambda_g$	D.	All L in cms.	
1.8	3.6	6.966	5.549	2.249	
1.9	3.8	5.921	4.717	2.845	
2.0	4.0	5.325	4.242	4.075	
Limiting Case	$\leq 2.112$	$\leq 4.224$	$\geq 4.898$	$\geq 3.902$	Imaginary.

#### 2.2.4. Variation of $H'_z$ in waveguide with y.

The variation of the longitudinal component of the magnetic field  $H'_z$ , in the waveguide is given by:-

$$H'_z = -j \frac{\pi \lambda}{2} \sqrt{\frac{\epsilon}{\mu}} \cdot \frac{1}{A^2} \cos \frac{\pi y}{A} e^{j(\omega t - \frac{2\pi z}{\lambda_g})}$$



Where,  $\epsilon$  = permittivity of guide filling.

$\mu$  = permeability.

$\omega$  = angular frequency.

Choosing a point where  $y = A$ , i.e. at the edge of the wave guide the equation reduces to:-

$$H'_z = K \frac{1}{A^2} e^{-j \frac{2\pi z}{\lambda_g}}, \quad \left( K = j \frac{\pi \lambda}{2} e^{j\omega t} \sqrt{\frac{\epsilon}{\mu}} \right)$$

The distance  $z$  of interest down the guide is the position opposite the coupling holes, (i.e. at  $H'_z$  maximum), or an integral number  $n$  of  $\lambda_g$ 's down the guide,  $z = n \cdot \lambda_g$ . We can therefore write  $e^{-j \frac{2\pi z}{\lambda_g}}$  as  $e^{-j 2\pi n}$  or a constant for a given position down the guide.

$$\therefore H'_z = \frac{N}{A^2}, \quad N = K e^{-j 2\pi n} = \text{a constant for a given point down the guide.}$$

The ratio of  $H'_z$  (at a given position in the guide), for two different waveguides is thus the ratio of  $\frac{A_1^2}{A_2^2}$ , where  $A_1$  and  $A_2$  are the respective dimensions in the  $y$  axis, i.e.

$$\frac{H'_z}{H'_z} = \frac{A_2^2}{A_1^2}$$

This ratio for the Standard British X Band wave guide, and a wave guide of cross section 1.9 x 1.27 cms. is 1 : 1.6, i.e. the wave guide of cross section 1.9 x 1.27 cms. shows an increase 60% in the value of  $H'_z$ .

The coupling efficiency increases with increasing  $H'_z$  and will therefore be increased by a reduction in the larger dimension of the wave guide.

#### 2.2.5. Variation of the Poynting Flux down the waveguide due to a change in A.

It is easily shown that an approximate reduction of 7% is caused in the Poynting Flux by reducing the waveguide dimensions from 2.54 x 1.27 cms. to 1.9 x 1.27 cms.

2.2.6. Final choice of dimensions. It was eventually decided to use a waveguide of dimensions 1.9 x 1.27 cms. for these experiments. Using a waveguide of these dimensions a resonator could therefore be constructed that conformed to the original condition. This choice results in a slight reduction in the Poynting Flux, but there is an appreciable increase in the  $H'_z$  field component in the guide. The value of A chosen is 0.212 cms below the critical size (i.e. where L becomes imaginary) which allows for slight differences between calculation and practice. Finally if

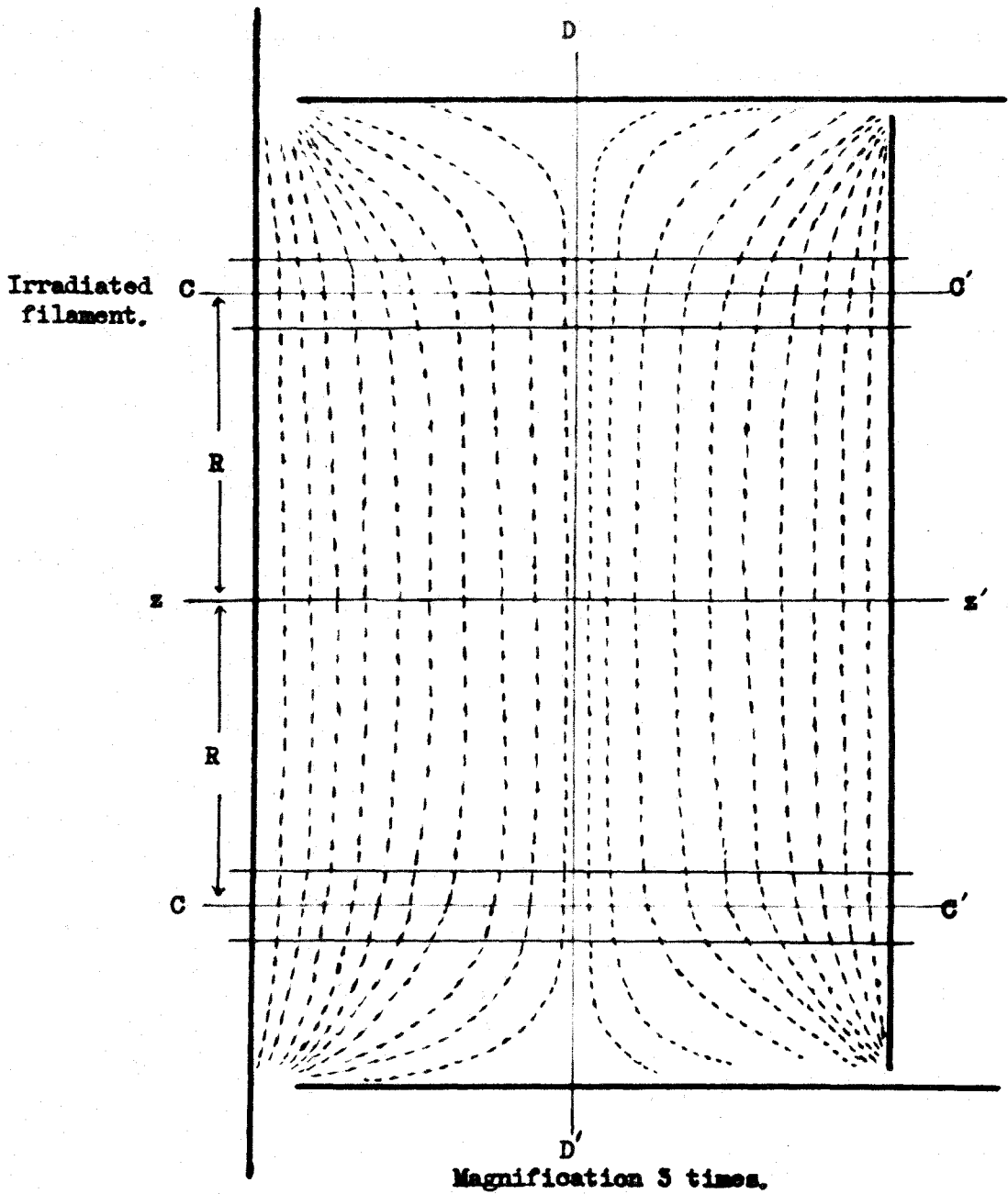


Fig. 26 . Distribution of equipotential lines (new resonator).



A were chosen too small the cross section would approach a square section, and a pure  $H_{01}$  wave would tend to become distorted in transmission down the guide. To avoid extremely difficult machining of the waveguide it was decided to only reduce one dimension.

The final dimensions were therefore:-

A = 1.9 cms.  
 B = 1.27 cms.  
 which gave D = 4.717 cms.  
 and L = 2.845 cms. at resonance  $H_{011}$  mode,  
 air dielectric.

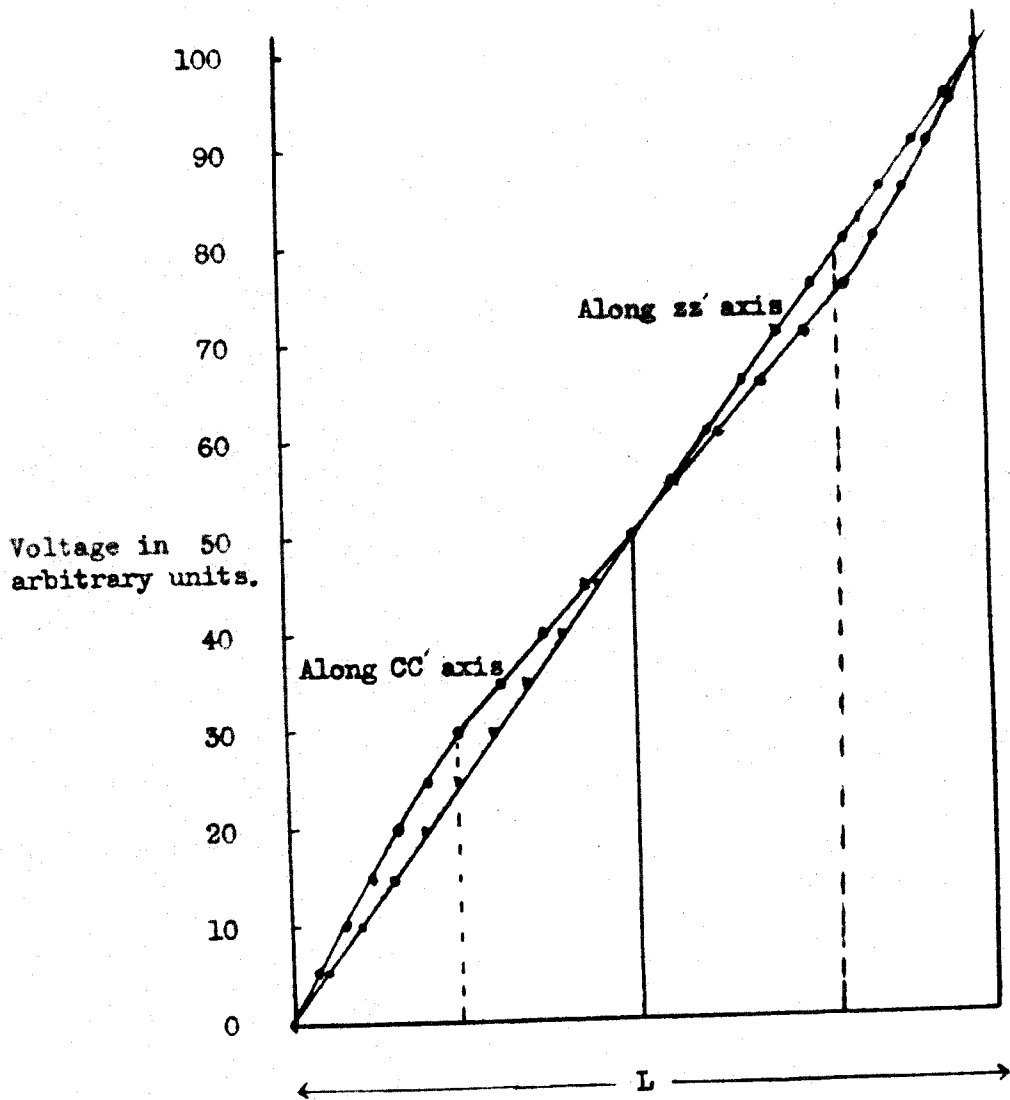
### 2.3. Steady field distribution within resonator.

It was then necessary to satisfy the most important condition of the design: that a unidirectional field could be applied at right angle to the ring of maximum electric stress, and be directed along the Z axis of the resonator.

This was accomplished by constructing the resonator of three sections, (the two ends and the cylindrical wall); each section insulated from its neighbour. As no current flow occurs in the  $H_{011}$  mode between the end plates and the curved wall such a design was possible. (Current flow diagram given in figure 7, Part I).

However before construction of such a resonator was undertaken, the distribution of the unidirectional field was explored by means of an electrolytic tank. A three times enlarged sectional model of the resonator was

Graph. 25. Voltage Distribution Along  $zz'$  &  $CC'$  Axes.



constructed, the section being taken along the  $Z$  axis of the resonator. The applied voltage was distributed so that half the voltage was applied between the movable piston and the cylinder, the remainder between the cylinder and the fixed end plate. (Figure 25). Using such an arrangement the distribution of equipotential lines, as shown in figure 26, was obtained; graph 25 shows a voltage plot along the  $Z$  axis, and along the line of maximum circuital stress, ( $CC'$ ). It can be seen that the distribution of the field in the filament of maximum circuital stress, (shaded area), is directed along the  $Z$  axis of the resonator. The voltage plot taken down the centre line  $ZZ'$  gives an even field distribution; the departure along the line  $CC'$  is small and is itself linear for the central portion, where  $E_0$  has its maximum value.

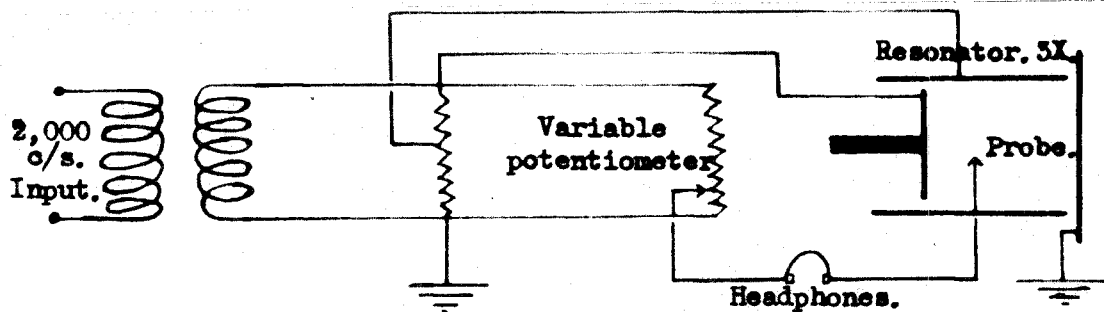


Fig. 25. Electrolytic tank circuit.

It was therefore considered that the field distribution was sufficiently uniform for the proposed

constructed, the section being taken along the  $Z$  axis of the resonator. The applied voltage was distributed so that half the voltage was applied between the movable piston and the cylinder, the remainder between the cylinder and the fixed end plate. (Figure 25). Using such an arrangement the distribution of equipotential lines, as shown in figure 26, was obtained; graph 25 shows a voltage plot along the  $Z$  axis, and along the line of maximum circuital stress, ( $CC'$ ). It can be seen that the distribution of the field in the filament of maximum circuital stress, (shaded area), is directed along the  $Z$  axis of the resonator. The voltage plot taken down the centre line  $ZZ'$  gives an even field distribution; the departure along the line  $CC'$  is small and is itself linear for the central portion, where  $E_0$  has its maximum value.

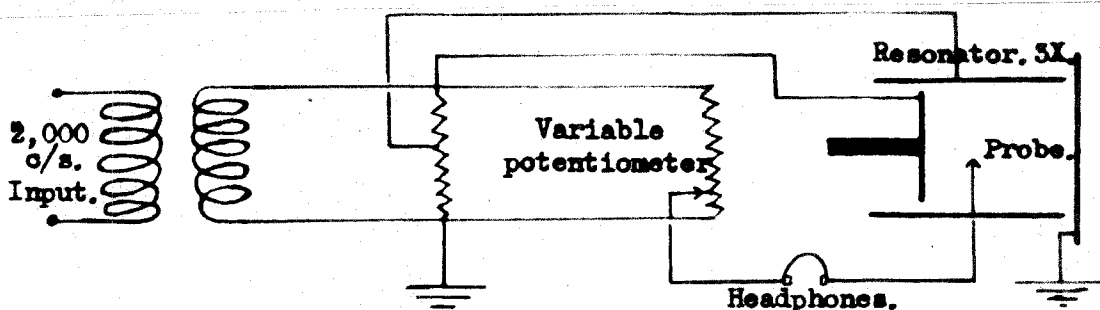
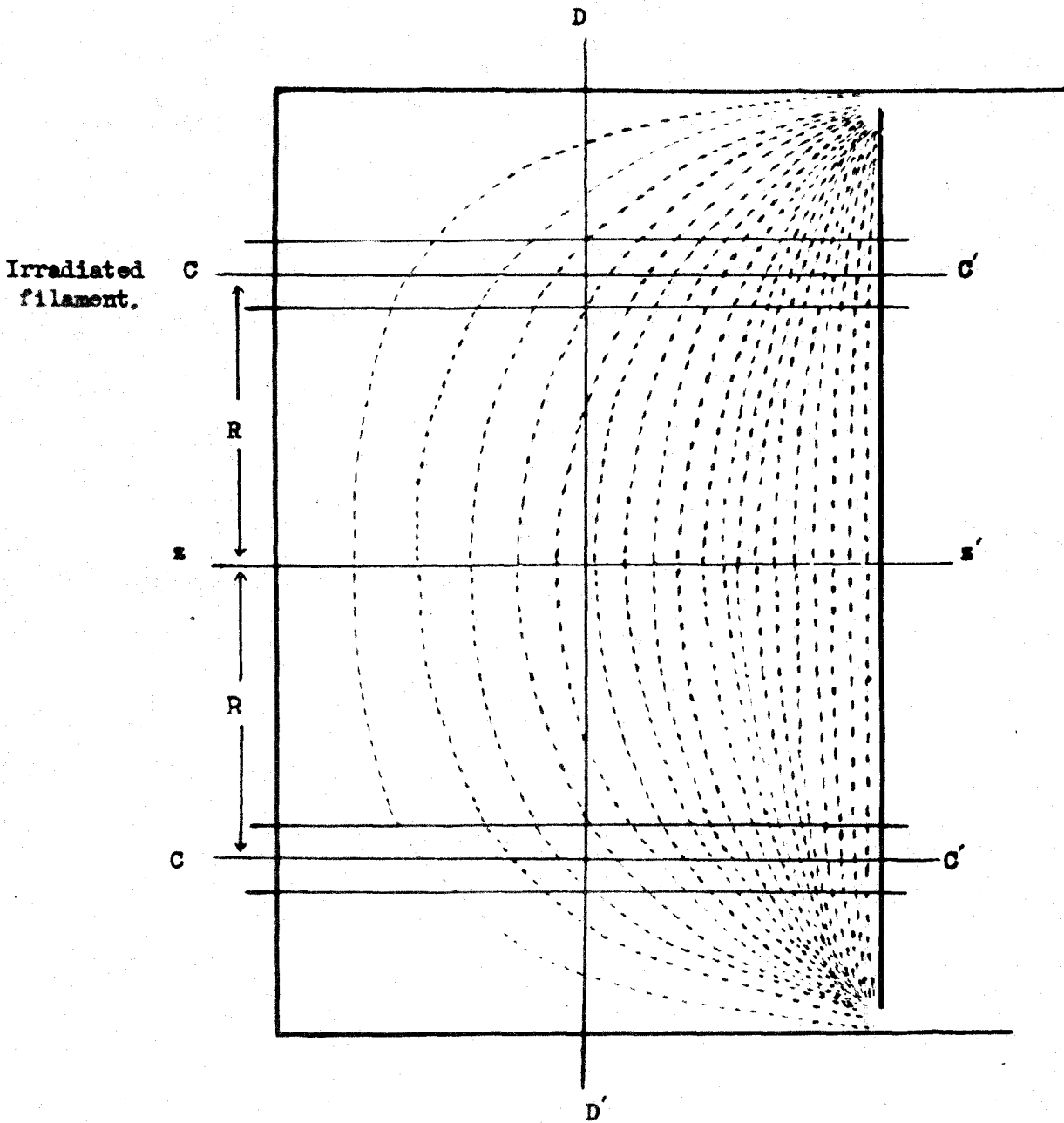


Fig. 25. Electrolytic tank circuit.

It was therefore considered that the field distribution was sufficiently uniform for the proposed



Magnification 3 times.

Fig. 27. Distribution of equipotential lines (old resonator).

experiments, and the unidirectional field value could easily be calculated for any required position.

An equipotential plot has also been included for the original type of resonator, where the full voltage was applied to the movable piston, the other end and the curved wall were in electrical contact and earthed. It can be seen that the field is directed almost at right angles to the required direction. (Figure 27).

#### 2.4. Constructional details of resonator.

The resonator can be divided into three sections the end plate, (A), rigidly attached to the waveguide, the cylindrical portion, (B), separated from the end plate by a polythene washer and screwed ebonite ring. Finally the movable piston, (C), carried as in the previous resonator on an ebonite rod. This plate is therefore insulated from the other two sections; its position is readily adjustable by means of the micrometer head. The resonator in section is shown in figure 28.

Two input ports were necessary in the end plate A, one for the magnetic pick up loop, the second for the capsule outlet tube, these two holes were also drilled as to be situated on the same circle, (concentric with the curved wall of the resonator) which also included the two coupling holes. In this way only the minimum number of the circuital

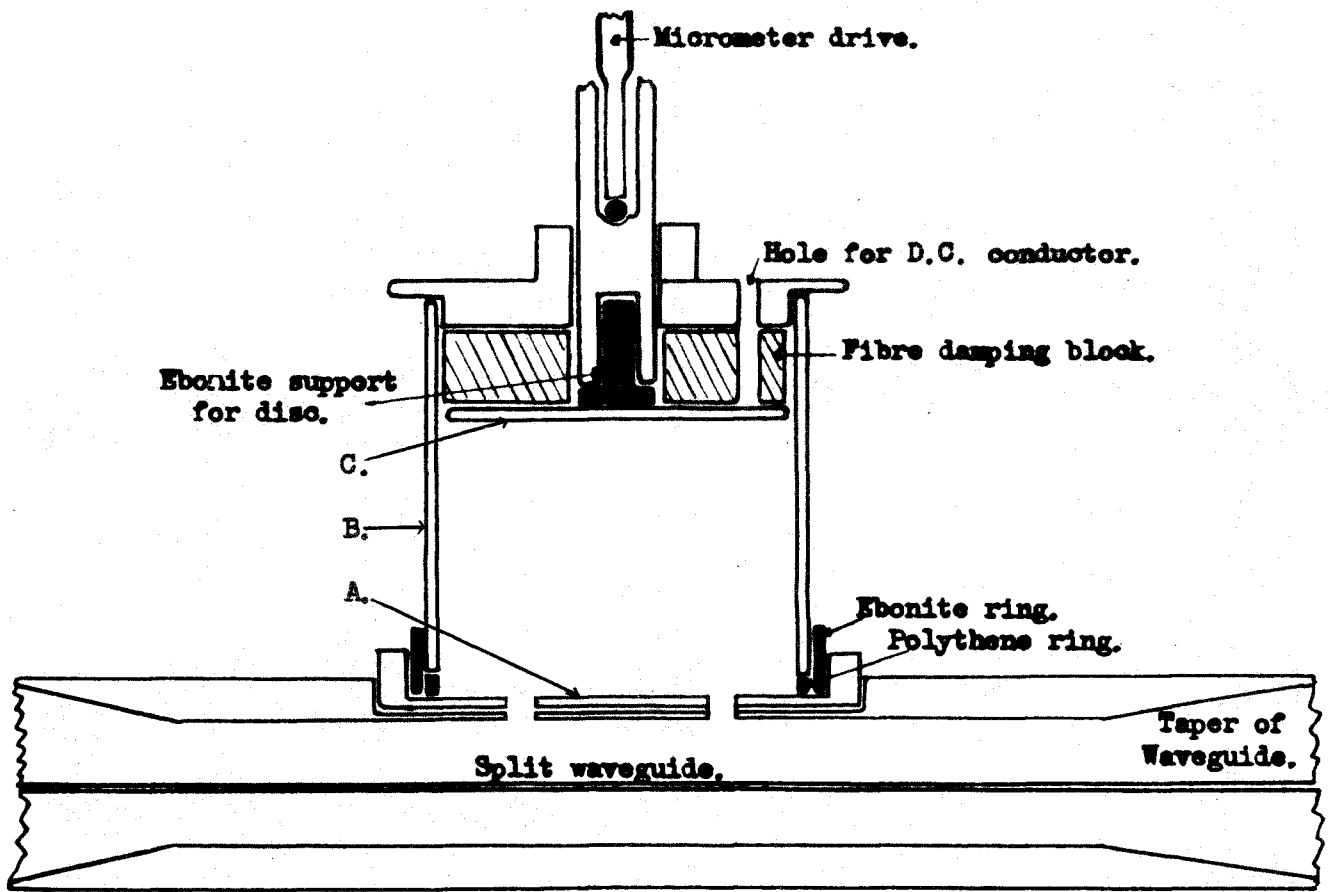


Fig. 28. Plan of resonator.

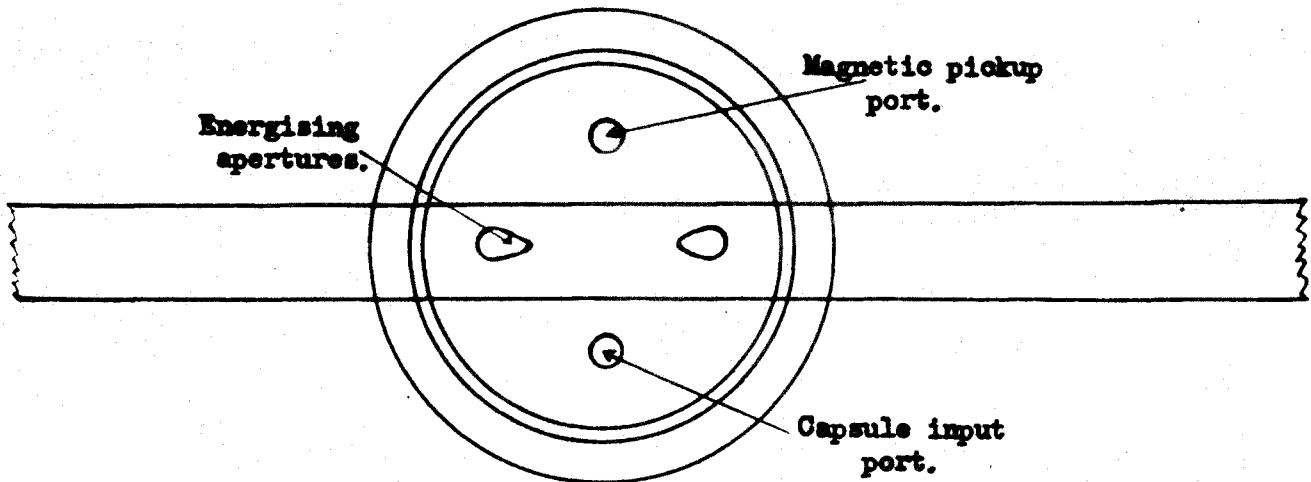


Fig. 29. Elevation of resonator.

current flow lines in the end plate were interrupted. (When working in the  $H_{011}$  mode).

## 2.5. The other microwave components.

### 2.5.1. The tapering waveguide section.

In order to permit easy access to the coupling holes a special length of waveguide was constructed, split longitudinally by a central cut parallel to the E direction in the waveguide<sup>49</sup>. As there is no current flow across the longitudinal split the arrangement did not affect the transmission of the  $H_{01}$  waveguide down the guide.

The taper in the waveguide from 2.54 cms to 1.9 cms. was gradual, the sloping faces exceeding  $2\lambda_g$  in length, thus reducing backward reflections to a minimum<sup>85</sup>.

### 2.5.2. The tuning stub sections.

These were two short pieces of standard British waveguide 2.54 cms. x 1.27 cms. with tuning stubs as shown in figure 31, and separated from each other by an odd number of quarter wavelengths, (i.e.  $\frac{\lambda_g}{4}$ ). To join these sections to the resonator waveguide section a special design of choke coupling was employed. This coupling served two purposes; to join the two sections of waveguide (i.e. tuning stub and resonator sections), and to join the two halves of the resonator waveguide section.

### 2.5.3. The choke couplings (Figure 30).

The depth of the slot in these couplers



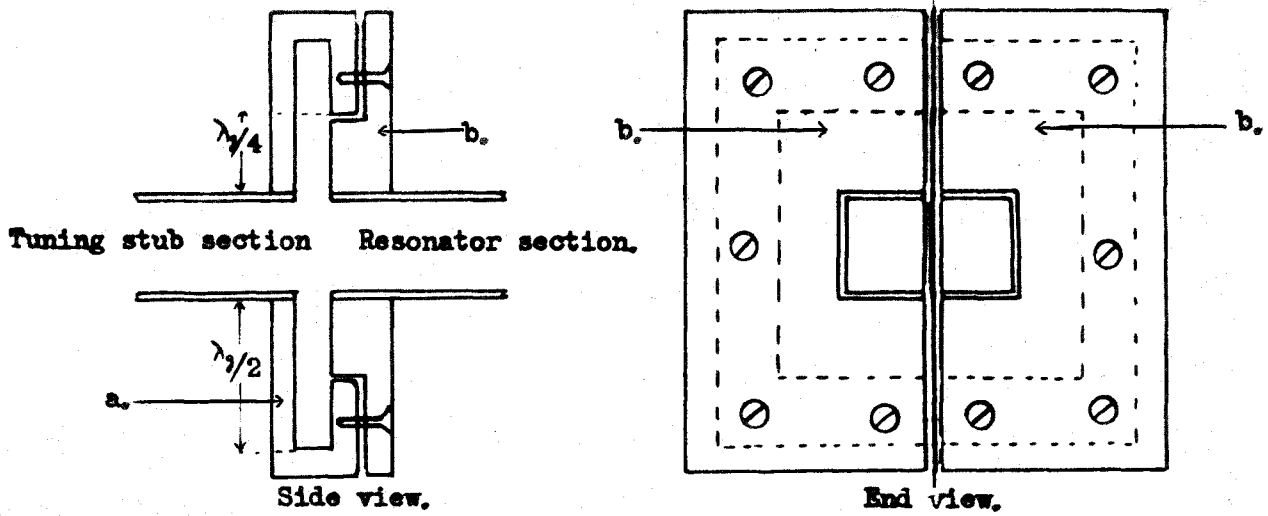


Fig. 30 , Coupler used between resonator & tuning stub sections.

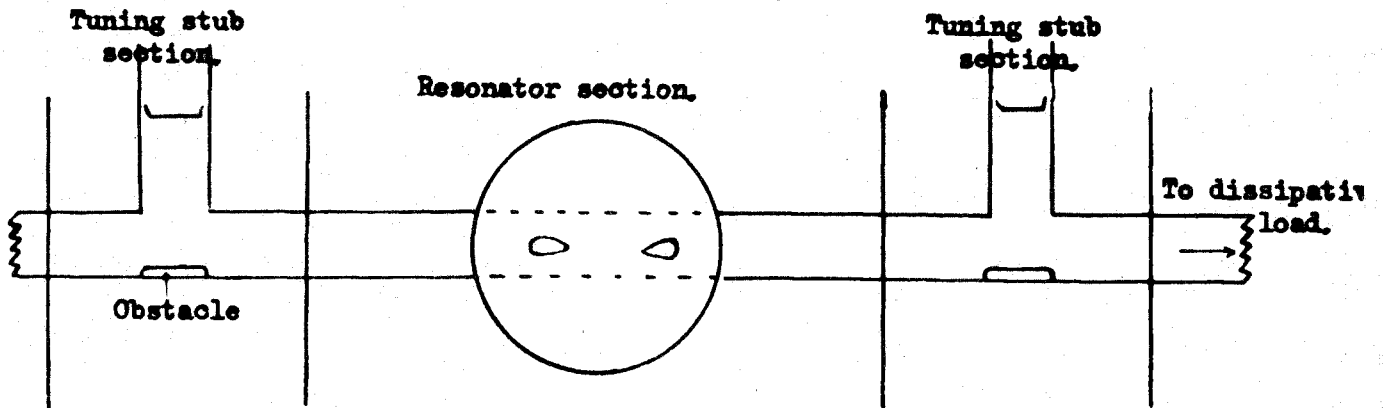


Fig. 31 , Arrangement of U.H.F. apparatus.

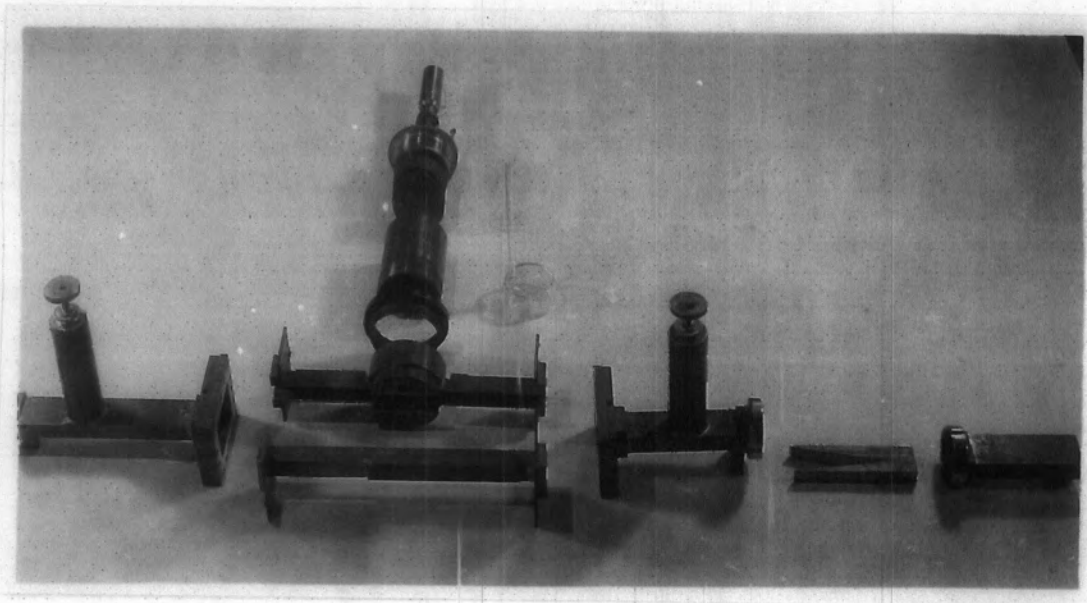
was  $\lambda/2$  thus the standing wave has an antinode of magnetic field in the slot entrance, and is continuous with the magnetic field in the wave guide. The section of the coupler (a), attached to the tuning stub section was in one piece; whilst the other side of the coupler, (b), was divided in a vertical direction, (i.e. cut in a line parallel to the E field direction in the waveguide). The two portions (b) were attached to the split section of waveguide and slotted into the single portion of the coupler attached to the tuning stub section of the waveguide (a); thus the two halves of the waveguide in the resonator section were tightly pressed together.

It will be noticed that the join in the coupling comes at a distance  $\lambda/4$  from the waveguide, the current flow is a minimum here, and a maximum at the end of the slot ( $\lambda/2$ ).

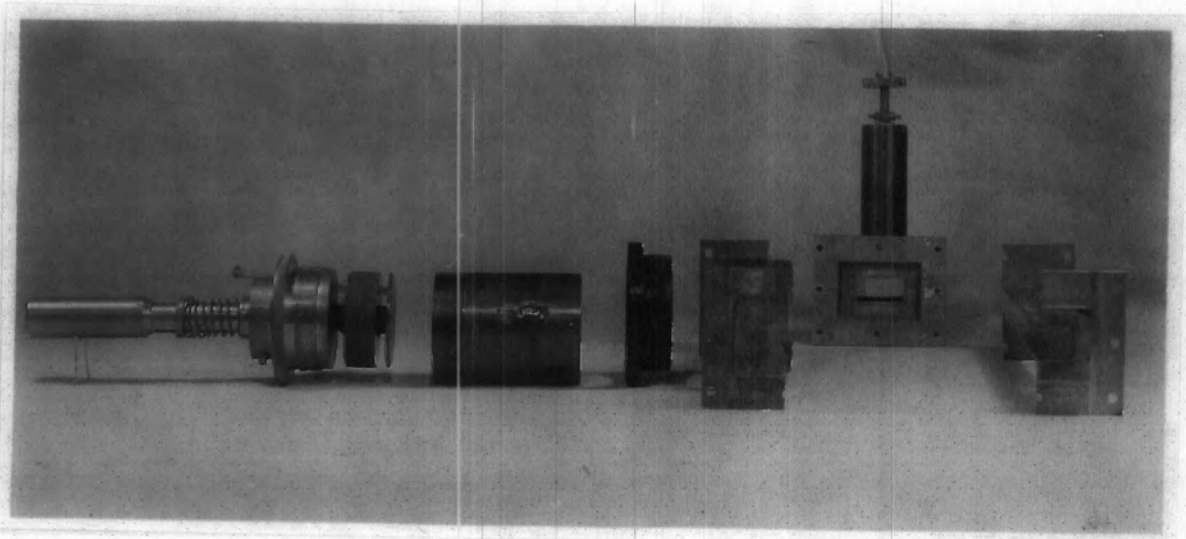
In all the waveguide and resonator joints care had to be exercised to avoid spurious sparking; it was found expedient to place a layer of thin lead or metal foil between the joints in the couplers.

#### 2.5.4. The magnetron load and feed sections.

The dissipative load consisted of a tapering block of wood, the sloping edges again being greater than  $2\lambda_g$  to reduce backward reflection to a minimum.



Figs. 32 & 33. Exploded view of microwave apparatus.



The complete microwave system was coupled to the magnetron output by means of an adjustable choke coupling when using the British magnetron, and a fixed choke coupling in the American model.

The load and magnetron sections were themselves joined to the tuning stubs sections by standard couplers.

A diagram of the microwave layout is given in figure 31, and the two photographs, figures 32 and 33, show the apparatus in an exploded form.

The measurement of the electric stress within the resonator was again accomplished by means of a small magnetic pick up loop, the output of which was displayed on an oscilloscope. The general arrangement was identical with that used in Part I.

#### 2.6. Coupling adjustments and initial use of apparatus.

Originally coupling between the resonator and the waveguide was accomplished by means of two holes  $\lambda/2$  apart. It was found that coupling holes large enough to energise the empty resonator were too small when the glass capsule was inserted, probably because of dielectric losses in the glass. The necessary increase of coupling was accomplished by elongating the holes. (Figure 29). The increase in the dielectric constant due to the insertion of the capsule moved the position of the movable piston for resonance

in the  $H_{011}$  mode slightly further out.

The system was so designed that the radiation from the irradiating spark, this time, intersected the filament of maximum circuital electric stress.

Initial experiments were conducted with the British magnetron, and breakdown in air could be achieved up to a pressure of about 50 m.m.Hg, a slightly lower limit than the previous resonator. However changing to the American magnetron breakdown could be produced up to about 70 m.m.Hg in air. (This represents about 40 K.volts round the  $E_0$  ring).

## 2.7. The unidirectional field.

### 2.7.1. General.

In the presence of a unidirectional field, the ions resulting from one discharge might be expected to form a coating on the walls of the glass capsule, and tend to neutralise the steady field across the capsule. In order to avoid this difficulty, the unidirectional field was applied in the form of pulses derived from the modulator supplying the magnetron. The pulse was obtained by means of a potential divider network; the full voltage was applied to the movable piston, half voltage to the circular walls of the resonator, the other end of the divider was connected to the fixed end wall of the resonator and earthed. The

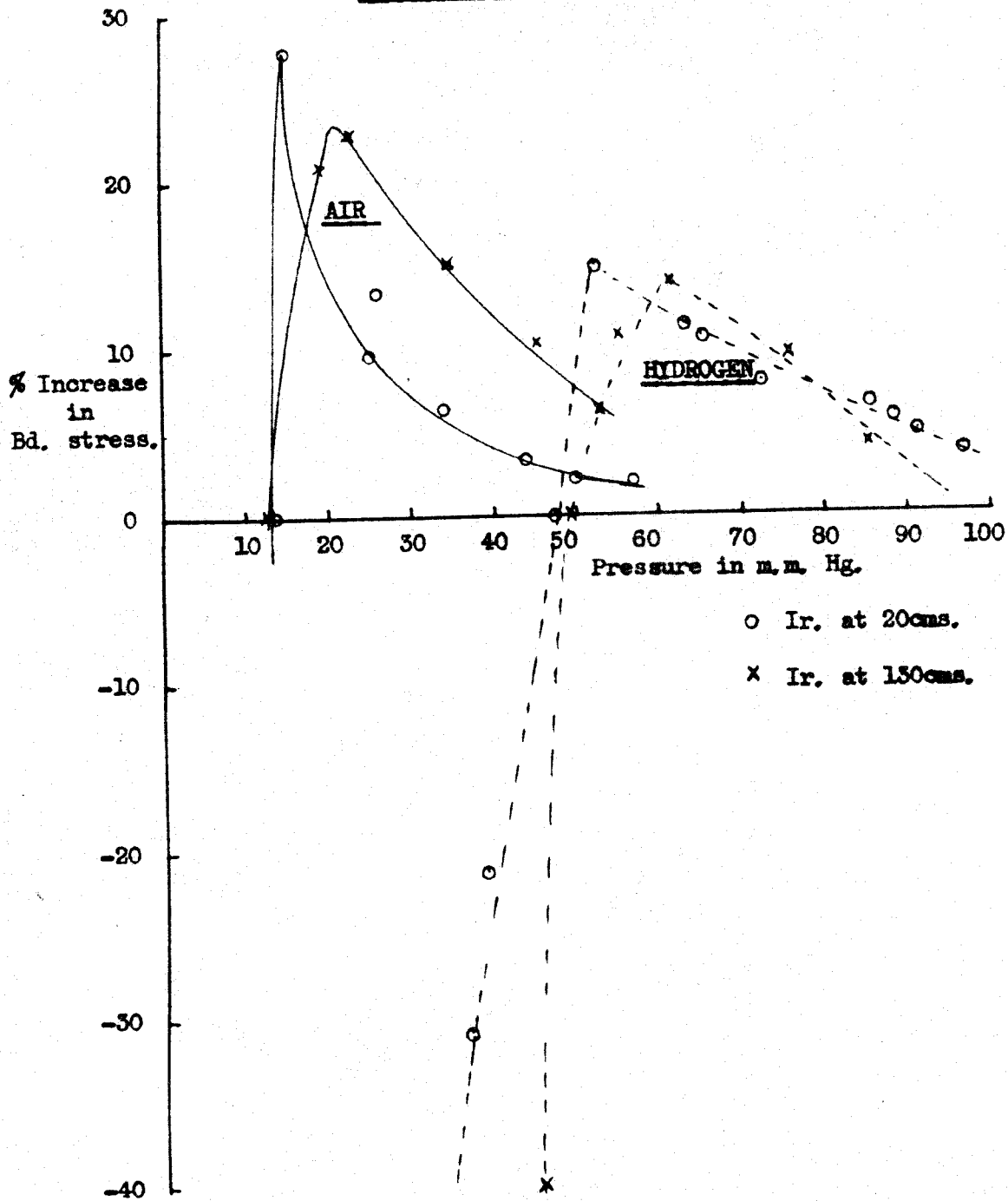
H.T. pulse was negative.

2.7.2. Measurement of the steady pulse magnitude.

The magnitude of the unidirectional pulse was measured by feeding a known fraction, (by means of a divider network), to a calibrated oscilloscope. The resulting pulse amplitude was found to have a maximum of 3.7K.volts. The incorporation of a potential divider network allowed the applied pulse to the resonator to be varied in twenty steps to a minimum of 185 volts.

The length of the resonator, L, at resonance with the glass capsule in position was 3.1 cms., and the unidirectional field produced at the position of maximum microwave circuital stress was therefore 1200 volts/cms., and could be reduced to a minimum of 60 volts.cm. The potential divider network was checked for linearity.

Graph 26 . AIR & HYDROGEN Percentage Increase in Breakdown Stress for No D.C. to Full D.C. v. Pressure.



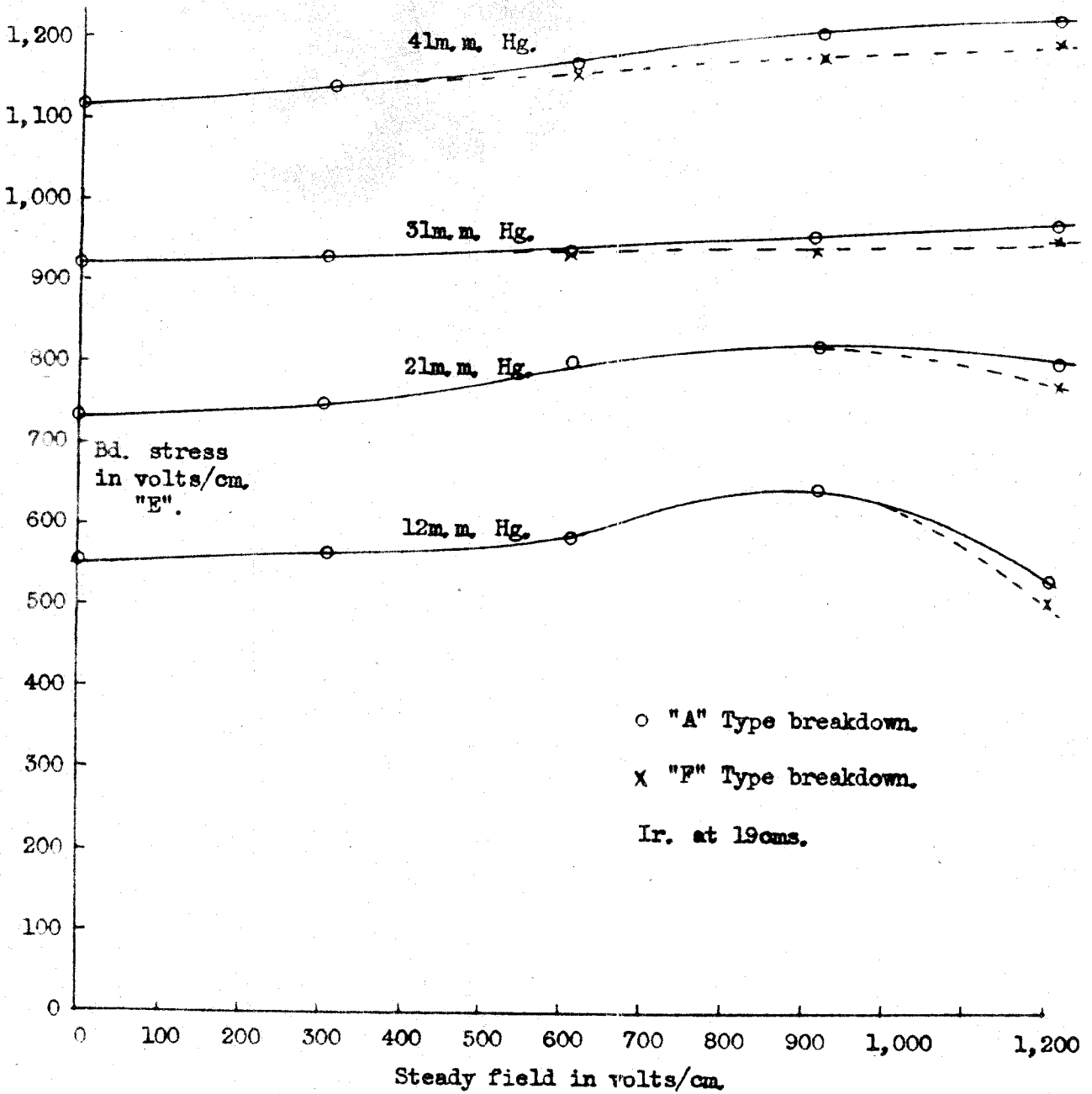
CHAPTER 2.Crossed fields, microwave and unidirectional fields.1. Initial results in air and hydrogen.

Exploratory experiments were undertaken using dry air, measuring the variation between the values of breakdown stress for the microwave field with and without the steady field present. Two positions of the irradiator were used and at first just the maximum value of the unidirectional field, i.e. 1200 volts/cm. In all cases for  $p > 22$  m.m.Hg. when the steady field was applied an increase in the value of the microwave field was necessary to produce breakdowns; this percentage increase with respect to pressure is shown in graph 26 for the two positions of the irradiator,

Similar results were found for cylinder hydrogen, and the reduction in stress for the lower pressures was more noticeable in hydrogen than air. The hydrogen results are also shown in graph 26 for two irradiator positions. In both gases recovery after a discharge was far more difficult when the unidirectional field was left switched on; i.e. switching off the microwave field and the irradiator, but on re-applying the microwave field the gas tended to breakdown spontaneously. A period up to thirty seconds or more had to be allowed to ensure complete gas recovery when



Graph 27 . AIR, U.H.F. Breakdown Stress v. Steady Field.



the steady field remained applied. This was not found to be the case when the steady field was also removed, the recovery in air then being instantaneous, and far quicker in hydrogen. The recovery troubles encountered in Part I for hydrogen were not found provided the fields were removed for a reasonable period of time, i.e. 30 seconds to one minute say. Time in all readings of up to 2 to 3 minutes was allowed between adjustments for statistical lags.

There also appeared to be a decrease in the statistical lag recorded for air, when both fields were operative, for both irradiator positions. Such lag variations were difficult to establish because of the length of the experiments.

It was felt that for quantitative purposes the variation of the microwave stress necessary for discharge with varying unidirectional fields would be easier to understand. Accordingly experiments of this type were performed: the results for each gas are considered separately.

## 2. Air (Dry).

Variation of the microwave field required to produce breakdown with the application of different unidirectional fields is shown in graph 27. Four steady field values were chosen and several such sets, taken over a

period of four months, gave similar microwave stress variations with applied unidirectional fields. For pressures less than about 20 m.m.Hg. a maximum in the curves became apparent, and the value of the steady field would seem to be almost high enough to produce normal steady discharge. This is more noticeable in the hydrogen results given in the next section.

Two types of breakdown were observed for the higher pressures in air, and these can be described as the 'F' and 'A' type of discharge:-

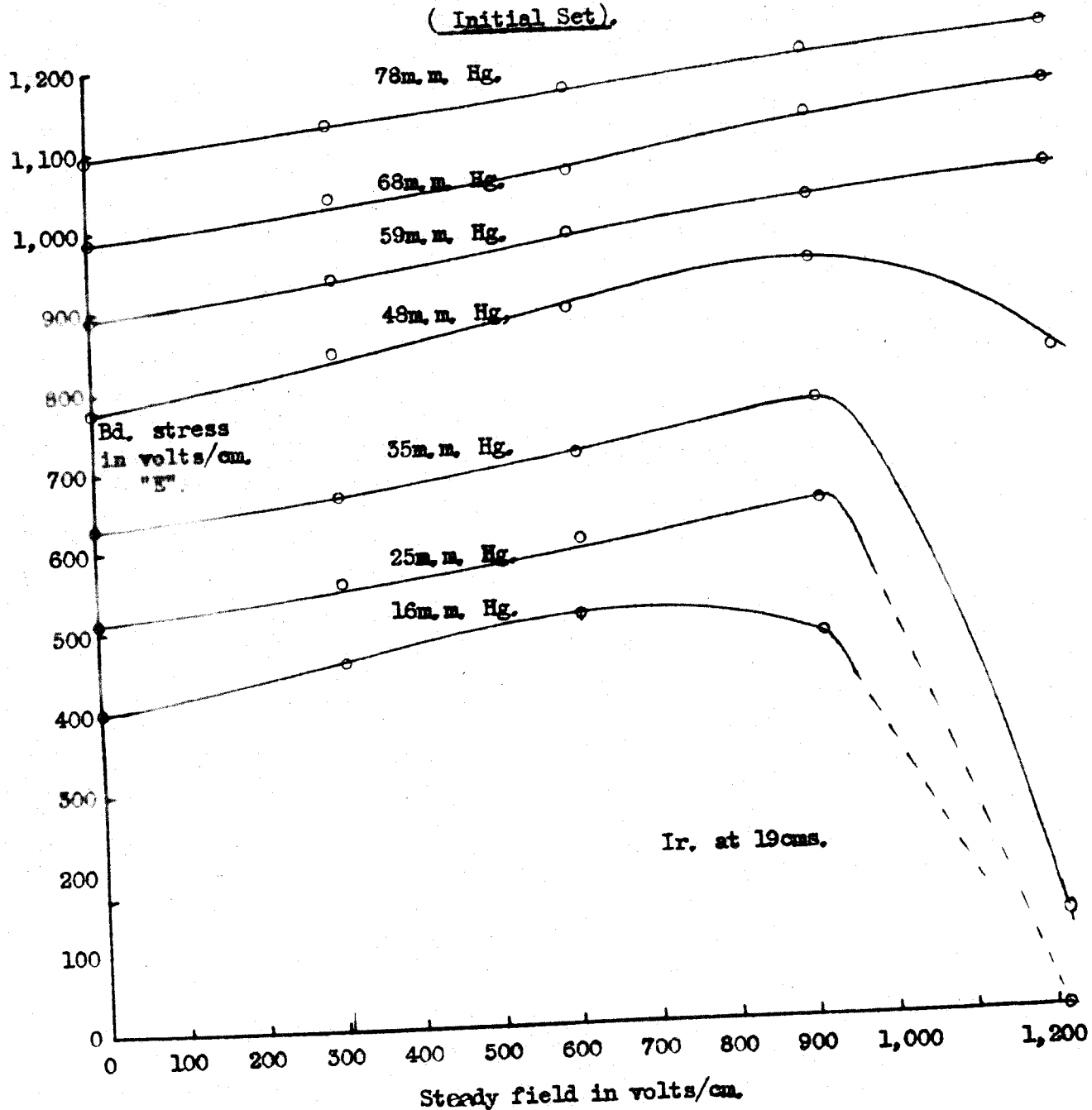
'F' type, or flick breakdown, when the pulse envelope was observed to collapse for a short duration, (1 to 2 seconds) and then recover; this field collapse recurred every 40 to 60 seconds. Switching off the irradiator stopped this type of discharge. (The pulse envelope refers to the envelope viewed on the oscilloscope screen).

'A' type, or absolute type, where complete collapse of the pulse envelope occurred remaining collapsed when the irradiator was switched off.

Variations between these two types were also occasionally observed, but they all only appeared for the higher pressures, and higher values of the applied unidirectional field.

Graph 28 . HYDROGEN, U.H.F. Breakdown Stress v. Steady Field.

( Initial Set )



These results in air were recorded with the irradiator positioned at a distance of 19 cms. from the resonator. The usual time allowance was made between resonator input adjustments for statistical lag.

### 3. Hydrogen.

The experiments in hydrogen were more extensive and were undertaken at three different times. The initial results, shown in graph 28, are substantially similar to the air results. The peaks in the curves occur at higher pressures, of the order 50 m.m.Hg.

A more detailed study revealed that, as for air various types of breakdown were apparent, four quite separate types were distinguished, and have been called the 'F', 'C', 'M' and 'A' types.

'F' type, a 'flick' was observed in the pulse envelope as viewed on the oscilloscope screen, not a complete collapse, could be described as an occasional collapse seen inside the main pulse envelope. Verified by visual observation along the capsule inlet tube.

'C' type, complete collapse of the pulse envelope, not maintained when the irradiator is switched off.

'M' type, remains collapsed when the irradiator is switched off, but does sometimes recover after several seconds.

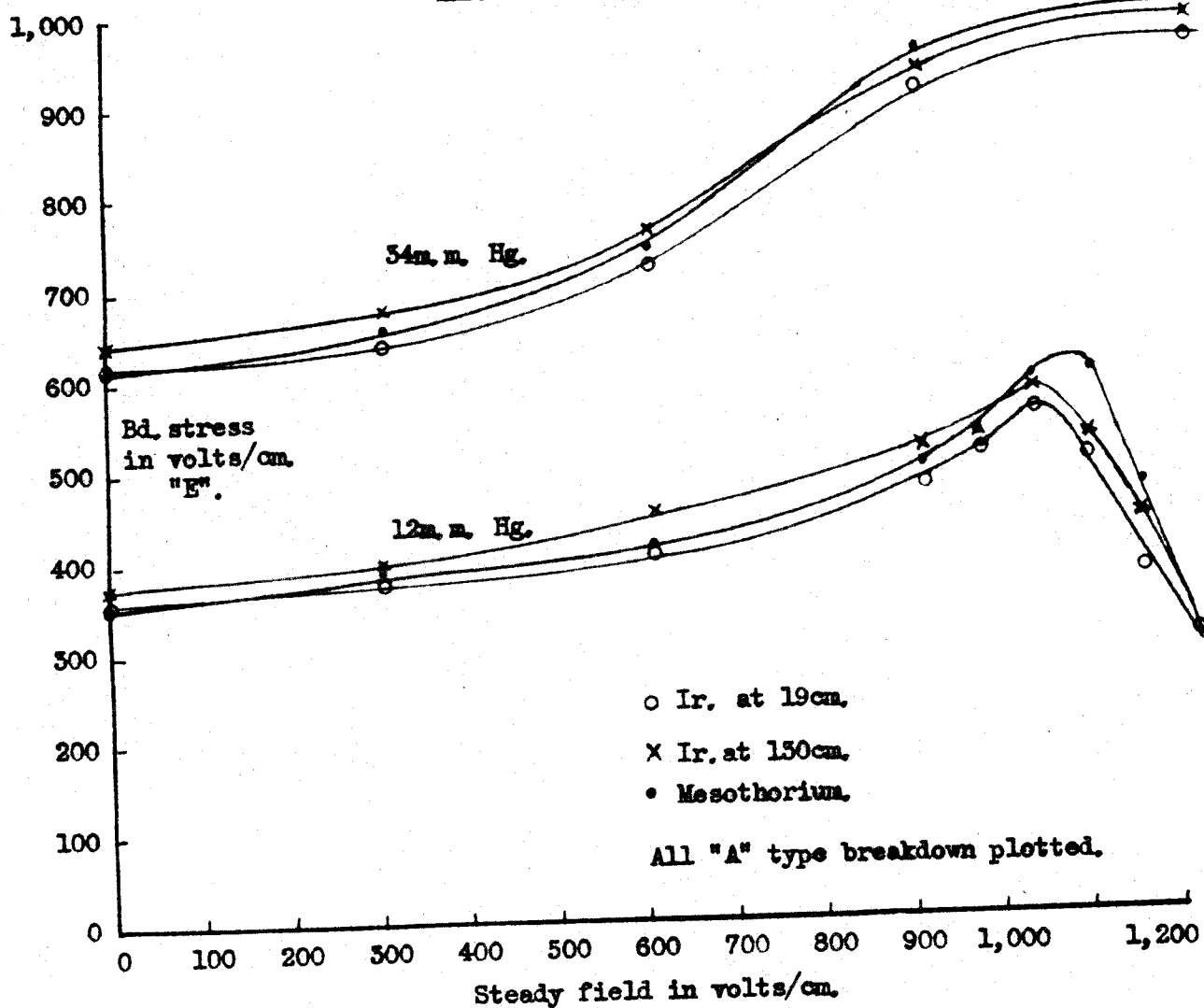
'A' type, no recovery at all after breakdown when irradiator is switched off.

The separation of the four types of discharge became more apparent at the lower pressures, and higher values of the applied unidirectional field. All pressures just gave the 'A' type for microwave breakdown with no applied steady field. It can generally be stated that the four types gradually became indistinguishable from the 'A' type as the pressure increased, and the applied unidirectional field decreased. The table below summarises the results; the microwave stresses are in an arbitrary scale. (The actual values shown are the displacement voltages required to displace the pulse envelopes a distance equal to their own heights; see section 3.2.1. Part I). The irradiator was situated at a distance of 19 cms. from the resonator.

TABLE 17. Microwave breakdown stresses, both fields operative.

$P$ m.m.Hg.No.D.C.	$\frac{1}{4}$ 305 volts/cm.	$\frac{1}{2}$ 610 volts/cm.	$\frac{3}{4}$ 915 volts/cm.	Full. 1220 volts/ cm.
Microwave breakdown stress in arbitrary units.				
11.    A 19.7	A 21	F 24 C 25 M 28.5 A 31	F 18 C 27 M 37 A 40	A 20.5
30.5    A 22.5	F+C 24.5 M+A 25.5	F 25.0 C 29.0 M 31.5 A 31.5	F 26.0 C 33.0 M 42.0 A 42.0	F 24 C 32.0 M 44.0 A 44.0

Graph. 29 . HYDROGEN, U, H, F. Breakdown Stress v. Steady Field  
for Irradiator at 19, & 150cms, & Mesothorium.



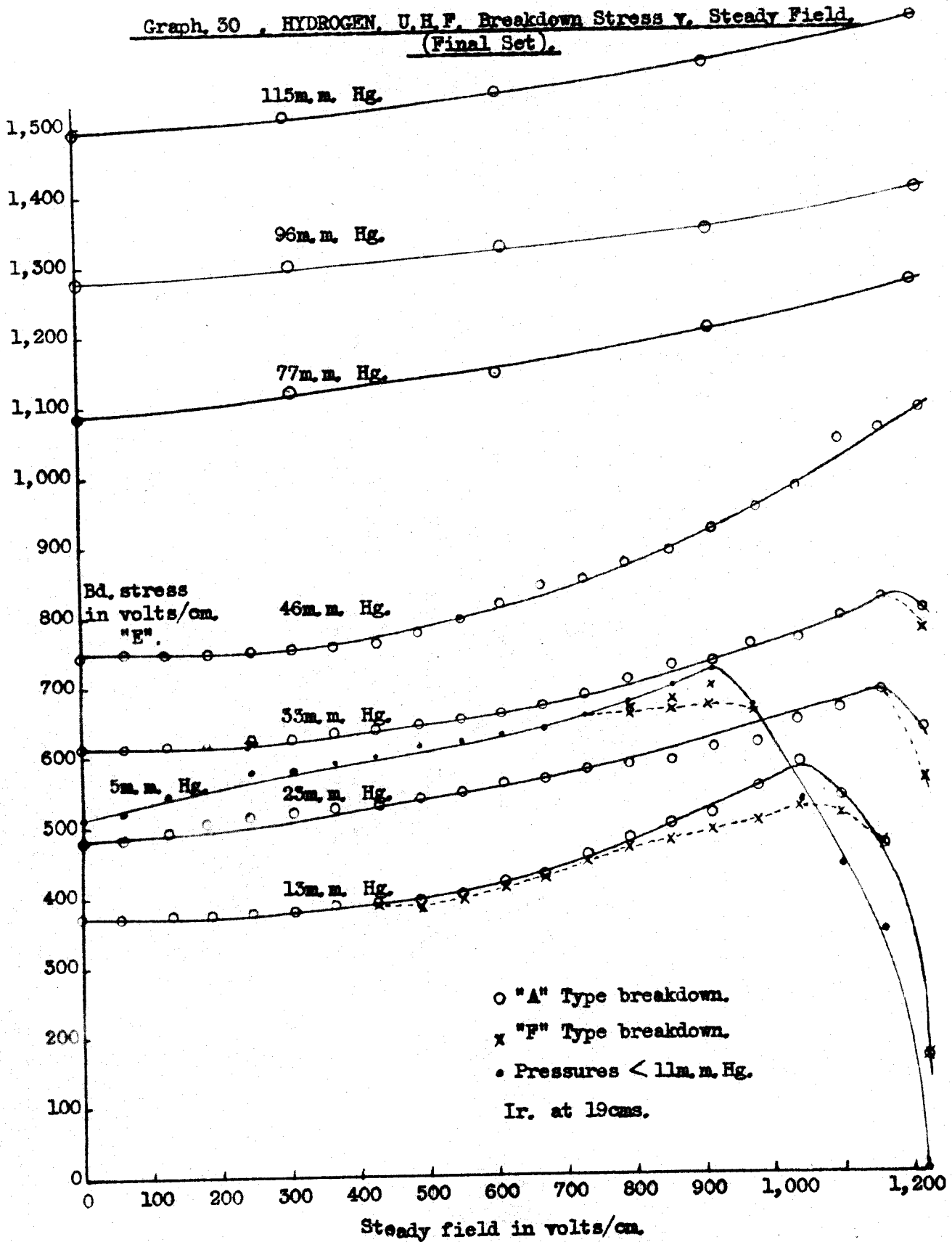
50.5	A 29	A 30.5	F 33 C 39 M 45 A 45	F 35 C 40.5 M 49.0 A 49.0	F 34.5 C 45.0 M 50.0 A 50.0
80	A 38.5	A 39.0	F 40 A 41.5	F 42 C 44.5 A 45.0	F 43.0 C 46.5 A 48.5
119	A 45.5	A 45.5	A 47.0	F 48.0 A 48.5	F 48.5 C 49.0 A 50
156	A 49.5	A 49.5	A 50.0	A 50.5	F 51 A 52
175	A 51.0	A 51.0	A 51.5	A 52.0	F 52.3 A 52.5

Results obtained with the irradiator at d maximum, i.e. 130 cms. showed that the separation of the types of breakdown was not distinguishable until lower pressures, and higher unidirectional fields than the results with the irradiator at 19 cms.

Variation of the microwave breakdown stress with applied unidirectional field was also explored using the mesothorium source as the ionising mechanism, the curves (Graph 29) follow the same general trend as the curves obtained with the irradiator at 19 and 130 cms. With the mesothorium source of ionisation the separation of the types of breakdown did not become noticeable until the lower pressures, and the higher values of the unidirectional field;



Graph. 30 . HYDROGEN, U.H.F. Breakdown Stress v. Steady Field.  
(Final Set).



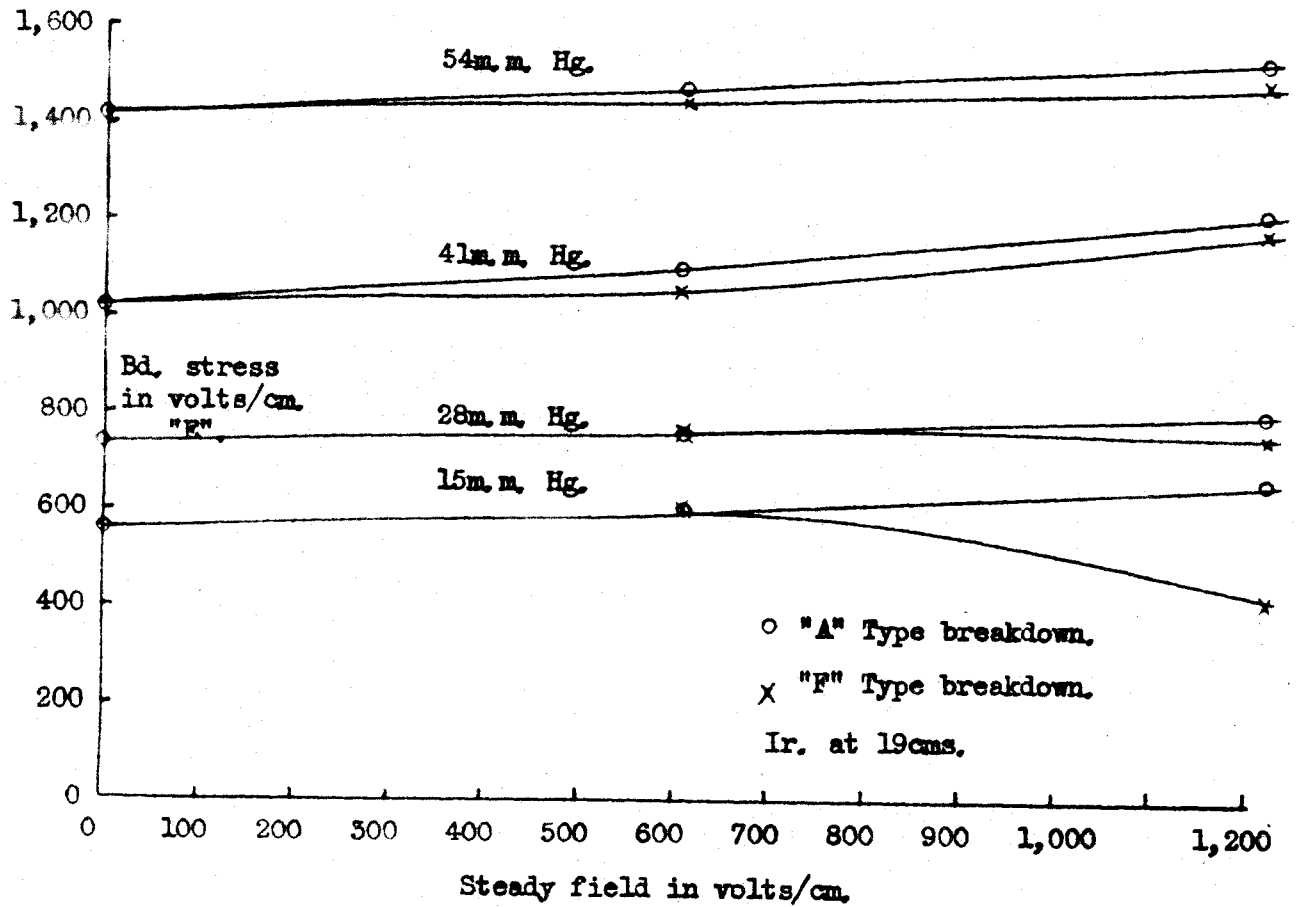
usually only the F and A types of breakdown were observed. The mesothorium results were therefore essentially similar in this respect to the results with the irradiator at 130 cms.

It is interesting to notice that the mesothorium values shown in graph 29 agree with the  $Ir = 19$  cms. results for breakdown with no unidirectional field applied; but are greater than the  $Ir = 19$  cms results for the higher values of the applied steady field. The mesothorium results exceed the values recorded with the irradiator at 130 cms. when the peak in the graph has been reached, this is shown for both pressures 12 and 34 m.m.Hg.

An analysis of the statistical lags recorded in these experiments shows that no general trends can be deduced: the lags seem quite random, except that they increase with irradiator distance, i.e., between  $Ir = 19$  and 130 cms; also the mesothorium results showed greater lags than the  $Ir = 19$  cms results.

Finally for hydrogen, because of the somewhat unsatisfactory nature of the two sets of results presented above, a further check was undertaken at a later date. Care and precision were observed, graph 30 shows the results; again the same increase in the microwave stress with increase

Graph 31, OXYGEN, U.H.F. Breakdown Stress v. Steady Field.



in the steady field is apparent. Only at the highest voltages and lower pressures did the various separate forms of breakdown occur. Then only the F and A types could be distinguished, the other variations if present could not be resolved.

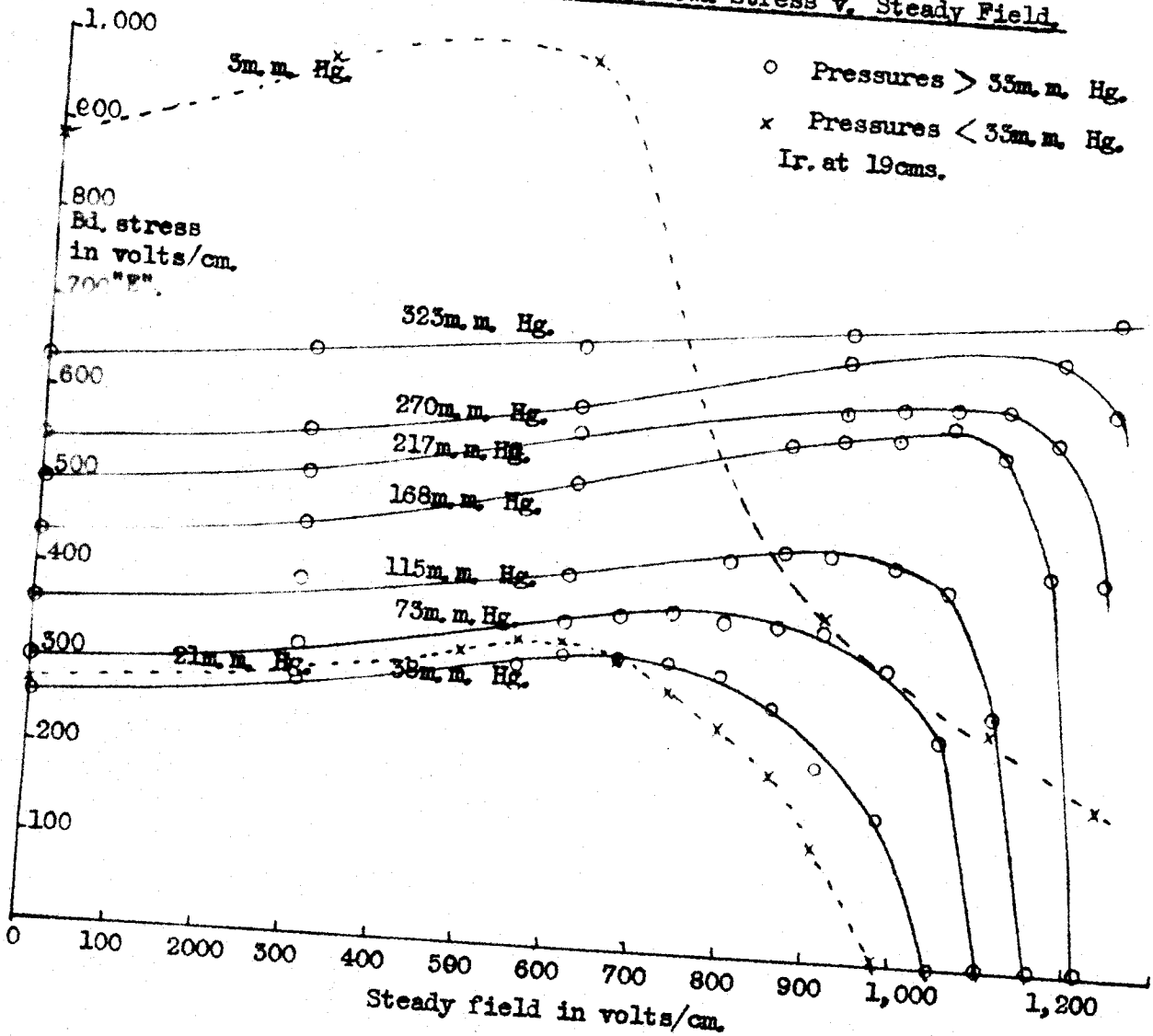
Many sets of results were taken during this final period, and the results observed in pure hydrogen and cylinder hydrogen were always found to be identical.

No explanation for the non-appearance of the four types of breakdown in the latter work is apparent, except that the latter work was mostly in pure hydrogen, while the earlier results were all obtained using cylinder hydrogen, apart from this all else was identical. It was felt that no more time could usefully be spared for further experiments of this type in hydrogen.

#### 4. Oxygen. (Cylinder).

A set of curves for oxygen is shown in graph 31, where the irradiator was placed at 19 cms., only A and F types of discharge could be distinguished; these became more apparent at the higher pressures, (similar to the air results). The experimental technique was as for the other two gases, due allowance being made for statistical lag at each microwave field adjustment. No gas recovery trouble was encountered provided the microwave field was switched

Graph 32. NEON. U.H.F. Breakdown Stress v. Steady Field.



off for a minute or so after a discharge.

#### 5. Neon. (Pure).

Spectroscopically pure neon gave the curves shown in graph 32 for the variation of the microwave breakdown stress with the value of the applied unidirectional field. The irradiator was in the near position, 19 cms; only the A type of breakdown could be detected, and the discharge was extremely sharp giving complete recovery on switching off the microwave field.

The position of interception of the graphs with the steady field axis was given by the value of the steady field which itself produced breakdown, when the gas was irradiated, (the microwave field not being present). An increase in the breakdown stress for the lower pressures, ( $< 21$  m.m.Hg) is clearly shown both for the microwave and steady field discharges.

#### 6. Discussion.

In interpretation of these results it is recognised that electrons may simply be moved by the unidirectional field out of the zone of maximum circuital electric stress, ( $E_e$ ).

Consider three regions in the gas, A. B and C. The region A is a zone where the circuital electric stress

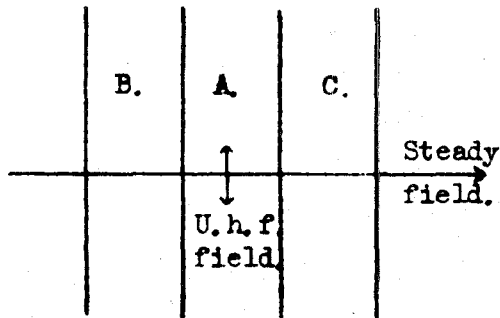


Fig 34.

is a maximum and sensibly constant over the area; B and C two neighbouring zones where the electric stress is less than maximum. An electron therefore moving from zones B, to A, to C, will not produce as many new

electrons by collision as an electron remaining in A. Also a population of electrons drifting under the influence of the unidirectional field through A will not produce as many new electrons as a stationary population, of the same density, in zone A. The auxiliary field may therefore cause a reduction in the ionising power if it displaces electrons a distance greater than that within which the microwave field is sensibly uniform. An increase in the microwave field would therefore be necessary for breakdown, when the auxiliary field was present, compared to the stress necessary for breakdown under the microwave field alone.

A slightly different approach to the problem is to consider the electron movement in one microsecond under the influence of the unidirectional field. One microsecond was the duration of the unidirectional pulses applied orthogonally

to the microwave field. The values quoted below are calculated by the methods fully explained in Chapter 6, Part II.

Hydrogen: pressure 115 m.m.Hg, and a steady field of 305 volts/cm the electron movement is of the order 10 m.m. in one microsecond, this value rapidly increases on increasing the steady field or decreasing the pressure.

(The electron ambit under the microwave field for pressures 5 to 115 m.m.Hg. is approximately 0.014 m.m. to 0.0025 m.m. in one half cycle of the microwave field).

Neon: at pressures greater than 180 m.m.Hg. and a steady field of 305 volts/cm. the electron movement is less than 30 m.m., and for the maximum pressure used in these experiments 323 m.m.Hg the electron movement is of the order 25 m.m. in one microsecond.

(The electron ambit under the microwave field for pressures 13 to 323 m.m.Hg., is 0.016 to 0.0013 m.m. approximately).

Air: the highest pressure, 41 m.m.Hg. gives an electron movement under a steady field of 305 volts/cm. of 35 m.m. in one microsecond.

Oxygen: for a pressure of 53.5 m.m.Hg. the electron movement under the unidirectional field of 305 volts/cm. is of the order 30 m.m. in one microsecond.

The length of the resonator was 31 m.m. at resonance and the internal length of the glass capsule, 22 m.m.; it can therefore be seen that even for the highest pressures the electron movement under the action of the steady field is of the same order as the capsule length. The electrons might therefore be swept to the capsule walls, (i.e. clean up)



during the steady pulse.

The possible explanations of the increase required in the microwave stress to produce breakdown, when a steady field was simultaneously applied to the gas, suggested the use of an alternating field in place of the steady field. The electric ambit would therefore be controlled by the choice of frequency of the alternating field. Experiments were next conducted with alternating fields of three frequencies; 1, 3 and 10 Mc/s; these are described in the following three chapters. The order given, i.e. 1,3 and 10 Mc/s. is not historically correct, but they are discussed in this sequence so that the development of the problem can be more easily followed.

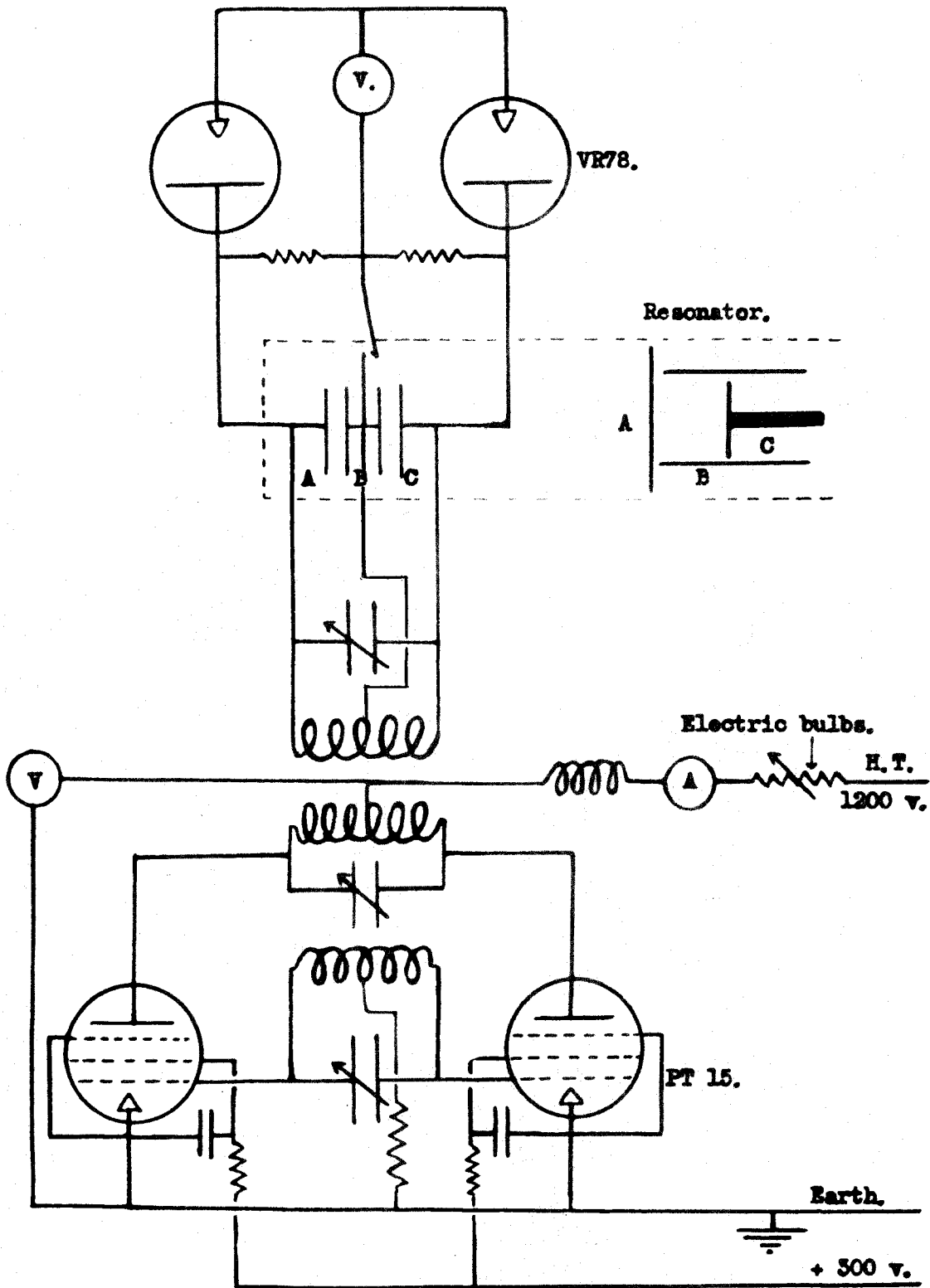


**Fig. 35 . Oscillator, and voltage measuring circuits.**

CHAPTER 3.Crossed fields, microwave and 0.86 Mc/s.  
fields.1. Introduction.

The slowest alternating field applied at right angles to the microwave field had a frequency of approximately 1 Mc/s; two gases were studied under the action of the crossed fields, hydrogen and neon. Each gas is discussed separately.

2. Apparatus.2.1. The oscillator.

The one megacycle oscillator was essentially a tuned anode tuned grid oscillator, with two pentodes working in push-pull. Due to the heavy anode current, (200 m.a.), ten 60 watt electric light bulbs formed the anode load. The bulbs could be switched out of circuit in pairs, thus facilitating an easy control of the anode voltage.

The resonator can be represented by two condensers in series, one between the movable piston and the cylindrical wall, (C.B.), the other between the cylindrical wall and the fixed end plate, (A.B.). (Figure 35). Thus by making the resonator one of the components in the tuned circuit, and loosely coupling this circuit to the oscillator,

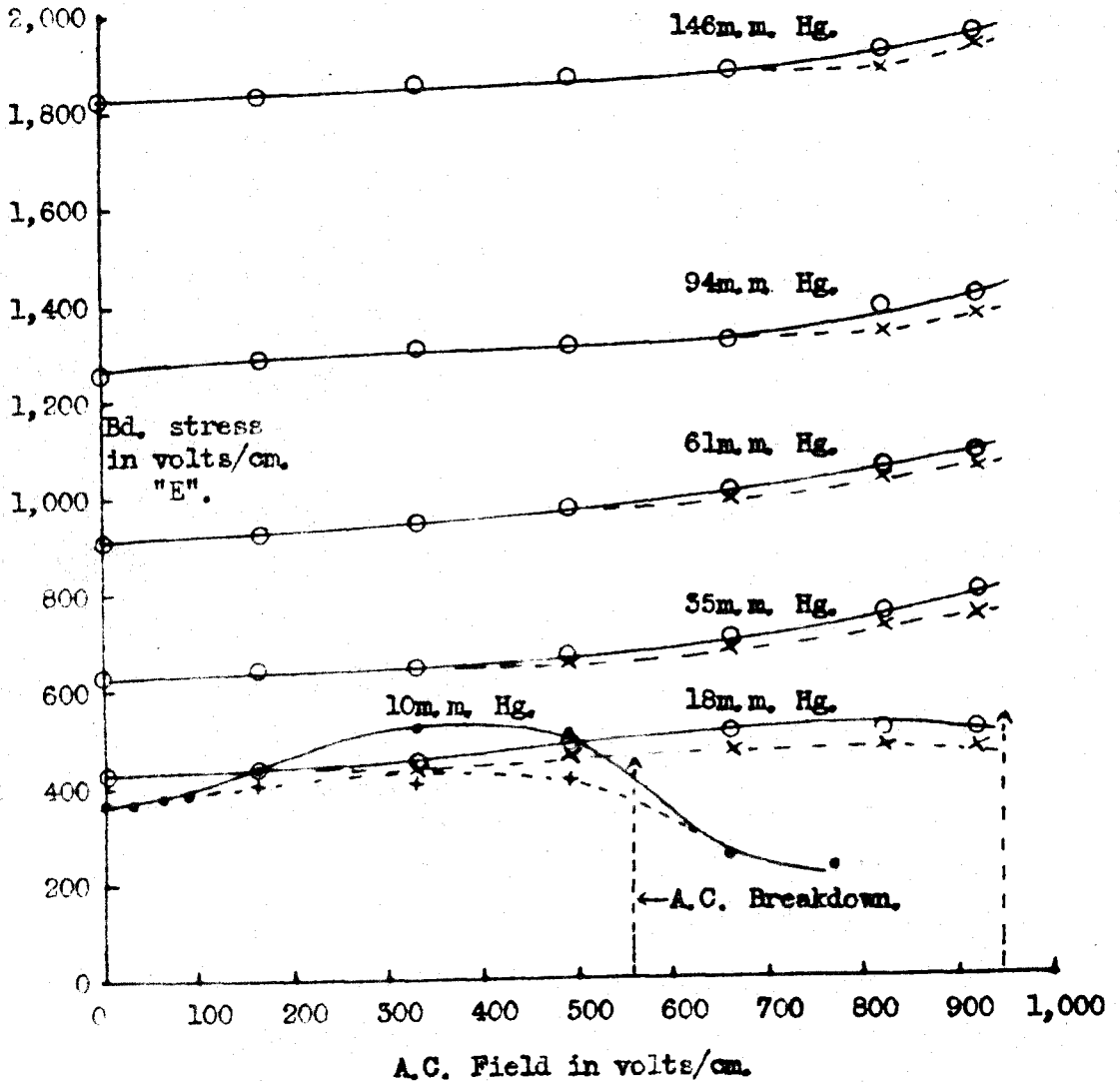
an alternating voltage could be produced across the resonator. To ensure the required even voltage distribution, as discussed in the previous chapter, the central section of the resonator was connected to a suitable point on the coil in this isolated tuned circuit, as shown in the diagram. This position was chosen so that the voltage between B and A was half the voltage between C and A. Variation of the coupling between the tuned circuit and the anode tuned circuit of the oscillator varied the applied voltage across the resonator.

The three coils used consisted of some 45 turns, 15 S.W.G. copper wire wound as a pancake coil on a wooden former, (diameter of coil 4" to 8"); the inductance was of the order 320  $\mu$ H. All connecting wires in the oscillator, and tuned circuit, were made of thick copper wire to obtain a high Q. The oscillator produced a peak voltage of about 3000 volts across the resonator, i.e. a maximum of approximately 1000 volts/cm at a frequency of 0.86 Mc/s.

## 2.2. Voltage measurement.

The voltmeter was similar to that used by Gill and von Engel<sup>44</sup> employing two diodes, (VR 78), and an electrostatic voltmeter, the reading of the meter being half the peak voltage.

Graph. 53 . HYDROGEN. U.H.F. Breakdown Stress v. A.C. Field (0.86Mc/s).



{ O "A" Type breakdown,  $p > 15$ m.m. Hg.  
 { X "F" do do  $p > 15$ m.m. Hg.  
 { • "A" do do  $p < 15$ m.m. Hg.  
 { + "F" do do  $p < 15$ m.m. Hg.  
 Ir at 19cms.

The centre point between the two resistances is at a potential equal to half the applied potential to the voltmeter; thus connecting this point to the cylindrical section of the resonator (B), no variation in the meter reading should be recorded if the voltage distribution on the resonator is that required. By the insertion of a tapping key in this line a constant check could be made that the full voltage was applied to the piston, and half voltage to the cylindrical wall, the other end of the resonator was earthed. The alternating field at the position of the maximum microwave circuital field was therefore longitudinal, and its value could easily be calculated.

### 3. Results.

#### 3.1. Pure electrolytic hydrogen.

##### 3.1.1. Variation of the microwave stress with alternating field.

The alternating field applied orthogonally to the microwave field produced an increase in the stress required for microwave discharge, clearly shown in graph 33. Two types of breakdown were again noticed and can still be referred to as the 'F' and 'A' types of breakdown. The separation of the two forms increased as the pressure decreased, and the alternating voltage increased.

No real recovery troubles were encountered provided the fields were switched off after a

discharge for the usual one to two minutes; due allowance was also made for any statistical lag.

The two vertical arrows on the graph represent the breakdown stress of hydrogen under the action of the alternating field alone for pressures of 10 and 18 m.m.Hg. The microwave stress values recorded to the right of these lines were obtained by visual observations, i.e. a general glow could be seen in the resonator caused by the alternating field breakdown, but on increasing microwave field this glow was seen to increase suddenly; this was taken as the point where the microwave breakdown began. These values, of course, are far more liable to error than the usual results to the left of this boundary.

However the oscilloscope trace did not collapse when the alternating discharge alone was present in the resonator, and it was found possible to still use the collapse of the pulse envelope as an indication of the microwave discharge; this approximately agreed with the visual method.

### 3.1.2. Auxiliary field cut off voltages.

If the microwave field was set so as to just produce breakdown, with no auxiliary field operative, the discharge could be extinguished by applying the auxiliary field; the irradiator could be on or off during these

experiments and did not vary the alternating voltage necessary to extinguish the discharge. A table is now given showing these alternating extinction (or cut off) voltages for the pressure range 15 to 142 m.m.Hg. The electron ambits are calculated, by the method outlined in Chapter 6, for a half cycle of the alternating field.

TABLE 18. Extinction, voltages and associated electron ambits hydrogen.

p m.m.Hg.	Microwave stress for breakdown No.a.c. field present.  Volts/cm.	A.C.stress for extinction Ir off or on.  Volts/cm.	Electron amb for $\frac{1}{2}$ cycle alternating field $5.8 \times 10^{-7}$ secs.  m.m.
15	390	< 30	2.7
23	480	59	3.1
35	625	153	5.2
51	800	164	4.6
66	960	252	5.2
76	1070	485	7.1
97	1345	545	6.7
118	1520	1045	10.1
142	1770	1180	9.9

Length of resonator 31 m.m., length of inside of capsule  
22 m.m.

The effect of a slight over-voltage of the microwave field increased these extinction voltages, as can be clearly seen in the following table; whether the irradiator was operative, or not, affected these



values, the lower values occurring for no irradiation.

TABLE 19. Extinction voltage (0.86 Mc/s) for slight microwave overvoltage.

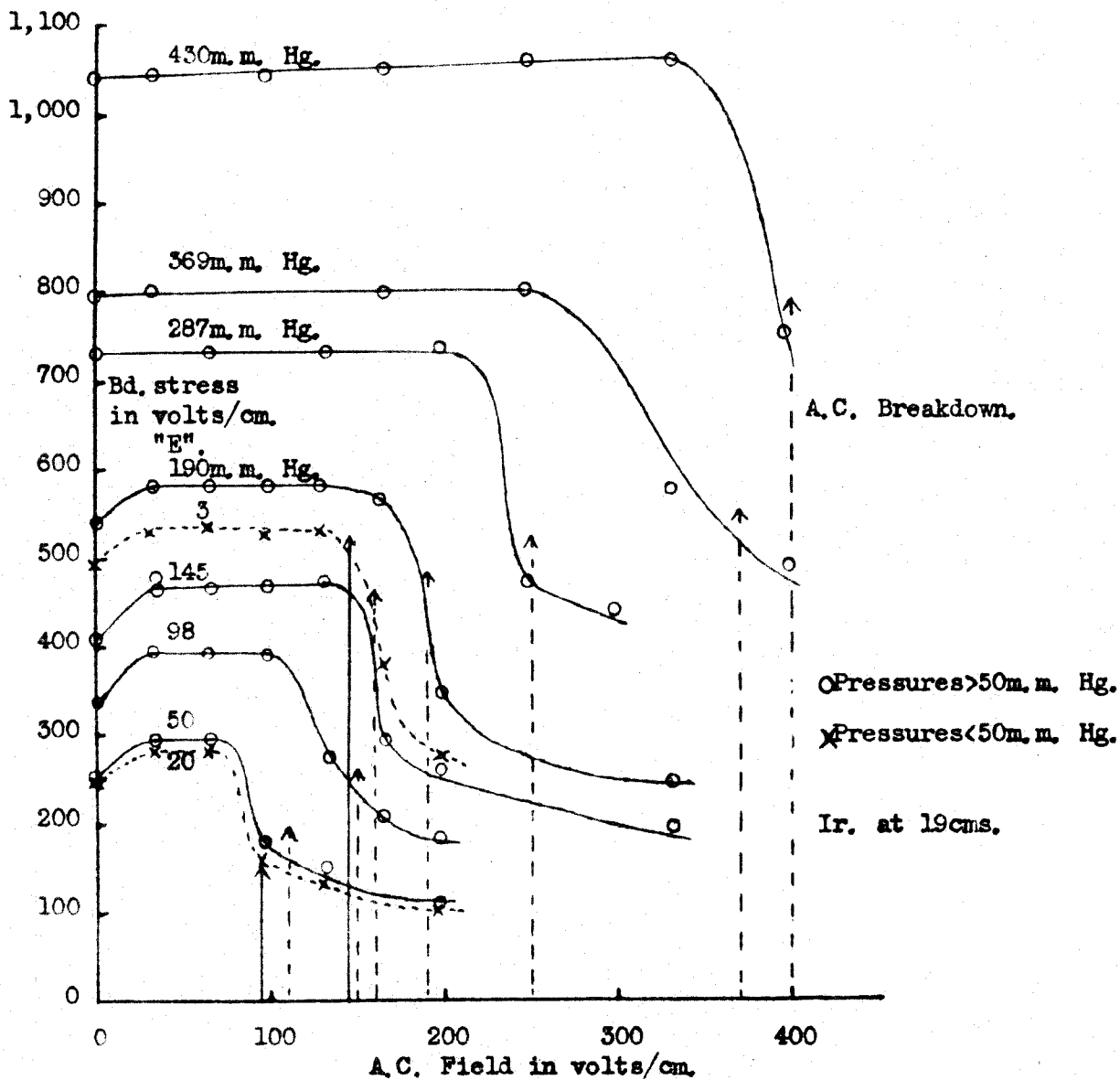
P m.m.Hg.	Microwave stress No a.c. field present.	Volts/cm. Applied microwave stress.	Alternating extinction voltages in volts/cm.	
			Ir off.	Ir on.
10	370	370	< 30	< 30
		415	125	156
		440	154	500
		470	500	N.E.
19	425	425	35	35
		455	370	450
		470	920	N.E.
61	910	910	250	250
		940	635	720
		955	660	885
		995	885	N.E.
94	1260	1260	530	535
		1290	690	720
		1310	980	N.E.

N.E. no extinction obtained with the voltage available (order of 1000 volts/cm).

### 3.1.3. General comments, hydrogen.

The electron orbit under the auxiliary field is such that the average microwave field acting is (at least in some cases) materially reduced, because the movement is large enough to prevent any electron from remaining in the strong filament of the ring electric field: this leaves

Graph 34 . NEON, U.H.F. Breakdown Stress v. A.C. Field (0,86Mc/s).



an ambiguous explanation. It was therefore proposed to use a higher frequency field, in which a given intensity is associated with a smaller electron displacement.

### 3.2. Spectroscopically pure Neon.

#### 3.2.1. Variation of the microwave stress with alternating field.

In neon a far greater pressure range could be covered, and graph 34 shows the variation of the microwave stress for breakdown when the orthogonally applied alternating stress is increased. The vertical arrows again give the alternating field breakdown stress for neon at 0.86 Mc/s. The sudden rise of the microwave stress in the first 33 volts of the applied auxiliary field was repeatable, for pressures less than about 200 m.m.Hg., for a number of different sets of results.

The microwave stresses recorded to the right of these vertical arrows were determined visually, this was facilitated by the difference in appearance of the microwave and alternating discharge in neon. The microwave discharge always showed the characteristic neon red colour; however the alternating discharge was a bright blue. There was such a marked change of colour that the microwave discharge could easily be seen within the general blue glow of the alternating discharge. The onset of the microwave

discharge was therefore easily determined visually, the onset was fairly sharp. The microwave stress recorded to establish a discharge within the already present alternating discharge was not dependent on whether the irradiator was on or off.

This blue neon discharge persisted down to a pressure of about 15 m.m.Hg. where any further pressure reduction caused a gradual change to pink in the colour of the alternating discharge, and at the still lower pressures red. The variation of the breakdown stress for neon, under the 0.86 Mc/s field, with pressure is given on graph 39, Chapter 4.

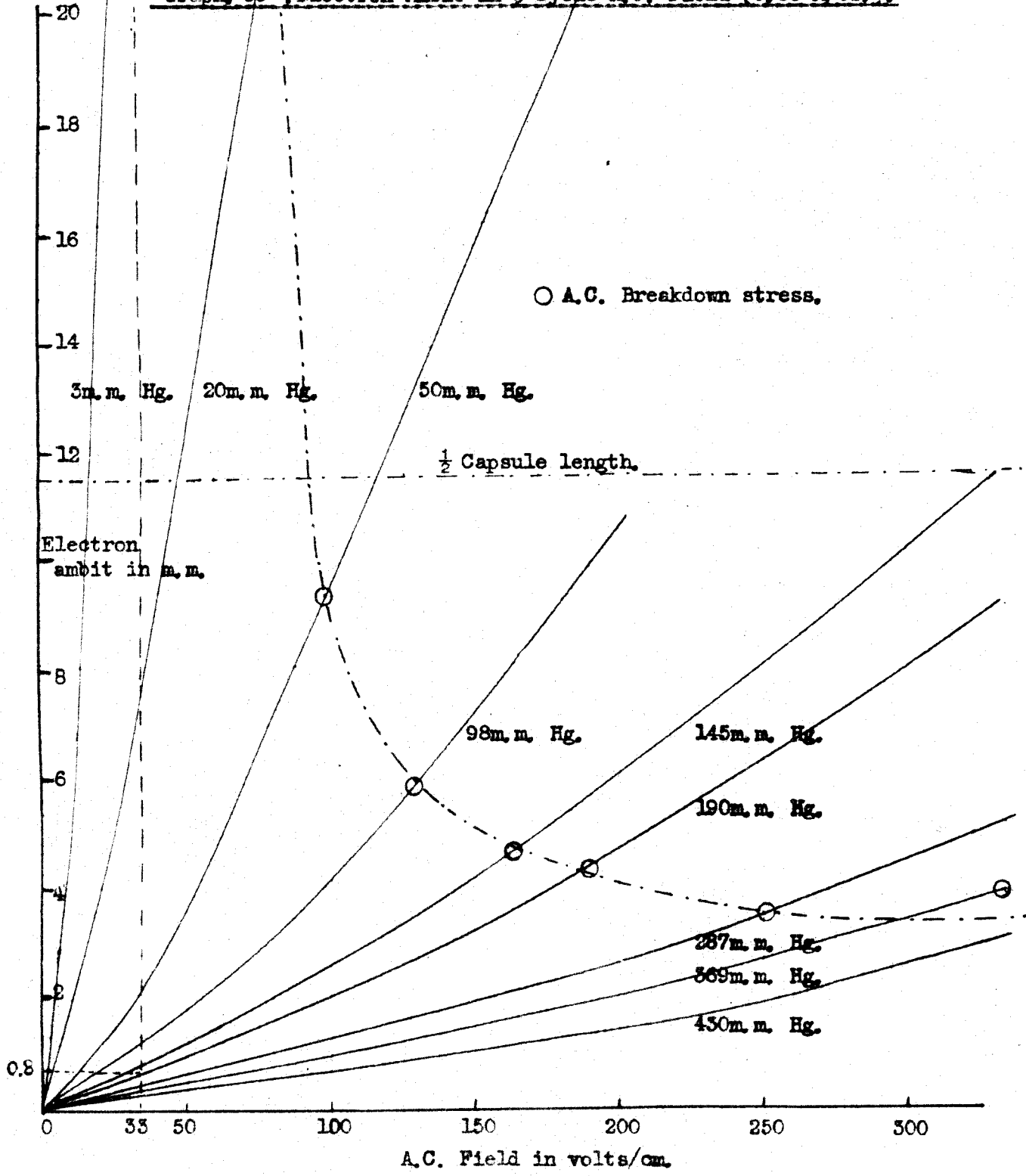
### 3.2.2. Auxiliary field cut off voltages.

The necessary alternating field stress to give extinction of an established microwave discharge was determined in a similar fashion to the method used for hydrogen, for a pressure range 98 to 190 m.m.Hg. The microwave stress was the minimum stress required to produce breakdown with no auxiliary field present.

TABLE 20. Extinction voltages and associated electron ambits.

p m.m.Hg.	Microwave stress for breakdown. No A.C. field present.  volts/cm.	A.C. stress for extinction.  volts/cm.	Electron ambit for $\frac{1}{2}$ cycle of alternating fie - $5.8 \times 10^{-7}$ se m.m.
190	540	118	2.05
145	440	52	1.86
98	340	45	1.35

Graph, 35. Electron Ambit in  $\frac{1}{2}$  Cycle A.C. Field (0,86 M/cs.).



These amplitudes are small in comparison with the dimensions of the gas chamber; however it is interesting to compare them with the electron amplitudes under the auxiliary field of 33 volts/cm., i.e. the point where the graphs flatten out. The two sets of values are of the same order of magnitude.

TABLE 21. Electron ambits under 33 volts/cm. A.C. field.

p m.m.Hg.	Electron ambit under 33 volts/cm. A.C. field 0.86 Mc/s for $\frac{1}{2}$ cycle in m.ms.	
430	0.39	
369	0.55	
287	0.62	
190	0.78	} Upsweep in microwave stress within 33 volts/ cm. A.C. field.
145	1.1	
98	1.2	
50	1.94	
20	7.5	
3	48 ?	

### 3.2.3. Electron ambits under crossed fields, Neon.

Graph 35 shows the electron ambits under the action of the alternating field when both fields are operative, the method of calculation is given in Chapter 6. The microwave field used in these calculations is the field necessary to produce breakdown in the presence of the

appropriate alternating field. The boundary, or dotted line, on the graph marks the electron ambits under the alternating field when the stress of the alternating field is sufficient to produce breakdown alone.

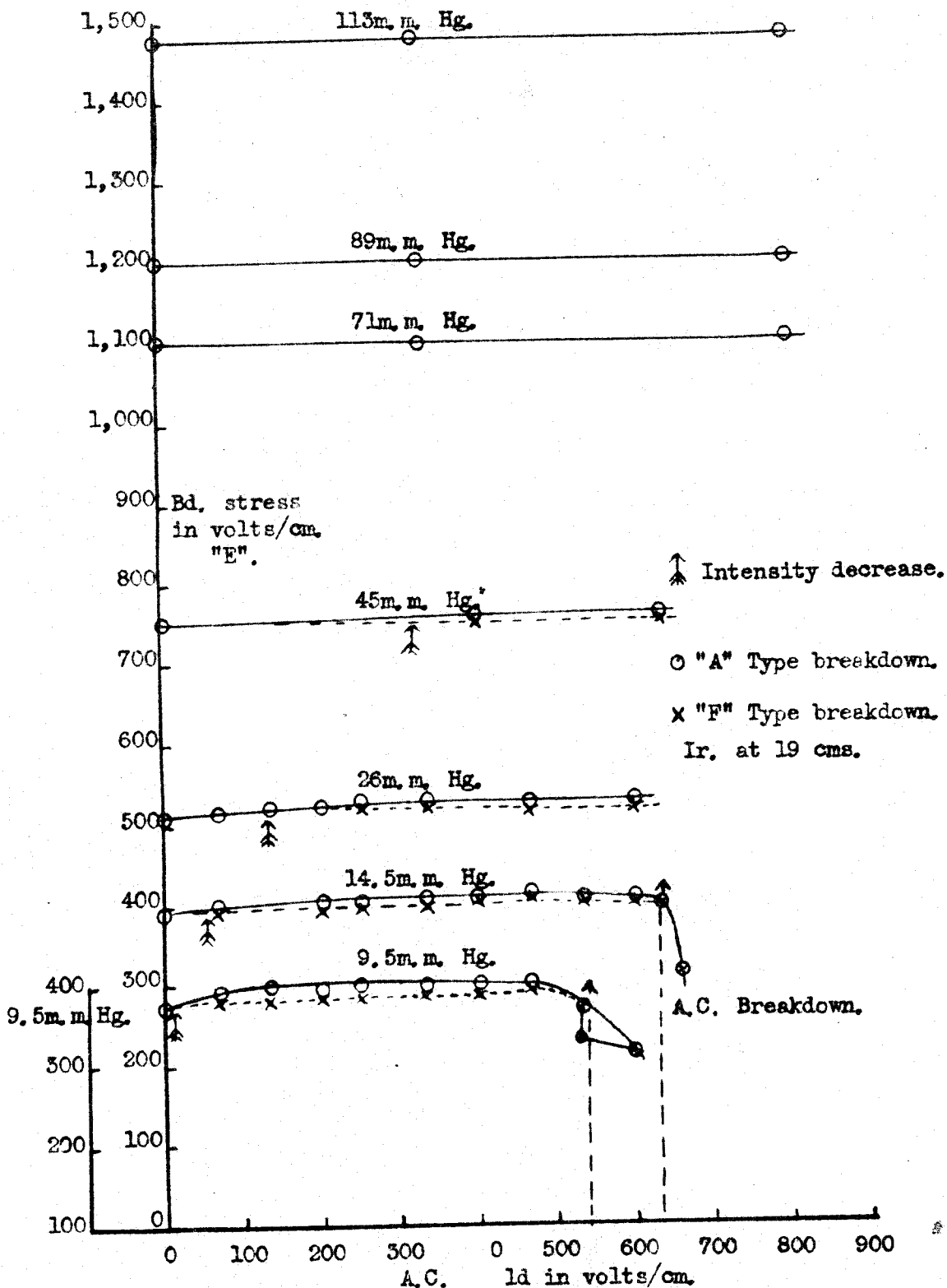
It can be seen that for alternating field values less than these breakdown stresses the electron ambit is small in comparison with the capsule length, except for low pressures. Unlike the hydrogen results no large movement of the electrons occurs due to the alternating field; therefore clean up cannot account for the increase in the microwave stress necessary to give breakdown in the presence of an orthogonal auxiliary field. This increase would appear to occur when the electron ambit under the auxiliary field exceeds 0.8 m.m. approximately. The flatness of the graphs is of considerable interest; discussion of this is reserved until a later Chapter, (Chapter 9).

The lowest alternating field voltage that could be easily read by the measuring system was approximately 20 volts/cm. At a pressure of 50 m.m.Hg. the microwave stress necessary for breakdown with an auxiliary field present of 20 volts/cm. was still greater than that required when no auxiliary field was present. The electron ambit under the alternating field (i.e. 20 volts/cm) was

now 1.14 m.m.; it was therefore still in excess of the minimum ambit quoted above, (i.e. 0.8 m.m.) Owing to the uncertainty of the measuring system for such low auxiliary fields further experiments were not continued. However, it was considered desirable to increase the frequency of the auxiliary field, results using a 3 Mc/s auxiliary field are given in the following chapter.



Graph 36 , HYDROGEN, U.H.F. Breakdown Stress v. A.C. Field (2.66Mc/s).



CHAPTER 4.Crossed fields, microwave and 2.66 Mc/s fields.1. Apparatus.

The oscillator was modified by substituting new coils; these consisted of some 16 turns, 10 S.W.G. copper wire with a diameter of 6 inches. The resonator feed and voltage measuring circuits were as before. The oscillator frequency was 2.66 Mc/s, with a peak output across the resonator of 2400 volts.

The five gases, hydrogen, neon, nitrogen, oxygen and air were used at this frequency; the results for each gas are given separately. Hydrogen and neon were studied more fully than the other gases.

2. Results.2.1. Pure electrolytic Hydrogen.2.1.1. Variation of the microwave breakdown stress with alternating field.

Little or no increase in the microwave stress was required to produce discharge on application of the auxiliary field. An increase could only be established for pressures below about 50 m.m.Hg. The two types of discharge, the F and A types, were also separately evident below this pressure. (Graph 36). Once the F type of discharge had been established switching off the alternating field caused a

change to the A type, however on reapplying the auxiliary field the discharge reverted to the F type.

Alternating field discharge could only be established for the two lowest pressures; shown by vertical arrows on the graph. The microwave breakdown stresses to the right of these boundaries were obtained, as before, visually observing the sudden increase in intensity of the discharge as the microwave stress was increased.

The rectangular shape of these graphs is of considerable interest showing an apparent complete independence of the two fields in establishing their own discharge, (see the discussion chapter for further comments).

The intensity of the observed discharge under crossed fields was lower than the microwave discharge alone. The auxiliary field voltages at which any decrease in the intensity of the discharge was seen are marked on the graphs by small arrows; they would appear to coincide approximately with the separation of the discharge into the two forms, (i.e. A and F types).

#### 2.1.2. Alternating field cut off voltages.

With the microwave field set for the minimum stress required (with no auxiliary field present), to produce breakdown at a given pressure, the necessary auxiliary field stresses to quench this discharge were determined and are tabulated below, together with the

electron ambits at these values. The electron ambits are of the same order of magnitude as those recorded at 0.86 Mc/s. The same general remarks apply to this frequency as to the previous set of results.

TABLE 22. Extinction voltages, and associated electron ambits, hydrogen.

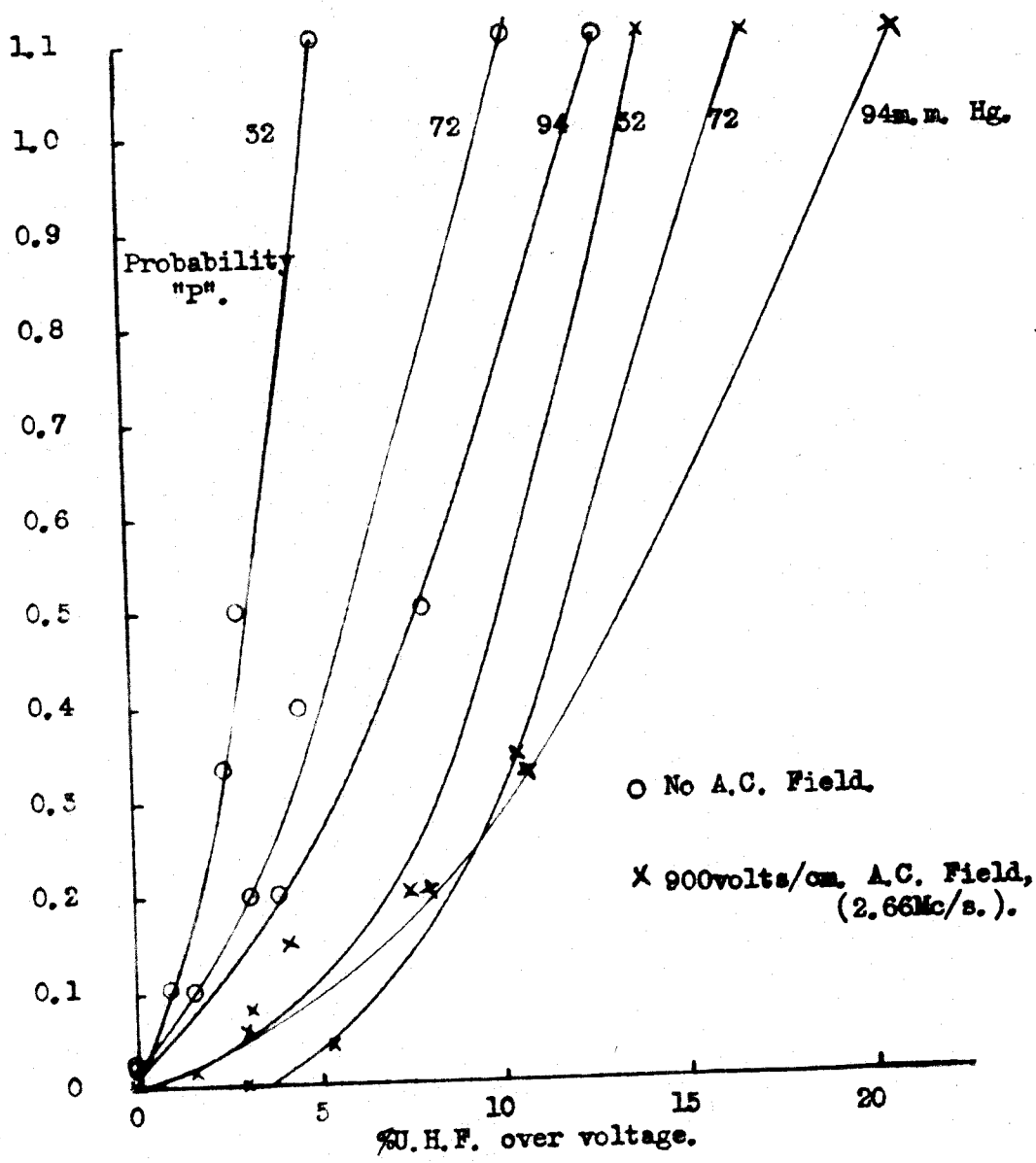
p m.m.Hg.	Microwave stress for breakdown. No A.C. field present. volts/cm.	A.C. stress for extinction. volts/cm.	Electron ambit for $\frac{1}{2}$ cycle of A.C. field - $1.88$ $\times 10^{-7}$ secs. m.ms.
45	750	550	4.5
26	525	120	1.8
14.5	410	100	2.1
9.5	390	90	2.66

2.1.3. Electron ambits under crossed fields, hydrogen.

In the table below (table 23) the electron ambits in one half cycle of the alternating field for the maximum applied auxiliary voltage are given, the microwave field being at the appropriate breakdown stress for the applied auxiliary field.

It will be seen that the electron ambits for pressures greater than 26 m.m.Hg. are well below half the capsule length, and it therefore seems improbable that electron clean up to the capsule walls is a major

Graph 37 . HYDROGEN, Probability of Breakdown v. % Over Voltage.



factor. The electron paths given are for the maximum applied auxiliary field, and they decrease rapidly as the auxiliary field is reduced.

TABLE 23. Electron ambits in alternating field, hydrogen.

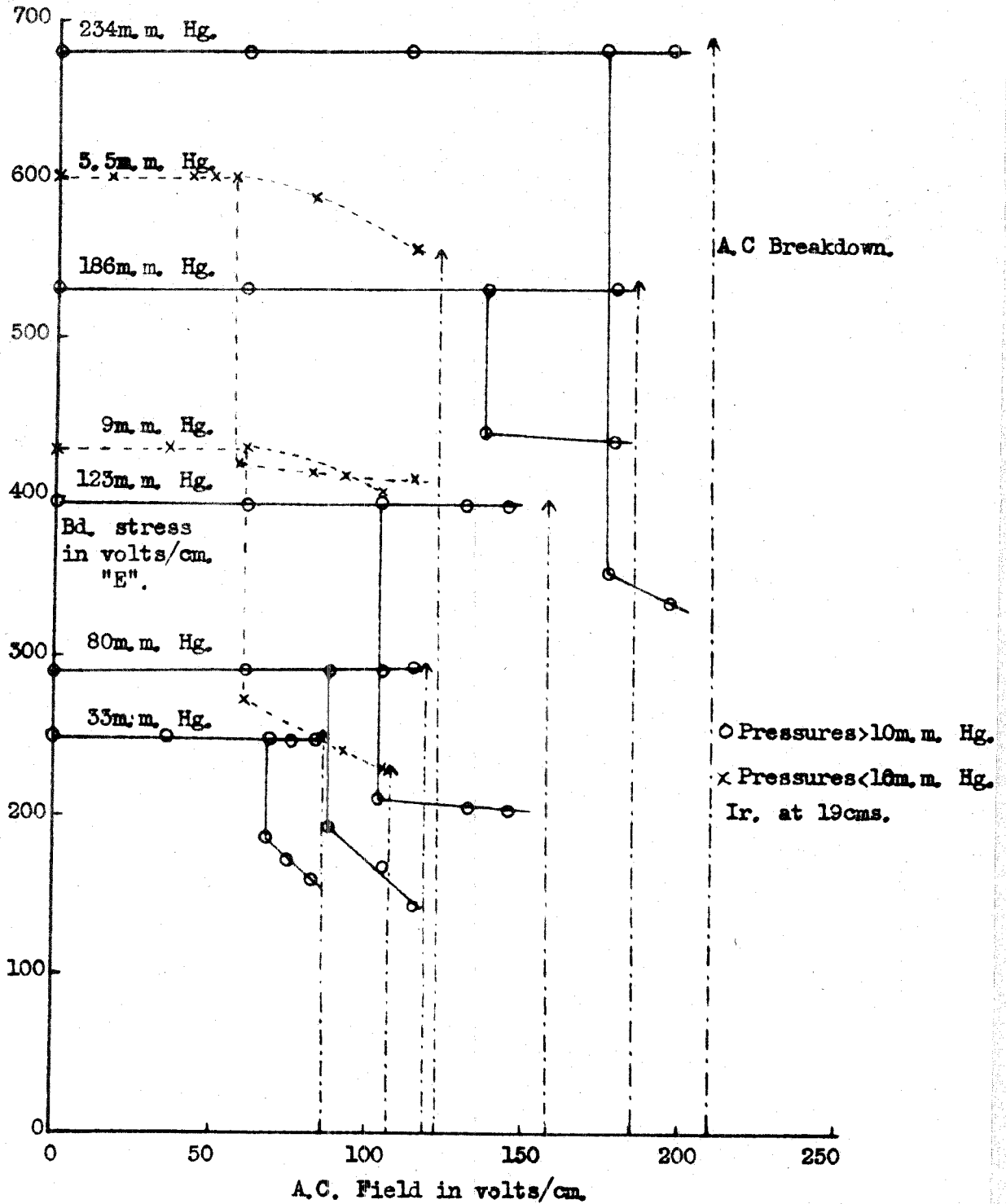
p m.m.Hg.	Microwave stress for breakdown. (A type)  volts/cm.	A.C.field.  volts/cm.	Electron ambit in $\frac{1}{2}$ cycle of A.C.field.  m.ms.
9.5	390	500	23
14.5	410	600	18.5
26	525	600	8.5
45	750	600	4.8
71	1100	600	3.2
89	1200	600	2.8
113	1480	600	2.5

2.1.4. Statistical lag variations with auxiliary field voltages.

It can be stated generally that the application of the auxiliary field, though it might not produce any increase in the microwave stress necessary for breakdown, did produce an increase in the observed statistical lag.

Graph 37 shows the variation in the probability per pulse for breakdown with microwave field overvoltage for two cases; (a) no applied auxiliary field,

Graph 38 . NEON. U.H.F. Breakdown Stress v. A.C. Field (2.66Mc/s).



and (b) with a large applied auxiliary field. (The probability per pulse is the reciprocal of the statistical lag, the lags measured in seconds). It is shown from these results that there is a definite decrease in the probability per pulse with the application of an alternating field applied orthogonally to the microwave field.

## 2.2. Neon Spectroscopically pure.

### 2.2.1. Variation of the microwave breakdown stress with alternating field.

Application of an alternating field at right angles to the microwave field gave no observable increase in the microwave stress necessary to initiate breakdown, this was true up to the auxiliary field breakdown stresses. The rectangular shaped graphs clearly illustrate this point, graph 38. The right hand boundaries, i.e. the vertical arrows, show the auxiliary field voltages necessary to initiate a discharge, (no microwave field operative). Pressures up to 465 m.m.Hg. were used and these higher pressures gave curves similar in general shape to the ones shown in graph 38.

Observations made with various values of amplifier gain gave similar graphs, thus ensuring that the constant microwave breakdown stress recorded could not be attributed to amplifier saturation. A slight increase in the microwave stress with the application of the auxiliary

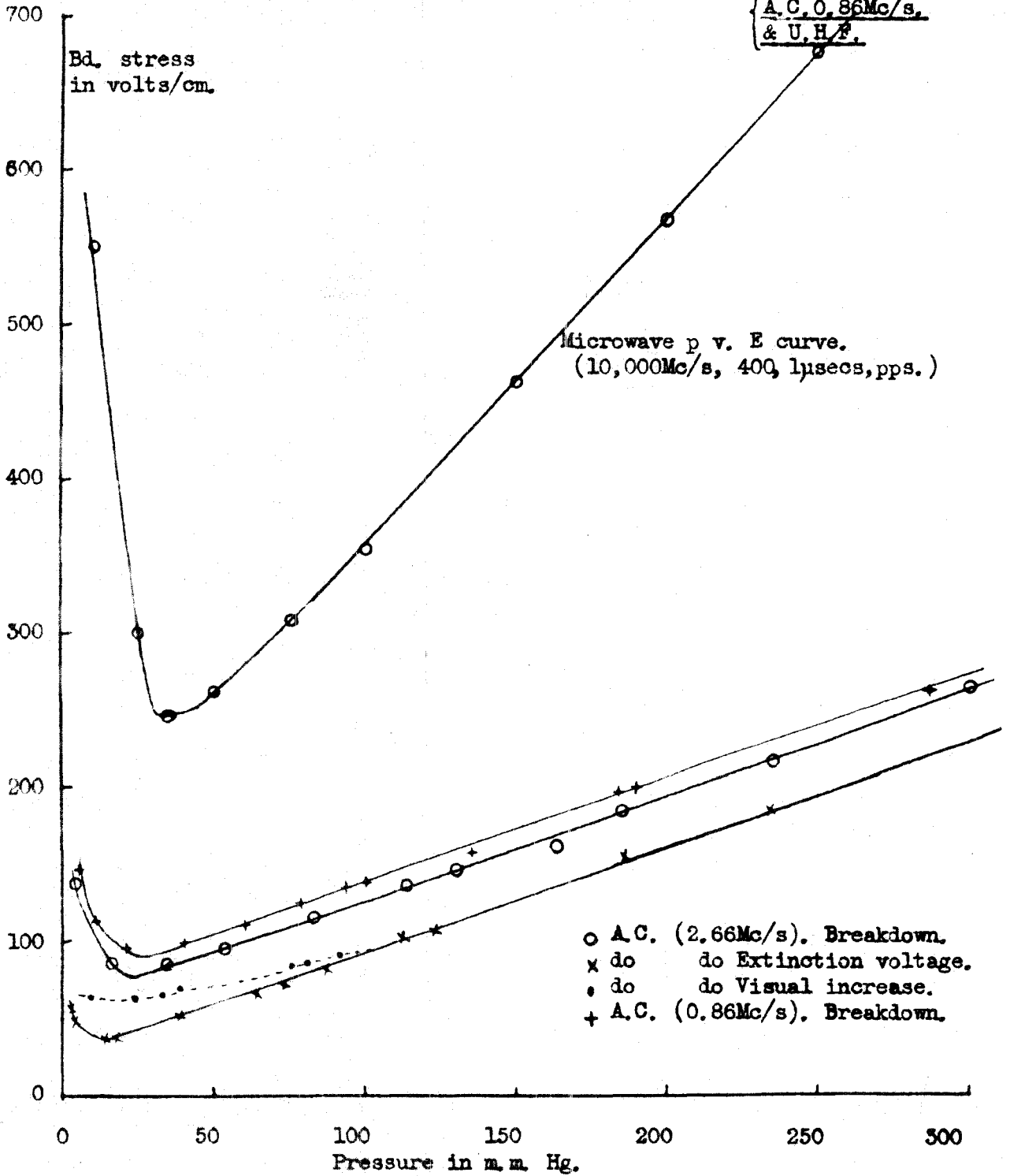


field was observed for the lower pressures, but was a maximum of 2 to 3 per cent. It can therefore be stated that for five separate sets of results, at all pressures, no increase in the microwave stress necessary for breakdown with the application of the auxiliary field was observed, except at very low pressures.

The neon discharge was blue in colour for pressures above 30 m.m.Hg. when excited by the alternating field alone, (similar to the colour observed at 0.86 Mc/s.) The colour changed to pink, and then the characteristic red as the pressure was decreased below 30 m.m.Hg.

Visual observations of the microwave discharge showed that as the auxiliary field was increased the intensity of the discharge first decreased and then suddenly increased. Due to the gradual reduction of the intensity as the auxiliary field increased it was impossible to record at what auxiliary field voltage the intensity reduction commenced. The auxiliary voltage at which the intensity of the microwave discharge increased was easily determined. This voltage (A.C.) was identified as the lowest auxiliary field necessary to maintain the discharge on removal of the microwave stress, the points at which the curves branch in graph 38 identify these voltages. (The auxiliary voltage necessary to initiate a discharge was

Graph 39 , NEON. Breakdown Stress v. Pressure, for (A.C. 2.66Mc/s.  
 A.C. 0.86Mc/s.  
 & U.H.F.)



considerably greater than this value of course).

The microwave stresses shown on the lower curve for any pressure were determined visually. A blue glow due to the alternating field discharge in the resonator was first observed and as the microwave stress increased a red glow fairly suddenly appeared within the blue glow; this was taken as the microwave discharge. If no alternating discharge was present the microwave stress had to reach the higher value before breakdown occurred.

The lowest auxiliary field voltages that would maintain the discharge, once started, were really the extinction voltages ( 'X' on graph) of the alternating discharge, and are plotted on graph 39. Pressure above 80 m.m.Hg gave a very sharp value for this auxiliary field voltage where the increase in the discharge intensity occurred. The auxiliary voltage at which the intensity of microwave discharge was observed to increase (plotted as '●' on graph 39) were found to be slightly greater than the alternating field extinction voltages for pressures below 80 m.m.Hg. However, it was difficult to state at these low pressures the exact voltage at which the discharge intensity visually increased.

The statistical lags were observed to be higher when the auxiliary field was also operative.

2.2.2. Breakdown of neon under the alternating field (2.66 Mc/s) alone.

The stress against pressure curve for neon breakdown under the action of the 2.66 Mc/s. field is shown on graph 39, (plotted as '0'); a linear relationship above about 20 m.m.Hg. These results were reproducible and agree with the boundary conditions, (vertical arrows on graph 38), established in the crossed field experiments.

The curve for 0.86 Mc/s. is also plotted, (plotted as '+'), and is slightly higher though parallel to the 2.66 Mc/s curve: the microwave stress curve is also shown. Attention is drawn to the fact that the microwave field was pulsed while the alternating fields were sustained.

2.2.3. Electron ambits under crossed fields, neon.

The table below gives the electron ambits under crossed field at the boundary conditions for one half cycle of the alternating field. These are the maximum values of the electron ambit under the combined field, higher auxiliary fields initiated discharge alone.

TABLE 24. Electron ambits in alternating field, neon.

p m.m.Hg.	Microwave stress.	Alternating field stress. Boundary value.	Electron ambit in $\frac{1}{2}$ cycle of A.C. field = $1.88$ $\times 10^{-7}$ secs.
	volts/cm.	volts/cm.	m.m.
465	1125	400	0.98
375	930	315	0.98
299	775	260	1.0
235	680	210	1.1
187	530	185	1.2
124	395	160	1.75
80	290	118	2.1
33	250	85	4.1
9	405	105	15.5
5.5	555	120	45

The electron ambits are considerably smaller than the dimensions of the capsule except at the lowest pressures; thus removal of the electrons by clean up cannot be operative in neon, except at the lowest pressures.

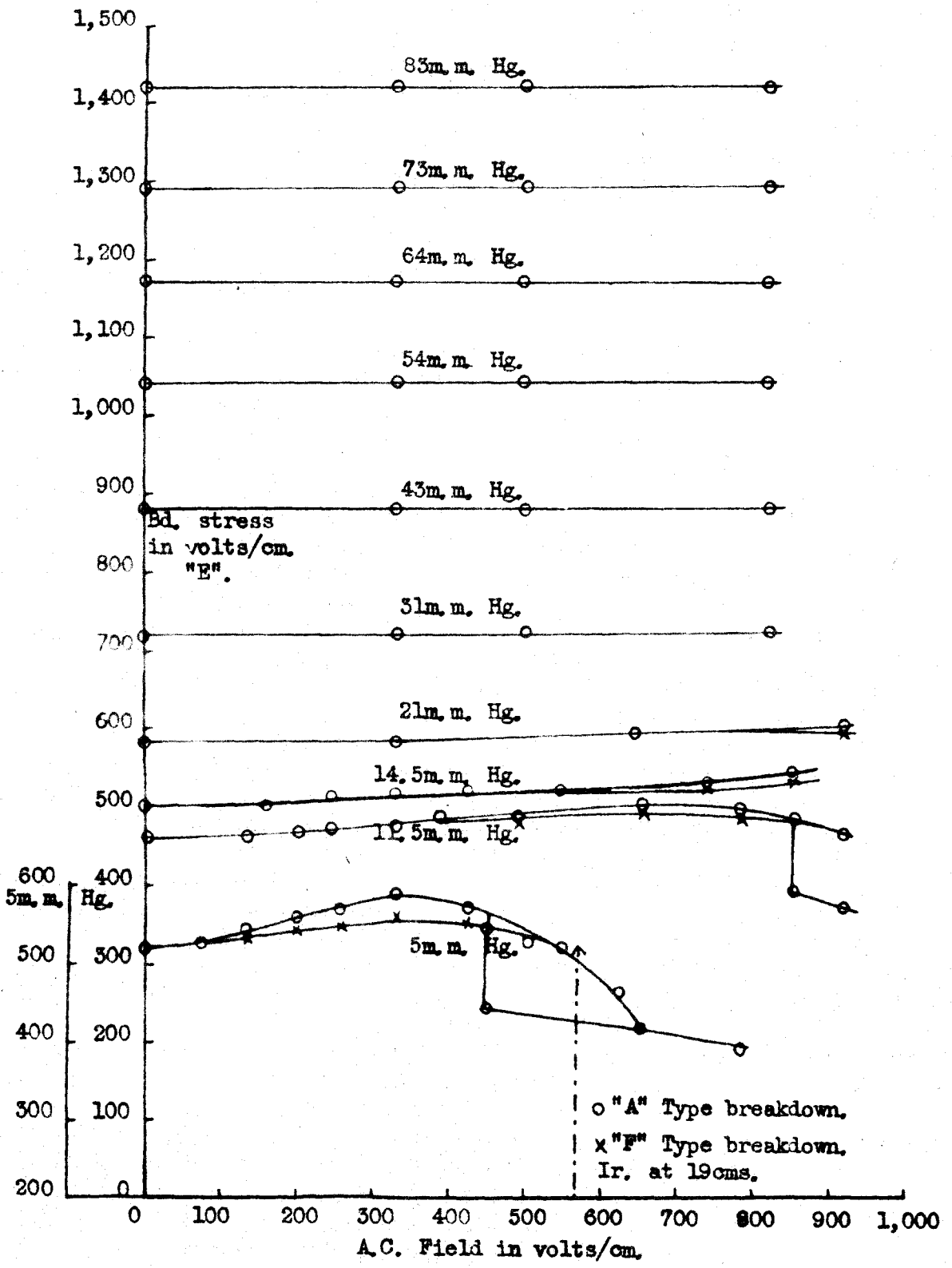
The neon results again show the apparent independence of the two fields right up to breakdown conditions of either field. Further discussion is reserved to a later chapter.

### 2.3 Spectroscopically pure nitrogen.

#### 2.3.1. Variation of the microwave breakdown stress with auxiliary field.

Curves very similar to the other two gases were obtained showing no general increase in the

Graph 40 . NITROGEN. Breakdown Stress v. A.C. Field (2.66Mc/s).



necessary microwave stress to initiate breakdown when the alternating field was applied orthogonally. At low pressures, below 21 m.m.Hg. a slight rise in the microwave stress was evident; two types of breakdown were again observed, the F and A type, for these low pressures. (Graph 40). The vertical line for 5 m.m.Hg. represents the necessary alternating voltage to produce breakdown alone; the microwave breakdown stress values to the right of this boundary and for the cases when the auxiliary voltage was greater than the extinction voltage, were obtained by noting when the pulse envelope on the oscilloscope collapsed. The presence of the alternating discharge in the resonator did not change the magnitude, or shape, of the pulse envelope; at very low pressures a slight blurring occurred.

The alternating voltages at which an increase in the microwave stress was necessary to initiate breakdown are of considerable interest, and the electron ambits at these voltages are given below. It will be seen that the increase occurs when the electron ambit is of the order half the length of the capsule.

TABLE 25 Electron ambits in A.C. field for pressures  $\leq$  21 m.m.Hg.

p m.m.Hg.	Alternating voltage volts/cm.	Electron ambit m.m.	Half length of capsule. m.m.
5	130	6.2	11
11.5	190	6.8	11
14.5	240	7.1	11
21	380	8.5	11

The statistical lag seemed to increase with increase in the applied auxiliary field; the time taken to ascertain actual values would have been prohibitive. The intensity of the discharge also seemed to decrease up to the point where the auxiliary field maintained the discharge on removal of the microwave field.

### 2.3.2. Alternating field cut off voltages.

Setting the microwave stress to the minimum value necessary to initiate discharge (no auxiliary field operative), this discharge could be extinguished by application of the auxiliary field. Extinction of a microwave discharge could only be obtained for the lower pressures, the auxiliary field values were reasonably consistent, 5% to 8%. Again the electron ambit seems to be of the order half the capsule length, (11 m.ms.)

TABLE 26. Electron ambit in A.C. extinction field.

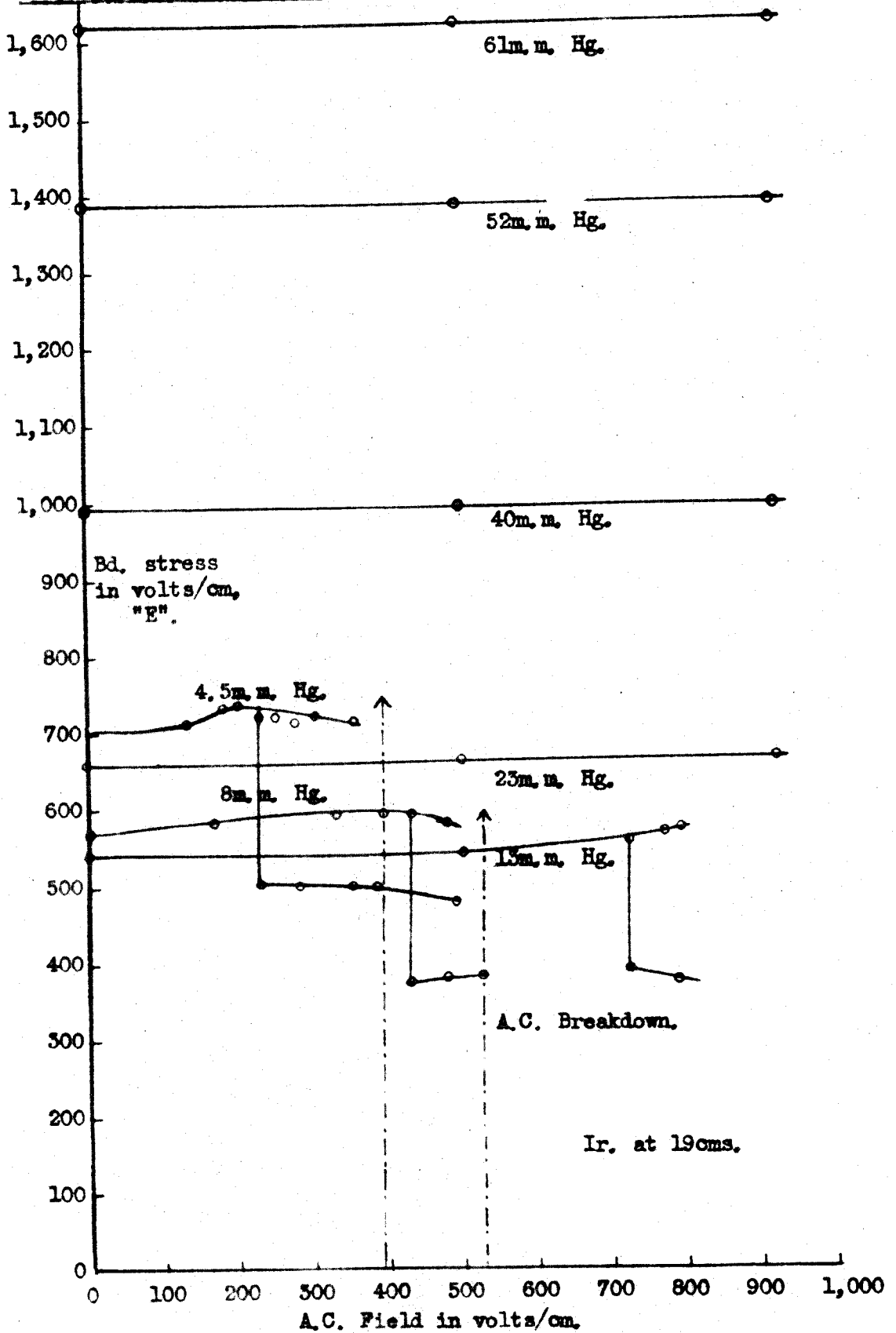
$p$ m.m.Hg.	Microwave field. volts/cm.	A.C. cut off volt- age volts/cm.	Electron ambit in $\frac{1}{2}$ cycle of A.C. m.m. (field)
5	520	75	4.0
11.5	460	230	7.7
14.5	500	240	7.4

### 2.4. Cylinder Oxygen.

#### 2.4.1. Variation of the microwave breakdown stress with auxiliary field.



Graph 41. OXYGEN. U.H.F. Breakdown Stress v. A.C. Field (2.66Mc/s).



No observable increase could be established in the microwave stress required to produce breakdown with an orthogonally applied auxiliary field for pressures greater than 12.5 m.m.Hg. The presence of an alternating discharge in the capsule did not alter the tuning of the resonator, and the pulse envelope was not disturbed as viewed on the oscilloscope, hence microwave breakdown could be established when there was already an alternating discharge in the resonator. Such microwave stresses are shown on the graphs by the lower curve for any particular pressure. (Applicable to pressures 13, 8 and 4.5 m.m.Hg. only). (Graph 41).

The statistical lags were extremely long in oxygen, but an increase in the lags could be established for the lower pressures as the auxiliary field increased, there appeared little effect at higher pressures.

The slight increases observed in the microwave stress as the auxiliary field increases again appeared to occur where the electron orbit under the alternating field is of the order half the length of the capsule.

Graph 42, AIR U.H.F. Breakdown Stress  $\gamma$ , A.C. Field (2.66Mc/s).

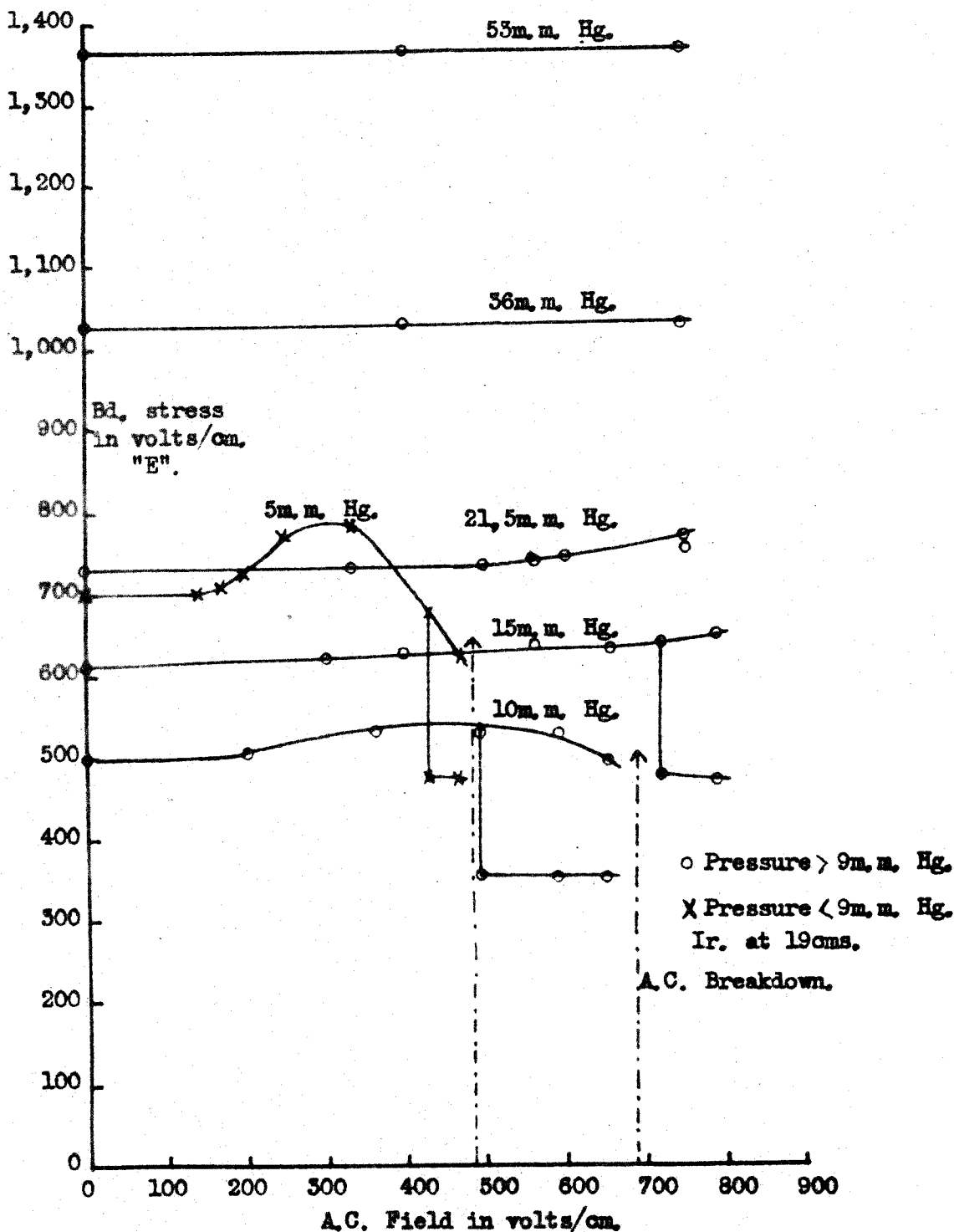


TABLE 27. Electron ambits in A.C. field (microwave stress increase).

p m.m.Hg.	Alternating field. volts/cm.	Electron ambit. m.m.
4.5	160	7.4
8.0	150	5.8
13.0	500	9.2

On removal of the fields the gas rapidly returned to an unexcited state in that reapplication of the microwave stress did not produce spontaneous breakdown, i.e. no recovery troubles were encountered. For the low pressures it was usually found advisable to allow 10 to 20 seconds for complete recovery of the gas.

Oxygen therefore exhibits the apparent complete independence of the two fields in initiating a discharge, except where the electron ambit becomes large, i.e. of the same order as the dimensions of the gas chamber.

### 2.5. Dry air.

#### 2.51. Variation of the microwave breakdown stress with auxiliary field.

The variation of the microwave stress for breakdown as the applied alternating field increases followed the same general pattern of the other gases, and the results can be seen in graph 42. Breakdown for the alternating field alone could only be established for the two lowest pressures, 5 and 10 m.m.Hg. A slight increase

in the breakdown stress could be determined up to a pressure of 21.5 m.m.Hg. The electron ambits appropriate to the alternating field stress at which an increase in the microwave stress was found necessary to initiate breakdown are given in the table below. They again appear to be the same order as half the length of the capsule.

TABLE 28. Electron ambits in AC field (microwave stress increase).

P m.m.Hg.	Alternating field. volts/cm.	Electron ambits. m.ms.
5	155	10.7
10	200	8.8
15	300	9.0
21.5	500	11.0

The statistical lags generally increased with the applied auxiliary field, even when the application of the auxiliary field did not necessitate an increase in the microwave field to produce breakdown.

#### 2.6. Résumé of the 2.66 Mc/s work.

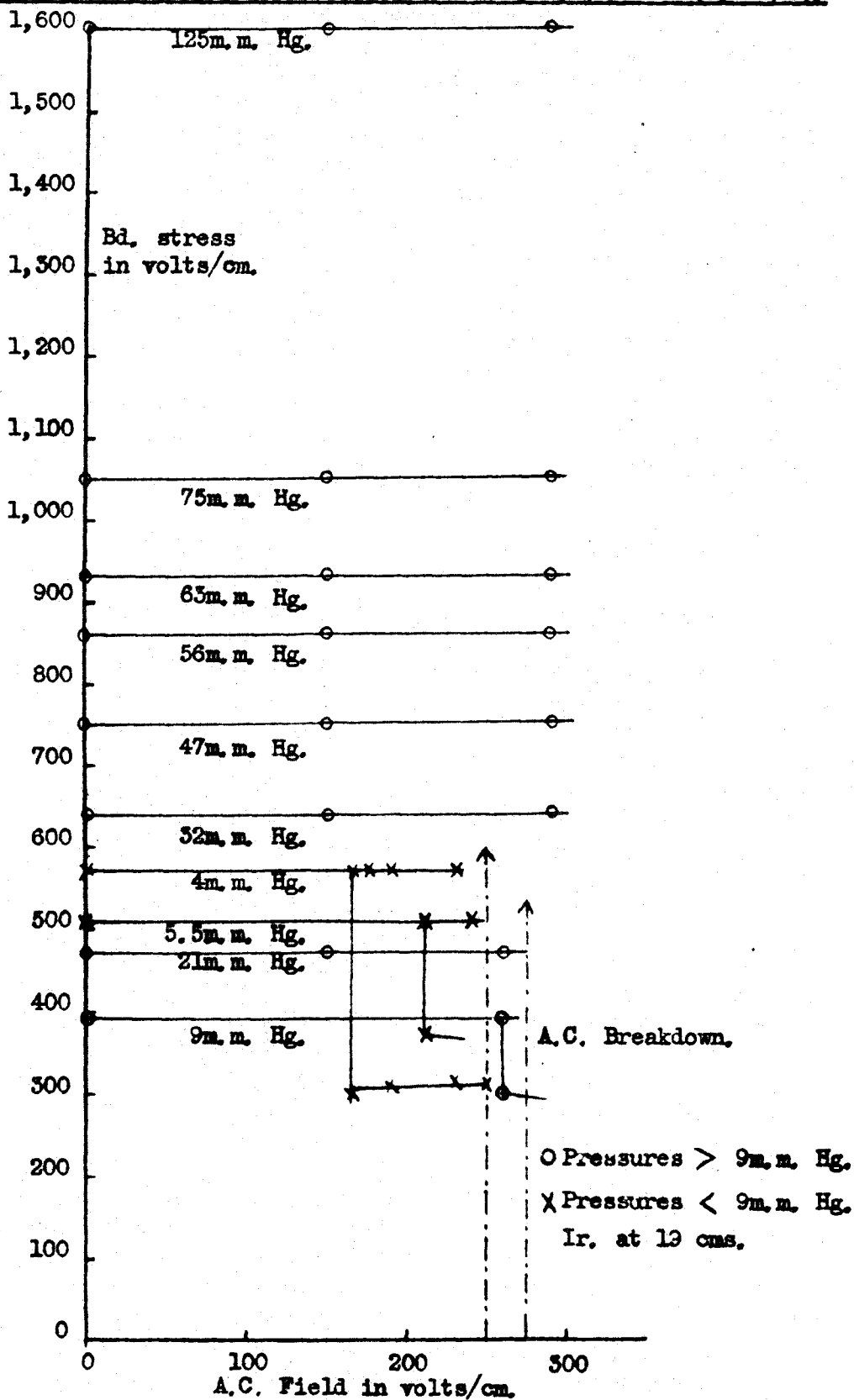
Apart from neon, the application of an orthogonal alternating field to the microwave field did not in general result in any variation in the microwave stress required to give breakdown. This was true up to

alternating voltages within 10 volts of the alternating field breakdown voltage; the two fields seemed to be completely independent in action.

A small increase in the microwave stress for breakdown became necessary at the low pressures as the auxiliary field increased; it would seem that the electron ambit at this point became comparable to half the length of the capsule. The alternating voltages necessary to extinguish the microwave discharge also gave a resultant electron ambit of the same order, probably indicating electron capture by the capsule walls.

The electron ambits are still rather large and finally the experiments were repeated using a higher auxiliary field frequency, (10 Mc/s). Air, hydrogen and neon were used for these trials; the results are given in the next chapter.

Graph 43, HYDROGEN, U. H. F. Breakdown Stress v. A.C. Field (9.7Mc/s).



CHAPTER 5.Crossed fields, microwave and 9.7 Mc/s. fields.1. Apparatus.

The coils for the low frequency oscillator consisted of 9 turns of 10 S.W.G. copper wire with a diameter of 2 inches; this gave a peak output of 880 volts at a frequency of 9.7 Mc/s. The voltage obtainable was less than in the previous oscillators, but proved sufficient for these experiments.

Three gases were subjected to the action of the crossed fields, hydrogen, neon and air; each gas is again considered separately.

2. Results.2.1. Pure electrolytic hydrogen.2.1.1. Variation of the microwave breakdown stress with auxiliary field.

No variation in the microwave field was required to produce breakdown with the 9.7 Mc/s field applied orthogonally; this was found to be true for the complete pressure range explored, i.e. 7.5 to 220 m.m.Hg, (Graph 43 gives the corresponding curves). The constancy of the microwave stress persisted right up to auxiliary field values that themselves initiated breakdown; the rectangular form of the graphs is again evident. Two positions of the



irradiator were used with similar results - no variation in the microwave breakdown stress.

The presence of an alternating discharge did not appear to de-tune the resonator, and the pulse envelope maintained its magnitude and shape. It was thus possible to establish the microwave breakdown stress required when an alternating field discharge was already present in the resonator. When the applied alternating field voltage was above the extinction voltage, the alternating discharge persisted when the microwave field was removed. On re-applying the microwave stress the voltage necessary for collapse of the pulse envelope was considerably lower than the microwave stress required to initiate discharge, when no alternating discharge was already present in the resonator. (The lower of the two curves on graph 43 for the pressures 4 and 5.5 m.m.Hg. show these voltages).

#### 2.1.2. Electron ambits under crossed fields, hydrogen.

Calculation of the electron amplitude of oscillation under the effect of the alternating field, when both fields were operative, shows that even at the lowest pressure and maximum alternating field the ambits were considerably smaller than the dimensions of the capsule.

Graph 44. NEON U.H.F. Breakdown Stress v. A.C. Field (9.7Mc/s).

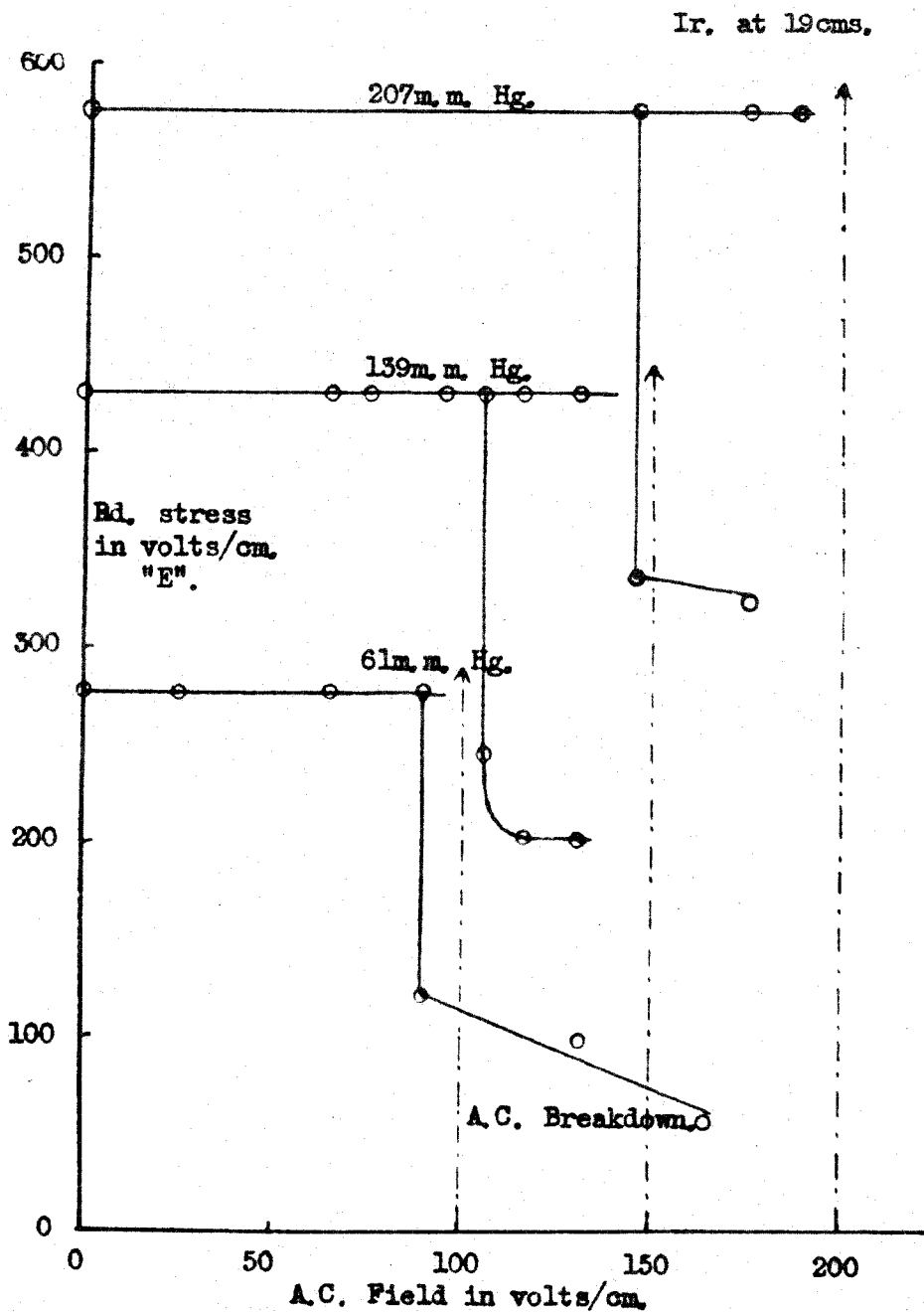


TABLE 29. Electron ambits in alternating field, hydrogen.

p m.m.Hg.	Alternating voltage.	Electron ambit for $\frac{1}{2}$ cycle of A.C.field.
	volts/cm.	m.m.
220	290	0.04
31.5	290	0.83
21.5	260	1.1
9	250	2.5
Bd conditions (5.5	275	4.9
under A.C.field (4	250	5.3

It would therefore seem improbable that the electrons are swept to the capsule walls and lost by the action of the alternating field.

## 2.2. Spectroscopically pure neon.

### 2.2.1. Variation of the microwave breakdown stress with auxiliary field.

No increase in the microwave stress necessary to produce a discharge in the capsule could be determined with the application of the 9.7 Mc/s field, even up to the breakdown stress for the auxiliary field. Graph 44 shows the curves obtained for the three pressures used, 61, 139 and 207 m.m.Hg; the vertical lines again indicate breakdown of the gas under the action of the alternating field alone. Values of the microwave field to the right of these boundaries could be established visually, by the fact that again the alternating discharge appeared blue, and the microwave

red. The microwave discharge could therefore be seen to suddenly start within the general blue glow of the alternating field discharge.

This procedure also enabled the values to the left of the boundaries where the alternating discharge still persisted (once triggered by the combined breakdown), to be established. By this method the lower values, for a given pressure, of the microwave stress were determined; of course if no alternating discharge was present in the resonator then the microwave stress had to be increased to the higher values shown. This was found to be true for all gases at the three auxiliary frequencies. The irradiator made no difference to the microwave stress recorded when the alternating discharge was already present in the capsule.

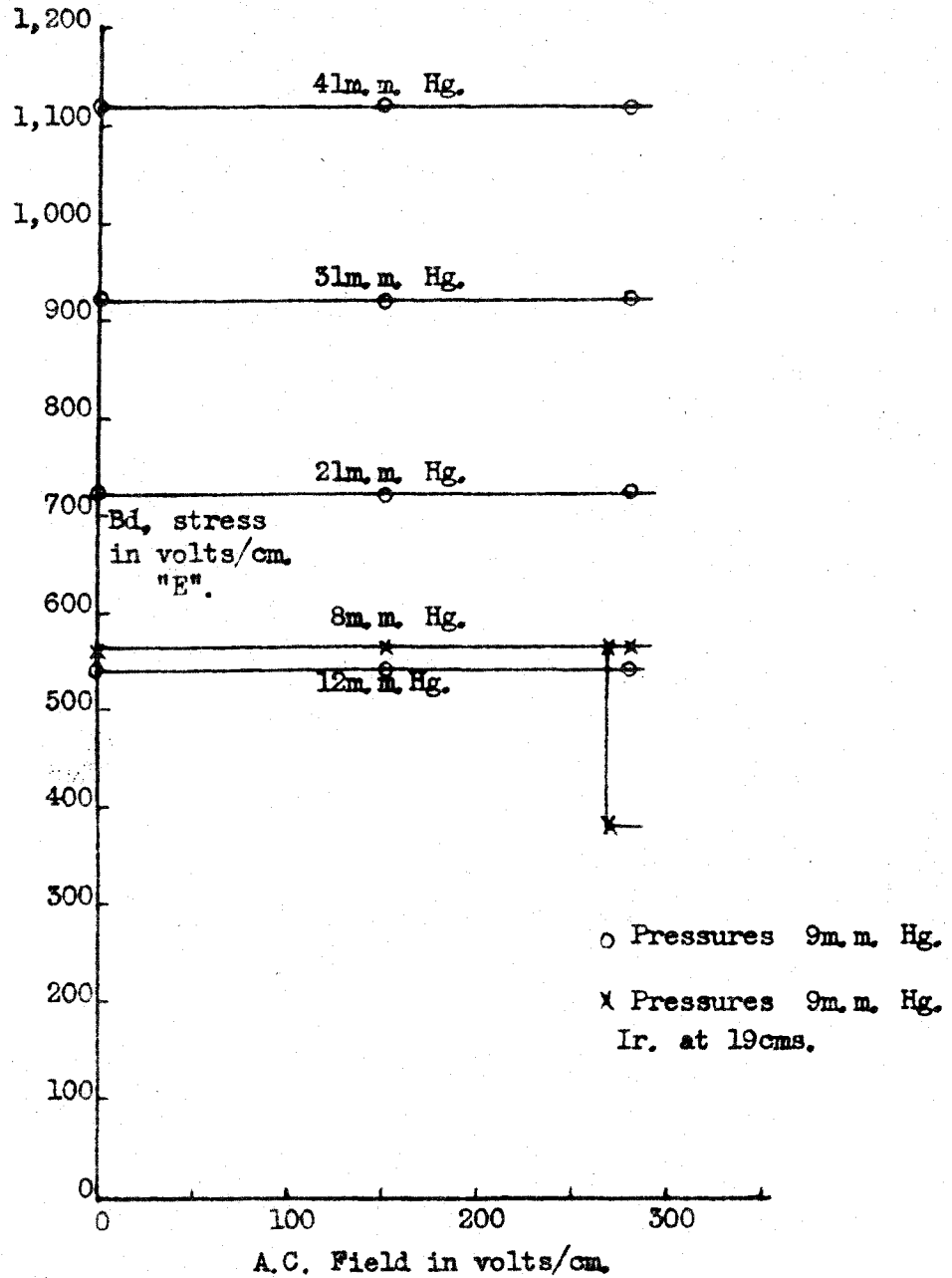
#### 2.2.2. Electron ambits under crossed fields, neon.

The electron ambits are given in the table below for the highest alternating voltages that could be applied before the alternating field initiated breakdown itself. The maximum electron ambit is approximately 1 m.m. and thus far smaller than the linear dimensions of the capsule.

TABLE 30. Electron ambits in alternating field, neon.

p m.m. Hg.	Alternating voltage volts/cm.	Electron ambits. m.m.
207	210	0.4
139	150	0.5
61	100	0.68

Graph 45 . AIR U.H.F. Breakdown Stress v A.C. Field (9.7Mc/s).



Electron removal to the walls of the capsule by the action of the alternating field can be considered negligible.

### 2.3. Dry Air.

#### 2.3.1. Variation of the microwave breakdown stress with auxiliary field.

Exactly similar results were found for air, no variation in the microwave field was required to initiate breakdown on application of the alternating field; this was true even for the lowest pressure used, 8 m.m.Hg. It was unfortunate that breakdown under the auxiliary field could not be reached; later work employing parallel plane electrodes showed air at 8 m.m.Hg. at a frequency of 11 Mc/s. to have a breakdown stress of approximately 400 volts/cm. However the alternating voltage was high enough to reach the extinction voltage at this pressure. The presence of the alternating discharge did not appear to change the pulse envelope as displayed on the oscilloscope. Thus with the alternating discharge present the microwave field could be increased and the onset of the microwave breakdown indicated by the collapse of the pulse envelope. The low values at this pressure, (8 m.m.Hg), were determined in this manner, (graph 45 refers). With no alternating discharge present the higher values were necessary for the microwave field to initiate breakdown.

2.3.2. Electron ambits under crossed fields, air.

Taking the two extreme pressures used and the maximum applied alternating voltage the electron amplitudes of oscillation were still small in comparison with the dimensions of the capsule.

TABLE 31. Electron ambits in alternating field, air.

p m.m.Hg.	Alternating voltage volts/cm.	Electron ambit. m.m.
8	280	3.3.
41	280	1.03

3. Discussion.

It was felt that before any explanation, or hypothesis, could be advanced to account for the apparent complete independence of the two fields, even up to breakdown conditions of either field, a somewhat more detailed study should be undertaken of the electron movement in the capsule. Therefore the following experiment was undertaken: to set up a parallel gap system and measure the electron amplitude under an alternating field of comparable frequency to the ones used above, and to compare the experimental and calculated electron ambits. The electron ambit can be

determined by gradually decreasing the separation of the parallel plates until the electrons become captured by the electrodes in one half cycle; this is evident by a sharp rise in the breakdown stress.

These experiments have been undertaken at 2.3 Mc/s and 11.5 Mc/s for hydrogen, and 11.5 Mc/s for air, oxygen and nitrogen; they are described in chapter 7

First, however, the different methods that can be used for calculating electron amplitudes of oscillation are compared in chapter 6; one method has been used in all the calculations so far presented, (the method given in section 2.2 chapter 6).



CHAPTER 6.

Calculation of electron ambits.

1. Electron drift velocity correction under crossed fields.

In the combined fields a charged particle in a viscous medium would execute a path similar to figure 36. Electron movement is complicated by diffusion effects and the dependence of drift velocity on random velocity

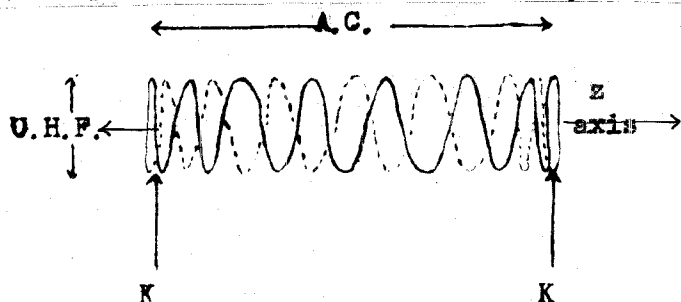
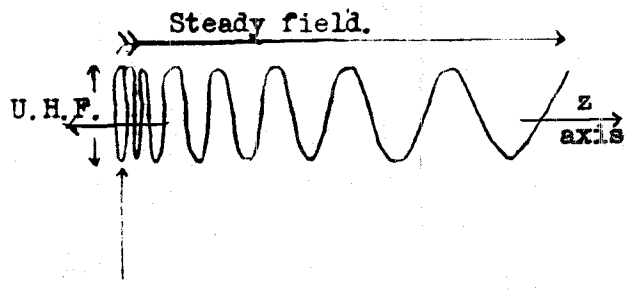


Fig. 36a Electron movement, U.H.F. + A.C. Field.



36b. K. Fig. Electron movement, U.H.F. + D.C. Field.

In working out typical electron tracks, diffusion is neglected, but it is assumed that the random velocity is always that appropriate to the magnitude of the combined

fields, averaged over a time interval long enough to allow of the adjustment of the random velocity, (e.g. random velocity will not change at same rate as the microwave field).

Let  $V_E$  random velocity of electron under microwave field E  
 $W_E$  drift " " " " " " E  
 $V_x$  random " " " " alternating " X

$W_x$	drift velocity of electron under alternating	field	X
and	" " " "	the combined	T
let $V_T$	random	fields	
		where $T = \sqrt{E^2 + X^2}$	

Experimental values of the random and drift velocities appropriate to the particular steady state of the field were taken from the literature<sup>87</sup>; the drift velocities were then corrected by a factor  $\frac{V_E}{V_T}$  or  $\frac{V_X}{V_T}$ .

The corrected drift velocities then became  $cW_E = W_E \frac{V_E}{V_T}$  and  $cW_X = W_X \frac{V_X}{V_T}$

these corrected drift velocities were then used in calculations of the electron ambits as discussed in the following sections.

## 2. Calculation of electron ambits using corrected drift velocities.

### 2.1. Most precise method.

The electron ambit 'q' under the action of a field can be written as :-

$$q = \int_{t_1}^{t_2} w dt$$

$$= \int_0^t w dt \quad (t_1=0, \omega t=0)$$

Therefore ambit for a half cycle of the applied field becomes

$$q = \frac{2}{\omega} \int_0^{\pi/2} w d\theta = \frac{2}{\omega} A$$

The value of A was determined in the following manner. After correcting the drift velocities for a

particular case by the procedure shown in section 1 above, a graph was drawn plotting the corrected drift velocity  ${}_cW_x$  against field strength  $X$  (See figure 37a).

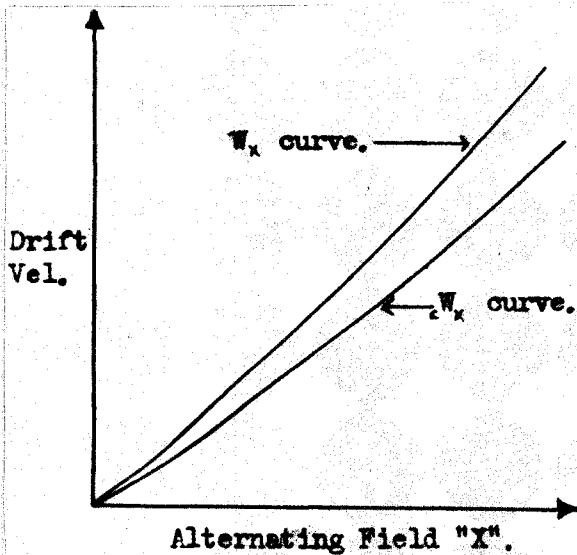


Fig. 37a Typical graph of Drift Velocity  
v. A.C. Field Stress,

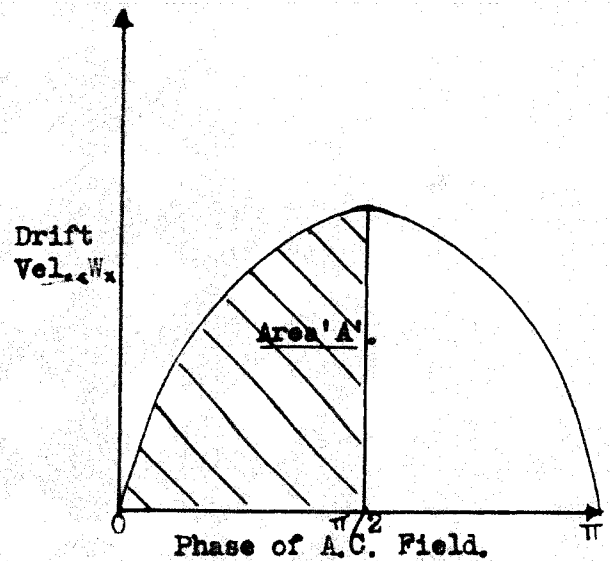


Fig. 37b. Typical graph of Drift Vel.  
v. Phase of A.C. Field.

A further graph was then required of  ${}_cW_x$  against  $\theta$ , where  $\theta$  is the phase angle of the sinusoidal field  $X$  in  $\theta$ , the area under this graph would then be  $A$ , (for  $\theta$ , 0 to  $\frac{\pi}{2}$ ). This second graph was easily obtained by determining the values of  ${}_cW_x$  from the first graph (37a) for each value of  $X$  in  $\theta$ , the type of graph thus obtained is shown in 37b.

The magnitude of the electron orbit under the action of the combined field along the  $Z$  axis of the resonator can therefore be determined. Each value of the alternating field (i.e. low frequency field 1, 3 or 10 mc/s),

necessitates its own particular graph 37b, this is a lengthy procedure.

An example of the values determined by this procedure for neon at 98 m.m.Hg. and an auxiliary field of 0.86 Mc/s is given below. The appropriate curve of E against X is plotted on graph 34, Chapter 3.

TABLE 32. Electron ambits, calculated as above.

Alternating field 0.86 Mc/s. X volts/cm peak.	Microwave field E. Volts/cm. peak.	Electron orbit under alternating field in $\frac{1}{2}$ cycle. m.m.
33	395	1.25
66	395	2.05
100	395	3.4
133	275	4.9
166	205	6.7
200	190	7.9

## 2.2. Sinusoidal variation of $cW_x$ .

The foregoing procedure could be considerably reduced if it is assumed that the corrected drift velocity follows the field variations precisely, i.e., the drift velocity on any instant is given by  $W_t = W_0 \sin \theta$  when the field is varying sinusoidally.

$$\text{Therefore } q = \int_{t_1}^{t_2} W \sin \theta dt \quad \omega t = \theta$$

$$\text{or } = 2 \int_0^{\frac{1}{4}\nu} W \sin \omega t dt \quad (t_1 = 0, t_2 = \frac{1}{2}\nu, \text{ for } \frac{1}{2} \text{ cycl}$$

$$\therefore q = \frac{W}{\pi \nu} \quad \text{where } \nu = \text{frequency of the applied field.}$$

The table below shows the electron ambits calculated using the above method for two cases:-

1. using  $W_x$  i.e. uncorrected, and
2. "  $cW_x$  i.e. corrected as in section 1.

TABLE 33. For neon at 98 m.m.Hg. and  $\nu = 0.86$  Mc/s.

Alternating field X	Electron ambit in m.m.		
	2nd method Sinusoidal variation of W		1st method for comparison.
	Either $W_x$	or $cW_x$	
33	2.0	1.2	1.26
66	2.7	2.05	2.05
100	4.25	3.45	3.4
133	6.1	5.2	4.9
166	7.65	7.1	6.7
200	9.15	8.5	7.9

The discrepancy between the electron ambits using the sinusoidal variation of the corrected drift velocities, and the more complicated first method is slight.

### 2.3 Using the R.M.S. value of the field.

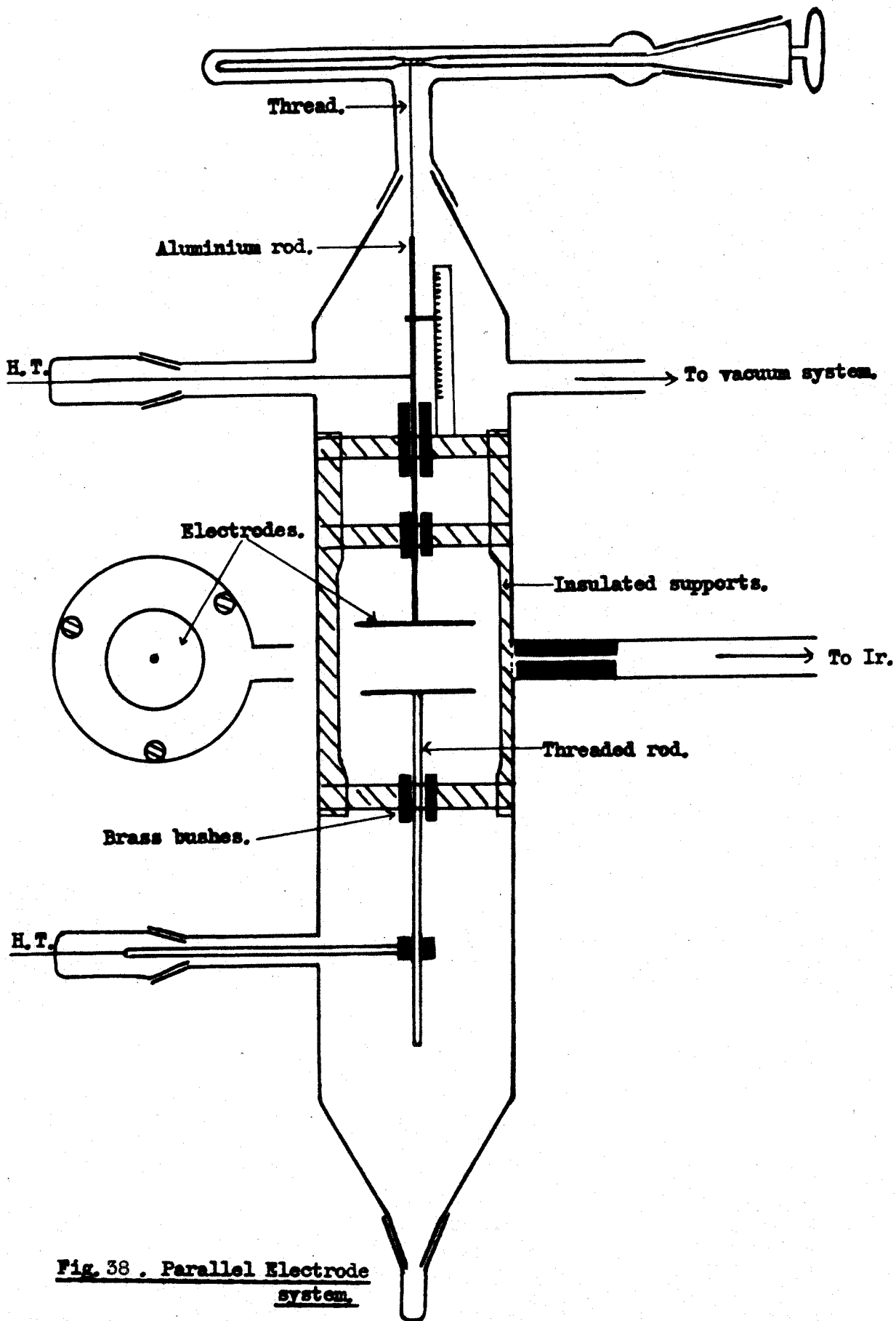
The value  $\frac{X}{\sqrt{2}}$  can be used for the applied field, and the corresponding drift velocities give the electron ambits shown in table 34 below; again two results can be deduced depending if the corrected or uncorrected drift velocity is used. The divergence from the first method is somewhat greater than the ambits calculated on a sinusoidal variation of the drift velocity.

TABLE 34. For neon at 98 m.m.Hg  $v = 0.86$  Mc/s.

Alternating field X  volts/cm.	Electron ambits using either		1st method for compari- son.  m.m.
	$W_x$ m.m.	or $\bar{W}_x$ m.m.	
33	1.44	2.85	1.26
66	2.3	3.95	2.05
100	3.75	5.2	3.4
133	4.9	6.85	4.9
166	8.6	9.6	6.7
200	10.1	10.9	7.9

### 3. Conclusions.

It was eventually decided to adopt the following method: correct the drift velocities by the random velocity correction procedure outlined in section 1, and then assume the sinusoidal variation of this corrected drift velocity, (section 2.2.) This method was used in all the electron ambit calculations presented in this thesis. For the unidirectional field experiments only the random velocity correction was used.



**Fig. 38 . Parallel Electrode system.**

CHAPTER 7.The parallel electrode work at 2.3 and 11.5 Mc/s.1. Introduction.

This chapter describes the investigations into the variation of the breakdown stress of a gas with electrode separation at frequencies of 2.3 and 11.5 Mc/s; these experiments were undertaken for the following three main reasons.

1. To try to establish whether the American diffusion theory for electrodeless discharge of a gas can be applied to the frequencies of the order 3 to 10 Mc/s. The diffusion theory requires a dependence of the breakdown stress of a gas on the electrode separation, see Introduction, page 17.

2. To check the electron orbit calculations as outlined in the previous chapter.

3. To compare the relative breakdown stresses of hydrogen, air, oxygen and nitrogen at 11.5 Mc/s. with the relative stresses as determined in the microwave experiments.

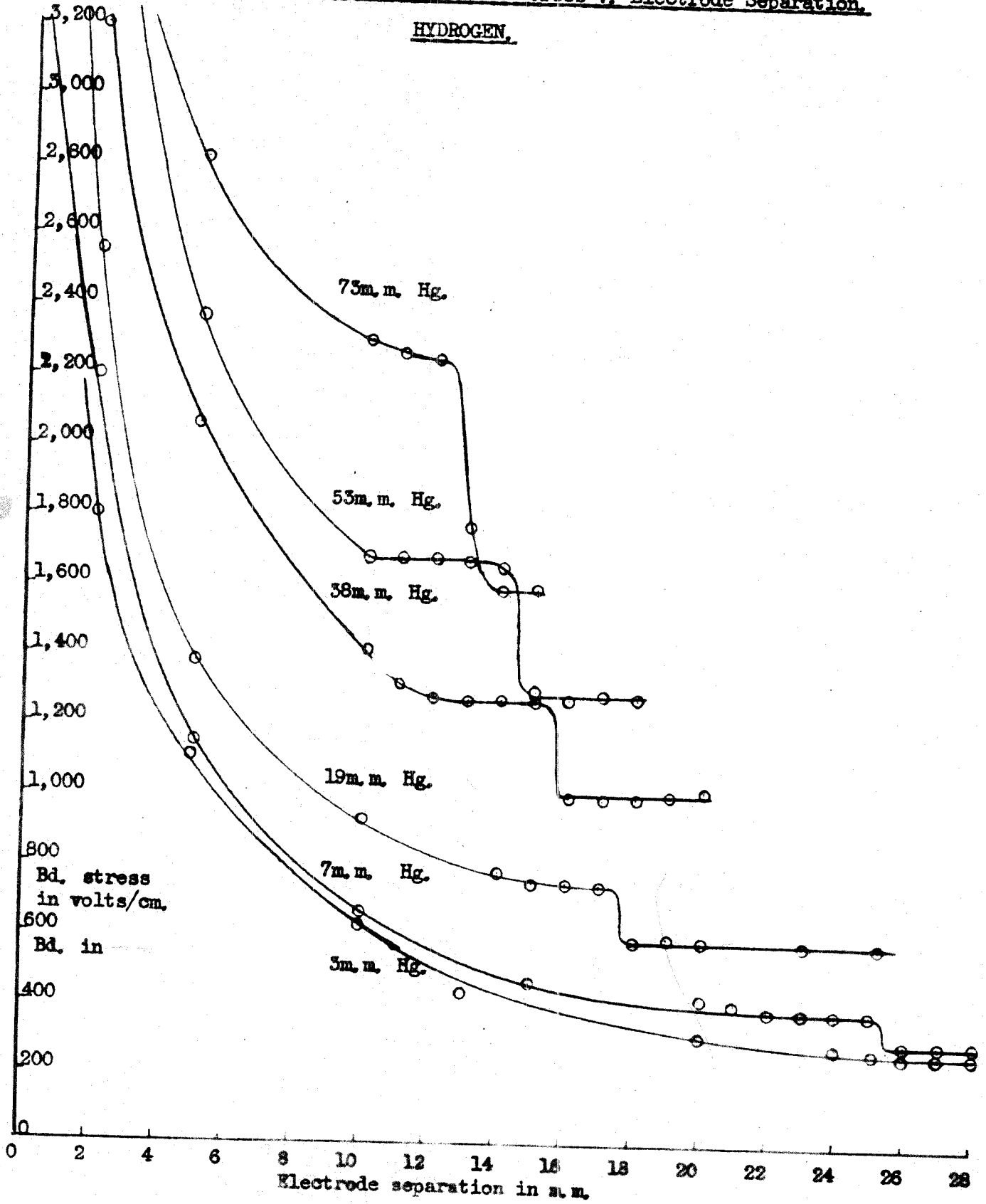
2. Apparatus.

The electrode system is shown in figure 38: the electrodes consisted of 1 cm. diameter aluminium discs, the lower electrode carried on a threaded rod, rotation of which varied the electrode separation. This could be described as the coarse adjustment, and could only be used when the



Graph 46 . A.C. ( 2, Mc/s). Breakdown Stress v. Electrode Separation.

HYDROGEN,



lower cone joint of the gas chamber was open. The use of 1 cm diameter electrodes gave a uniform field between the electrodes provided the separation did not exceed 30 m.m.<sup>87</sup> .

The upper electrode position was easily varied by rotation of the glass top. To ensure that the electrodes remained parallel the aluminium rod attached to the upper electrode slid through two accurately set brass bushes, as shown. Electrode separate could therefore be easily varied without breaking the vacuum of the system; this arrangement worked well.

The same oscillator and measuring circuits as used in the previous work were employed; this time the oscillator frequency was 2.3 Mc/s, or 11.5 Mc/s, with a peak output of 2800 volts

### 3. Results.

#### 3.1. The 2.3 Mc/s experiments.

##### 3.1.1. Hydrogen, pure electrolytic.

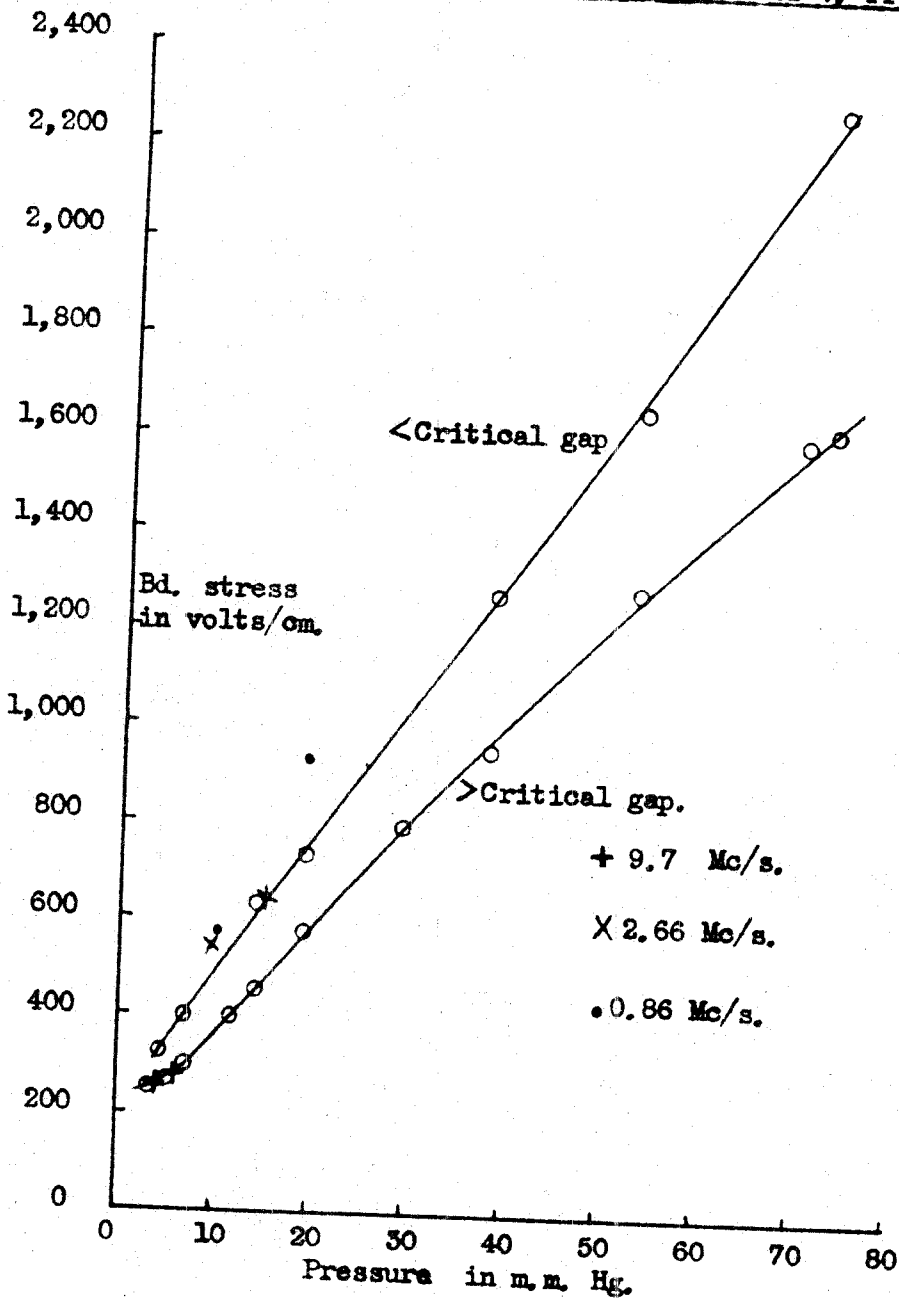
Electrolytically produced hydrogen, dried by phosphorous pentoxide was the only gas used at this frequency (2.3 Mc/s). Graph 46 shows the variation of the breakdown stress of hydrogen with the separation of the electrodes. A sharp drop is evident as the electrode separation increases, the breakdown stress then remaining constant within experimental area as the electrode spacing

is further increased. The experimental error was estimated to be of the order  $\pm 5\%$ . It was concluded from previous work that the sharp drop in the breakdown stress normally appears when the electron ambit fills the inter-electrode space. Assuming this to be true, calculations were made, the results of which are set out in the table below. The electron ambits in column 'A' are calculated using the field strength observed just before the sudden drop, (i.e. the top of the step), the ambits in column 'B' were deduced for the field strength on the lower part of the drop, (i.e. the bottom of the step). The electrode separation between which the sudden fall in breakdown stress occurred is shown in the final column 'C'.

TABLE 35. Calculated and experimental electron ambits (2.3 Mc/s).

p m.m.Hg.	Column 'A'	'B'	'C'
	Using field strength at top of step.	at bottom of step.	Electrode separations between which drop observed.
	Electron ambits. m.m.		m.ms.
73	14.8	11	13 to 12
70.5	14.8	11.3	13 to 12
53	15.6	12.5	15 to 14
38	17	13	16 to 15
29	20	14.4	16 to 15
19	20	16.3	18 to 17
14	22.5	17.9	20 to 19
11.5	26.5	19.4	21 to 20
7	28	22.3	26 to 25
4.5	-	33.5	Not reached at 30
3	-	37	-do-

Graph 47 . HYDROGEN A.C. (2.5Mc/s), Breakdown Stress v. Pressure.



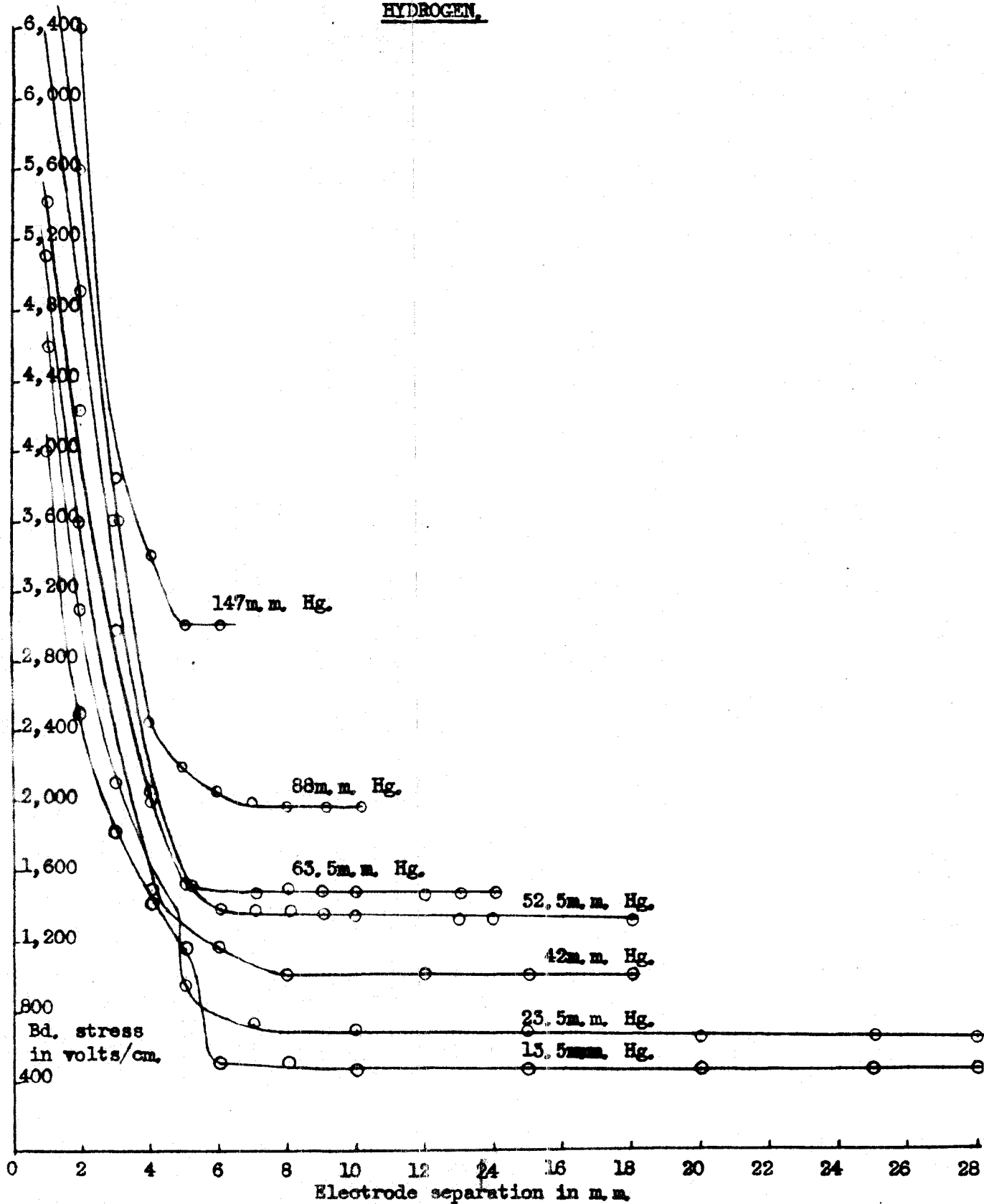
The experimental values in the final column fall in all cases between the calculated boundaries for the electron ambits; thus showing that the sudden drop in the breakdown stress as the electrode separation increases can be attributed to the point where the electron ceases to cross the inter-electrode space in one half cycle of the field oscillation. The electrode separation at which this drop in breakdown stress occurs will be described as the critical gap width.

The striking result of these curves is the constant value, within experiment error, of the breakdown stress once the electrode separation exceeds this critical value. To further investigate these flat regions of the curves required either an increase in the available voltage, or a higher frequency, the latter course was adopted and the frequency increased to 11.5 Mc/s.

Graph 47 shows the variation of the breakdown stress of hydrogen with pressure for gap widths greater than the critical value, and just less than the critical gap. The values of breakdown stresses determined in the earlier work for 0.86, 2.66 and 9.7 Mc/s are also shown; it will be remembered that these were the positions of the vertical arrows on graphs 33, 36 and 43 respectively. Calculations establish that for 0.86 Mc/s and 2.66 Mc/s the electron ambits

Graph 48 . A.C. (11.5Mc/s), Breakdown Stress v. Electrode Separation.

HYDROGEN.



at the pressures shown were greater than the capsule length, it is therefore to be expected that these breakdown stress values would appear above the 'less than critical gap curve'. The 9.7 Mc/s. results were for electrodeless breakdown and are seen to appear on the appropriate line on graph 47, i.e. 'the greater than critical gap curve'.

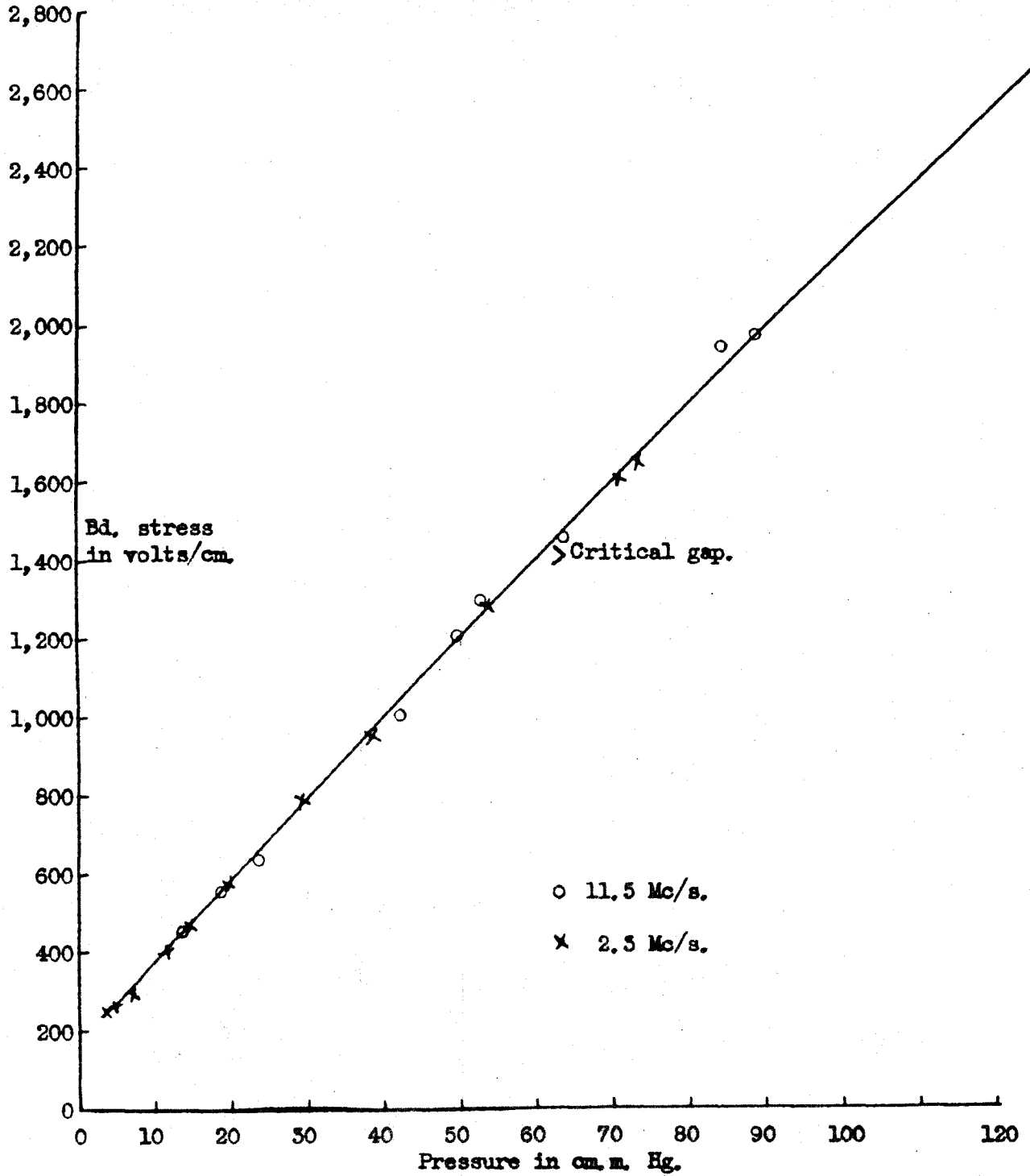
### 3.2. The 11.5 Mc/s experiments.

3.2.1. Hydrogen. The experimental technique was as before and very similar curves were obtained (Graph 48) the drop in the breakdown stress curves now occurring at a smaller electrode separation. The critical gap width again agreed with electron ambit calculations, and a summary of such calculations is given in table 36. Because of the uncertainty of the top of the step in the curves, only the electron ambit associated with the stress observed at the lower section of the step could be determined. It is therefore to be expected that the calculated value would be somewhat lower than the observed values.

TABLE 36. Calculated and experimental electron ambits (11.5 Mc)

p m.m.Hg.	Electron ambit. Using stress at lower part of step.	Electrode separation between which drop observed in graphs.
	m.m.	m.m.
170	1.9	2-3
163	2.0	2-3
147	2.0	3-4
88	2.3	3-4
63.5	2.5	3-4
52.5	2.6	3-4
42	2.7	3-4
23.5	3.0	3.5 - 4.5
13.5	3.6	4-5

Graph 49 . HYDROGEN, A.C. (11.5 Mc/s.), Breakdown Stress v. Pressure.





Two distinct forms of discharge could be distinguished, their appearance dependent on the electrode separation. For small gaps less than critical an intense form of discharge was observed, the I type, and consisted of an intense column of discharge with bright ends at the electrodes. The column became more diffuse as the pressure was reduced. The I type of discharge again became manifest at the very long gaps, i.e. at the extreme right hand side of the graphs shown.

At gap widths equal to and just greater than the critical gap a diffuse type of discharge, D, became evident, quite distinct in character from the I type. The D form of discharge tended to be situated in the centre of the electrode space.

The sequence as the gap width increased was:-

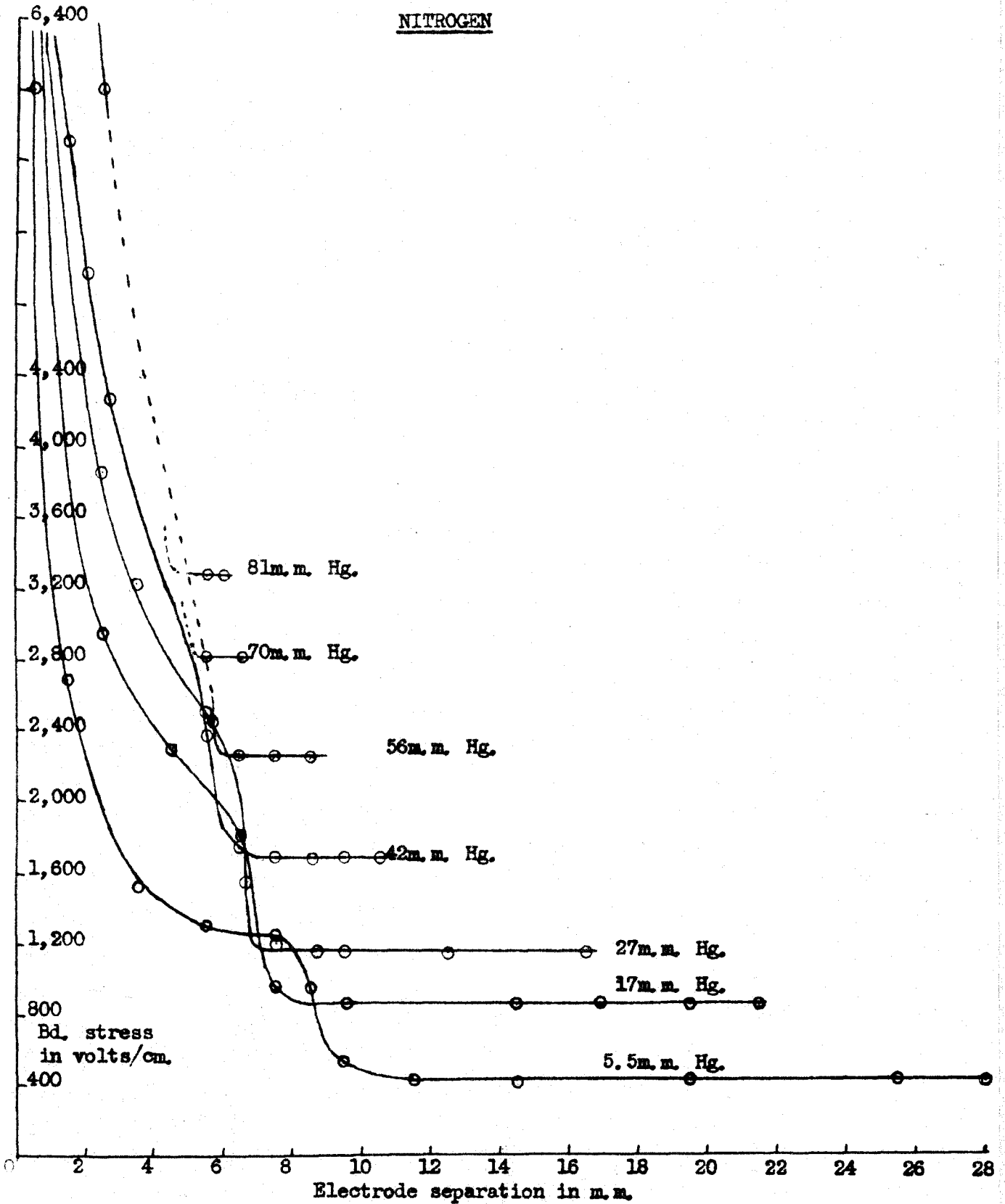
Pressure	< Critical gap	Critical gap	> Critical gap	>> Critical gap
Low	I type	D+I	D	D+I
High	I "	I	D	D+I

This sequence in the form or appearance of the discharge was found for all the sets of results taken with hydrogen at 11.5 Mc/s.

Other points of difference between the two types of discharge were:-

Graph 50 . A.C. (11.5Mc/s), Breakdown Stress v. Electrode Separation.

NITROGEN



1. The I type caused a large fall in the voltmeter reading.  
     " D " " " small " " " "
2. The I type caused a marked reduction in the anode current of the oscillator.  
     " D " " " small " " " "

and 3. The D type occasionally changed spontaneously to the I form of discharge; increasing the applied voltage usually changed the D type to the I form.

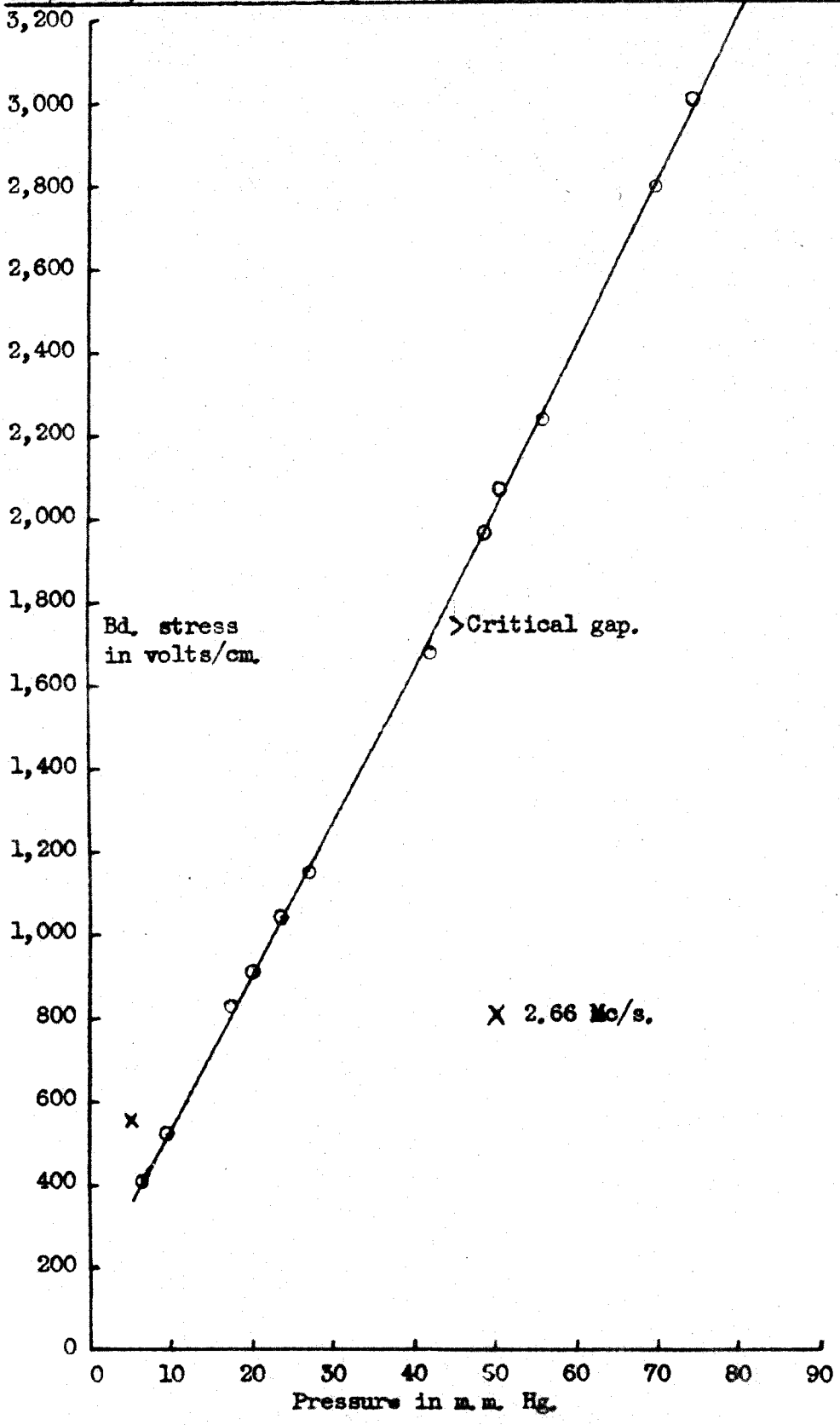
The second graph (49) shows the variation of the breakdown stress with pressure, the 2.3 Mc/s results are also plotted and they follow the same variation.

### 3.2.2. Nitrogen

An exactly similar experimental technique was used for nitrogen, resulting in similar curves to those found for hydrogen. A complete independence of the breakdown stress was found (measured in volts/cm) with the gap width provided the gap width exceeded the critical value and the discharge could be described as electrodeless in character.

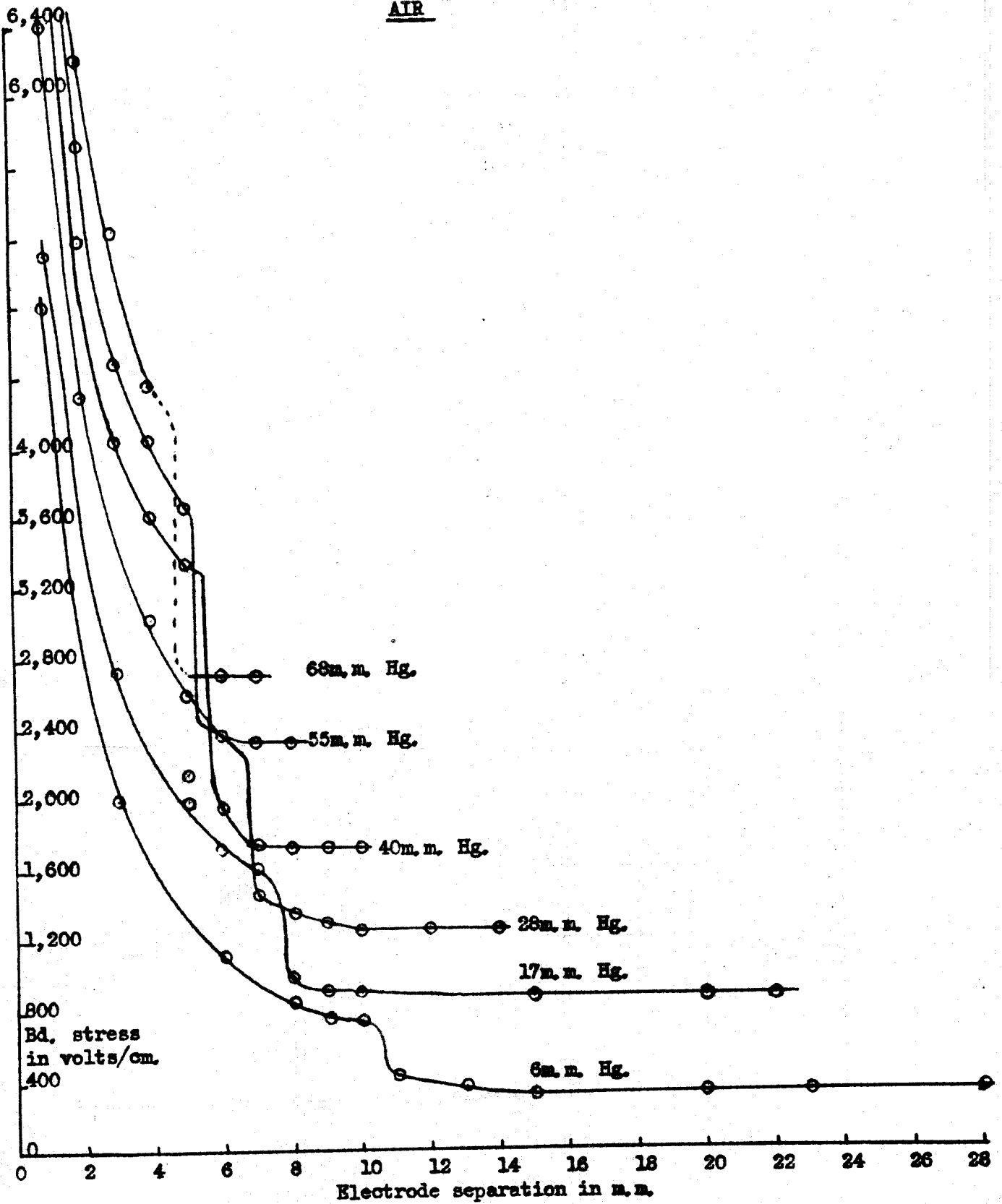
Spectroscopically pure and cylinder nitrogen gave similar results. The two types of discharge described above were encountered, occurring under approximately similar conditions. The intense form of discharge before the critical gap width was reached, for a gap greater than critical the diffuse form changing to a

Graph 51 , NITROGEN A.C. (11.5 Mc/s.), Breakdown Stress v. Pressure.



Graph 52, A.C. (11,5Mc/s), Breakdown Stress v. Electrode Separation

AIR



combination of both forms as the electrode spacing was increased. The maximum gap widths resulted in the intense form of discharge once again; the two forms of discharge were quite distinct in appearance.

The variation of breakdown stress with pressure appeared linear for the pressure range explored, 5 to 80 m.m.Hg. (graph 51). The value for 2.66 Mc/s breakdown stress from the crossed field work is also shown; calculation showed that the electron orbit for this discharge was greater than the length of the capsule, (see graph 40).

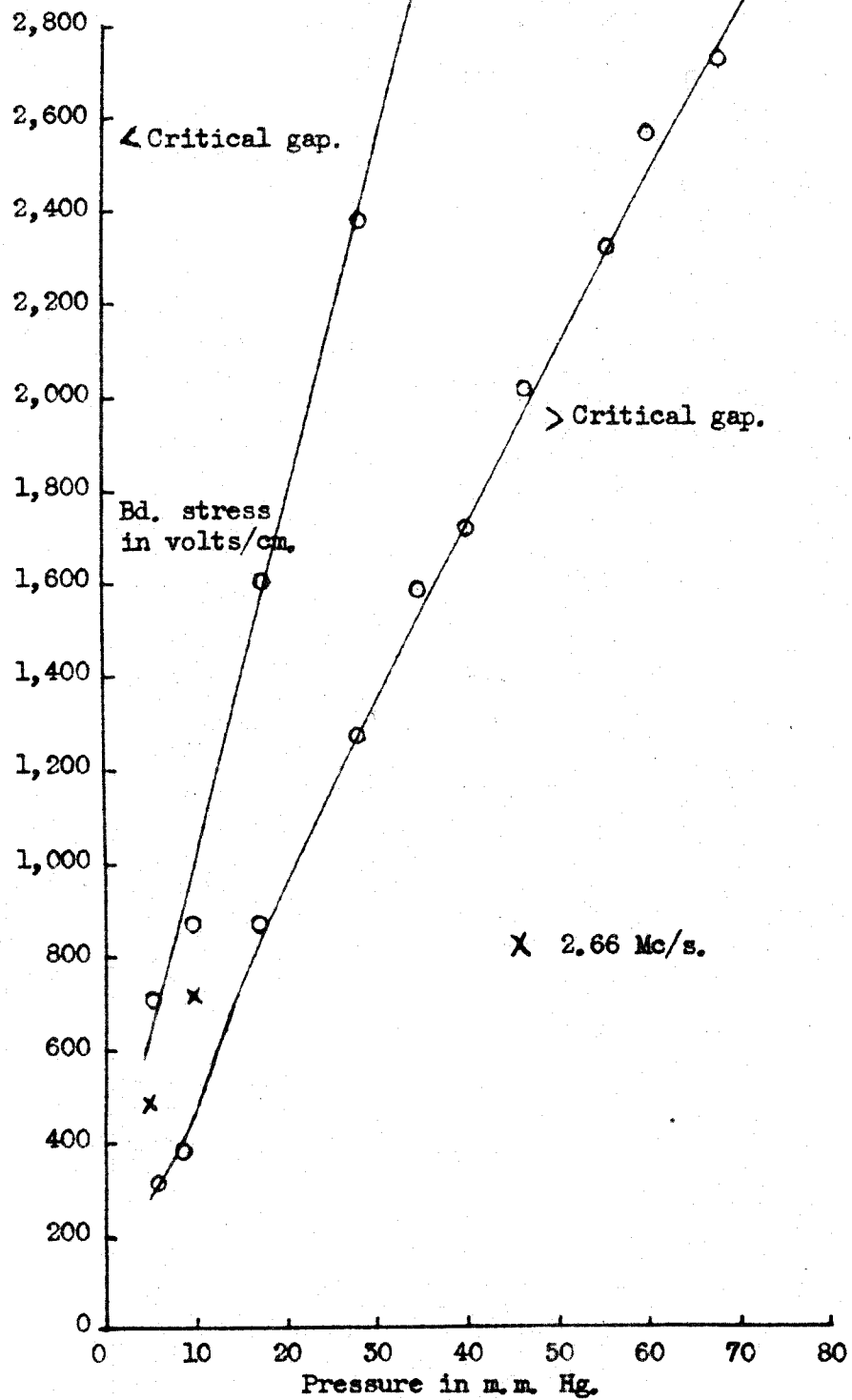
Slight recovery trouble after a discharge was encountered for nitrogen, but by allowing up to one minute between readings this could be overcome.

### 3.2.3. Dry Air.

Air is the only gas for which a unique value for the breakdown stress has been established, provided the discharge is electrodeless in character; this is again upheld by the curves shown in graph 52. A constant value of the stress required to initiate discharge is evident for gap widths exceeding the critical gap widths.

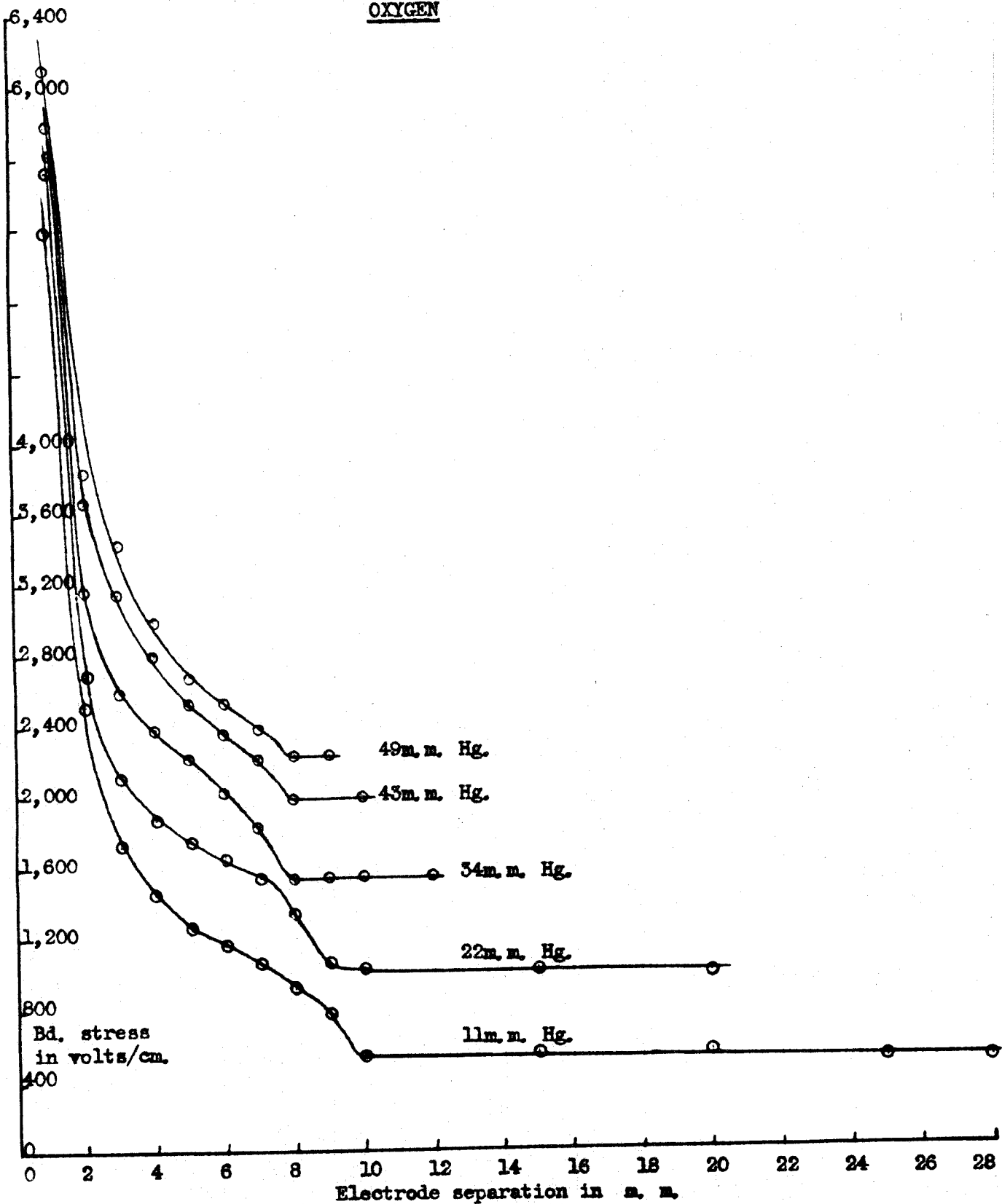
The two forms of discharge were again seen, the intense type consisted of an intense blue glow around the electrodes and a faint reddish inter electrode

Graph 55, AIR A.C. (11.5Mc/s), Breakdown Stress v. Pressure.



Graph 54. A.C. (11.5Mc/s), Breakdown Stress v. Electrode Separation.

OXYGEN





glow, while the D type consisted of just the reddish glow. The general variation followed that outlined for the other gases.

Two X against p graphs are shown, one for gaps greater than critical, and the other for gaps less than critical. (See graph 53). The breakdown voltages from the crossed field work at 2.66 Mc/s are also plotted, calculation again shows that these are for gaps less than the critical gap. (Graph 42 refers to the 2.66 Mc/s results).

#### 3.2.4. Cylinder Oxygen.

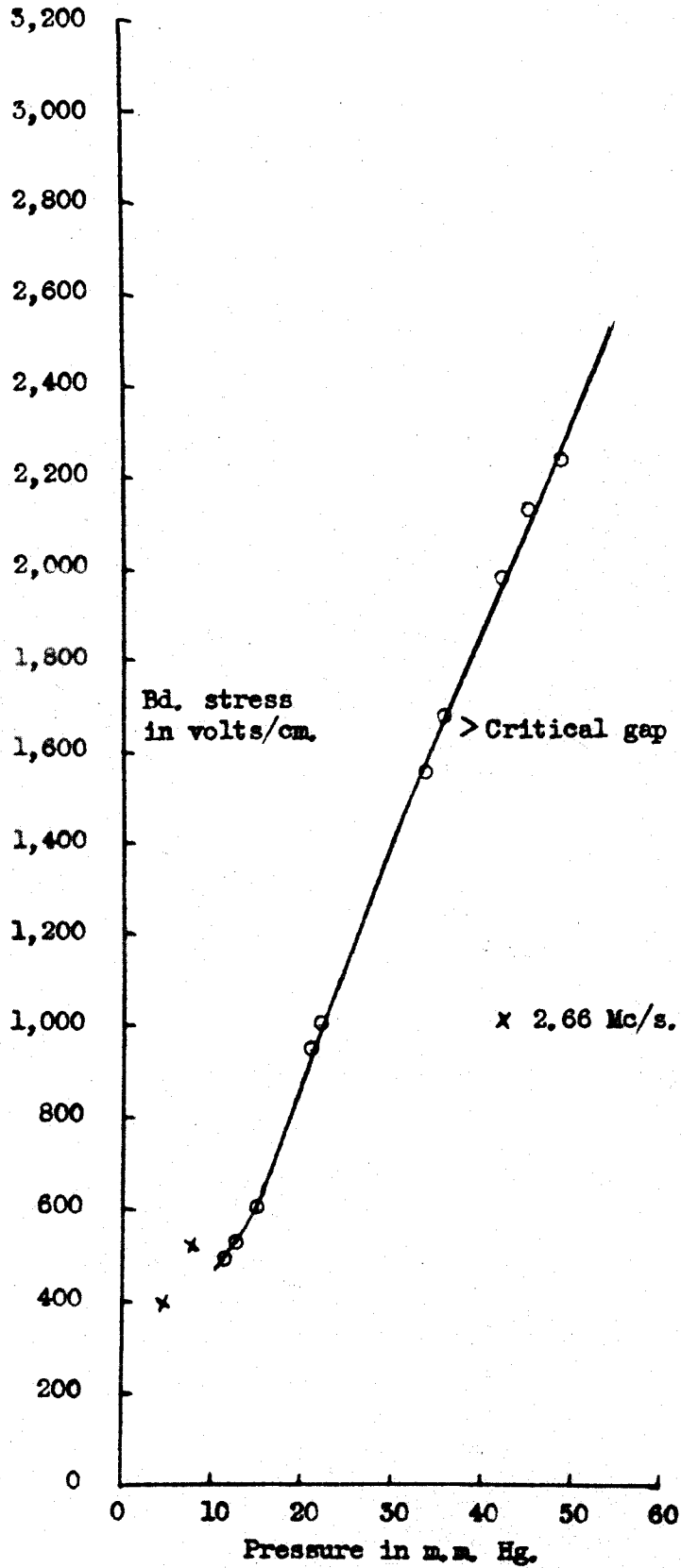
Finally cylinder oxygen was used with similar results to those found for the other three gases; the independence of breakdown stress on electrode separation provided the electrode separation exceeded the critical value. The results for oxygen are shown in graphs 54 and 55, the breakdown stress values for the 2.66 Mc/s. work are also shown, and again the electron ambit was greater than the capsule length, it is therefore to be expected that the values should be above the curve shown.

#### 4. Conclusions.

The results of the parallel electrode work can be summarised as follows:-

1. Provided the separation of the electrodes is greater than the critical separation the stress necessary to initiate a discharge was found to be independent of the

Graph 55 . OXYGEN A.C. (11.5Mc/s), Breakdown Stress v. Pressure.



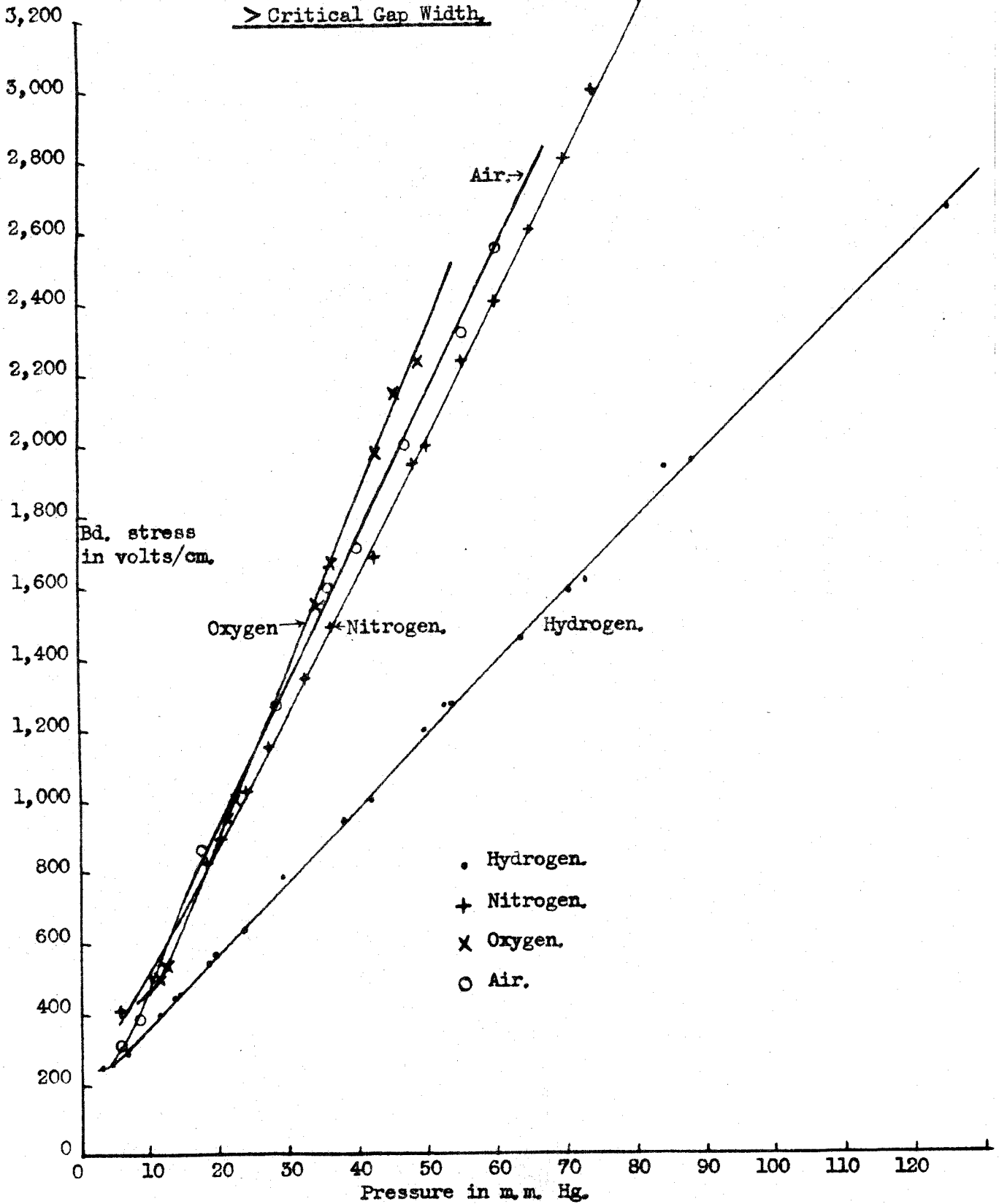
electrode separation; shown to be true for hydrogen, nitrogen, air and oxygen at 11.5 Mc/s, and hydrogen at 2.3 Mc/s. This result supports the idea that the breakdown stress for a high frequency discharge in a uniform field is a unique value, characteristic of the gas only. Such a statement has been verified for air by Pim and Cooper. (Introduction). The gases used in the present experiments include monatomic, polyatomic, non-attaching and polyatomic attaching gases, which all gave similar results. These results are at variance with the American diffusion theory of breakdown where the breakdown stress is a function of the gap widths. (See discussion, Chapter 9).

2. The final graph (56) in this chapter displays the  $X$  against  $p$  curves for all four gases, and it is interesting to compare this graph with the similar one found for the microwave discharge experiments (Graph 57) shown in Chapter 8. The separation of the air, oxygen, nitrogen curves is greater in the latter case, but once again the oxygen curve falls more steeply than the air curve for the lower pressures. Further comparison between the two sets of results has been deferred to the next chapter.

3. The Similarity Theorem<sup>70</sup> is upheld in the case of hydrogen at the two frequencies used 2.3 and 11.5 Mc/s; the same values of breakdown stress were recorded for similar pressures at the two frequencies.

Graph 56. A.C. (11.5Mc/s). Breakdown Stress v. Pressure.

> Critical Gap Width.



4. The experimentally determined electron ambits agreed with the calculated values.

## CHAPTER 8.

### Microwave breakdown stresses.

#### 1 Calibration of 10,000 Mc/s. E-p curves.

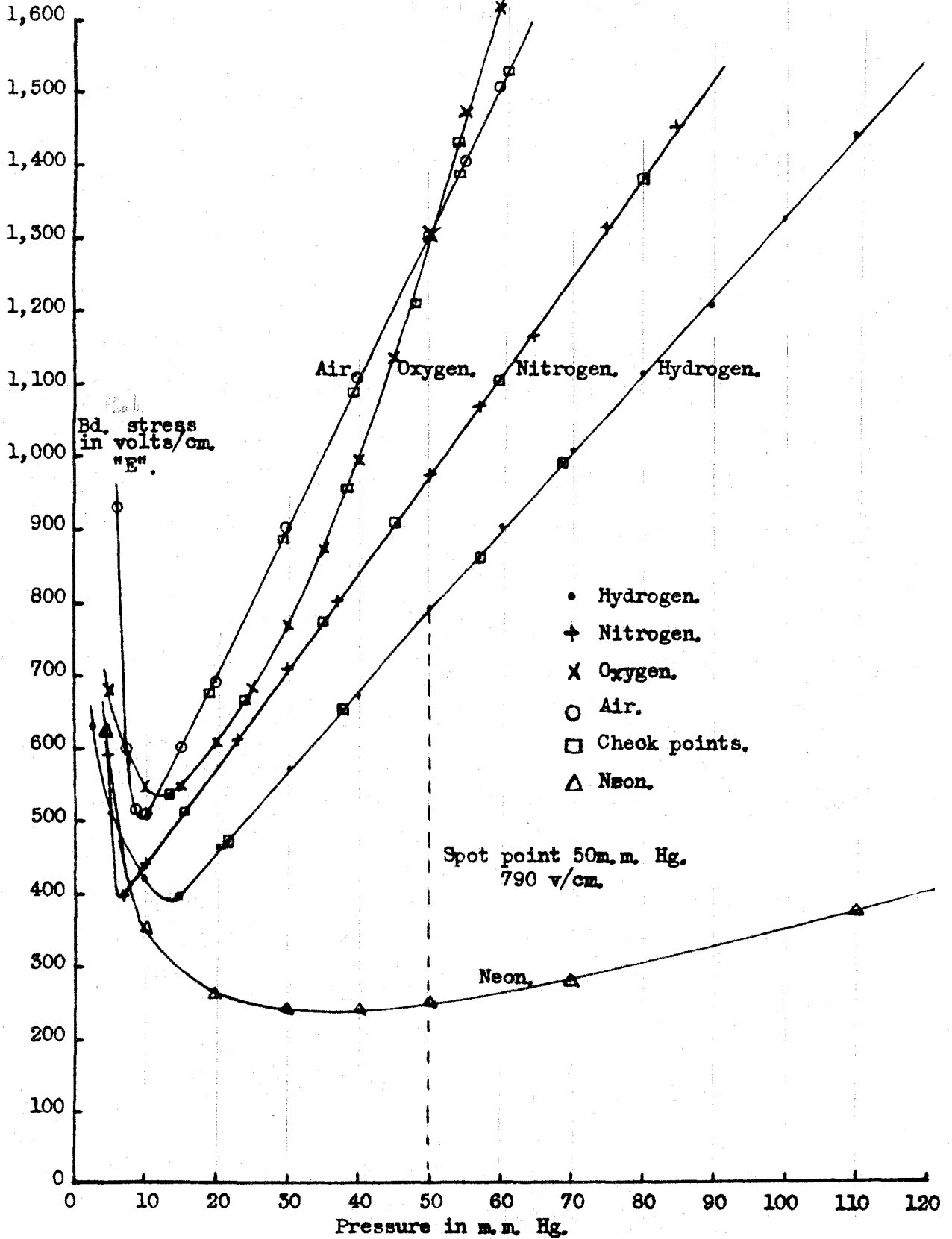
The chief object of the experiments was the elucidation of discharge mechanisms, but the actual values of the breakdown stresses are of technical importance, therefore an attempt was made to determine these stresses. They are to be accepted with reserve because of the difficulty in arriving at suitable standards of reference.

For the sake of clearness and brevity the curves showing the variation of the breakdown stress with pressure will be described as Paschen<sup>88</sup> curves, though the term is not strictly applicable. In particular the minimum has little relationship with the Paschen minimum.

Very little information on the numerical value of the breakdown stresses for any gas is available at this frequency (10,000 Mc/s). Labrum<sup>49</sup> measured breakdown stress for air at 10,000 Mc/s over the pressure range 5 to 20 m.m.Hg., somewhat similar experiments by Cooper<sup>47</sup> at the same frequency covered the pressure range 5 to 760 m.m.Hg; his results differed widely from Labrum's results over the 5 to 20 m.m.Hg. range. However the value 28,000 Volts/cm. for air at 760 m.m.Hg. determined by Cooper agreed with Pim's<sup>36</sup> determination for the lower frequency of 200 Mc/s. Due to the discrepancy in the pressure region 5 to 100 m.m.Hg. in the breakdown stress values recorded by several workers it was considered unsuitable to standardise the microwave stress results from the air curves.

However Prowse and Jasinski<sup>65</sup> employing a frequency of 2,800 Mc/s established the Paschen curve for hydrogen down to a pressure of approximately 30 m.m.Hg; their curve agreed within experimental error with the results of Githens<sup>41</sup> at 11 Mc/s. Githens determined the breakdown stress of hydrogen at 11 Mc/s. by an absolute method and estimated his experimental error not to exceed 2%. The slope of this curve agrees with the slope of the Paschen curve established in the present experiments at 10,000 Mc/s; it was therefore decided to take a spot value from the Prowse and Jasinski results and thus calibrate all

Graph 57. U.H.F. Breakdown Stress Calibration Graph.



the 10,000 Mc/s curves. The spot value chosen was the breakdown stress of pure hydrogen at 50 m.m.Hg., this being 790 Volts/cm.

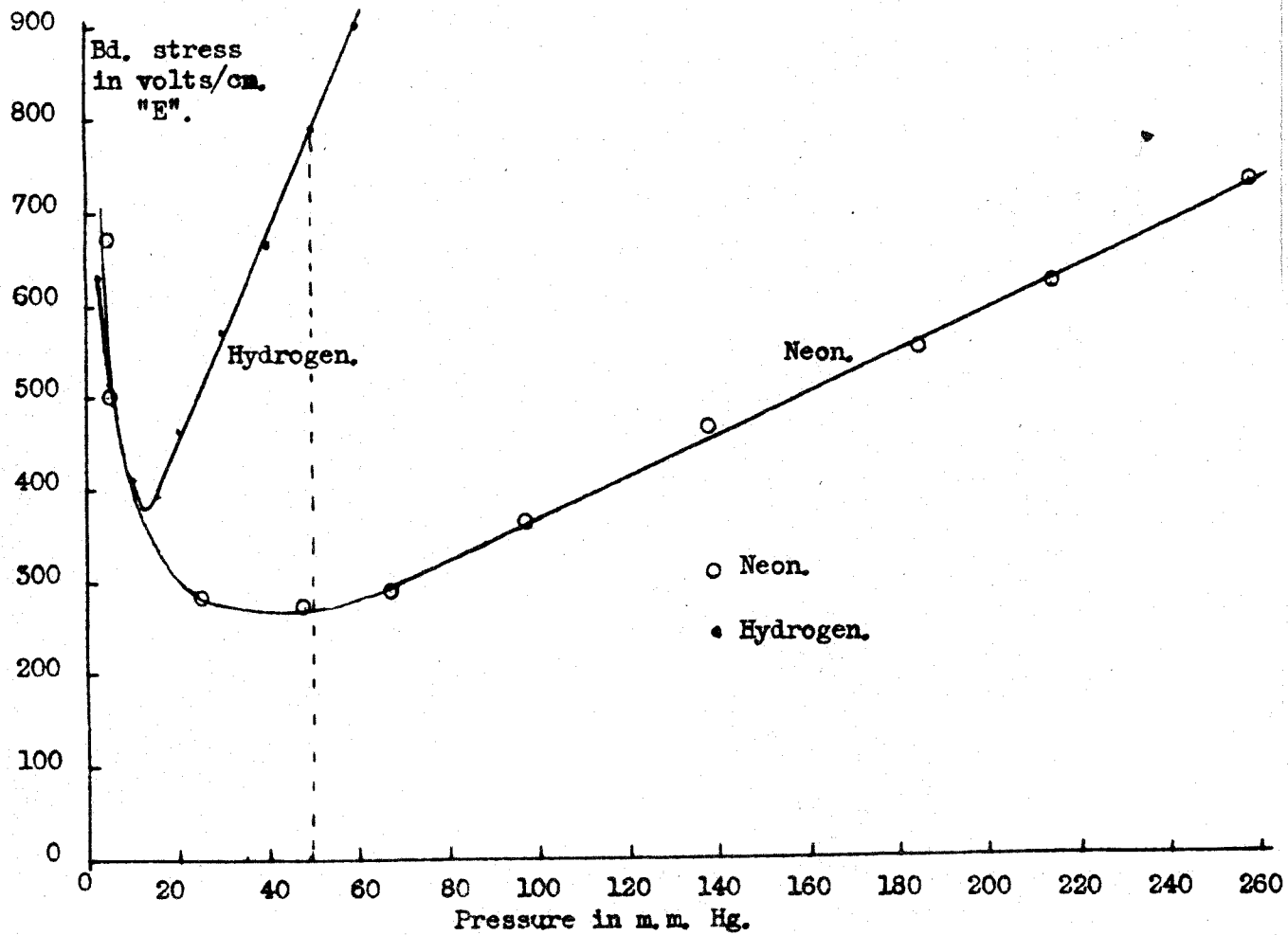
The resulting Paschen curves for hydrogen, nitrogen, air, oxygen and neon are shown on graph 57, the values shown are peak values of the stress. All these curves, therefore, are dependent on the breakdown stress of hydrogen at 50 m.m.Hg., they are a self consistent set of results. The curves were found to be reproducible within experimental error, and check points are shown taken many months after the original curves. The air, nitrogen and hydrogen curves are linear, except for the lower portion of the hydrogen curve, (below 35 m.m.Hg.)

The neon curves were not quite so reproducible; but over the three years of the experiments the variation between many calibration curves of neon to hydrogen never exceeded 6%. This is considered very reasonable as the breakdown stress of neon is markedly reduced by traces of impurity<sup>89</sup>.

The air was thoroughly dried; oxygen was from commercial cylinders. The use of spectroscopically pure, or cylinder, nitrogen did not alter the breakdown stresses recorded. The hydrogen was generated by the electrolysis of barium hydroxide as described, (Appendix 4)



Graph 58. U.H.F. Breakdown Stress Calibration Graph for NEON.



but no variation could be found between electrolytically produced, cylinder, or spectroscopically pure cylinder hydrogen.

2. Comparison with the 2,800 Mc/s. results of Prowse and Jasinski.

Comparison between these curves and the curves found by Prowse and Jasinski is of interest. In both sets the breakdown stress of oxygen is greater than the corresponding values for air above 50 m.m.Hg., and for Nitrogen for all pressures. The 10,000 Mc/s. work shows a reduction in the oxygen breakdown stresses compared with the corresponding values for air, below 50 m.m.Hg.; the 2,800 Mc/s. work also showed an irregularity at these lower pressures. (The radius of curvature of the graph however was in the opposite sense). A reversal in the relative breakdown stresses for low pressures for air and oxygen was also found at 11 Mc/s. in the present work. (Graph 56).

The curve for air at 10,000 Mc/s. is somewhat lower than the corresponding curve found by Prowse and Jasinski (2,800 Mc/s.). They calibrated all their curves from a spot value for air of 28,000 Volts/cm. at 760 m.m.Hg., now the 10,000 Mc/s. curves have been calibrated from the hydrogen curve of Prowse and Jasinski, but the resulting air curve (at 10,000 Mc/s). falls well below the 2,800 Mc/s. curve. Such a comparison between the 2,800 Mc/s and the 10,000 Mc/s.

curves however is only directly possible at the extreme range of either curve, (i.e. 10,000 mc/s from 5 to 70 m.m.Hg. and 2,800 Mc/s. from 70 to 760 m.m.Hg).

A comparison is given in the table below between the 10,000 Mc/s, 11 Mc/s. and the Prowse and Jasinski 2,800 Mc/s curves, with respect to hydrogen.

TABLE 37. Breakdown stress of various gases in terms of that for hydrogen at the same pressure.

p m.m.Hg.	Gases.	10,000 Mc/s.	11 Mc/s.	2,800 Mc/s.
20	{ H <sub>2</sub> = 1	-	-	-
	{ N <sub>2</sub>	1.235	1.54	-
	{ Air	1.48	1.63	-
	{ O <sub>2</sub>	1.3	1.56	-
40	{ N <sub>2</sub>	1.26	1.67	-
	{ Air	1.66	1.78	-
	{ O <sub>2</sub>	1.48	1.90	3.4
60	{ N <sub>2</sub>	1.21	1.72	-
	{ Air	1.66	1.82	-
	{ O <sub>2</sub>	1.79	-	3.95
80	{ N <sub>2</sub>	1.24	-	2.4
	{ Air	1.02	-	3.0
	{ O <sub>2</sub>	-	-	4.2
100	{ N <sub>2</sub>	1.25 Extrapo- lated	-	2.28
	{ Air	1.65 "	-	2.8
	{ O <sub>2</sub>	- "	-	3.3

### 3. Comparison with the American work.

No comparison has yet been drawn to the American results of Herlin and Brown<sup>51</sup> for air, and MacDonald and

Brown<sup>55</sup> for hydrogen. These results as has been stated support the diffusion theory; the results are therefore dependent on the gap width used. However, the results obtained for air using the greatest electrode separation, (0.318 cms.) coincide almost exactly with the air results from the present experiments; their frequency was 3,000 Mc/s. However for the smaller gaps 0.157 and 0.0635 cms. far greater stresses were recorded. The hydrogen results for the large electrode separations 2.5 cms. and 0.476 cms. fall below and above the hydrogen curve from the present experiments respectively; the discrepancy is of the order 20%. Discussion on the American results is deferred until the next chapter.

#### 4. The minimum pressure on the E - p graphs.

Calculation of the electron collision frequency at the minima on the E against  $p$  curves reveals a consistency between the five gases; nitrogen being the only one that differs largely from the rest.

The collision frequency is simply the quotient of the electron random velocity,  $V$ , and the mean free path at the appropriate E/p value, i.e.  $f = \frac{V}{L_p}$ , the data used ( $L_p$ ) to calculate these collision frequencies were obtained from Townsend<sup>86</sup>.

TABLE 38. Collision frequencies.

Gas	E min. Volts/cm.	p min. m.m. Hg.	f Collision frequency c/s.
Air	500	9.5	$4.05 \times 10^{10}$
H <sub>2</sub>	365	11.5	4.06 "
O <sub>2</sub>	530	12.0	4.02 "
N <sub>2</sub>	400	7.0	3.20 "
Ne	240	35	4.08 "

The frequency of the applied field was 10,000 Mc/s, i.e.  $10^{10}$  c/s., it can therefore be assumed that the minimum in the Paschen curves can be attributed to the fact that the collision frequency of the electron with molecules is of the same order as the frequency of the applied field.

In conclusion it can be stated that the set of curves given for the five gases is a self consistent set of results all based on hydrogen, thus if the value assumed for hydrogen is, by future experiments, found to be in error, all the set can be recalibrated; the relative stress values will, of course, remain constant.

CHAPTER 9.Discussion.1. Comparison of the 11 Mc/s and 10,000 Mc/s results with the American Diffusion Theory.

The American diffusion theory (this is actually a quantitative account of the earlier Townsend<sup>68</sup> theory) for breakdown at microwave frequencies, and high frequencies, demands that the production of electrons by ionising collisions, between electrons and neutral gas molecules, replaces the loss of electrons by diffusion to the walls of the discharge chamber. However as has been stated by Prowse and Jasinski<sup>64</sup> for pulsed microwave discharges diffusion to the electrodes cannot be the removal mechanism; the short times involved, (i.e. order of microseconds) so limit the diffusion radii.

The same conclusions apply to the present microwave work where the pulse length was one microsecond. Assuming that a diffusion radius of 5 m.ms. is necessary before diffusion can be considered to be a serious removal mechanism; the table below gives the pressures for the five gases used, below which the diffusion radii would exceed 5 m.m. There is a rapid decrease in these radii as the pressures increase above the values stated.

TABLE 39. Pressures at which diffusion radii  $> 5.0$  m.m.

Gases used.	p, in m.m.Hg.
H <sub>2</sub>	< 15
N <sub>2</sub>	< 13
O <sub>2</sub>	< 17
Air	< 15
Ne	< 150

The pressure for neon is considerably higher than the pressure for the polyatomic gases, but it should be remembered that the pressures actually employed for neon were relatively greater, up to 500 m.m.Hg.

Therefore for the polyatomic gases the loss of electrons by diffusion is not significant for pressures exceeding some 15 m.m.Hg. The diffusion theory is not therefore applicable to pulsed microwave breakdown above these pressures.

However if the criterion for breakdown under a sustained high frequency field is the balance between the production of electrons and their loss by diffusion, then this theory should apply to the parallel plate 11 Mc/s. experiments.

The diffusion theory gives the general equation:-

$$\xi = \frac{u}{CE_1^2}$$

where  $E_1$  = R.M.S. Breakdown stress

C = Diffusion coefficient of electrons in the gas.

$U$  = net electron production  
per electron per second.

$\xi$  is called the high frequency  
ionisation coefficient and is analogous to Townsend's  $\alpha$

The breakdown condition can take a modified form  
for a parallel plate system :-  $\xi = \frac{\pi^2}{\ell^2 E_1^2}$

where  $\ell$  = separation of the electrodes  
in cms.

The breakdown stress of a gas is therefore a  
function of the electrode separation.

None of the 2.3 Mc/s or the 11.5 Mc/s. results  
for hydrogen, air, oxygen, or nitrogen gives any evidence,  
provided the discharge is electrodeless in character, that  
the breakdown stress is a function of the electrode separation.  
A constant breakdown stress was recorded, within experimental  
error, for each gas at any given pressure provided the gap  
width was greater than the critical gap width. (It will be  
remembered that the breakdown stress rapidly decreased for  
electrode separation just greater than the critical separation,  
and then remained constant as the gap was further increased,  
i.e., the electrons failed to cross the gap in one half cycle  
of the applied field). This idea from the 2.3 and 11.5 Mc/s  
work that the high frequency breakdown stress of a gas is a



true characteristic of the gas independent of the gap width (provided the gap is greater than the critical value), is supported by the work of Pim<sup>36</sup>, Prowse and Jasinski<sup>65</sup>, Pim working in air obtained a constant breakdown stress for various gap widths at the same pressure. It has been suggested that air being an attaching gas might partly explain the discrepancy between the earlier results and the diffusion theory. However the present work has been undertaken in two attaching gases, air and oxygen, and two non-attaching gases, nitrogen and hydrogen, with similar results for both groups.

The calculations of Brown and MacDonald<sup>55</sup> over a wide range of results in hydrogen led to a single curve relating  $\zeta$  and  $E_1/p$ . It is of interest to calculate the appropriate value of  $\zeta$  from the 11.5 Mc/s. hydrogen results. As can be seen there are two possible methods.

1st Method using  $\zeta = \frac{\pi^2}{l^2 E_1^2}$ , the results used in this calculation are taken from graph 49.

TABLE 40 - Calculation of  $\zeta$

p m.m.Hg.	$E_1/p$	$l_1$ cms.	$l_2$ cms.	$\zeta_{l_1}$	$\zeta_{l_2}$
13.5	23.7	1.0	2.8	$9.8 \times 10^{-5}$	$1.24 \times 10^{-5}$
23.5	19.2	0.9	2.8	6.1 "	0.59 "
42.0	16.9	1.0	1.8	1.98 "	0.61 "
63.5	16.2	0.6	1.4	2.6 "	0.48 "
88	15.6	0.7	1.0	1.06 "	0.52 "

The two values of  $\ell$  chosen are the values between which a constant breakdown stress was recorded. The values taken from the paper by MacDonald and Brown are now given for comparison.

TABLE 41. Values of  $\zeta$  after MacDonald and Brown.

$E_1/p$	$\zeta$
10	$\ll 10^{-6}$ (Extrapolated).
15	$10 \times 10^{-5}$
20	37 "
25	70 "
30	115 "

These results (Table 40) demand, for a plot of  $\zeta$  against  $E_1/p$ , a vertical line for each value of  $E_1/p$ , there being no unique value of  $\zeta$  for a particular value of  $E_1/p$  as required by MacDonald and Brown. The values determined by MacDonald and Brown do, however, indicate a very rapid increase in  $\zeta$  with an increase in  $E_1/p$  for the range of pressures in the present work.

2nd Method using  $\zeta = \frac{\mu}{CE_1^2}$ . This is a more difficult procedure because of the variable  $\mu$ , the net electron production rate per electron. However let it be assumed that each collision between an electron and a gas molecule is an ionising collision, which is certainly incorrect but may be useful in assessing the trend of the

results.  $\therefore \mu = \frac{V}{L_p}$   
 where  $L_p =$  m.f.p. of electron in cms.  
 $V =$  random vel. in cms/sec.

and  $C = \frac{V L_p}{3} \text{ (Townsend}^{86}\text{)}.$

Again for hydrogen at 2.3 and 11.5 Mc/s. the values of  $\zeta$  are tabulated below.

TABLE 42. Calculated values for  $\zeta$ .

p m.m.Hg.	$E./p$	$\zeta$
5	37.6	1.2
10	27.0	3.58
20	20.5	8.65
30	18.7	11.2
50	17.0	15.2
70	16.1	17.3
100	15.5	19.6
120	15.0	21.5

These disagree by a factor of the order  $10^{-5}$  with the previous results, indicating the assumption that each collision was an ionising collision is far from the truth; an expected result. The values of  $\zeta$  do show an increase with a decrease of  $E./p$  as opposed to the previous calculation also the results illustrate the vertical form of a graph displaying  $\zeta$  against  $E./p$ .

It would therefore seem from this work that the diffusion theory cannot apply to (1) pulsed microwave breakdown at pressures, for polyatomic gases, greater than

15 m.m.Hg; (2) the relatively low frequency parallel plate work. The idea that breakdown is a true characteristic of the gas and independent of the gap width requires an infinite variation of  $\xi$  for any value of  $E/p$ . The diffusion theory gives an almost vertical plot for  $\xi$  against  $E/p$  for air and hydrogen when the pressure is in excess of about 10 m.m.Hg.

The diffusion theory might offer a possible explanation of breakdown in the lower pressure regions but not at the higher pressures, especially for pulsed work.

Disregarding the neon results for the present, the beaten zone hypothesis for a high frequency discharge is now considered. As has been explained, this hypothesis postulates that the excitation, or activation, of the gas by the electrons is a prerequisite of breakdown. Thus an electron produces, by continued inelastic collisions, an atmosphere of excited states, and because of its drift motion under the action of the microwave field, it will return through its own excited atmosphere thus increasing the probability of further excitation and ionisation. Diffusion to the walls of the discharge chamber at the higher pressures is, as has been shown, not considered to produce any serious electron loss during the build up of the electron concentration for breakdown. Consideration

of the lives of the excited states, and the frequency of the applied field, shows that there is sufficient time for the electron to return into its own excited atmosphere before this atmosphere decays. The average life of excited states for the gases used are of the order  $10^{-8}$  to  $10^{-9}$  secs, while the period of the applied field is  $10^{-10}$  secs.

Volume Recombination processes are too infrequent to be effective in the removal of electrons at low concentrations, and especially in the short times involved  $10^{-6}$  seconds.

The chief object of this work was to explore the hypothesis that the return of an electron through its own excited atmosphere is an important factor in microwave gas discharge, the results seem to support the original postulate.

## 2. The work under crossed fields.

### 2.1. A possible expected result with orthogonally applied fields.

#### 2.1.1. Case 1

##### Microwave and unidirectional fields.

It is not unreasonable to assume that the electron velocity necessary to produce ionisation in the gas, and hence breakdown, is determined by the magnitude of the resultant electric field.

Let the microwave field be represented by  $E \cos \omega t$ , and the unidirectional field by  $X$ .

The resultant field is therefore  $(\frac{E^2}{2} + X^2)^{1/2}$  where the mean value of  $E^2 \cos^2 \omega t = \frac{E^2}{2}$

The condition for breakdown is therefore  $(\frac{E^2}{2} + X^2)^{1/2} = \text{constant}$ , the curve plotting microwave field against steady field is clearly a circular quadrant for breakdown conditions. (If the breakdown stress depends on the frequency, the curve will be an elliptical quadrant).

### 2.1.2. Case 2.

#### Microwave field and alternating field.

Let the alternating field be represented by  $X \cos \omega t$ , as before the same assumptions apply and hence the condition for breakdown is  $(E^2 + X^2)^{1/2} = \text{constant}$ . The resulting curve would therefore be of the same form as before, i.e. a quadrant.

The curves realised in the actual experiments did not take the form indicated above, their general shape was rectangular, see graphs 36, 38, 43, 44 and 45, etc.

### 2.2. Summarised results.

1. Unidirectional field. The microwave breakdown stress of hydrogen, neon, air and oxygen was increased, when a unidirectional field was simultaneously orthogonally applied, compared to the microwave stress

recorded when no auxiliary field was present.

2. 0.86 Mc/s. Auxiliary field.

1. Hydrogen gave similar increases in the microwave field necessary for breakdown to those for a steady field.

2. Neon showed an increase in the microwave stress as the auxiliary field increased from 0 to 33 Volts/cm.; the microwave stress then remained constant as the auxiliary field was increased even up to the alternating field breakdown stress for neon.

3. 2.66 Mc/s auxiliary field.

Hydrogen, neon, air, oxygen and nitrogen all gave flat (i.e. rectangular) graphs, except at very low pressures, where small increases in the microwave field, compared to the stress required for breakdown with no auxiliary field present, were necessary to give breakdown.

4. 9.7 Mc/s. auxiliary field. Hydrogen, neon and air gave flat graphs (within experimental error) for all pressures used right up to values of the auxiliary field which themselves produced breakdown

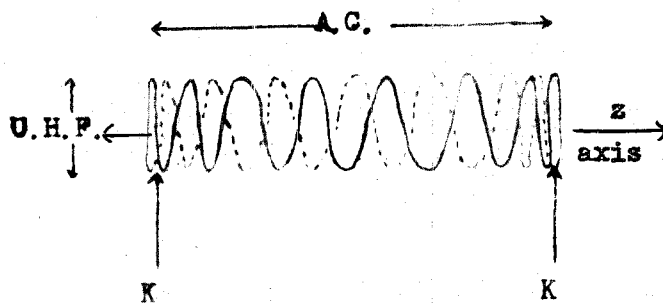


Fig. 39. Electron movement, U.H.F. + A.C. Field.

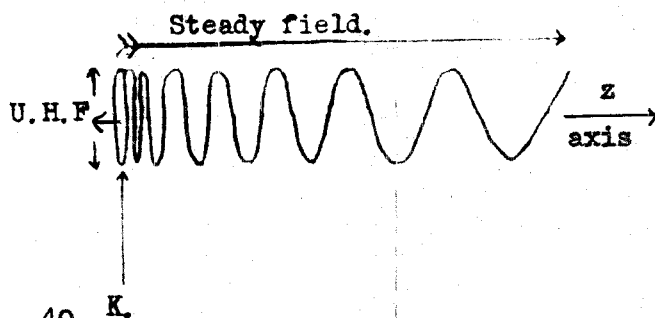


Fig. 40. Electron movement, U.H.F. + D.C. Field.

Figures 39 and 40 show an electron orbit under the action of the combined fields; either microwave and a unidirectional field, or microwave and an alternating field. The movement in the direction of the microwave field is extremely exaggerated for clarity, (i.e. of the order  $10^3$  to  $10^4$  times).

### 2.3. Discussion of the results obtained under the action of the combined fields.

1. Unidirectional field. The increase in the microwave field necessary to produce breakdown in the presence of a steady orthogonally applied field has been



discussed in Chapter 2, Part II. The increase is thought to be caused by clean up of the electrons by the steady field during the microsecond pulse.

2. 0.86 Mc/s. auxiliary field. The electron orbit calculations showed that for hydrogen the movement in the direction of the auxiliary field during one microsecond was comparable to the capsule dimensions; the increase in the microwave field necessary to produce breakdown in the presence of the 0.86 Mc/s. field may be explained in the same way as the corresponding increase for the unidirectional field results.

The auxiliary field voltages that produced extinction of the established microwave breakdown (i.e. cut off voltage) are of interest. The electron orbit in the direction of the auxiliary field for these voltages were shown to be of the order 3 to 10 m.m., that is, comparable to half the capsule length (11 m.m.) The auxiliary field may therefore sweep electrons originally in the central region of the resonator to the end walls and so cause the extinction of the discharge.

The results for neon are separately discussed below. (Page 232).

3. 2.66 Mc/s. auxiliary field. At the positions marked with a letter 'K' in figure 39, the

electron under the microwave field returns along its own track, i.e. it can be said to be travelling back through its own excited atmosphere. If breakdown under the action of a microwave field is determined by the electron returning through its own excited atmosphere, it could be said that such a condition exists at the positions indicated (K). This could explain why no increase in the microwave field was found necessary to produce breakdown even when the electrons were swept in and out of the intense field zone by the auxiliary field. Some 'ends' (K region) will always be in the strong  $E_0$  filament if the ambit (along the  $Z$  axis of the resonator) is less than half the capsule length.

Experiments in the lower pressure regions showed that an increase in the microwave field was necessary for breakdown as the auxiliary field increased. However, as stated, this increase occurred where the electron ambit under the auxiliary field was of the order  $\frac{L_c}{2}$ , ( $L_c$  - length of capsule). The electron ambits under the auxiliary field at which an increase in the microwave field became necessary to produce breakdown are given in the following table.

TABLE 43. Calculated electron ambits under 2.66 Mc/s. field.

Gas.	Pressure. m.m.Hg.	Electron ambit. m.m.
Dry air	21.5	11
	15	9.0
	10	8.8
	5	10.7
Oxygen	12.5	9.2
	8.0	5.8
	4.5	7.4
Nitrogen	21	8.5
	14.5	7.1
	11.5	6.8
	5	6.2

$\frac{L_c}{2} = 11 \text{ m.m.}$

It was difficult to say in hydrogen at what auxiliary field value an increase in the microwave stress became necessary to produce breakdown. There was for pressures below 45 m.m.Hg. a slight increase in the microwave stress necessary to initiate a discharge in the presence of the maximum auxiliary field, (600 Volts/cm). The electron ambits under the maximum 2.66 Mc/s field voltage are given in Table 23, Chapter 4.

The auxiliary voltage (2.66 Mc/s) necessary to quench the microwave discharge in nitrogen also gave electron ambits of the order  $\frac{L_c}{2}$ . The hydrogen cut off voltages for the 2.66 Mc/s. gave electron ambits

somewhat lower in value, 2 to 5 m.m.; however the ambits associated with the 0.86 Mc/s cut off voltages for hydrogen were of the order  $\frac{L_c}{2}$  (i.e. they were between 3 and 10 m.ms.) The resulting discharge under the crossed fields for hydrogen (microwave and 2.66 Mc/s.) showed a reduction in intensity at a fairly definite auxiliary voltage, (see section 2.1.1. Chapter 4), the electron ambits under the 2.66 Mc/s. field at these points were in the region 1 to 3 m.m.; i.e., similar to the cut off ambits for an auxiliary field of 2.66 Mc/s.

#### 4. 9.7 Mc/s. auxiliary field.

The greatest value of the calculated electron ambit in hydrogen was 5.3 m.m. and in this gas the microwave stress showed no dependence on the value of the auxiliary stress. This is in complete agreement with the foregoing argument.

#### 2.4. Further considerations.

##### 2.4.1. Formative time for discharge.

An electron is able to return under the action of the microwave field through its own excited atmosphere, i.e. at the positions marked K on figure 39 as discussed. If breakdown is dependent on this occurrence then the time spent in these regions (K) must be sufficient for the initiation of breakdown. Assume that the electron

spends  $\frac{1}{10}$ <sup>th</sup> of the auxiliary field cycle in these end regions, this is probably a low estimate. Then the times spent in these zones are :-

For an auxiliary field of 0.86 Mc/s,	$\frac{t}{10} = 1.16 \times 10^{-7}$	secs.
" " " " " 2.66 Mc/s,	$\frac{t}{10} = 3.76 \times 10^{-8}$	"
" " " " " 9.7 Mc/s,	$\frac{t}{10} = 1.03 \times 10^{-8}$	"

The formative times observed by Prowse and Jasinski<sup>65</sup> were, for the gases hydrogen, oxygen, air and nitrogen, less than the resolution time of their apparatus,  $10^{-8}$  seconds. It would therefore seem reasonable that the electron spends sufficient time in these end regions to initiate the discharge.

#### 2.4.2. Diffusion at the ends of the trajectories

It is worth while seeing how far an electron would diffuse during this period  $\frac{t}{10}$  seconds, particularly as this expresses the indefiniteness of the electron trajectory.

Let the corresponding movement of the electron under the auxiliary field in this time  $\frac{t}{10}$  be  $x$ ; then if  $x$  is approximately equal to the diffusion distance for a time  $\frac{t}{10}$ , the electron is at the end of its alternating field trajectory for a time  $\frac{t}{10}$  within the limits of electron-and-gas behaviour.

Examples of these values are given below for hydrogen, two values for the diffusion distances are given, one for the maximum value of the circuital field ( $E_0$ ) and one for the microwave field ( $E_c$ ) appropriate to the position a distance equal to electron ambit along the Z axis of the resonator. (The microwave circuital field varies sinusoidally along the Z axis). See Chapter 1, Part II).

TABLE 44. Diffusion radii in  $\frac{t}{10}$  secs.

p m.m.Hg.	Frequency of auxiliary field. Mc/s.	Ambit under A.C. field in $\frac{1}{2}$ cycle (t) m.m.	Diffusion for $E_0$ max. in $\frac{t}{10}$ secs. m.m.	Diffusion for $E_c$ in $\frac{t}{10}$ secs. m.m.
35	0.86	5.2	0.78	0.80
-97	0.86	6.7	0.4	0.43
45	2.66	4.5	0.35	0.36
113	2.66	2.05	0.22	0.23
5.5	9.7	4.9	1.2	1.32
21.5	9.7	1.1	0.32	0.33

The difference between the two values of E is small, and any diffusion calculations can only be taken as an indication of the electron spread. It can be seen that the diffusion distance at the ends of the ambits are of the same order as the electron movement under the combined fields for a similar period of time,  $\frac{t}{10}$  seconds.

#### 2.4.3. Variation of statistical lag with applied auxiliary field.

Breakdown it has been postulated can only

take place in the end regions, K K on figure 41.

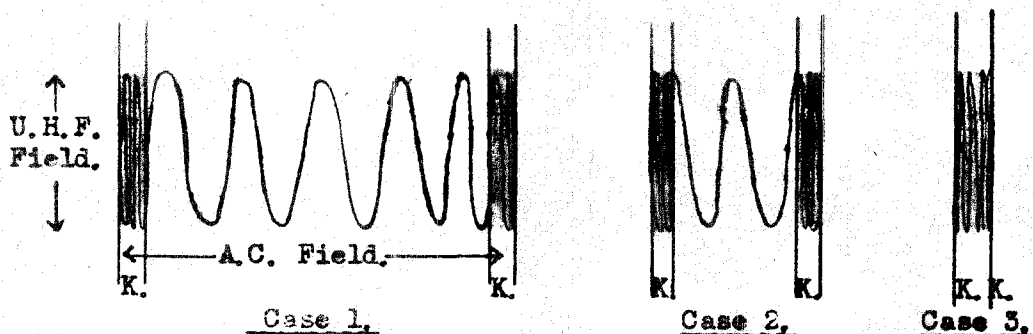


Fig. 41 . Electron movement under crossed fields.

Three possible cases are shown for decreasing auxiliary field. The time available for breakdown in case 1 is less than case 2, which is in turn less than case 3. If breakdown is conditioned by a random onset then the statistical lags ( $t_s$ ) should increase with increasing auxiliary field, i.e.,  $t_s > {}_2t_s > {}_3t_s$ . This was generally observed, the actual increase is seen on graph 37, Chapter 4, for hydrogen with an auxiliary field of 2.66 Mc/s.

### 3. The neon results.

3.1. General. The conception of an excited atmosphere built up in the beaten zone of the oscillating electron is not equally applicable to the monatomic gases. Small transference of energy from the oscillating electron to the gas molecules (resulting in an excited molecule) does

not occur; the collisions remain elastic until the electron energy reaches a value corresponding to the first excitation potential, (i.e. produces a metastable state in the neon atoms). Thus the beaten zone could be considered to be an area of metastable neon atoms rather than excited atoms.

To account for the fact that the breakdown stress of neon varied with the pulse length of the applied field, Labrum<sup>49</sup> proposed the following hypothesis: the breakdown condition is that a requisite number of electrons  $N_D$  should be present in the gap, and during a pulse the ionisation grows exponentially with time, thus we can write:-

$$N = N_0 e^{(Q-S)t}$$

where  $Q$  = No. of ion. pairs produced per electron per second.  
 $S$  = No. of electrons which disappear per second.  
 $N_0$  = No. of electrons at time,  $t=0$ .  
 $N$  = " " " " " " ,  $t=t$ .

Assuming a pulse length  $T$  and that  $N_D$  electrons are required for instability, the condition for discharge becomes:-

$$Q-S > \frac{1}{T} \text{Log} \frac{N_D}{N_0}$$

Neon is a non-attaching gas and thus diffusion is the only removal process. It has been shown



for 1 microsecond pulses provided the pressure was greater than 150 m.m.Hg. such losses were small, therefore 'S' is very small. (Table 39, page 216).

Thus the breakdown stress determined for neon is a function of the pulse length. (Figure 5).

The variation of breakdown stress for neon with pressure in the present work at 10,000 Mc/s. is in good agreement with Labrum's 'Paschen' curves for the same pulse length and pulse repetition frequency, (1  $\mu$ sec., and 400 p.p.s). The comparison however can only be made at the extreme opposite ranges of the results; Labrum used pressure up to maximum 30 m.m.Hg., and the present work extended from 5 to 465 m.m.Hg. The variation in the microwave breakdown stress with pulse repetition rate in Labrum's work for the same duration pulse is explained by residual ionisation in the gap from one pulse to the next.

It is therefore to be expected that the lowest breakdown stresses would be recorded for a given pressure when the gas is subjected to a sustained oscillating field. Gill and von Engel<sup>45</sup> have recorded a value of 465 volts/cm. at 760 m.m.Hg; compared with the 11 Mc/s parallel plate results which by extropolation, assuming a line-or relationship from 465 to 760 m.m.Hg., give a value of 660 volts/cm. at a pressure of 760 m.m.Hg.

### 3.2. The neon results for the crossed field experiments.

1. Unidirectional field. The necessary microwave breakdown stress had to be increased to give breakdown as the steady field increased. The interpretation is probably clean up of the electron as discussed in the previous sections.

2. 0.86 Mc/s auxiliary field. For pressure less than 200 m.m.Hg. a sudden increase in the microwave breakdown stress was found necessary for very low auxiliary fields, and then no variation in the microwave stress for breakdown right up to values of the auxiliary field which itself initiated a discharge. The interpretation of the sudden increase in the microwave stress is uncertain, but the following observations are made. It occurred within 33 Volts/cm of the auxiliary field and the electron drift movement under the auxiliary field at this voltage varied from 0.8 to 7.5 m.ms. for pressures 180 to 20 m.m.Hg. respectively. These electron ambits are of the same order as the ambits corresponding to the auxiliary field voltages necessary to quench an established microwave discharge, (i.e. cut off voltages, see Chapter 3 section 3.2.2.).

The flat portion of the graphs would seem interpretable in the same manner as for the polyatomic gases. The electron ambits for all pressures greater than

50 m.m.Hg. were far less than  $\frac{L_c}{2}$ ; thus clean up to the capsule wall was unlikely.

### 3. 2.66 and 9.7 Mc/s. auxiliary field.

At these two frequencies for the auxiliary field the results were similar in character, no increase in the microwave field with an orthogonally applied alternating field. The electron ambits in all cases were small in comparison with the capsule length, even at the highest alternating field stresses, (i.e. breakdown conditions for the auxiliary field). The two pressures 9 and 5.5 m.m.Hg gave calculated ambits of 15.5 and 45 m.m. under the maximum alternating field where a decrease in the microwave stress necessary to initiate breakdown was recorded. However at such low pressures the picture is further complicated as the collision frequency of electrons and gas molecules is less than the frequency of the microwave field.

### 3.3. Further considerations for neon.

It was assumed that the formative time for breakdown in the polyatomic gases was of such an order that breakdown could occur in the estimated time of  $\frac{1}{10} T^k$  cycle of the auxiliary field. Neon however has a large formative time; in Labrum's proposed mechanism the formative time is the time required to build up to a certain number

of electrons ( $N_D$ ) by normal collision processes. Prowse and Jasinski<sup>65</sup> showed that neon had a considerable formative time, this was dependent on the overvoltage, and values of the order 2 microseconds were recorded, decreasing to less than the resolution time of the apparatus ( $10^{-8}$  secs) as the percentage overvoltage increased.

The breakdown stresses recorded in the present work employing 1 microsecond pulse are higher than the stresses required for breakdown under a sustained field at the same pressure, (see graph 39) Whether breakdown can occur in a time equal to  $\frac{t}{10}$  (where  $t$  the period of the auxiliary field, i.e. from  $1.16 \times 10^{-7}$  to  $1.03 \times 10^{-8}$  secs), for the same percentage overvoltage is a doubtful suggestion unless the decrease in formative lag for the given percentage of overvoltage is very rapid.

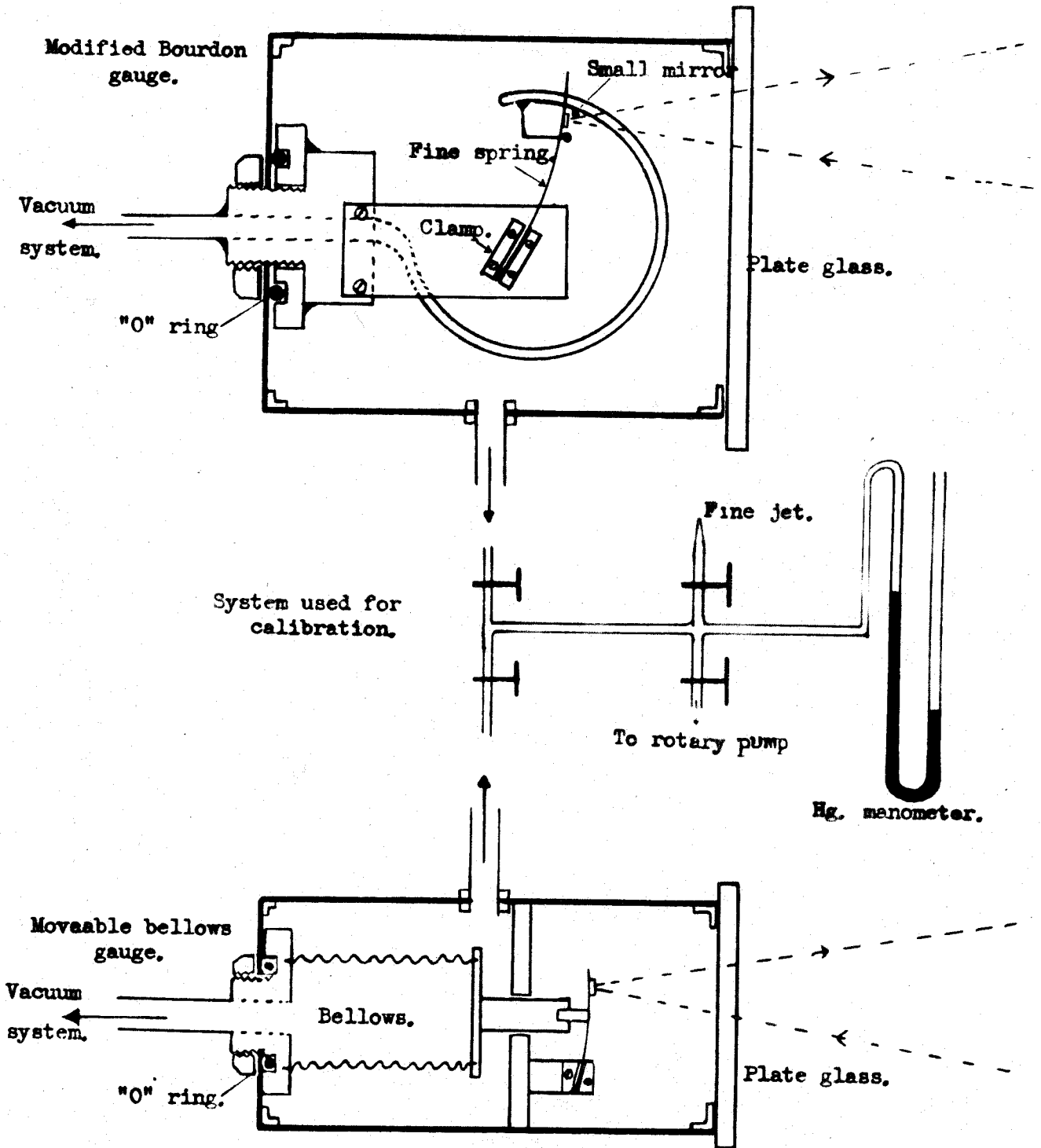


Fig. 42. Pressure gauges.

APPENDIX 1. The pressure gauges.

The modified differential Bourdon gauge as used throughout the experiments is shown opposite. This gauge was used in preference to the moving bellows gauge, the latter had a very limited pressure range. The gauges were constructed to be of a differential form to obviate the necessity of connecting, for calibration purposes, a mercury manometer to the high vacuum system.

To calibrate the gauge the following procedure was adopted:-

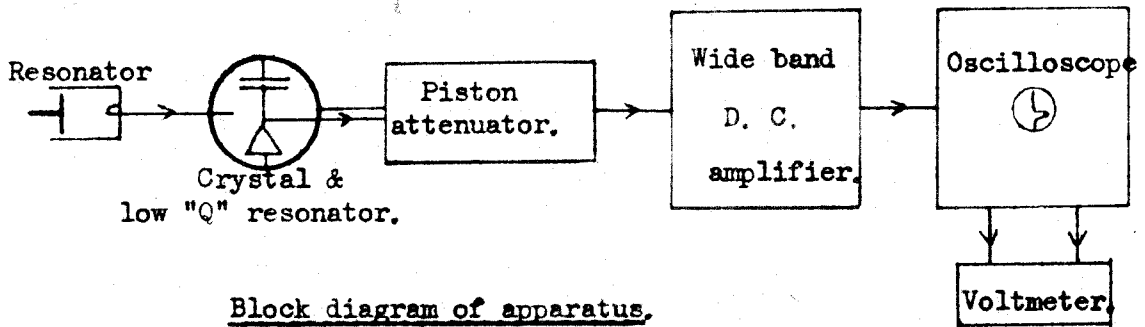
1. The inner portion of the gauge was evacuated by the high vacuum line.

2. Then the outer casing was evacuated by means of a rotary pump. The gauge now read zero - no pressure difference between the inner and outer compartments. The manometer of course read atmospheric pressure.

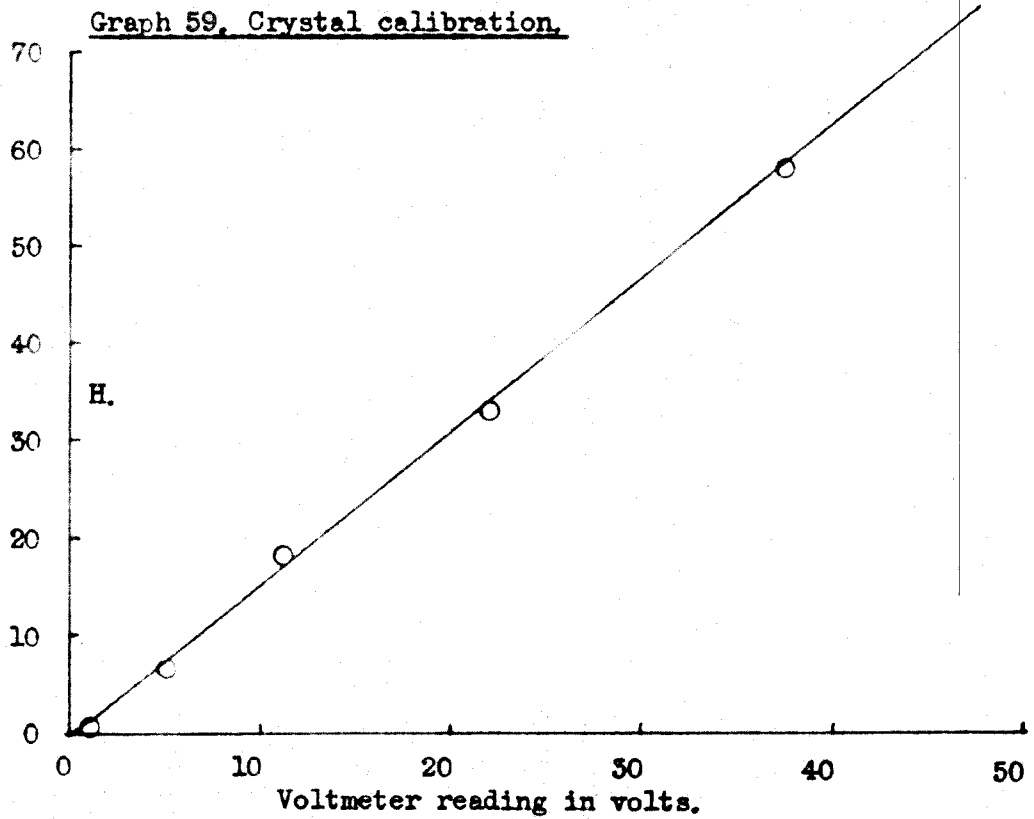
3. A small quantity of air was then allowed to enter the outer casing, by means of the fine jet shown, the change in the manometer reading was the pressure difference between the inner and outer sections of the gauge.

4. In this manner a calibration curve was easily obtained for either gauge. The Bourdon gauge was linear over the pressure range 10 m.m. to approximately 480 m.m.Hg; a slight departure from linearity occurred below 10 m.m.Hg., the complete range extended from 1 to 480 m.m.Hg.

Appendix 2 .



Block diagram of apparatus.



APPENDIX 2.Calibration of crystal diodes.

To calibrate the crystal diodes a calibrated piston alternator was inserted between the low Q resonator, plus crystal, and the wide band amplifier, as shown.

The energy input to the resonator from the waveguide was kept constant and the amplitude of the pulse envelope, as seen on the oscilloscope screen, was measured for a known amount of attenuation in the piston attenuator. In this manner the calibration curve was obtained, the voltmeter reading is the voltage required to displace the pulse envelope a distance equal to its own height. The field strength,  $H$ , in the resonator is plotted in arbitrary units. The linearity of the amplifier had already been established for the range of gain used in the experiments.

It can therefore be assumed that the field strength within the resonator was directly proportional to the height of the pulse envelope viewed on the oscilloscope screen.



Appendix 3 .

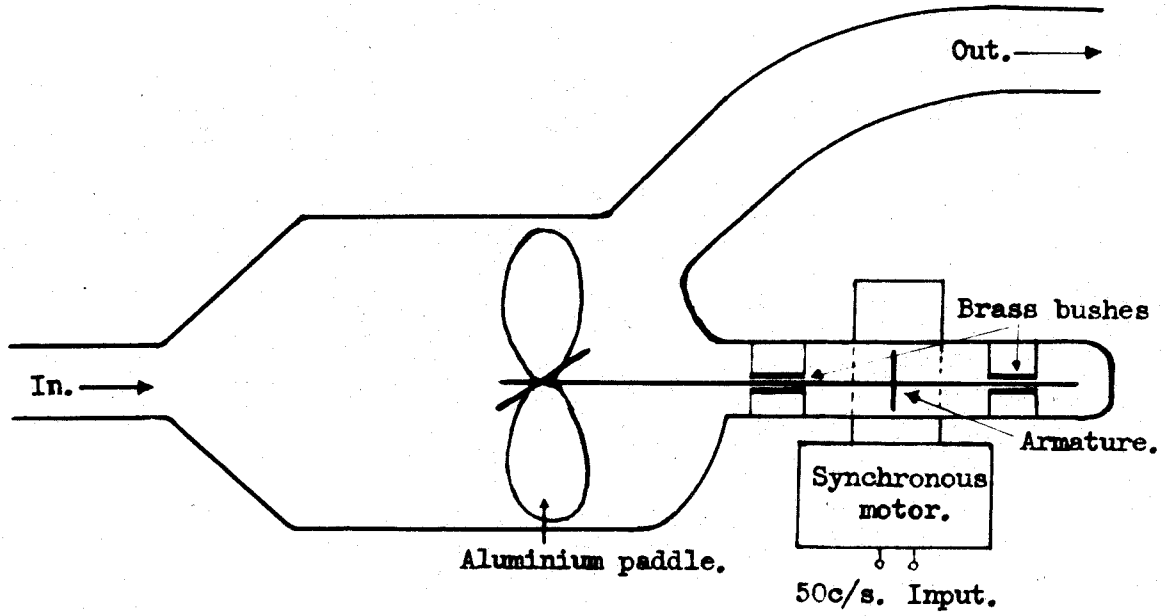


Fig 45. Circulating motor for vacuum apparatus.

APPENDIX 3.The circulating pump.

The circulating pump consisted of an aluminium four bladed paddle mounted on a light spindle; the spindle also carried the armature of a synchronous motor. Two small brass bushes carried the spindle as shown; the field coils of the motor were mounted outside the high vacuum system, thus a minimum of metal was introduced into the vacuum system.

The diagram opposite is approximately 3/4 full size.

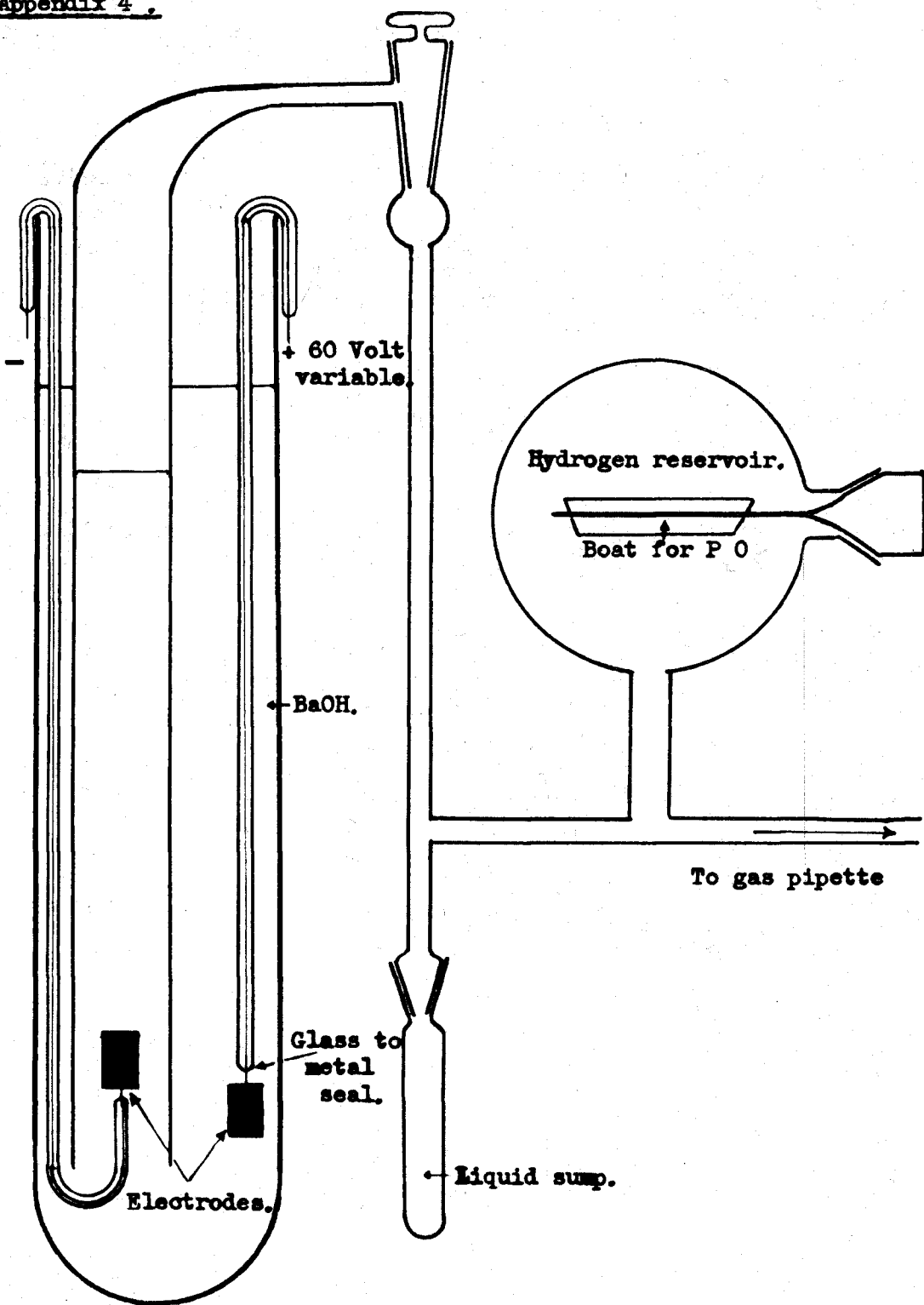


Fig. 44. Electrolysis apparatus for pure hydrogen.

APPENDIX 4.Hydrogen generating plant.

Pure hydrogen was obtained by the electrolysis of barium hydroxide<sup>38</sup>. The apparatus was constructed so that (1) the hydrogen could be easily tapped off into the vacuum apparatus,

and (2) the hydrogen could not be contaminated with oxygen. This was achieved by placing, as shown, a sleeve over the negative electrode.

The gas was dried by allowing it to stand in a reservoir containing a phosphorous pentoxide boat, it could then be pipetted into the vacuum apparatus as required.

In case of emergency, i.e. liquid entering the reservoir section of the apparatus, a liquid sump was incorporated, thus ensuring that no liquid could pass this T joint.

Appendix 5

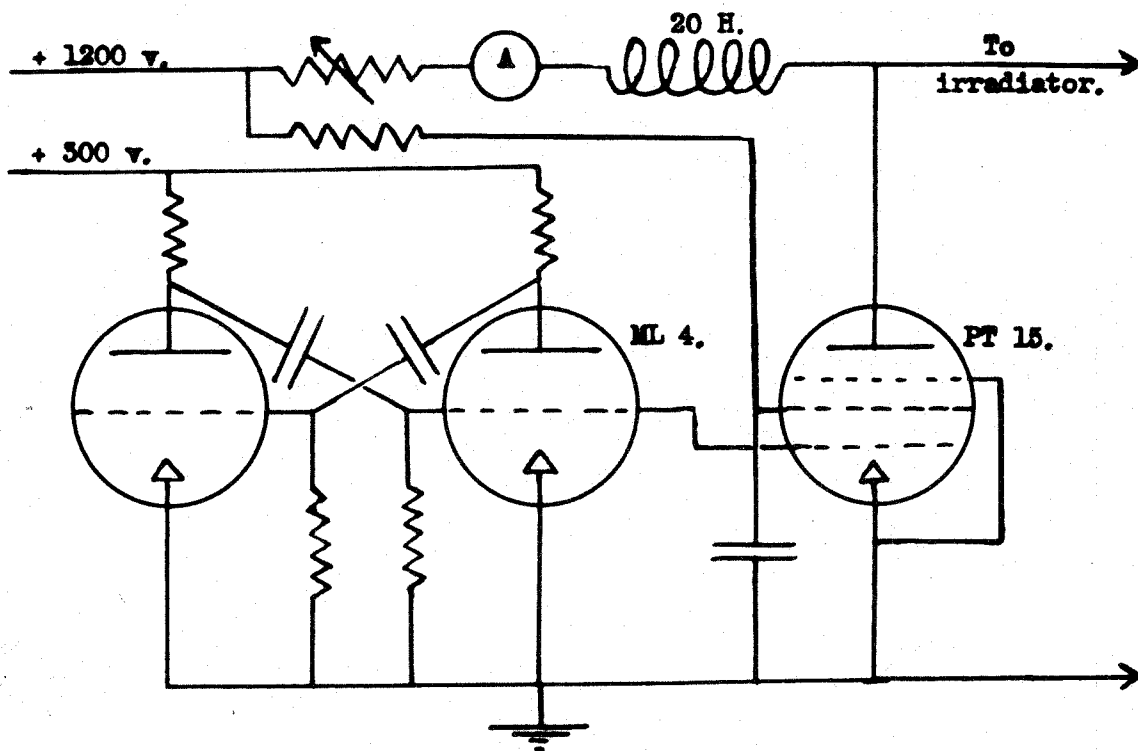


Fig. 45 . H.T pulse circuit for irradiator.

APPENDIX 5.Irradiator pulse generator.

The irradiator pulse was derived by cutting off an inductively loaded pentode; the negative pulse required to bias off the pentode was derived from a simple multivibrator circuit. The repetition rate of this multivibrator was adjusted to be approximately 400 pulses per second. An anode load resistance controlled the steady current through the pentode and therefore the resulting output pulse. The ammeter in series with this variable resistance was used to identify the magnitude of the output pulses, (i.e. Ia 9, 10, 13, 15, 19 m.a.).

BIBLIOGRAPHY.

1. Coulomb C.A., Mém.de l'Acad.des Sc., 612, 1875.
2. Faraday M., Researches in Electricity,  
London, 1844.
3. Righi A., Nuovo Cimento, (2), 16, 97, 1876.
4. Mehta G.K., J. University of Bombay, 16, Part 5,  
1948.
5. Morgan G.D., Science Progress, 161, January, 1953.
6. Thomson J.J., Phil.Mag., 32, 321 and 445, 1891.
7. Hittorf W., Wied. Ann., 52, 437, 1884.
8. Lehrmann W., Wied. Ann., 47, 427, 1882.
9. Tesla N., Electrical Engineer, July, 1891.
10. Lecher Phys. Zeits., 5, 179, 1904.
11. Steiner Wien. Ber., 113a, 403, 1904.
12. Thomson J.J., Conduction of Electricity through  
Gases, Vol. 11, Cambridge  
University, Press 1933.
13. Wiedemann E., and Ebert Wied. Ann., 1, 221, 1, 1893.
14. Thomson J.J., Proc. Phys. Soc., 40, 79, 1928.
15. Thomson J.J., Phil. Mag., 4, 1128, 1927.
16. Townsend J.S., and Donaldson, R.N., Phil. Mag., 5, 178, 1928.
17. Mackinnon K.A., Phil. Mag., 8, 605, 1929.
18. Knipp C.T., Phys. Rev., 37, 756, 1931.
19. Smith H., Lynch W.A. and Hilberry N., Phys. Rev., 37, 1091, 1931.
20. Yarnold G.D., Phil. Mag., 13, 1179, 1932.
21. Brasefield C.J., Phys. Rev., 37, 82, 1931.
22. Clark J.C., and Ryan H.J., Proc. Am. I. E. E., 2, 937, 1914.
23. Gill E.W.B., and Donaldson R.H., Phil. Mag., 2, 129, 1926.
24. Taylor J. and W., Proc. Camb. Phil. Soc., 24, 259, 1928.
25. Hulbert E.O., Phys. Rev., 20, 127, 1922.
26. Thomson J., Phil. Mag., 10, 280, 1930.
27. Lassen Arch. f Elek., 25, 322, 1931.
28. Kirchner F., (Ann. d Physik., 77, 289, 1925.  
(Phys. Rev. 72, 348, 1947.
29. Rohde Ann. d Physik., 12, 569, 1932.
30. Cambell N., Phil. Mag., 38, 215, 1919.
31. Darrow K.K., Bell Syst. Tech. J., 2, 576, 1932.





65. Prowse W.A., and Jasinski W., I.E.E. Monograph, 32, March, 1952.
66. Gill E.W.B., and Townsend J.S. Phil.Mag., 26, 290, 1938.
67. Margenau H., (Phys.Rev. 69, 508, 1946.  
" " 73, 297, 1948.)
68. Townsend J.S. Electricity in Gases, Clarendon Press, Oxford.
69. Holm R., Phys.Zeits., 25, 316, 1924.
70. Llewellyn-Jones F., and Morgan G.D., Proc.Phys.Soc.,B, 64, 560, 1951.
71. -do- Proc.Phys.Soc., 64, 574, 1951.
72. Llewellyn-Jones F., Morgan G.D., and Williams G.C. Proc.Phys.Soc., 66, 17, 1952.
73. Fisher L.H., and Bedersen B. Phys.Rev., 81, 109, 1951.
74. Kachickas G.A., and Fisher L.H. " " 88, 878, 1952.
75. Menes M., and Fisher L.H. " " 86, 134, 1952.
76. Biondi M.A., and Brown S.C. " " 76, 1647, 1949.
77. Biondi M.A., ( " " 82, 453, 1952.  
" " 88, 660, 1952.)
78. Massey H.S.W. Advances in Physics 2, 1, 1952.
79. Prowse W.A., Laverick E., and Jasinski W. Brit.E.A.I.R.A., L/T 295, Feby. 1953.
80. Penning F.M., Naturwiss., 15, 818, 1927.
81. Loeb L.B., Electrical Discharge in Gases, John Wiley, New York, 1947.
82. Varela A.A., Phys.Rev., 71, 124, 1947.
83. Montgomery G.C., Technique of Microwave Measurements, McGraw Hill, 1951.
84. Jaknke-Emde, Tables of Functions, Dover Publications, 1949.
85. Huxley L.G.H., The Principles and Practices of Waveguides, C.U.P., 1947.
86. Townsend J.S., Electrons in Gases, Hutchinsons Publications, 1947.
87. von Engel A., and Steenbeck M., Elektroische Gasentladungen, - Band 2, 1944.
88. Paschen F., Wied.Ann., 37, 69, 1889.
89. Hayman R.L., Phil.Mag., V, 586, 1929.